

Copyright  
by  
David Arnold Glasscock

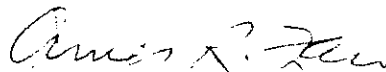
1990

MODELLING AND EXPERIMENTAL STUDY OF CARBON DIOXIDE  
ABSORPTION INTO AQUEOUS ALKANOLAMINES

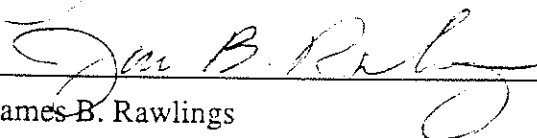
APPROVED BY  
SUPERVISORY COMMITTEE:



Gary T. Rochelle



James R. Fair



James B. Rawlings



Robert S. Schechter



Kamy Sepehrnoori

MODELLING AND EXPERIMENTAL STUDY OF CARBON DIOXIDE  
ABSORPTION INTO AQUEOUS ALKANOLAMINES

by

DAVID ARNOLD GLASSCOCK, B.S., M.S.

DISSERTATION

Presented to the Faculty of the Graduate School of

The University of Texas at Austin  
in Partial Fulfillment  
of the Requirements  
for the Degree of

DOCTOR OF PHILOSOPHY

THE UNIVERSITY OF TEXAS AT AUSTIN

August 1990

To Kathleen

## Acknowledgements

I am grateful to Dr. Gary Rochelle for his guidance in this research. I never cease to be amazed by his quick perception of concepts and his ability to intuitively analyze complex problems. I also appreciate the guidance and support of many faculty members. I have been able to learn much from the members of my committee, Professors Jim Fair, Jim Rawlings, Robert Schechter, and Kami Sepehrnoori. All of these distinguished people have been of assistance to me beyond the expectations of committee members. I am also grateful to Dr. Linda Hayes, who was a committee member for some time.

One of the most valuable resources a graduate student has is other graduate students. There are numerous graduate students from whose contact I have benefited. Dave Austgen and Jim Critchfield, both now of Shell Development were of great assistance. I have also learned much from my association with Steve Beaudoin, Todd Carey, Joe Peterson, and Jerry Toman. I will always miss Cini Gage and Cindy Gleason. I have known Stephanie Butler for years, and consider her to be not only a good friend, but also an outstanding chemical engineer. In addition, I have enjoyed learning from and getting to know numerous other graduate students.

Above all, I must thank my wife Kathleen for her support of my graduate and undergraduate education. She is not only a wonderful wife and mother to our son, Aaron, she is an exceptionally intelligent and caring person. I am especially grateful to Dr. Mayis Seapan, who hired me as an undergraduate assistant at Oklahoma State University, and encouraged me to pursue a graduate education. I am also grateful to my parents for their encouragement of my graduate education.

Finally, I am grateful for the financial support of the Separations Research Program. The Center for High Performance Computing provided the supercomputer time without which much of this work would have been impractical. I also appreciate the financial support of Texaco Chemical and the opportunity to work with Tom Moore and Ed Sheu of the Texaco Chemical Austin Laboratory.

# MODELLING AND EXPERIMENTAL STUDY OF CARBON DIOXIDE ABSORPTION INTO AQUEOUS ALKANOLAMINES

Publication No. \_\_\_\_\_

David Arnold Glasscock, Ph.D.  
The University of Texas at Austin, 1990

Supervising Professor: Gary T. Rochelle

A comprehensive model for the simulation of CO<sub>2</sub> absorption and desorption with chemical reaction is presented. The activity coefficients for the alkanolamine systems studied are estimated using the Electrolyte-NRTL equation. It takes into account both long-range and short-range interactions between the species in solution. A generalized framework is constructed for the diffusion and reaction of species in ionic solutions. The differential material balance equations are solved numerically to obtain liquid-phase concentration profiles and flux rates for CO<sub>2</sub> at the gas-liquid interface. This general model is used to extract kinetic information from mass transfer experiments and predict system behavior under industrially relevant conditions.

The model has been used to study the reaction kinetics for CO<sub>2</sub> with MEA (monoethanolamine), DEA (diethanolamine), MDEA (methyldiethanolamine), and the mixtures MEA/MDEA, and DEA/MDEA. In addition to data taken by other authors, experimental data are presented for absorption of CO<sub>2</sub> into 0.5 and 1.0 molal DEA at 40°C, 1.0 molal MDEA at 25 and 40°C under a range of CO<sub>2</sub> partial pressures up to 1

atm, and 0.1/0.9 and 0.3/0.7 molal DEA/MDEA mixtures at 40°C. The MDEA data indicate that the apparent reactivity of MDEA is a function of the CO<sub>2</sub> partial pressure and loading. By detailed treatment of the reaction kinetics in nonideal solutions, absorption and desorption data for DEA have been successfully reconciled by assuming the reaction rate constants "increase" with ionic strength. It is also demonstrated that MDEA interacts in the DEA kinetic expression, but the model can simulate MEA/MDEA mixed amine data without kinetic interaction.

Model results show that, under many conditions, a simple pseudo first-order approximation will be accurate to within 10%. This is certainly true for the MDEA system, which provides little if any enhancement of the CO<sub>2</sub> absorption rate under the typically high mass transfer coefficients found in packed and plate columns. For faster reacting amines, the use of a more rigorous approximation is suggested.

## TABLE OF CONTENTS

<b>Acknowledgements .....</b>	<b>v</b>
<b>Abstract.....</b>	<b>vi</b>
<b>List of Tables.....</b>	<b>xii</b>
<b>List of Figures .....</b>	<b>xiii</b>
<b>Chapter One: Introduction.....</b>	<b>1</b>
1.1 Acid Gas Treating Technologies.....	1
1.2 Removal of Acid Gases Using Aqueous Alkanolamine Solutions.....	3
1.3 Effect of Chemical Reaction on Gas Absorption.....	5
1.3.1 Equilibrium Considerations .....	5
1.3.2 Nonequilibrium Considerations.....	7
1.4 Overview of This Work.....	9
<b>Chapter Two: Chemistry of CO<sub>2</sub>-Alkanolamine Systems.....</b>	<b>14</b>
2.1 Reactions of CO <sub>2</sub> in Aqueous Solutions.....	16
2.2 CO <sub>2</sub> Reactions with Primary and Secondary Alkanolamines.....	17
2.2.1 Mechanisms .....	17
2.2.2 Literature Data on Primary Amines (MEA and DGA).....	21
2.2.3 Literature Data on Secondary Amines (DEA) .....	22
2.3 CO <sub>2</sub> Reactions with Tertiary Alkanolamines .....	23
2.3.1 Mechanisms .....	23
2.3.2 Literature Data on Tertiary Amines (TEA and MDEA).....	24
2.4 Rate Equations for CO <sub>2</sub> Reactions in Mixed Amine Systems .....	25
<b>Chapter Three: Equilibrium Models for Aqueous CO<sub>2</sub>-Alkanol-amine Systems.....</b>	<b>32</b>
3.1 Formulation of Equilibrium Equations in Combined Phase/Chemical Equilibria.....	32
3.2 Activity Coefficients in Electrolyte Systems.....	35
3.2.1 Long-Range Contributions .....	36
3.2.2 Short-Range Contribution .....	37
3.3 Standard States of the Electrolyte-NRTL Model.....	41
3.4 Solution of the Combined Phase/Chemical Equilibrium Problem .....	41
3.4.1 The Nonstoichiometric Algorithm .....	43
3.4.2 Application of the Nonstoichiometric Algorithm to the Acid Gas-Alkanolamine System .....	45
3.4.3 Conversion of Equilibrium Constants into Standard-State Chemical Potentials.....	46



<b>Chapter Four: Mass Transfer with Reversible Chemical Reaction in Electrolyte Systems.....</b>	<b>48</b>
4.1 The Theory of Irreversible Processes (TIP).....	48
4.2 Diffusion in Nonideal Electrolyte Systems.....	51
4.2.1 The Flux Expression for Diffusion in Electrolyte Systems.....	51
4.2.2 The Henderson Formula for the Electrical Potential Gradient.....	53
4.3 On the Consistency Between Chemical Kinetics and Reaction Equilibria .....	57
4.4 Incorporation of Flux Expressions into Material Balance Equations .....	60
4.5 Two Alternative Formulations of the Material Balance Equations for Multiple Instantaneous Reactions.....	61
4.6 Mass Transfer Equation Systems for Acid-Gas Absorption/Desorption with Alkanolamine-Based Systems.....	64
4.6.1 CO <sub>2</sub> Absorption into Mixed Amine Systems.....	64
4.6.2 CO <sub>2</sub> Absorption into Mixed Amine Systems with Buffer Additives.....	65
4.6.3 Simultaneous H <sub>2</sub> S/CO <sub>2</sub> Absorption into Mixed Amine Systems.....	66
<b>Chapter Five: Models for Gas Absorption into a Turbulent Liquid Phase .....</b>	<b>67</b>
5.1 Mass Transfer Models - An Overview .....	67
5.2 Unsteady-State Mass Transfer Theories .....	70
5.2.1 Penetration Theory .....	72
5.2.2 Surface Renewal Theory.....	77
5.3 Steady-State Mass Transfer Theories .....	80
5.3.1 Film Theory .....	80
5.3.2 Eddy Diffusivity Theory.....	81
5.3.3 Approximate Film Theory.....	83
5.4 Quantitative Effect of Chemical Reaction on the Gas Absorption Rate.....	84
<b>Chapter Six: Numerical Methods .....</b>	<b>86</b>
6.1 Review of Literature Methods for Gas Absorption with Chemical Reaction.....	86
6.1.1 Unsteady-State Theories.....	86
6.1.2 Steady-State Theories .....	90
6.2 Numerical Methods used in This Work.....	94
6.2.1 Spatial Dimension .....	94
6.2.2 Unsteady-State Theories.....	95
6.2.3 Steady-State Theories .....	96

6.3	Verification of Model.....	99
6.4	Parameter Estimation.....	99
6.5	Performance Enhancements .....	107
6.5.1	Machine Independent Performance Enhancement .....	107
6.5.2	Machine Dependent Performance Enhancement - Vectorizability.....	108
<b>Chapter Seven: Experimental Apparatus and Procedure.....</b>		<b>110</b>
7.1	Procedure.....	111
7.2	Apparatus Assembly and Operation .....	113
7.3	Calibration and Use of Supplemental Equipment.....	115
7.4	Calibration of the Reactor.....	116
7.5	Measurement of Chemical Absorption Rates.....	117
<b>Chapter Eight: Comparison of Mass Transfer Theories.....</b>		<b>120</b>
8.1	Second-Order, Reversible Reaction .....	120
8.2	CO <sub>2</sub> Absorption into Aqueous MDEA .....	124
<b>Chapter Nine: Simulation of CO<sub>2</sub> Absorption/Desorption.....</b>		<b>137</b>
9.1	Equilibrium Data Regression.....	140
9.2	Rate Data Regression.....	143
9.2.1	MDEA system.....	143
9.2.2	DEA system .....	151
9.2.3	DEA/MDEA system .....	153
9.2.4	MEA/MDEA system.....	159
9.3	Comparison with Previous Data .....	159
9.3.1	MDEA system.....	159
9.3.2	DEA and DEA/MDEA systems .....	164
9.4	Concentration Profiles Obtained using the Rate Model .....	166
9.5	Useful Results Using the Combined Equilibrium/Rate Model .....	166
<b>Chapter Ten: Conclusions and Recommendations .....</b>		<b>178</b>
10.1	Summary .....	178
10.2	Conclusions .....	178
10.3	Recommendations for Future Work.....	180
<b>Appendix A: Derivations of the Equations of Continuity in Transformed Coordinates.....</b>		<b>181</b>
A.1	Penetration and Surface Renewal Theories.....	181
A.2	Eddy Diffusivity Theory.....	187
<b>Appendix B: Error Analysis.....</b>		<b>192</b>
B.1	Introduction .....	192
B.2	Gas Phase Error Analysis .....	193
B.3	CO <sub>2</sub> Partial Pressure Error Analysis .....	196
B.4	Error in Concentration Measurements.....	198
<b>Appendix C: Experimental Data .....</b>		<b>199</b>

<b>Appendix D: Physical Property Correlations</b> .....	217
D.1 Viscosity of the Unloaded Solution .....	217
D.2 Viscosity of the Loaded Solution .....	218
D.3 Density of the Solution.....	218
D.4 Diffusion Coefficients.....	219
D.4.1 Diffusion Coefficient of CO <sub>2</sub> .....	219
D.4.2 Diffusion Coefficient of the Amines.....	220
<b>Appendix E: Program Documentation</b> .....	221
E.1 Program Execution Overview.....	221
E.2 Location of Subroutines .....	226
E.3 Input Files .....	226
E.4 Output Files .....	227
E.5 Include Files.....	227
E.6 Selection of Chemical System.....	239
E.7 Execution of Mass-Transfer Simulation .....	239
E.7.1 One Case Only .....	239
E.7.2 Multiple Cases .....	239
E.8 Execution of Equilibrium Simulation.....	239
E.9 Nonlinear Parameter Estimation of Equilibrium and Rate Parameters.....	240
<b>Appendix F: SRP Annual Report - Modelling and Experimental Study of CO<sub>2</sub> Absorption into Aqueous Amines</b> .....	241
<b>Nomenclature</b> .....	250
<b>Bibliography</b> .....	253

## LIST OF TABLES

Table 3.1	Equilibrium Constants for the CO <sub>2</sub> -Amine Reactions.....	42
Table 6.1	Summary of Numerical Studies of Absorption With Chemical Reaction for the Unsteady-State Theories .....	91
Table 6.2	Summary of Numerical Studies of Absorption with Chemical Reaction Using Film Theory .....	93
Table 6.3	Comparison of Numerical Results for a Second-Order, Reversible Reaction.....	100
Table 7.1	Summary of Conditions for Chemical Absorption Data .....	119
Table 8.1	Model Parameters for the MDEA System at 318K .....	129
Table 9.1	Scheme of Reactions for the CO <sub>2</sub> -Amine System .....	139
Table 9.2	Range of Data Used in Equilibrium and Rate Regression .....	141
Table 9.3	Equilibrium Regression Results .....	142
Table 9.4	Typical Activity Coefficients Calculated Using the Electrolyte-NRTL Model.....	144
Table 9.5	Comparison of Regression Results for the MDEA System.....	145
Table 9.6	Analysis of Effect of Impurities on the Absorption Rate of CO <sub>2</sub> into MDEA .....	152
Table 9.7	Comparison of Regression Results for the DEA and DEA/MDEA Systems.....	154
Table 9.8	Comparison of Results with Literature Data.....	161
Table 9.9	Effective Rate Constants and Activation Energy for the Reaction of CO <sub>2</sub> with MDEA.....	165
Table 9.10	Effectiveness of the Welleck Correlation for CO <sub>2</sub> Enhancement Factors .....	177
Table E.1	Summary of Subroutines Written by the Author.....	228
Table E.2	Definition of Chemical Systems .....	232

## LIST OF FIGURES

Figure 1.1	Typical Absorber/Scrubber System for Acid Gas Removal.....	4
Figure 1.2	Equilibrium of CO <sub>2</sub> with a (a) Physical System (b) Chemical System.....	6
Figure 1.3	Comparison of CO <sub>2</sub> Fugacity for a Physical System (water at 313K) and a Chemical System (10%DEA,40%MDEA at 313K).....	8
Figure 1.4	Concentration Profiles Under High-Driving Force Absorption .....	10
Figure 2.1	Molecular Structure of Typical Amines Used in Acid Gas Treating Processes .....	15
Figure 2.2	Second-Order Rate Constant for the CO <sub>2</sub> -MDEA Reaction .....	26
Figure 5.1	Liquid-Phase Mass Transfer Models.....	68
Figure 5.2	Enhancement Factor for a Second-Order, Reversible Reaction using Surface Renewal Theory .....	85
Figure 7.1	Liquid-Phase Mass Transfer Coefficient for Various Types of Equipment.....	112
Figure 7.2	Stirred Tank System Used in CO <sub>2</sub> Absorption Experiments.....	114
Figure 7.3	Mass Transfer Coefficients Determined by CO <sub>2</sub> Absorption into Water and Aqueous Ethylene Glycol.....	118
Figure 8.1	Enhancement Factor for a Second-Order, Reversible Reaction, $K_{eq} = 350$ .....	122
Figure 8.2	Comparison of Mass Transfer Theories to Surface Renewal Theory for a Second-Order, Reversible Reaction, $K_{eq} = 350$ .....	123
Figure 8.3	Comparison of Mass Transfer Theories to Surface Renewal Theory for a First-Order, Irreversible Reaction.....	125
Figure 8.4	Enhancement Factor for a Second-Order, Reversible Reaction, $K_{eq} = 1$ .....	126
Figure 8.5	Comparison of Mass Transfer Theories to Surface Renewal Theory for a Second-Order, Reversible Reaction, $K_{eq} = 1$ .....	127
Figure 8.6	Effect of CO <sub>2</sub> Interfacial Concentration and Hydroxide Reaction for the MDEA System .....	130
Figure 8.7	Concentration Profiles for the MDEA System with the Film Theory Solution, Enhancement Factor = 17.5.....	132
Figure 8.8	Concentration Profiles for the MDEA System with the Film Theory Solution, Enhancement Factor = 11.9.....	133
Figure 8.9	Comparison of Mass Transfer Theories to Surface Renewal Theory for the MDEA System .....	134

Figure 8.10	Effect of CO <sub>2</sub> Interfacial Concentration and Hydroxide Reaction for the MDEA System .....	135
Figure 9.1	Fit of MDEA High- and Low-Driving Force Data with the Simplified Kinetic Mechanism.....	148
Figure 9.2	Fit of MDEA High- and Low-Driving Force Data with the Simplified Kinetic Mechanism.....	149
Figure 9.3	Fit of MDEA High- and Low-Driving Force Data with the Hydroxide Kinetic Mechanism .....	150
Figure 9.4	Fit of DEA Absorption/Desorption Data Using Constant Forward Rate Constants.....	155
Figure 9.5	Fit of DEA Absorption/Desorption Data Assuming Forward Rate Constants Increase with Increasing Ionic Strength.....	156
Figure 9.6	Fit of DEA/MDEA Data Using Simplified MDEA Kinetic Mechanism.....	157
Figure 9.7	Fit of DEA/MDEA Data Using Hydroxide Kinetic Mechanism for MDEA .....	158
Figure 9.8	Simulation of MEA/MDEA Experimental Data Using a Non-Interactive Kinetic Model.....	160
Figure 9.9	Apparent Rate Constant for the CO <sub>2</sub> -MDEA Reaction.....	163
Figure 9.10	Concentration Profiles Under Low-Driving Force Absorption Conditions.....	167
Figure 9.11	Concentration Profiles Under High-Driving Force Absorption Conditions.....	168
Figure 9.12	Concentration Profiles Under Desorption Conditions .....	169
Figure 9.13	Concentration Profiles for Low-Driving Force Absorption into MDEA .....	170
Figure 9.14	Absorption Enhancement Factor for 30wt% DEA and 50wt% MDEA .....	171
Figure 9.15	Absorption Enhancement Factor for 10wt% DEA/40wt% MDEA and 5wt% MEA/45wt% MDEA .....	173
Figure 9.16	Comparison of Actual to First-Order Enhancement Factors.....	174
Figure E.1	Subroutine Call Chain From the Main Program.....	222
Figure E.2	Subroutine Call Chain from PROP70.....	224
Figure E.3	Subroutine Call Chain from CONT .....	225
Figure E.4	Input File RXN70.IN.....	229
Figure E.5	Input File EQUIL.IN .....	231

Figure E.6	Input File PARM.IN.....	232
Figure E.7	Output File RXN70.DAT .....	233
Figure E.8	Output File RXN70.OUT .....	237
Figure F.1	Enhancement Factor for a Second-Order, Reversible Reaction.....	244
Figure F.2	Fit of MDEA High- and Low-Driving Force Data with the Simplified Kinetic Mechanism.....	245
Figure F.3	Fit of MDEA High- and Low-Driving Force Data with the Hydroxide Kinetic Mechanism .....	246
Figure F.4	Concentration Profiles for Low-Driving Force CO <sub>2</sub> Absorption into MDEA .....	247
Figure F.5	Enhancement Factor for 10wt% DEA/40wt% MDEA and 5wt% MEA/45wt% MDEA .....	248

# Chapter One

## Introduction

Acid gas treating is a technology that has been in use industrially for over half a century. It was in 1930 that Bottoms patented a process to remove  $\text{CO}_2$  using alkanolamines. The idea was to remove an acidic component from the vapor-phase by using a basic species with which it can react. Today, we still practice acid gas treating in this manner. One may wonder if the potential exists for academic research in a field so mature. Nevertheless, there is much about acid gas treating which we do not understand. A fundamental understanding of acid gas treating processes requires utilizing complex kinetic mechanisms, electrolyte thermodynamics, mass transfer with chemical reaction in nonideal systems, theories for gas absorption into a turbulent liquid phase, various numerical methods for solving the equilibrium and rate equations, and nonlinear parameter estimation of kinetic and thermodynamic parameters. Indeed, these subjects represent a brief outline of the topics discussed in this dissertation.

In this chapter, we will widen the scope by reviewing the basic technology of acid gas treating processes. There are a number of different types of solvents and methods for removing acid gases such as  $\text{CO}_2$  and  $\text{H}_2\text{S}$  from a process stream. How do alternative methods compare with the technology we are studying? Finally, we will restrict the scope to the removal of  $\text{CO}_2$  by aqueous alkanolamines in preparation for the main text. It will be shown that the work presented in this dissertation is an appropriate mixture of theory and practical application.

### 1.1 Acid Gas Treating Technologies

The book by Kohl and Reisenfeld (1985) is a most authoritative review of acid gas treating technologies. They separate techniques for removing acid gases into 3 categories: adsorption onto a solid, catalytic conversion in the vapor-phase, and absorption into a liquid phase. We divide the third category - absorption into a liquid phase - into subcategories, since this dissertation is concerned with absorption, and absorption is the most important of the 3 basic types of processes:



## I. Reactive Absorption

### A. amines

1. aqueous solvent
2. nonaqueous solvent

### B. hot potassium carbonate

### C. ammonia

## II. Physical Absorption

### A. water

### B. specialty physical solvents

This work is concerned with the removal of  $\text{CO}_2$  by reactive absorption using alkanolamines in an aqueous solvent. As can be seen, this is only one of a number of technologies, and the particular technology used is dictated, of course, by process economics. Reactive absorption is generally used over physical absorption due to the higher capacity of the solution. Physical absorption has the advantage of easier removal of the acid gases from the loaded solution, but is useful only when the partial pressure of the acid gas to be removed is relatively high. There are several types of processes available to remove  $\text{CO}_2$  and/or  $\text{H}_2\text{S}$  by reactive absorption. The alkanolamine technology is the most common. Aqueous solvents have the advantage of lower cost, however nonaqueous solvents combine the physical absorption characteristics of the nonaqueous solvent with the reactivity of the amine. Hot potassium carbonate solutions are generally used in conjunction with ammonia plants. In this situation, the gas to be treated is typically high in  $\text{CO}_2$  partial pressure and temperature, conditions at which the hot potassium carbonate process is better suited than alkanolamines, in which the equilibrium considerations would make absorption at the high temperatures difficult (Astarita et al., 1983). Ammonia-based processes are rarely used due to the higher corrosivity of the loaded solutions and the complex flow scheme compared to the alkanolamine- and hot potassium carbonate-based processes. They do have the advantage, however, of less expensive solution, and can be used to remove  $\text{CO}_2$  when the initial partial pressure of the gas to be treated is small.

We have provided only a brief sketch of the considerations that must be taken into account when selecting a process to treat acidic gases. The texts by Astarita et al. (1983) and Kohl and Reisenfeld (1985) provide a detailed comparison of the different

processes. There are many considerations, largely dictated by process feasibility and economics. In addition to the kinetic and equilibrium behavior, which can be largely measured in the laboratory and predicted using models such as the one developed in this work, there are many other considerations which we will not address. For example, corrosion is a major consideration, and the types of materials required in process construction can have a profound influence on the process economics. Degradation of the chemical reactants is a consideration rarely found in the literature, but affects the type of process used. Foaming of the process solution is another consideration which is difficult to characterize from a scientific point of view, but must be taken into consideration. We cannot hope to address all of these issues, but we can provide information on the thermodynamic and kinetic considerations that are of use not only from a scientific standpoint, but in process development as well.

## 1.2 Removal of Acid Gases Using Aqueous Alkanolamine Solutions

A general process schematic for removing acid gases is shown in Figure 1.1. A feed gas consisting typically of hydrocarbons ( $\text{CH}_4$ ,  $\text{C}_2\text{H}_6$ ,  $\text{C}_3\text{H}_8$ , etc.) along with the acidic components is contacted countercurrently in a packed or plate column with the aqueous solution. The reason for the countercurrent contacting is that the reactions are equilibrium limited. It has been proposed (Blauwhoff et al., 1985) that a series of cocurrent packed columns be used for selective  $\text{H}_2\text{S}$  removal since these columns have a higher ratio of gas to liquid-phase mass transfer coefficients, nevertheless, most contacting is countercurrent. The sweet gas comes out from the top of the absorption column. The loaded solution may be carried through a flash tank in order to remove any of the hydrocarbons. The solution is then fed to the stripper where it is typically heated at slightly above ambient pressure. Energy is provided to the reboiler for two reasons: (1) to produce enough water vapor so that the vapor-phase partial pressure of  $\text{CO}_2$  is low enough to provide a driving force for desorption, and (2) to provide enough energy to reverse the reactions which occur in the absorber. In fact, the reactions of  $\text{CO}_2$  with aqueous alkanolamine solutions are highly exothermic, releasing energy in the absorber and requiring energy in the stripper. Economic analysis of this type of process shows that the reboiler heat duty is the most significant operating cost

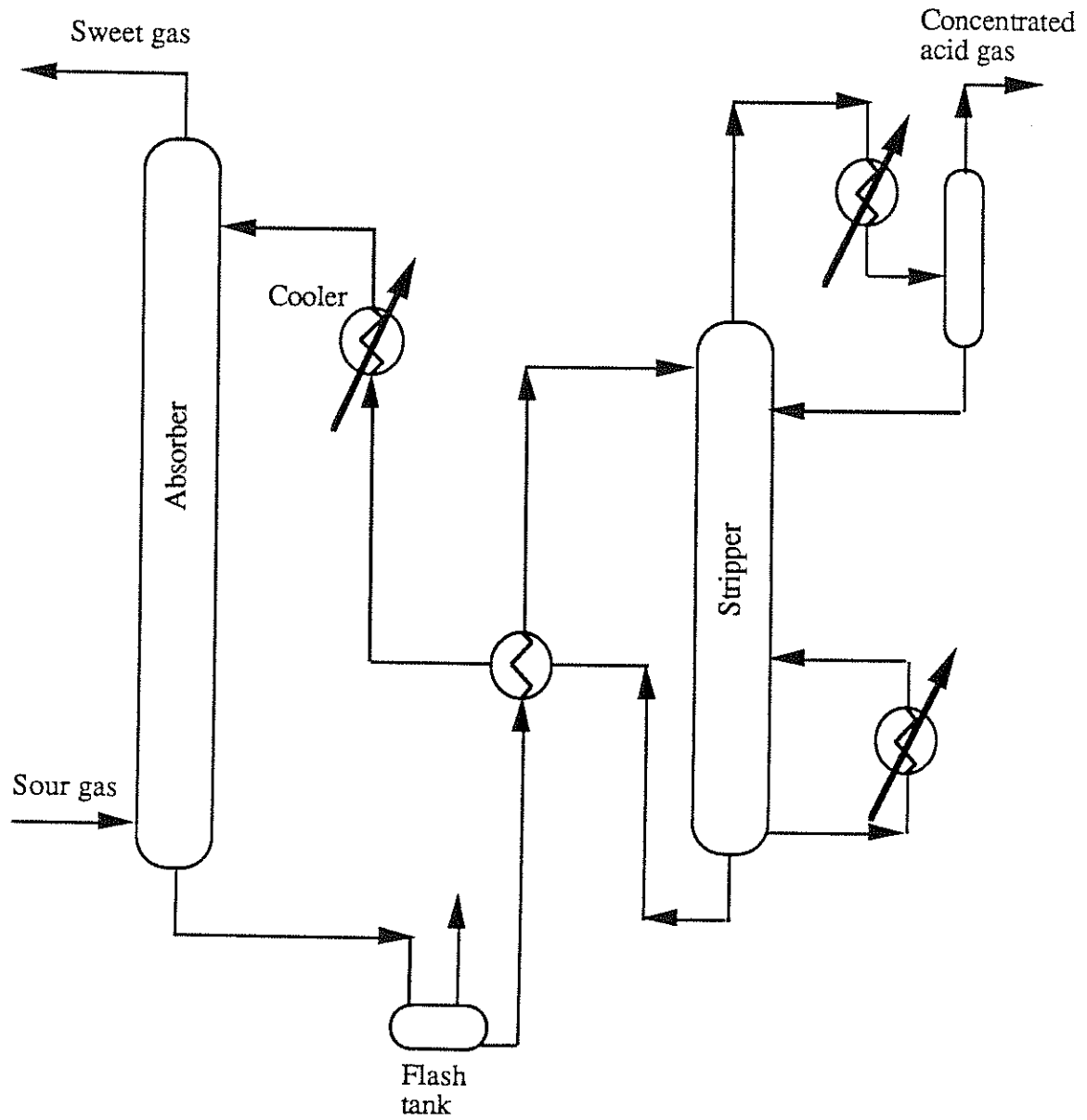


Figure 1.1 Typical Absorber/Scrubber System for Acid Gas Removal

of this system (Blauwhoff et al., 1985). It is desirable, therefore, to find solvents and/or operating modes which reduce this reboiler heat duty.

Alkanolamines are ideally suited for the removal of acid gases. The basicity is provided by the amine function, and this provides reactivity to remove the acid gases. The hydroxyl groups serve to increase the solubility of the amine in water. This effect reduces the vapor pressure of the amines so that less is lost out the top of the absorber or stripper. Since  $\text{CO}_2$  reacts with amines at a finite rate and  $\text{H}_2\text{S}$  reacts instantaneously, the selectivity of the solution towards  $\text{CO}_2$  can be controlled by changing the type of amine, or, in a mixed amine system, the ratio of various amines in solution.

### **1.3 Effect of Chemical Reaction on Gas Absorption**

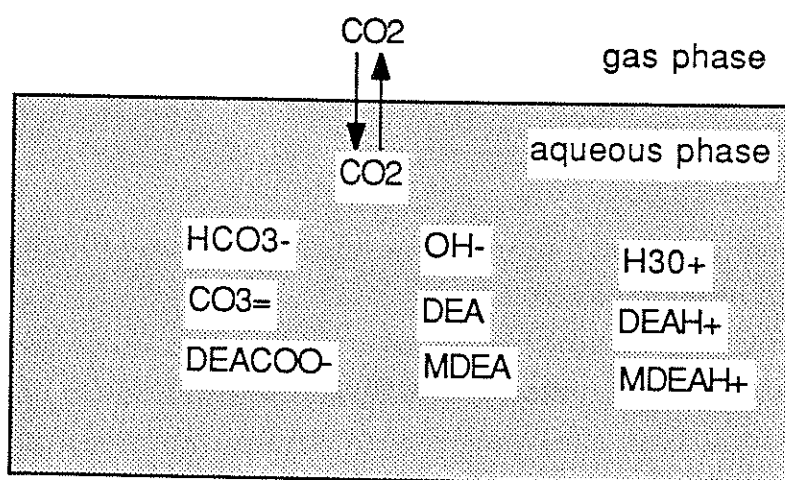
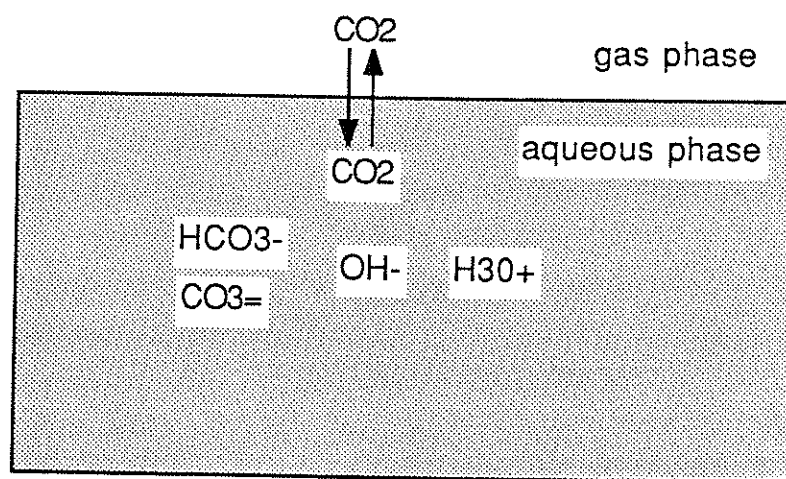
The effect of chemical reaction on gas absorption can be separated into two categories: equilibrium effects and nonequilibrium effects. We will review each of these effects separately.

#### ***1.3.1 Equilibrium Considerations***

Let us write the expression for the mass transfer rate in terms of the overall gas-phase mass transfer coefficient:

$$R = \frac{P - P^*}{\frac{1}{k_g} + \frac{H}{E k_l}} = K_g (P - P^*) \quad [1.1]$$

For the moment, let us neglect the mass transfer coefficient in this formulation and concentrate on the driving force  $P - P^*$ .  $P^*$  is the equilibrium partial pressure corresponding to the concentration of acid gas in solution. For a given concentration of acid gas, we obtain the equilibrium partial pressure from the solution of an equilibrium model. The effect of chemical reaction is to lower this equilibrium partial pressure for a particular concentration of acid gas in solution. We take, for example, the  $\text{CO}_2$ -DEA-MDEA system and compare it to  $\text{CO}_2$  in water. The  $\text{CO}_2$ -water case is represented by case (a) in Figure 1.2 (Astarita et al., 1983), whereby the molecular  $\text{CO}_2$  in the liquid



---

Figure 1.2      Equilibrium of  $\text{CO}_2$  with a (a) Physical System (b) Chemical System

---

phase is in equilibrium with the vapor-phase and other ionic species in the liquid phase. In this case of  $\text{CO}_2$  in water, the ionic equilibria may be neglected under most conditions (this assumption also applies to  $\text{H}_2\text{S}$ , but not to  $\text{SO}_2$ , see cited reference). For the  $\text{CO}_2$ -DEA-MDEA system, the behavior is that of case (b). In this case, the concentration of  $\text{CO}_2$  in chemically combined forms is significant, and in fact dominates at all but extremely high loadings, well beyond the validity of the equilibrium models developed here. We see the ramifications of this behavior on the equilibrium partial pressure of  $\text{CO}_2$  as a function of the  $\text{CO}_2$  concentration in the liquid phase shown in Figure 1.3 calculated by the equilibrium model developed in this work. Compare this to the equilibrium partial pressure of  $\text{CO}_2$  in pure water calculated by the Henry's constant. We see that the reactions between  $\text{CO}_2$  and basic species greatly decrease this equilibrium partial pressure, and would therefore increase the driving force for the absorption rate of the acid gases relative to the nonacidic gases such as methane, which do not react with the amines.

### ***1.3.2 Nonequilibrium Considerations***

We saw in the last section that chemical reaction can have a profound influence on the solubility of reactive gases in solution. This will in turn affect the absorption rate by increasing the driving force for absorption. However, the primary objective of this work is to understand the nonequilibrium, or rate, phenomena associated with alkanolamine-based acid gas treating processes. This type of information is necessary for the rate-based approach to acid gas treating (Astarita et al., 1983; Seader, 1989). Consider the transport equation for the flux shown in equation [1.1]. This expression is equivalent to the standard expression for physical absorption except for the presence of the parameter  $E$ , the enhancement factor, which is defined as the rate of absorption with reaction to that without reaction. For a given concentration of acid gas species in solution, the equilibrium model will provide the equilibrium partial pressure,  $P^*$ . However, it is the rate model which must provide the enhancement factor. Under certain conditions, the enhancement factor may be approximated by the following expression (Danckwerts, 1970):

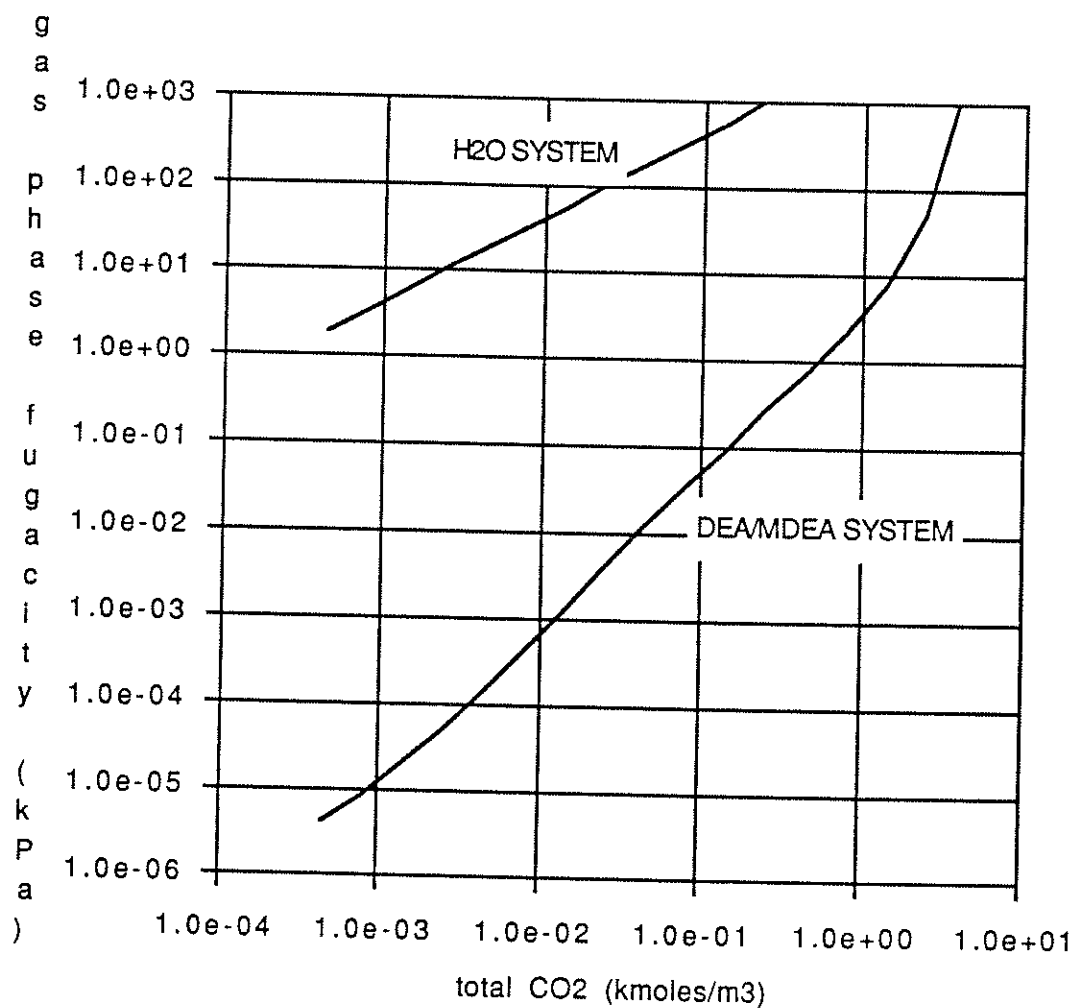


Figure 1.3 Comparison of CO<sub>2</sub> Fugacity for a Physical System (water at 313K) and a Chemical System (10%DEA,40%MDEA at 313K)

$$E = \sqrt{\frac{k_2 B^0 D_A}{k_1 a^2} + 1} \quad [1.2]$$

However, this equation is valid only for a simple reaction scheme under very specific conditions, namely, no depletion of reactants or accumulation of products at the gas-liquid interface. Under many conditions encountered experimentally, these simplifying assumptions do not hold. The reason why chemical reaction increases the absorption rate beyond that of physical absorption is that the gas is consumed at the gas-liquid interface. Typical profiles are shown for the DEA/MDEA system in Figure 1.4. The reaction causes an increase in the concentration gradient of the absorbing gas at the gas-liquid interface, and hence an enhancement of the gas absorption rate. Notice also that there are significant concentration gradients of the reactants and products at the interface. At the condition shown in Figure 1.4, the enhancement factor is 7.2, compared to 9.2 which would have been predicted by equation [1.2]. This error is not uncommon, and could be much more severe at higher partial pressures or lower mass transfer coefficients. This type of phenomenon, the origin of equation [1.2] and its limitations will be the subject of much of this work.

#### 1.4 Overview of This Work

In this dissertation, we will concentrate in the absorption/desorption of carbon dioxide with aqueous-based alkanolamine solutions - MDEA (methyldiethanolamine), DEA (diethanolamine), MEA (monoethanolamine), and mixtures of DEA/MDEA and MEA/MDEA. Currently, DEA is the most commonly used alkanolamine while MDEA and MDEA-based solvents are increasing in popularity (Moore, 1989).

Critchfield and Rochelle (1987, 1988) studied the kinetics of these systems by means of a stirred cell absorber. Data were taken for a range of CO<sub>2</sub> partial pressures and loadings, covering both absorption and desorption conditions. It was found that the CO<sub>2</sub> desorption from DEA and MDEA solutions was greater than expected from absorption measurements. This effect was especially pronounced in the MDEA system, and attributed to primary and secondary amine contaminants which would enhance the reaction rate. This explanation was also used by Versteeg (1986) to



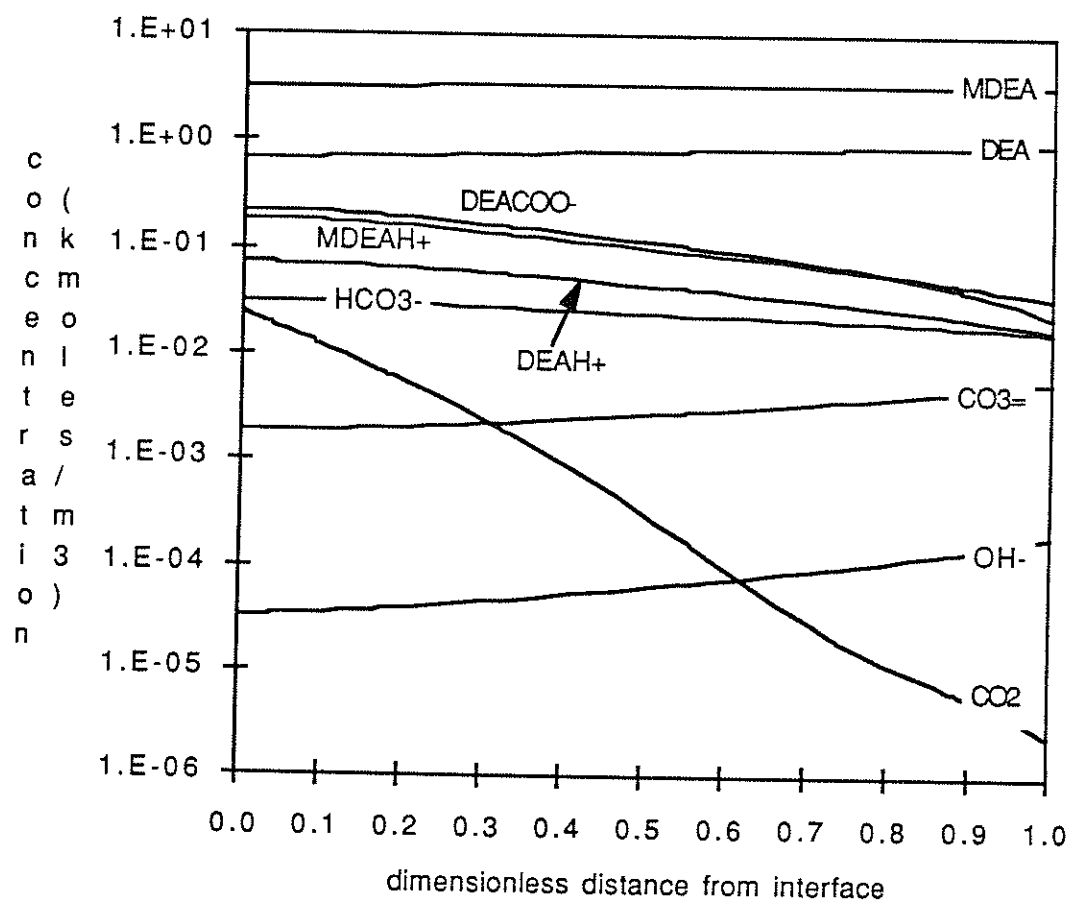


Figure 1.4 Concentration Profiles Under High-Driving Force Absorption  
 Conditions. 10wt% DEA, 40wt% MDEA, loading = 0.01, 313K,  $k_1^0 = 10^{-4}$  m/sec,  $P = 118$  kPa.

explain the discrepancy in the literature data and the apparent effect of  $\text{CO}_2$  partial pressure on the effective  $\text{CO}_2$ -MDEA reaction rate.

The previous work of Critchfield and Rochelle has been extended in several ways: More data have been taken to supplement those data taken previously. We have obtained absorption data at both low and high  $\text{CO}_2$  partial pressures for the MDEA- $\text{CO}_2$  system with the specific intent of observing the driving force phenomenon. In addition, we have taken data at higher temperatures for the mixed amine system DEA/MDEA to aid in prediction of amine system performance under conditions actually used in industry. Finally, we have taken a "rigorous" approach in the modelling of mass transfer rates and equilibrium phenomena.

There are several approaches available to estimate the effect of chemical reaction on gas absorption rates:

- (1) Fundamental modelling based upon the differential equations for mass transfer with reaction. Even this approach relies on an approximation to the liquid-phase hydrodynamic characteristics.
- (2) A hybrid approach which attempts to take into account the interaction of mass transfer effects and reaction kinetics (e.g. DeCoursey, 1982 and Onda et al., 1970a, 1970b). These approaches comprise the solution of algebraic, not differential, equations and are usually iterative in nature.
- (3) A pseudo first-order approximation which neglects the mass transfer effects of the liquid-phase reactants (Danckwerts, 1970).

The first approach is not practical except for research purposes and requires much computational power. The second approach is the best for the practical simulation of gas-liquid contactors, however, the need exists for a fundamental model with which to check the approximations (an example of this approach is the use of DeCoursey's approximation in absorber simulation by Hermes and Rochelle (1987)). The simplified approximation for  $\text{CO}_2$  is valid only at low acid gas partial pressures and high mass transfer coefficients. Since we are conducting detailed kinetic analysis using absorption data, we opt for the first approach in order to remove mass transfer effects on kinetic data interpretation. We are able to regress experimental data with the mass transfer model only by the availability of a supercomputer (CRAY X-MP/24).

Several hydrodynamic theories are available to use for the experimental data interpretation. The oldest and simplest of the theories is the classic film theory (Lewis

and Whitman, 1924). It will be shown that a simplified eddy diffusivity model can also be used for the rate simulation, and the results should be more accurate than for film theory, but with similar computation time.

This work also emphasizes the interpretation of experimental data and the simulation of CO<sub>2</sub> absorption into and desorption from aqueous-based alkanolamine solutions - MDEA, DEA, and MEA. These systems have been studied before, however most cases were limited to pseudo first-order conditions and/or negligible reverse reaction rates. The latter limitation was removed by Critchfield (Critchfield and Rochelle, 1988) who studied both absorption and desorption, but this work was still limited to pseudo first-order conditions for the data interpretation. Versteeg (1986) has developed a rigorous mass transfer model based on penetration and film theories, but the secondary amine data interpretation is for pseudo first-order conditions only, and at low loadings, so this does not provide a check on the mass transfer model at these conditions. Bosch (1989) has extended the work of Versteeg to include both desorption and absorption data, however, he has noted difficulties in predicting the desorption rates as well. He indicates the importance of a good equilibrium model in simulating the desorption process. In this dissertation, we will analyze the experimental data using a comprehensive mass transfer model based on the simplified eddy diffusivity theory. We will show that the combined mass transfer and equilibrium model can simulate the CO<sub>2</sub>-amine data under a wide range of conditions, covering both absorption and desorption.

The solutions of aqueous amines loaded with CO<sub>2</sub> are characterized by high ionic strength, causing the activity coefficients to vary greatly over the range of conditions encountered. In order to provide a realistic simulation of the data, we decided it was necessary to use a "rigorous" activity coefficient model, namely the Electrolyte-NRTL model (Chen and Evans, 1986) for the activity coefficients of the liquid-phase species. The parameters used in the model are based largely on the work done by Austgen et al. (1990), with some minor differences to be detailed later. This approach is in contrast with the neglect of activity coefficients in the model of Kent and Eisenberg (1976), and a less rigorous activity coefficient approach of Chakravarty (1985), as used by Bosch (1989) (In all fairness, the less rigorous approach of Chakravarty has advantages compared to the Electrolyte-NRTL model with respect to computation time).

The approach taken in this work has been rigorous, however, as indicated in section 1.3.2, the data are necessary for practical rate-based simulation of absorption/stripping systems. In order to bridge the gap between academic research and application, we examine the validity of simplifying approximations for the prediction of enhancement factors under industrial conditions, since it is impractical to use a differential equation-based model within a rate-based simulator due to the computation time involved.

In summary, several mass transfer models will be compared for the effect of chemical reaction on gas absorption rates. It will be demonstrated that a steady-state theory, the simplified eddy diffusivity theory, can be used rather than surface renewal theory, an unsteady-state theory. The resulting reduction in computation time is especially advantageous for such time intensive tasks as kinetic parameter estimation. The Electrolyte-NRTL model is used to estimate the activity coefficients of species in the liquid phase. Parameters for this model have been regressed from literature data on the systems CO<sub>2</sub> with aqueous MDEA (methyldiethanolamine), DEA (diethanolamine), MEA (monoethanolamine) and the mixtures DEA/MDEA and MEA/MDEA. Kinetic parameters have been estimated from literature and currently obtained experimental data for MDEA, DEA and the mixture DEA/MDEA. The issues of reaction kinetics in nonideal systems and alternative mechanisms for the reaction of CO<sub>2</sub> with alkanolamines will be discussed in light of the experimental data.

The comparison of mass transfer theories has been summarized by Glasscock and Rochelle (1989) and the regression of rate parameters for amine systems using the mass transfer model has been presented by Glasscock and Rochelle (1990).

## Chapter Two

### Chemistry of CO<sub>2</sub>-Alkanolamine Systems

The fundamental mechanism for the reaction of CO<sub>2</sub> with alkanolamines is still not fully understood; however, much progress has been made in accumulating rate data and developing kinetic expressions which can represent the experimental data reasonably well. Within the context of alkanolamines, the most distinguishing characteristic separating the reactants is the number of carbon-containing groups attached to the nitrogen atom. The amine is referred to as a primary, secondary or tertiary amine if one, two or three carbon-containing groups are attached to the nitrogen atom, respectively. Figure 2.1 shows the molecular structure of amines one often finds discussed in the literature. The primary amines MEA and DGA are noted for their fast reaction rates with CO<sub>2</sub>. The secondary amines DEA and DIPA have intermediate reaction rates, and finally TEA and MDEA, being tertiary amines, have much slower reaction rates with CO<sub>2</sub>. Historically, TEA was the first alkanolamine used in the gas processing industry (Kohl and Reisenfeld, 1985). It has, however, been largely replaced by the primary and secondary amines for bulk CO<sub>2</sub> removal, and MDEA for selective H<sub>2</sub>S removal (mixed amine systems can also be used for bulk CO<sub>2</sub> removal, as will be discussed later). While TEA has properties similar to MDEA, it has a larger molecular weight, hence, a larger weight fraction of TEA is required to accomplish the same task as MDEA. It must also be mentioned that the traditional aqueous alkanolamine systems must now compete with combined physical solvent/amine systems and the so-called hindered amines for many applications. A hindered amine, an example of which is AMP shown in Figure 2.1, is defined as "a primary amine in which the amino group is attached to a tertiary carbon atom, or a secondary amine in which the amino group is attached to a secondary or a tertiary carbon atom" (Sartori and Savage, 1983).

The purpose of this chapter is to review the existing literature on reaction rates of CO<sub>2</sub> with amines and discuss the possible mechanisms from which kinetic expressions can be derived. The development of a kinetic mechanism is, of course, a prerequisite to the mass transfer/reaction modelling of CO<sub>2</sub> with amine systems.

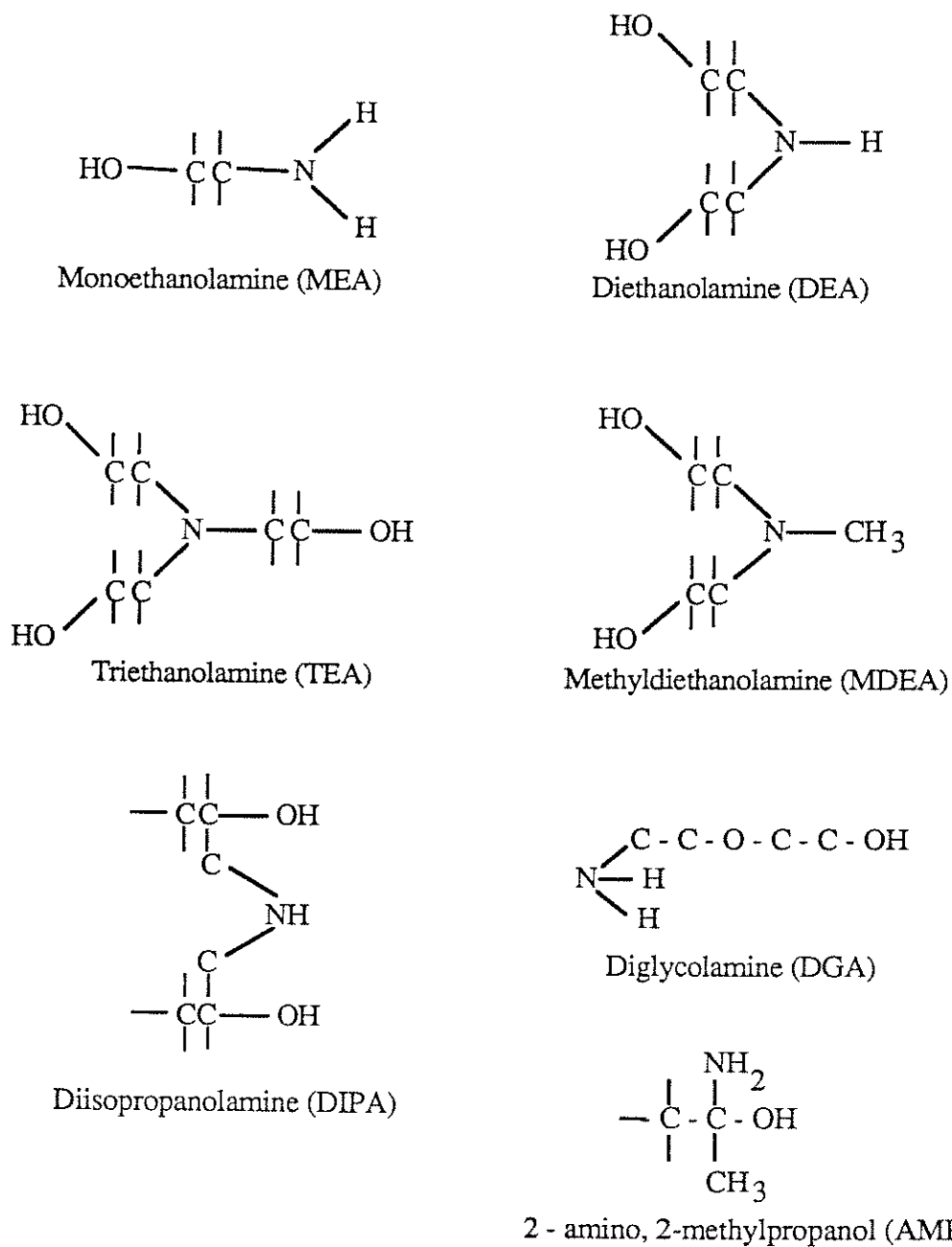


Figure 2.1 Molecular Structure of Typical Amines Used in Acid Gas Treating Processes

---

## 2.1 Reactions of CO<sub>2</sub> in Aqueous Solutions

In aqueous solution CO<sub>2</sub> reacts with hydroxide and water to form bicarbonate and carbonic acid, respectively:



The second-order rate constant for the reaction of CO<sub>2</sub> with hydroxide has been correlated by Sherwood et al. (1975) and corrected for ionic strength by Astarita et al. (1983):

$$\log_{10} k_{\text{OH}^-} = 13.635 - \frac{2895.}{T} + 0.08 I_c \quad [2.3]$$

where  $k$  is in units of m<sup>3</sup>/kmole/s, and  $I_c$  is the concentration-based ionic strength:

$$I_c = \frac{1}{2} \sum_{i=1}^N C_i z_i^2 \quad [2.4]$$

The first-order rate constant for the water reaction is also correlated by Sherwood et al.:

$$\log_{10} k_{\text{H}_2\text{O}} = 329.80 - 110.541 \cdot \log_{10} T - \frac{17265.4}{T} \quad [2.5]$$

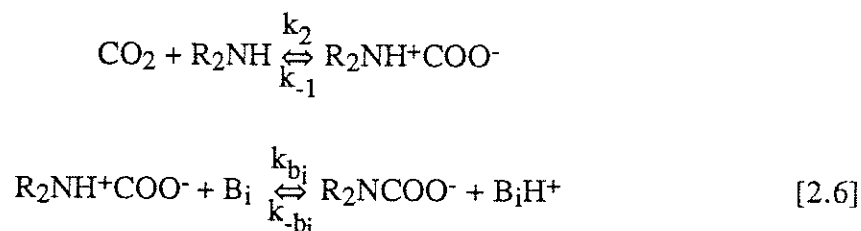
This reaction is usually negligible compared to the hydroxide reaction for alkaline solutions. However, it has been shown conclusively to be catalyzed by "anions of weak acids or by molecules having a high affinity for protons" (Sherwood et al., 1975).

## 2.2 CO<sub>2</sub> Reactions with Primary and Secondary Alkanolamines

### *2.2.1 Mechanisms*

Before covering the specific amine systems, it would be advantageous to discuss the mechanism for the reaction of CO<sub>2</sub> with alkanolamines in general. There has been much disagreement as to the mechanism and the order of reaction. In 1968, Caplow presented a hypothesized mechanism for the carbamate formation involving the formation of an intermediate zwitterion (a locally ionic, net neutral, molecule). Danckwerts (1979) introduced this mechanism into the chemical engineering literature, and Blauwhoff et al. (1984) showed that this mechanism reconciled much of the data in the literature, especially for DEA. In 1987, Critchfield and Rochelle introduced reversibility into this mechanism, which must necessarily be included for one to describe both absorption and desorption conditions. Presented below is a derivation of the mechanism, leading to a rate law describing the rate of reaction of CO<sub>2</sub> with primary or secondary amines.

Consider the two-step zwitterion mechanism:



The B<sub>i</sub> term designates any species in solution that can act as a base to abstract the proton from the zwitterion in the second reaction step. The first step in describing the rate for this reaction is to assume a pseudo-steady state concentration for the zwitterion (this is consistent with the evidence that the zwitterion intermediate has a very short lifetime (Johnson and Morrison, 1972)):



$$\begin{aligned} \frac{\partial[Z]}{\partial t} &= k_2(\text{CO}_2)(\text{R}_2\text{NH}) + \sum k_{-b_i}(\text{R}_2\text{NCOO}^-)(\text{B}_i\text{H}^+) - k_{-1}(\text{Z}) - \sum k_{b_i}(\text{Z})(\text{B}_i) \\ &= 0 \end{aligned} \quad [2.7]$$

The summation is over all of the bases in solution. The parenthesis designates activities, as opposed to concentration, since we will be basing the reaction rates on activities (see Chapter 4). We can solve for the zwitterion activity:

$$(\text{Z}) = \frac{k_2(\text{CO}_2)(\text{R}_2\text{NH}) + \sum k_{-b_i}(\text{R}_2\text{NCOO}^-)(\text{B}_i\text{H}^+)}{k_{-1} + \sum k_{b_i}(\text{B}_i)} \quad [2.8]$$

The rate of reaction of  $\text{CO}_2$  via the zwitterion mechanism is given by equation [2.9]:

$$\begin{aligned} r_{\text{CO}_2, \text{zwit}} &= k_2(\text{CO}_2)(\text{R}_2\text{NH}) - k_{-1}(\text{Z}) \\ &= \frac{(\text{CO}_2)(\text{R}_2\text{NH}) - \frac{k_{-1}(\text{R}_2\text{NCOO}^-) \sum k_{-b_i}(\text{BH}^+)}{\sum k_{b_i}(\text{B})}}{\frac{1}{k_2} + \frac{k_{-1}}{k_2 \sum k_{b_i}(\text{B})}} \end{aligned} \quad [2.9]$$

It is also possible to write equation [2.9] in terms of the equilibrium concentration of  $\text{CO}_2$ ,  $(\text{CO}_2)_e$ , as opposed to using the reverse rate constants (Critchfield, 1988):

$$r_{\text{CO}_2, \text{zwit}} = \frac{(\text{R}_2\text{NH}) \{(\text{CO}_2) - (\text{CO}_2)_e\}}{\frac{1}{k_2} + \frac{k_{-1}}{k_2 \sum k_{b_i}(\text{B})}} \quad [2.10]$$

We can also write a rate expression for the consumption of each base in the zwitterion mechanism:

$$r_{\text{B}, \text{zwit}} = k_{b_i}(\text{Z})(\text{B}) - k_{-b_i}(\text{R}_2\text{NCOO}^-)(\text{BH}^+) \quad [2.11]$$

It is necessary to point out that the individual rate constants,  $k_{bi}$ , cannot be obtained from data regression using equation [2.9], but only the groups  $\frac{k_2 k_{bi}}{k_{-1}}$ . However, we can rewrite the rate expression in terms of the combined constants:

$$r_{B, \text{zwit}} = \frac{k_2 k_{bi}}{k_{-1}} \frac{k_{-1}}{k_2} (Z)(B_i) - k_{-b} (R_2 \text{NCOO}^-)(B_i \text{H}^+) \quad [2.12]$$

We can multiply equation [2.8] for the zwitterion activity by  $\frac{k_{-1}}{k_2}$ :

$$\frac{k_{-1}}{k_2} (Z) = \frac{(\text{CO}_2)(R_2 \text{NH}) + \frac{1}{k_2} \sum k_{-bi} (R_2 \text{NCOO}^-)(B_i \text{H}^+)}{1 + \frac{1}{k_2} \sum \frac{k_2 k_{bi}}{k_{-1}} (B_i)} \quad [2.13]$$

Therefore, we can substitute this equation into the equation for the reaction of each individual base [2.12].

The next problem is to determine the rate constants, or groups of rate expressions,  $\frac{k_2 k_{bi}}{k_{-1}}$ ,  $k_2$ , and  $k_{-bi}$ . The first two rate constants can be determined from absorption data, and we can obtain the reverse rate constant by assuming detailed balancing for each of the reversible reactions for the proton extraction:

$$\frac{k_{bi}}{k_{-bi}} = \frac{(R_2 \text{NCOO}^-)(B_i \text{H}^+)}{(Z)(B_i)} \quad [2.14]$$

and

$$\frac{k_2}{k_{-1}} = \frac{(Z)}{(\text{CO}_2)(R_2 \text{NH})} \quad [2.15]$$

Therefore,

$$\frac{k_{b_i}k_2}{k_{-b_i}k_{-1}} = \frac{(R_2NCOO^-)(B_iH^+)}{(CO_2)(R_2NH)(B_i)} \quad [2.16]$$

Therefore, from the equilibrium speciation, and knowledge of the combined rate constants, we can determine the reverse rate constant. For the amine systems, the bases considered are  $OH^-$ ,  $H_2O$ , and the amine itself. The corresponding protonated bases are  $H_2O$ ,  $H_3O^+$ , and the protonated amine, respectively.

The utility of the zwitterion mechanism lies in its ability to explain the apparently varied reaction orders of amines (DEA in particular) with respect to the amine. Let us consider only the irreversible part of the rate expression:

$$r = \frac{(CO_2)(R_2NH)}{\frac{1}{k_2} + \frac{k_{-1}}{k_2 \sum k_{b_i}(B_i)}} \quad [2.17]$$

The apparent reaction order with respect to the amine is given by equation [2.18] (neglecting activity effects):

$$n = \frac{\partial \log_e r}{\partial \log_e (R_2NH)} \quad [2.18]$$

Taking the logarithm of the reaction rate:

$$\log_e r = \log_e \{k_2(CO_2)\} + \log_e (R_2NH) - \log_e \left\{ 1 + \frac{k_{-1}}{\sum k_{b_i}(B_i)} \right\} \quad [2.19]$$

Differentiating and solving for n, we obtain:

$$n = 1 + \frac{k_{-1} k_{b \text{ amine}} (R_2NH)}{\left\{ 1 + \frac{k_{-1}}{\sum k_{b_i}(B_i)} \right\} \left\{ \sum k_{b_i}(B_i) \right\}^2} \quad [2.20]$$

An equivalent, but more useful expression is obtained by multiplying the fractional term by  $k_2^2/k_{-1}^2$ :

$$n = 1 + \frac{\frac{k_2 k_{b\text{amine}}}{k_{-1}} (R_2NH)}{\left\{ \frac{1}{k_2} + \frac{k_{-1}}{\sum k_2 k_{b_i}(B_i)} \right\} \left\{ \sum \frac{k_2 k_{b_i}}{k_{-1}} (B_i) \right\}^2} \quad [2.21]$$

In the limit that  $k_2$  becomes very fast, the zwitterion expression reduces to:

$$r = (CO_2)(R_2NH) \left\{ \sum k_{b_i}(B_i) \right\} \quad [2.22]$$

So now the apparent order of reaction with respect to the amine is:

$$n = 1 + \frac{\frac{k_2 k_{b\text{amine}}}{k_{-1}} (R_2NH)}{\left\{ \sum \frac{k_2 k_{b_i}}{k_{-1}} (B_i) \right\}} \quad [2.23]$$

In this work, it was found that the simplified rate expression [2.22] fit the data within experimental uncertainty, and it is used exclusively throughout this work.

### 2.2.2 Literature Data on Primary Amines (MEA and DGA)

The primary amine MEA has been studied extensively in the literature (Astarita, 1961; Barth et al., 1986; Blauwhoff et al., 1984; Danckwerts, 1979; Donaldson and Nguyen, 1980; Hikita et al., 1977; Laddha and Danckwerts, 1981; Leder, 1971; Sada et al., 1976). The data for  $CO_2$  with MEA are in very good agreement, and all authors have found a first-order dependence for the reaction rate of  $CO_2$  with MEA, leading to the rate equation:

$$r_{CO_2} = k_2 (CO_2)(MEA) \quad [2.24]$$

Blauwhoff et al. (1984) studied all of the data available in the literature and concluded that the rate expression of Hikita et al. (1977) fits the data extremely well over the range of 5 - 80°C:

$$\log_{10} k_2 = 10.99 - \frac{2152}{T} \quad [2.25]$$

$k_2$  is in units of  $\text{m}^3/\text{kmole}\cdot\text{s}$ . Barth et al. (1986) studied the reaction rate at a later date, and found that the results compared very well with the previous literature data.

Barth et al. (1986) studied the reaction rate of  $\text{CO}_2$  with DGA at temperatures of 20 and 25°C. Interestingly enough, they found the rates to be indistinguishably similar to MEA.

### 2.2.3 Literature Data on Secondary Amines (DEA)

Diethanolamine is a commonly used solvent in the acid gas treating industry because it has a relatively high reactivity towards  $\text{CO}_2$ , like MEA, however it is much less corrosive and has a lower exothermic heat of reaction. Because of its prevalence, the literature data covering DEA is extensive (Jorgensen, 1956; Barth et al., 1983; Barth et al., 1984; Blanc and Demarais, 1984; Blauwhoff et al., 1984; Critchfield, 1988; Donaldson and Nguyen, 1980; Hikita et al., 1977; Laddha and Danckwerts, 1981; Nunge and Gill, 1963; Rangwala et al., 1989; Sada et al., 1976; Versteeg and Oyevaar, 1989; Versteeg and van Swaaij, 1988b). However, there is general disagreement as to the order of reaction with respect to DEA. The reason for the discrepancy is most likely due to an assumed simplified mechanism for the  $\text{CO}_2$ -DEA reaction. As seen from section 2.2.1, the most probable mechanism would indicate a shift in reaction order with respect to DEA depending on the experimental conditions. Blauwhoff et al. (1984) found that the zwitterion mechanism resolved much of the discrepancy in the literature data. In both the work of Blauwhoff et al. (1984) and Versteeg and van Swaaij (1988b), a rate expression of the form [2.17] was assumed, however it was found that the value  $k_2$  was so high that the expression essentially simplified to that of [2.22], which was used in this work. Laddha and Danckwerts

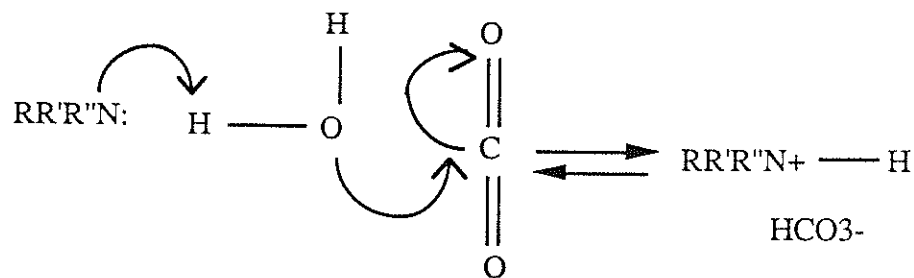
(1981) and Critchfield (1988) used expression [2.17], however, DEA was the only base considered.

## 2.3 CO<sub>2</sub> Reactions with Tertiary Alkanolamines

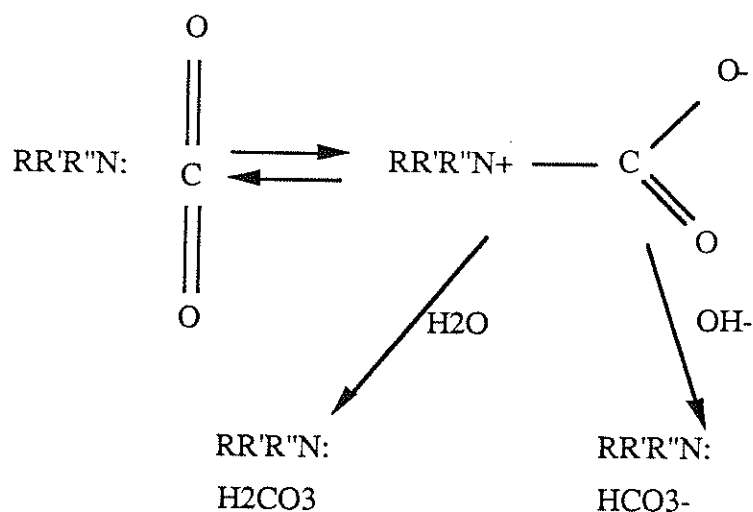
### *2.3.1 Mechanisms*

Some of the early research into tertiary amines was concerned with whether or not the enhanced CO<sub>2</sub> absorption rate could be explained by the hydroxide reaction (Barth et al., 1981; Jorgensen and Faurholt, 1954; Jorgensen, 1956). It has been demonstrated by numerous authors that this reaction alone does not account for the enhanced absorption rates. It has been proposed, however, that the amine serves to catalyze the CO<sub>2</sub> hydrolysis reaction rate. This is not the only possibility, however. Despite the fact that their conclusions concerning MDEA reaction rate data are erroneous, Barth et al. (1981) provide an enlightening discussion of the possible mechanisms for the reaction of CO<sub>2</sub> with alkanolamines, and the following mechanistic discussion follows their work.

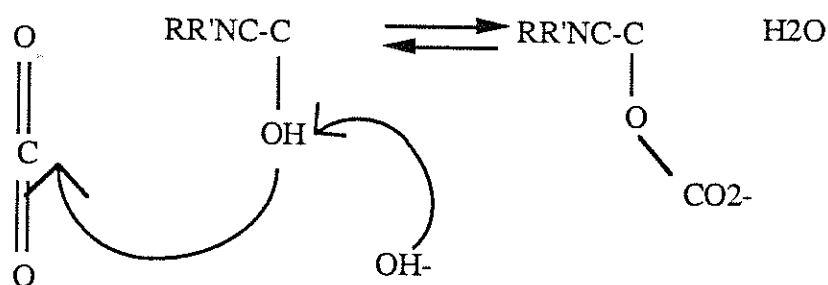
The most common theory is that the amine enhances the reaction rate of CO<sub>2</sub> by a homogeneous catalytic effect:



However, two other possibilities exist which should not be ignored. The first is the possibility of forming an intermediary such as in the zwitterion mechanism.



The other possibility is the formation of alkylcarbonates, which is generally considered unlikely except in solutions of very high pH (Blauwhoff et al., 1984):



### 2.3.2 Literature Data on Tertiary Amines (TEA and MDEA)

Triethanolamine (TEA) was the first ethanolamine used commercially for acid gas treating (Kohl and Riesenfeld, 1985). It has been largely displaced by other amines which are either more reactive towards  $\text{CO}_2$  (MEA and DEA) or have a lower molecular weight (MDEA). The reason why MDEA is generally considered superior is that more moles of amine are available for a given volume of solution, since it has a lower molecular weight (the specific gravity of the unloaded aqueous alkanolamine solutions is generally between 1 and 1.1, however, the specific gravity of loaded solutions can be

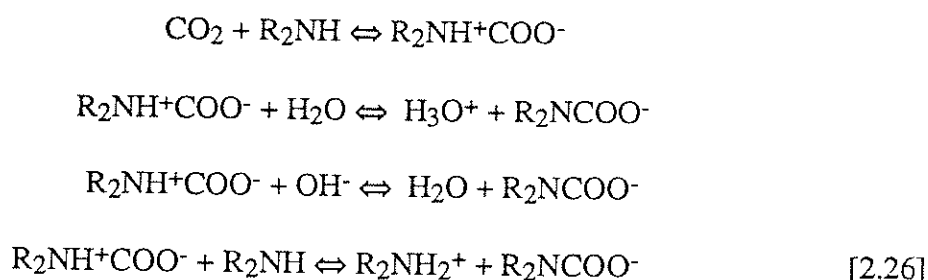
much greater). TEA does have limited industrial significance, and is of scientific interest since it has a  $pK_a$  which is lower than that of MDEA (7.76 vs. 8.52). This allows for a comparison of the rates of TEA and MDEA based on the Bronsted correlation (Weston and Schwarz, 1972). Data on the reaction rates of TEA with  $CO_2$  are abundant (Jorgensen and Faurholt, 1954; Jorgensen, 1956; Barth et al., 1981; Blauwhoff et al., 1984; Donaldson and Nguyen, 1980; Hikita et al., 1977; Sada et al., 1976; Versteeg and van Swaaij, 1988c). There is some dispute as to the actual rate constant and mechanism of TEA.

Methyldiethanolamine (MDEA) is currently being studied with fervor due to its industrial significance (Barth et al., 1981; Critchfield, 1988; Haimour et al., 1987; Haimour and Sandall, 1984; Hikita et al., 1977; Tomcej et al., 1986; Tomcej and Otto, 1989; Versteeg and van Swaaij, 1988c; Yu et al., 1985). Its widespread use is due to the fact that it has a relatively low heat of reaction with  $CO_2$ , as compared with DEA and MEA, and it can be used for selective  $H_2S$  removal since its reaction rate with  $CO_2$  is relatively slow. As with TEA, there is much discrepancy in the literature for the reaction rate of  $CO_2$  with MDEA, most likely due to the fact that the reaction mechanism is more complex than that which most authors assume. This discrepancy will, in fact, be a major topic of discussion in Chapter 9, and is best shown in Figure 2.2 where the data of various authors are presented.

## 2.4 Rate Equations for $CO_2$ Reactions in Mixed Amine Systems

We conclude this chapter by summarizing the complete set of reaction equations which must be solved in the mass transfer model. For the absorption of  $CO_2$  into mixed amines, the entire reaction scheme considered is shown below.

Secondary amine zwitterion mechanism:





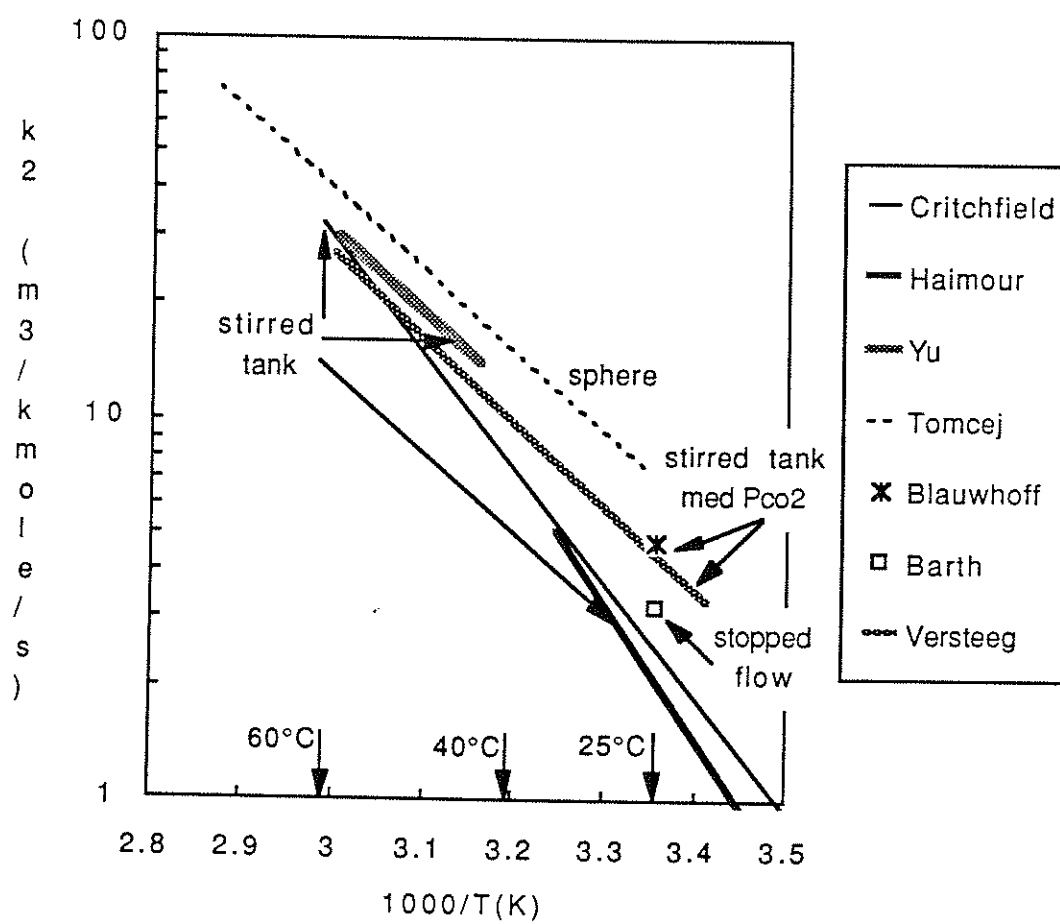
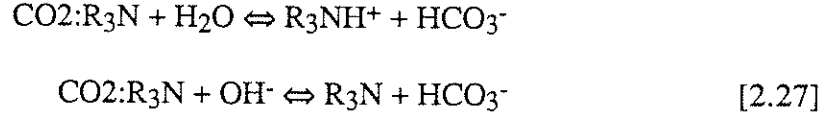


Figure 2.2 Second-Order Rate Constant for the  $\text{CO}_2$ -MDEA Reaction (adapted from Critchfield, 1988)

Tertiary amine mechanism:



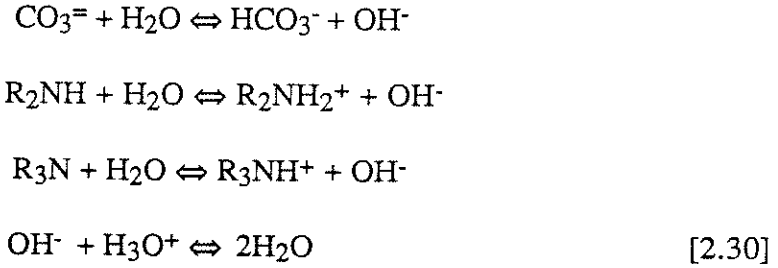
Interaction between primary (or secondary) amine and tertiary amine:



Hydroxide reaction:



Instantaneous buffer equilibria:



We neglect water as a chemical species (assuming its concentration is constant throughout the boundary layer), so we write reaction equations for 10 species -  $\text{CO}_2$ ,  $\text{HCO}_3^-$ ,  $\text{CO}_3^{2-}$ ,  $\text{R}_2\text{NH}$ ,  $\text{R}_2\text{NH}_2^+$ ,  $\text{R}_2\text{NCOO}^-$ ,  $\text{R}_3\text{N}$ ,  $\text{R}_3\text{NH}^+$ ,  $\text{OH}^-$ ,  $\text{H}_3\text{O}^+$ .

For  $\text{CO}_2$ , we have the following reaction rates due to the primary (secondary) amine, the tertiary amine, and hydroxide itself.

$$-\mathcal{R}_{\text{CO}_2} = \frac{(\text{CO}_2)(\text{R}_2\text{NH}) - \frac{k_{-1(1)}}{k_{2(1)}}(\text{R}_2\text{NCOO}^-) \frac{\sum k_{b_i(1)}(\text{B}_{i(1)}\text{H}^+)}{\sum k_{b_i(1)}(\text{B}_{i(1)})}}{\frac{1}{k_{2(1)}} + \frac{k_{-1(1)}}{k_{2(1)} \sum k_{b_i(1)}(\text{B}_{i(1)})}}$$

$$\begin{aligned}
& + \frac{(\text{CO}_2)(\text{R}_3\text{N}) - \frac{k_{-1(2)}}{k_{2(2)}}(\text{HCO}_3^-) \frac{\sum k_{-b(2)}(\text{B}_{i(2)}\text{H}^+)}{\sum k_{b_i(2)}(\text{B}_{i(2)})}}{\frac{1}{k_{2(2)}} + \frac{k_{-1(2)}}{k_{2(2)} \sum k_{-b_i(2)}(\text{B}_{i(2)})}} \\
& + k_{\text{OH}} \{ (\text{CO}_2)(\text{OH}^-) - \frac{1}{K_{\text{OH}}} (\text{HCO}_3^-) \} \\
& = r_{\text{CO}_2(1)} + r_{\text{CO}_2(2)} + r_{\text{CO}_2, \text{OH}} \quad [2.31]
\end{aligned}$$

The first, second, and third terms correspond to  $\text{CO}_2$  reaction through the carbamate mechanism, the tertiary amine mechanism, and the hydroxide mechanism, respectively.\* The bases considered in the carbamate mechanism are the amine itself,  $\text{R}_2\text{NH}$ , and water (hydroxide is neglected in this formulation). The bases considered in the tertiary mechanism are water and hydroxide. Hydroxide could also be important in the carbamate mechanism, however, the contribution of the amine has been shown to predominate. For the tertiary amine, we will assume a mechanism similar to the primary and secondary amines with an intermediate species  $I$  analogous to the zwitterion. This is an assumption of convenience and, if necessary, the resulting rate expression used for the tertiary amine reaction rate can default to the standard second-order reaction.

For carbamate, the rate of formation is equal to the rate of reaction of  $\text{CO}_2$  in the zwitterion mechanism:

$$R_{\text{R}_2\text{NCOO}^-} = r_{\text{CO}_2(1)} \quad [2.32]$$

For bicarbonate, the rate of formation is equal to the rate of reaction of  $\text{CO}_2$  in the tertiary amine mechanism plus the hydroxide mechanism minus the rate of carbonate formation:

---

\*  $R_i$  corresponds to the net rate of production of a species,  $i$ . Therefore,  $-R_i$  is the summation of all reaction rates in which component  $i$  is involved.

$$-R_{HCO_3} = -r_{CO_2(2)} - r_{CO_2,OH} + r_{HCO_3} \quad [2.33]$$

where,

$$r_{HCO_3} = k_{HCO_3} \left\{ (HCO_3^-)(OH^-) - \frac{1}{K_{CO_3}} (CO_3^{=})(H_2O) \right\} \quad [2.34]$$

For carbonate, we consider its "equilibrium" reaction to bicarbonate:

$$-R_{CO_3} = -r_{HCO_3} \quad [2.35]$$

with a very high rate constant (say  $10^9$ ) for this reaction.

For the tertiary amine and its protonated derivative, we may write the following two reactions:

$$-R_{R_3N} = r_{CO_2(2)} + r_{R_3N,R_3NH} \quad [2.36]$$

$$-R_{R_3NH} = -r_{CO_2(2)} - r_{R_3N,R_3NH} \quad [2.37]$$

The second term in equations [2.36] and [2.37] represent the rate of reaction of the amine to its protonated form:

$$r_{R_3N,R_3NH} = k_{R_3N,R_3NH} \left\{ (R_3N)(H_2O) - \frac{1}{K_{R_3N,R_3NH}} (R_3NH^+)(OH^-) \right\} \quad [2.38]$$

The rate constant for this reaction is set to a very high value.

In this formulation, we must use equation [2.13] to determine the activity of the zwitterion for the carbamate mechanisms, and the intermediate complex for the case of the tertiary amine mechanism (note from section 2.2.1 that we cannot solve for the zwitterion activity itself, but only a combination of the zwitterion activity and the rate constants):

$$\frac{k_{-1(1)}}{k_{2(1)}} (Z) = \frac{(\text{CO}_2)(\text{R}_2\text{NH}) + \frac{1}{k_{2(1)}} \sum k_{-b_i(1)}(\text{R}_2\text{NCOO}^-)(\text{B}_{i(2)}\text{H}^+)}{1 + \frac{1}{k_{2(1)}} \sum \frac{k_{b_i(1)}k_{2(1)}}{k_{-1(1)}}(\text{B}_{i(1)})} \quad [2.39]$$

Once again, we are really interested in the activity of the zwitterion, as opposed to its concentration. A similar expression provides the activity of the intermediate complex for the tertiary amine mechanism:

$$\frac{k_{-1(2)}}{k_{2(2)}} (I) = \frac{(\text{CO}_2)(\text{R}_3\text{N}) + \frac{1}{k_{2(2)}} \sum k_{-b_i(2)}(\text{HCO}_3^-)(\text{B}_{i(2)}\text{H}^+)}{1 + \frac{1}{k_{2(2)}} \sum \frac{k_{b_i(2)}k_{2(2)}}{k_{-1(2)}}(\text{B}_{i(2)})} \quad [2.40]$$

Now we may determine the reaction rate of the species involved as proton abstractors in the carbamate and tertiary mechanisms. First, for the primary (secondary) amine:

$$\begin{aligned} -\mathcal{R}_{\text{R}_2\text{NH}} &= k_2(\text{CO}_2)(\text{R}_2\text{NH}) - k_{-1}(Z) \\ &+ k_{\text{R}_2\text{NH}(1)}(Z)(\text{R}_2\text{NH}) - k_{\text{R}_2\text{NH}(1)}(\text{R}_2\text{NH}_2^+)(\text{R}_2\text{NCOO}^-) \\ &+ \mathcal{R}_{\text{R}_2\text{NH},\text{R}_2\text{NH}_2} \end{aligned} \quad [2.41]$$

$$\begin{aligned} -\mathcal{R}_{\text{R}_2\text{NH}_2} &= -k_{\text{R}_2\text{NH}(1)}(Z)(\text{R}_2\text{NH}) + k_{\text{R}_2\text{NH}(1)}(\text{R}_2\text{NH}_2^+)(\text{R}_2\text{NCOO}^-) \\ &- \mathcal{R}_{\text{R}_2\text{NH},\text{R}_2\text{NH}_2} \end{aligned} \quad [2.42]$$

where

$$\mathcal{R}_{\text{R}_2\text{NH},\text{R}_2\text{NH}_2} = k_{\text{R}_2\text{NH},\text{R}_2\text{NH}_2} \{ (\text{R}_2\text{NH})(\text{H}_2\text{O}) - \frac{1}{K_{\text{R}_2\text{NH},\text{R}_2\text{NH}_2}} (\text{R}_2\text{NH}_2^+)(\text{OH}^-) \} \quad [2.43]$$

Once again, this reaction is considered to be very fast. The remaining two species are hydroxide and the hydronium ion:

$$\begin{aligned}
-\mathcal{R}_{\text{OH}} = & k_{\text{OH}(1)}(\text{Z})(\text{OH}^-) - k_{\text{OH}(1)}(\text{H}_2\text{O})(\text{R}_2\text{NCOO}^-) \\
& + k_{\text{OH}(2)}(\text{I})(\text{OH}^-) - k_{\text{OH}(2)}(\text{H}_2\text{O})(\text{HCO}_3^-) \\
& + r_{\text{OH},\text{H}_2\text{O}} + r_{\text{CO}_2,\text{OH}}
\end{aligned} \tag{2.44}$$

$$\begin{aligned}
-\mathcal{R}_{\text{H}_3\text{O}} = & -k_{\text{H}_2\text{O}(1)}(\text{Z})(\text{H}_2\text{O}) + k_{\text{H}_2\text{O}(1)}(\text{H}_3\text{O}^+)(\text{R}_2\text{NCOO}^-) \\
& - k_{\text{H}_2\text{O}(2)}(\text{I})(\text{H}_2\text{O}) + k_{\text{H}_2\text{O}(2)}(\text{H}_3\text{O}^+)(\text{HCO}_3^-) \\
& + r_{\text{OH},\text{H}_2\text{O}}
\end{aligned} \tag{2.45}$$

where

$$r_{\text{OH},\text{H}_2\text{O}} = k_{\text{OH},\text{H}_2\text{O}} \left\{ (\text{OH}^-)(\text{H}_3\text{O}^+) - \frac{1}{K_{\text{OH},\text{H}_2\text{O}}} (\text{H}_2\text{O})^2 \right\} \tag{2.46}$$

A discussion will follow in Chapter 4 to describe how these rate equations are implemented into the mass transfer model.

## Chapter Three

### Equilibrium Models for Aqueous CO<sub>2</sub>-Alkanolamine Systems

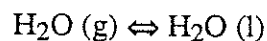
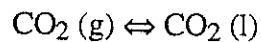
Before we can describe the nonequilibrium aspects of acid gas treating, we must have an understanding of the equilibrium behavior. It may be said that the equilibrium behavior is an important subset of the rate behavior problem - equilibrium establishes the driving force for absorption or desorption. This dependence is easily seen through equation [3.1] for the absorption rate (neglecting gas-phase resistance):

$$R = \frac{k_1^0}{H} E (P_A - P_A^*) \quad [3.1]$$

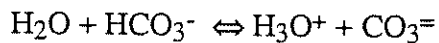
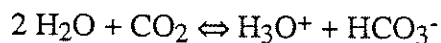
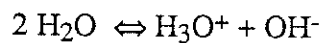
The kinetics of the reactions will determine the magnitude of E, the enhancement factor. However, the value of E is of only secondary importance to P\*, the equilibrium partial pressure of species A corresponding to a given liquid-phase concentration. There are a number of approaches used to correlate the effect of acid gas concentration on the partial pressure (Austgen, 1989; Chakravarty, 1985; Kent and Eisenberg, 1976). In this work, we choose the most rigorous approach (Austgen, 1989) in which the activity coefficients for the individual ionic species and molecules are calculated. Most of the work in this chapter is based upon the work of Austgen (1989) who thoroughly studied the equilibrium behavior of acid gas systems with a range of alkanolamines.

#### 3.1 Formulation of Equilibrium Equations in Combined Phase/Chemical Equilibria

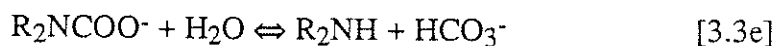
For the CO<sub>2</sub>-alkanolamine system, we must write the equations for vapor-liquid equilibria of CO<sub>2</sub>, water, and the amines:



We also have the equations corresponding to equilibrium reactions in the liquid phase:



R designates alkyl groups, and possibly protons for the case of primary and secondary amines. Furthermore, for primary and secondary amines, we have the carbamate reaction:



Corresponding to the vapor-liquid equilibria and chemical reactions, we have the following equations (neglecting the Poynting correction factor in [3.4]):

$$y_{\text{CO}_2} \phi_{\text{CO}_2} P_{\text{tot}} = x_{\text{CO}_2} \gamma_{\text{CO}_2} H_{\text{CO}_2, \text{w}}$$

$$y_{\text{H}_2\text{O}} \phi_{\text{H}_2\text{O}} P_{\text{tot}} = x_{\text{H}_2\text{O}} \gamma_{\text{H}_2\text{O}} P_{\text{H}_2\text{O}}^{\text{s}} \phi_{\text{H}_2\text{O}}^{\text{s}}$$

$$y_{\text{am}} \phi_{\text{am}} P_{\text{tot}} = x_{\text{am}} \gamma_{\text{am}} P_{\text{am}}^{\text{s}} \phi_{\text{am}}^{\text{s}} \quad [3.4]$$



$$\begin{aligned}
K_{a,h2o} &= \frac{(H_3O^+) (OH^-)}{(H_2O)^2} \\
K_{a,hco3} &= \frac{(H_3O^+) (HCO_3^-)}{(H_2O)^2 (CO_2)} \\
K_{a,co3} &= \frac{(H_3O^+) (CO_3^{=})}{(H_2O) (HCO_3^-)} \\
K_{a,am} &= \frac{(H_3O^+) (R_3N)}{(H_2O) (R_3NH^+)} \\
K_{a,amcoo} &= \frac{(RNH_2) (HCO_3^-)}{(RNHCO_2^-) (H_2O)} \quad [3.5]
\end{aligned}$$

A number of approaches have been used to model the equilibrium behavior of acid-gas alkanolamine systems. The approach used by Kent and Eisenberg (1976) was to "ignore" the nonideal behavior of the solution, and adjust the amine protonation constant [3.5d] and the carbamate stability constant [3.5e] in order to provide the best fit of the data. This approach is obviously approximate and cannot be relied upon to provide accurate concentrations of the individual species in solution. An extension of this approach was used for the MDEA system by Critchfield (1988) in that an equilibrium constant was made into a function of ionic strength. This approach would of course provide a better fit of the data, but is still inferior to an activity coefficient approach. The work of Austgen (1989) concentrated on modelling the thermodynamic behavior of acid gas systems and used a "rigorous" activity coefficient model, and since the individual activity coefficients are of importance in modelling the rate phenomena of amine systems, we chose this approach. We will discuss the method used in this work to model activity coefficients of CO<sub>2</sub> - alkanolamine systems.

In the work done presently, the amine volatility was neglected, and the following correlation was used for the mole-fraction based Henry's constant:

$$\log_e H_{CO_2} \text{ (Pa)} = 170.7126 - 8477.711/T - 21.9574 \cdot \log_e(T) + 0.005781 \cdot T \quad [3.6]$$

### 3.2 Activity Coefficients in Electrolyte Systems

The activity coefficients in electrolyte systems are considered to be a function of both long-range and local contributions. Unlike molecule-molecule interactions through dipole-dipole interactions, which vary as  $r^{-6}$ , ion-ion interactions vary as  $r^{-1}$ . Therefore, the long-range contributions are much more important in electrolyte systems. Fortunately, we have a good approximation to this long-range contribution from the Debye-Huckel theory. We assume that a local contribution can be added linearly into the total Gibbs excess free energy:

$$G^{\text{ex}} = G^{\text{ex},\text{sr}} + G^{\text{ex},\text{lr}} \quad [3.7]$$

Recall that the activity coefficient is obtained by differentiating the excess Gibbs free energy with respect to the mole number of a given species:

$$\ln \gamma_i = \frac{1}{RT} \left( \frac{\partial G^{\text{ex}}}{\partial n_i} \right)_{T,P,n_j} \quad [3.8]$$

We will present expressions in terms of the activity coefficients, instead of the Gibbs excess free energy, since the activity coefficient form is more useful for computation. We see that the combined activity coefficient is now a product of the activity coefficients from the short- and long-range contributions:

$$\gamma = \gamma^{\text{sr}} \gamma^{\text{lr}} \quad [3.9]$$

We will first discuss the long-range contribution to the activity coefficient.

### 3.2.1 Long-Range Contributions

The Pitzer-Debye-Huckel equation (Pitzer, 1980) accounts for the change in activity coefficients due to the ionic strength:

$$\ln \gamma_i^{\text{pdh}} = - \left( \frac{1000}{M_m} \right)^{1/2} A_\phi \left\{ \left( \frac{2z_i^2}{\rho} \ln (1 + \rho I_x^{1/2}) \right) + \frac{(z_i^2 I_x^{1/2} - 2I_x^{3/2})}{(1 + \rho I_x^{1/2})} \right\} \quad [3.10]$$

The constant  $A_\phi$  is a function of the dielectric constant  $D_m$  and density  $d_m$  of the medium:

$$A_\phi = \frac{1}{3} \left( \frac{2 \pi N_o d_m}{1000} \right)^{0.5} \left( \frac{e^2}{D_m k T} \right)^{1.5} \quad [3.11]$$

The Born term accounts for the change in the infinite dilution activity coefficients of ionic species due to a change in the dielectric constant from water to the mixed solvent:

$$\ln \gamma_{i,\text{BORN}}^\infty = \left( \frac{e^2}{2kT} \right) \left( \frac{z_i^2}{r_i} \right) \left( \frac{1}{D_m} - \frac{1}{D_w} \right) \quad [3.12]$$

For the case of alkanolamine systems, we have a mixed amine system, and the dielectric constant is assumed to vary in a weight fraction average of the individual dielectric constants. The distance  $r_i$  is the ionic radius for species  $i$ , assumed to be  $3\text{\AA}$ .

### 3.2.2 Short-Range Contribution

The standard NRTL contribution for molecule-molecule interactions is of the form:

$$\ln \gamma_{m,NRTL} = \frac{\sum_j X_j G_{jm} \tau_{jm}}{\sum_k X_k G_{km}} + \sum_{m'} \frac{X_{m'} G_{mm'}}{\sum_k X_k G_{km}} \left( \tau_{mm'} - \frac{\sum_k X_k G_{km'} \tau_{km'}}{\sum_k X_k G_{km'}} \right) \quad [3.13]$$

where

$$G_{km} = \exp(-\alpha_{km} \tau_{km}) \quad [3.14]$$

and  $\alpha_{km}$  is a nonrandomness factor fixed at 0.2 for our cases.\* The objective of the work of Chen and Evans (1982, 1986) was to utilize 2 key assumptions about the behavior of electrolyte solutions. The first is the assumption of like-ion repulsion, in which it is assumed that ions of a common charge cannot reside next to each other in solution, and hence have no short-range contribution. The second assumption is that of local electroneutrality, in which it is assumed that the net charge of cations and anions around a molecule is zero. By making these assumptions, we have a more realistic characterization of electrolyte systems. The expression for the Electrolyte-NRTL model is then:

---

\* In the present discussion,  $m$  designates a molecule,  $k$  designates any species in solution,  $a$  designates an anion, and  $c$  designates a cation. Summations over  $k$ ,  $m$ ,  $a$  and  $c$  designate summations over all species, all molecules, all anions, and all cations, respectively.

$$\begin{aligned}
\ln \gamma_{m,NRTL} = & \frac{\sum_j X_j G_{jm} \tau_{jm}}{\sum_k X_k G_{km}} \\
& + \sum_{m'} \frac{X_{m'} G_{mm'}}{\sum_k X_k G_{km}} \left( \tau_{mm'} - \frac{\sum_k X_k G_{km'} \tau_{km'}}{\sum_k X_k G_{km'}} \right) \\
& + \sum_c \sum_{a'} \frac{X_{a'}}{\sum_{a''} X_{a''}} \frac{X_c G_{mc,a'c}}{\sum_k X_k G_{kc,a'c}} \\
& \times \left( \tau_{mc,a'c} - \frac{\sum_k X_k G_{kc,a'c} \tau_{kc,a'c}}{\sum_k X_k G_{kc,a'c}} \right) \\
& + \sum_a \sum_{c'} \frac{X_{c'}}{\sum_{c''} X_{c''}} \frac{X_a G_{ma,c'a}}{\sum_k X_k G_{ka,c'a}} \\
& \times \left( \tau_{ma,c'a} - \frac{\sum_k X_k G_{ka,c'a} \tau_{ka,c'a}}{\sum_k X_k G_{ka,c'a}} \right) \tag{3.15}
\end{aligned}$$

where

$$G_{ka,c'a} = \exp(-\alpha_{ka,c'a} \tau_{ka,c'a}) \tag{3.16}$$

(A similar expression holds for all binary interaction parameters, and all values of  $\alpha$  are set to the default value of 0.2). At infinite dilution in water, we obtain the following expression for the activity coefficient:

$$\ln \gamma_m^{\infty} \text{NRTL} = \tau_{wm} + G_{mw} \tau_{mw} \quad [3.17]$$

This expression is useful since we use the infinite dilution value as a reference state for molecular solutes.

For the cations and anions, we have the following expressions:

$$\begin{aligned} \frac{1}{Z_c} \ln \gamma_c \text{NRTL} = & \sum_{a'} \frac{X_{a'}}{\sum_{a''} X_{a''}} \frac{\sum_k X_k G_{kc.a'c} \tau_{kc.a'c}}{\sum_k X_k G_{kc.a'c}} \\ & + \sum_m \frac{X_m G_{km}}{\sum_k X_k G_{km}} \left( \tau_{cm} - \frac{\sum_k X_k G_{km} \tau_{km}}{\sum_k X_k G_{km}} \right) \\ & + \sum_a \sum_{c'} \frac{X_{c'}}{\sum_{c''} X_{c''}} \frac{X_a G_{ca.c'a}}{\sum_k X_k G_{ca.c'a}} \\ & \times \left( \tau_{ca.c'a} - \frac{\sum_k X_k G_{ka.c'a} \tau_{ka.c'a}}{\sum_k X_k G_{ka.c'a}} \right) \end{aligned} \quad [3.18]$$

$$\ln \gamma_{c \text{ NRTL}}^{\infty} = Z_c \left\{ G_{cw} \tau_{cw} + \frac{\sum_{a'} x_{a'} \tau_{wc.a'c}}{\sum_{a''} x_{a''}} \right\} \quad [3.19]$$

$$\begin{aligned} \frac{1}{Z_a} \ln \gamma_{a \text{ NRTL}} &= \sum_{c'} \frac{X_{c'}}{\sum_{c''} X_{c''}} \frac{\sum_k X_k G_{ka.c'a} \tau_{ka.c'a}}{\sum_k X_k G_{ka.c'a}} \\ &+ \sum_m \frac{X_m G_{km}}{\sum_k X_k G_{km}} \left( \tau_{am} - \frac{\sum_k X_k G_{km} \tau_{km}}{\sum_k X_k G_{km}} \right) \\ &+ \sum_c \sum_{a'} \frac{X_{a'}}{\sum_{a''} X_{a''}} \frac{X_c G_{ac.a'c}}{\sum_k X_k G_{ac.a'c}} \\ &\times \left( \tau_{ac.a'c} - \frac{\sum_k X_k G_{kc.a'c} \tau_{kc.a'c}}{\sum_k X_k G_{kc.a'c}} \right) \end{aligned} \quad [3.20]$$

$$\ln \gamma_{a \text{ NRTL}}^{\infty} = Z_a \left\{ G_{aw} \tau_{aw} + \frac{\sum_{c'} x_{c'} \tau_{wa.c'a}}{\sum_{c''} x_{c''}} \right\} \quad [3.21]$$

The objective is then to adjust the binary interaction parameters,  $\tau$ , in order to best fit the experimental data. Default values for most of the interaction parameters are assumed based upon the work of Chen and Evans (1986) and Mock et al. (1986). All water-ion pair and ion pair-water parameter default values were 8 and -4, respectively. All alkanolamine-ion pair and ion pair-alkanolamine parameters, and all acid gas-ion

pair and ion pair-acid gas parameters were fixed at 15 and -8, respectively. All molecule-molecule parameters and ion pair-ion pair parameters are, by default, fixed at zero.

### 3.3 Standard States of the Electrolyte-NRTL Model

The standard state for the activity coefficients is defined as the point at which the activity coefficient is unity. This is important only in the sense that the equilibrium constants must be defined with respect to the standard states. The equilibrium constants were obtained from Austgen (1989) and shown in Table 3.1. The standard states for these equilibrium constants are:

$$\begin{aligned}\gamma_{\text{H}_2\text{O}} &\Rightarrow 1 \text{ as } x_{\text{H}_2\text{O}} \Rightarrow 1 \\ \gamma_{\text{AM}} &\Rightarrow 1 \text{ as } x_{\text{AM}} \Rightarrow 1 \\ \gamma_{\text{CO}_2} &\Rightarrow 1 \text{ as } x_{\text{H}_2\text{O}} \Rightarrow 1 \\ \gamma_{\text{ions}} &\Rightarrow 1 \text{ as } x_{\text{ions}} \Rightarrow 0, x_{\text{H}_2\text{O}} \Rightarrow 1\end{aligned}\quad [3.22]$$

The reason for defining the activity coefficients of the ionic species as unity at infinite dilution in water is so that equilibrium constants for the ionic reactions are consistent with the literature. Note, however, that equilibrium constants involving the amine itself uses a mixed convention. Austgen (1989) provides much discussion on that standard states of the equilibrium constants, and the equilibrium constant conversion between various standard states.

### 3.4 Solution of the Combined Phase/Chemical Equilibrium Problem

The obvious approach to solving the equilibrium problem given the equilibrium constants and activity coefficient function is to now find the solution of equations [3.4] and [3.5] using the appropriate correlations for the activity coefficients and gas-phase fugacity coefficients. The straightforward approach is, however, most difficult since the concentration of the components may vary by 10 orders of magnitude. This scaling



Table 3.1      Equilibrium Constants for the CO<sub>2</sub>-Amine Reactions (Austgen, 1989)  
 $\log_e K = C_1 + C_2/T + C_3 \log_e(T) + C_4 T$

Rxn	C <sub>1</sub>	C <sub>2</sub>	C <sub>3</sub>	C <sub>4</sub>
H <sub>2</sub> O [3.5a]	132.899	-13445.9	-22.4773	0.0
CO <sub>2</sub> [3.5b]	231.465	-12092.10	-36.7816	0.0
HCO <sub>3</sub> <sup>-</sup> [3.5c]	216.049	-12431.70	-35.4819	0.0
MEA [3.5d]	2.12112	-8189.38	0.0	-0.007484
DEA [3.5d]	-6.7936	-5927.65	0.0	0.0
MDEA [3.5d]	-9.4165	-4234.98	0.0	0.0
MEA [3.5e]	2.8898	-3635.09	0.0	0.0
DEA [3.5e]	4.5146	-3417.34	0.0	0.0

problem makes the solution of the nonlinear algebraic equations most difficult. A tremendous amount of work has been done on efficient methods for solving the equilibrium problem, and one of the best references on the subject is the text by Smith and Missen (1982). After trying several methods for the solution of the equilibrium problem, we found the nonstoichiometric algorithm of Smith and Missen (1988) to be by far the most reliable and efficient method used. We briefly describe this method and implementation for the acid gas systems below. The reader is referred to the excellent text of Smith and Missen (1982) for a detailed discussion of the equilibrium problem. It is shown in the cited reference that the nonstoichiometric algorithm is equivalent to the stoichiometric algorithm (p. 48) which is in turn equivalent to the equilibrium constant formulation (p. 62) often used to solve equilibrium problems.

### 3.4.1 The Nonstoichiometric Algorithm

The criterion for equilibrium is the minimization of the Gibbs free energy. This minimization is subject to material balance constraints and the entire problem can be posed mathematically as follows:

$$\min G(\mathbf{n}) = \sum_{i=1}^N n_i \mu_i$$

subject to

$$\sum_{i=1}^N a_{ki} n_i = b_k \quad k = 1, \dots, M \quad [3.23]$$

$N$  is the number of species in solution,  $M$  is the number of elements,  $\mu_i$  is the chemical potential,  $a_{ki}$  are the elements of the elemental abundance matrix, and  $b_k$  is the total amount of each element in the system. This problem is solved by the method of Lagrange multipliers. The resulting system of equations is then (Smith and Missen, 1982):

$$\mu_i - \sum_{k=1}^M a_{ki} \lambda_k = 0 \quad i = 1, \dots, N \quad [3.24]$$

$$b_k - \sum_{i=1}^N a_{ki} n_i = 0 \quad k = 1, \dots, M \quad [3.25]$$

The  $\lambda_k$  are the Lagrange multipliers, and we now have a total of  $N+M$  simultaneous equations to solve. The inherent difficulty of this problem is that, while equations [3.25] are linear in the mole numbers,  $n_i$ , equations [3.24] includes the chemical potentials which are nonlinear in the mole numbers. For the liquid phase we have equation [3.26]:

$$\mu_i = \mu_i^0 + RT \ln (C_i) + RT \ln (\gamma_i) \quad [3.26]$$

For the vapor phase, we can also write an expression for the chemical potential:

$$\mu_i = \mu_i^0 + RT \ln (P_i) + RT \ln (\phi_i) \quad [3.27]$$

In our case, we can neglect the effect of the vapor phase on the liquid-phase composition. This is possible for 2 reasons:

- (1) The total amount of CO<sub>2</sub> in the liquid phase will be specified through equation [3.23], and not by the partial pressure of the CO<sub>2</sub> over solution.
- (2) The pressures encountered in this work are such that the Poynting correction factor does not affect the liquid-phase chemical potentials.

Therefore, we can solve the equilibrium problem for the liquid phase only, then find the CO<sub>2</sub> partial pressure over solution by means of the VLE equation [3.4a].

The actual problem is based on Smith and Missen's extension (1988) of the RAND variation of the BNR algorithm. Fundamentally, equations [3.24] and [3.25] are solved by a local linearization of [3.24] with respect to mole numbers, and then an iterative procedure is used to converge on the compositions. A number of refinements have been put into the algorithm based upon the vast experience of Smith and Missen, and we merely list the equations used here:

$$\delta n_i^{(m)} = n_i^{(m)} \left( \sum_{k=1}^M \lambda_k^{(m)} a_{ki} - \mu_i^{(m)} \right) \quad i=1, \dots, N \quad [3.28]$$

$$\sum_{k=1}^M \lambda_k^{(m)} \sum_{i=1}^N a_{ki} n_i^{(m)} = \delta b_i^{(m)} + \sum_{i=1}^N a_{ii} n_i^{(m)} \mu_i^{(m)} \quad l = 1, \dots, M \quad [3.29]$$

$$\sum_{i=1}^N a_{ki} \delta n_i^{(m)} = b_k - b_k^{(m)} = \delta b_k^{(m)} \quad k = 1, \dots, M \quad [3.30]$$

These equations are solved at each iteration, then the mole vector is updated at each iteration using a dampening parameter to aid in convergence:

$$n_i^{(m+1)} = n_i^{(m)} + \omega^{(m)} \delta n_i^{(m)} \quad [3.31]$$

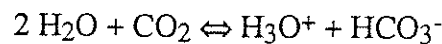
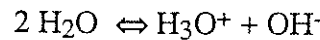
For the nonideal system, we use a pseudo-standard state chemical potential:

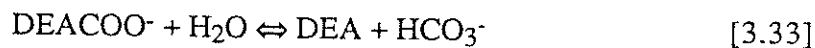
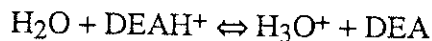
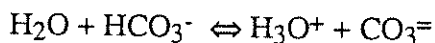
$$\mu_i^* = \mu_i^0 + RT \ln (\gamma_i) \quad [3.32]$$

After solving for the composition, the activity coefficients are calculated using the Electrolyte-NRTL model, then the equilibrium problem is solved again as if the solution was ideal. In this work, much effort was put into nonlinear parameter estimation, and a technique used to reduce the computation time was to save the activity coefficients for a given composition at one estimate of the parameters, then re-use the old values instead of assuming that the solution was ideal for an initial guess. This technique saves much computation time with minor effort.

### ***3.4.2 Application of the Nonstoichiometric Algorithm to the Acid Gas-Alkanolamine System***

The concepts presented in section 3.4.1 are best demonstrated by means of example. We will take the CO<sub>2</sub>-DEA system, and show how the nonstoichiometric algorithm would be formulated for this system. For this system, we have 9 components: CO<sub>2</sub>, DEA, H<sub>2</sub>O, HCO<sub>3</sub><sup>-</sup>, CO<sub>3</sub><sup>=</sup>, DEAH<sup>+</sup>, DEACOO<sup>-</sup>, H<sub>3</sub>O<sup>+</sup>, and OH<sup>-</sup>. For this system, we can only write 5 independent equilibrium equations:





At this point, we need to specify the  $M \times N$  elemental abundance matrix. The technique developed in this work was to consider actual molecules as elements when convenient. In this case, we would use DEA, C, O, and H. The elemental abundance matrix for this system is then:

$$\begin{bmatrix} 0. & 1. & 0. & 0. & 0. & 1. & 1. & 0. & 0. \\ 1. & 0. & 0. & 1. & 1. & 0. & 1. & 0. & 0. \\ 2. & 0. & 1. & 3. & 3. & 0. & 2. & 1. & 1. \\ 0. & 0. & 2. & 1. & 0. & 1. & -1. & 3. & 1. \end{bmatrix} \begin{bmatrix} \text{CO}_2 \\ \text{DEA} \\ \text{H}_2\text{O} \\ \text{HCO}_3^- \\ \text{CO}_3^{2-} \\ \text{DEAH}^+ \\ \text{DEACOO}^- \\ \text{H}_3\text{O}^+ \\ \text{OH}^- \end{bmatrix} = \begin{bmatrix} \text{total DEA} \\ \text{total C} \\ \text{total O} \\ \text{total H} \end{bmatrix} \quad [3.34]$$

In our case, we specify an initial overall composition by specifying the total amine, water, and  $\text{CO}_2$  loading. From this composition, the amount of each "element" may be calculated using equation [3.34], we may then proceed with the algorithm of Smith and Missen.

### 3.4.3 Conversion of Equilibrium Constants into Standard-State Chemical Potentials

In order to solve for the equilibrium composition using the nonstoichiometric algorithm, we must know standard state chemical potentials. However, the data that are available are in the form of equilibrium constants (Austgen et al., 1989). The solution to this problem is found in Smith and Missen (1982, pp. 214-217) where activity based equilibrium constants can be converted to reference chemical potentials by solving the following system of equations:

$$\sum_{i=1}^N v_{ij} \mu_i^0 = \Delta G_j^0; \quad j = 1, \dots, n_{\text{rex}} \quad [3.35]$$

with

$$\Delta G_j^0 = -RT \ln(K_{aj}) \quad [3.36]$$

The quantities  $\Delta G_j^0$  are the change in the Gibbs free energy for each reaction,  $j$ . If we take, for example, the DEA-CO<sub>2</sub> system, we have a speciation problem with 9 unknowns, and only 5 independent equilibrium reactions may be written for this system. The  $v_{ij}$  are the elements of the stoichiometric matrix for any of the 5 independent chemical reactions which may be written for this system. For our example with the DEA-CO<sub>2</sub> system, any 4 of the reference chemical potentials are arbitrary and may be set to zero (as long as  $N^T \mu^0$  is of rank  $n_{\text{rex}}$ , where  $N$  is the matrix of stoichiometric vectors,  $v_1 \dots v_{n_{\text{rex}}}$  - this means that we cannot set all of the chemical potentials of species corresponding to a single reaction equal to zero), then equation [3.35] becomes a problem of 5 equations with 5 unknowns.

## Chapter Four

### Mass Transfer with Reversible Chemical Reaction in Electrolyte Systems

The objective of this chapter is to develop the theory used to determine mass transfer rates in multicomponent electrolyte systems. One can choose from varying levels of sophistication, ranging from simplistic Fick's law models to the more complex models which arise from the Theory of Irreversible Processes (all of the models we consider will be from a macroscopic, phenomenological point of view). We choose to keep the equations for the reaction/diffusion system as simple as possible, using only as much sophistication as is necessary to interpret the experimental data. There are several reasons for this approach:

- 1) It is easier to transfer the technology to individuals who may wish to use this approach for practical simulation problems.
- 2) There is a lack of data to evaluate all of the parameters, such as cross-coupling coefficients, needed in the more complex models.
- 3) It is necessary to keep computation time to a minimum, in order that such an approach be practical for application in experimental data interpretation or design.

However, it is appropriate to review the more sophisticated theories in order that we can appreciate our simplifications, and note where such simplified models are not applicable. Therefore, let us briefly review the concepts of the Theory of Irreversible Processes as it applies to multicomponent mass transfer with chemical reaction. We cannot do justice to this theory in the short review provided, however, we hope to broaden the reader's view of mass transfer processes in the following discussion:

#### 4.1 The Theory of Irreversible Processes (TIP)

The classical view of the Theory of Irreversible Processes (TIP), also known as the Theory of Irreversible Thermodynamics, postulates that a flux is produced from the contribution of all forces in the system:

$$J_i = \sum_{j=1}^m L_{ij} X_j \quad [4.1]$$

$J_i$  are the fluxes related linearly to the forces,  $X_j$ , through the phenomenological coefficients,  $L_{ij}$ . There is some ambiguity as to what exactly constitutes a "force" and a "flux" (Yourgrau et al., 1982), but we can think of forces as temperature gradients, concentration gradients, density gradients, etc., and fluxes of mass, heat or momentum. The classical reference in this field is the book by de Groot and Mazur (1962), however, the book by Yourgrau et al. (1982) provides a more comprehensible introductory view, along with the contemporary thought in this area. Note that, as presented in equation [4.1], we are discussing a *linear* theory. It is also a constitutive equation, a function of the property of the system under consideration, and subject to verification.

One of the classical results of the Theory of Irreversible Processes (TIP) is to place restrictions on the phenomenological coefficients of equation [4.1] by use of the Onsager Reciprocal Relations (Onsager, 1931). In essence, Onsager showed that the Principle of Microscopic Reversibility imposes a symmetry condition on the phenomenological coefficients:

$$L_{ij} = L_{ji} \quad [4.2]$$

It should be noted that the Principle of Microscopic Reversibility does not hold in all situations, such as magnetic fields. This property is useful, however, because it can be shown (Standart et al., 1979) it implies that the binary diffusion coefficients of the Stefan-Maxwell formulation are also symmetric, allowing a large reduction in data that must be collected, as well as a check on the consistency of redundant data. However, the generalized Fick's Law diffusion coefficients are not symmetric.

The thermodynamic forces considered here are the forces due to temperature gradients, chemical potential gradients, external forces, and the chemical affinity for a reaction:



$$X_q = -\frac{1}{T^2} \nabla T \quad [4.3]$$

$$X_k = -\nabla \frac{\mu_k}{T} + \frac{1}{T} F_k \quad [4.4]$$

$$X_j = -\frac{1}{T} A_j \quad [4.5]$$

One of the interesting results of TIP can be obtained by solving for the rate of entropy production given the forces and fluxes (de Groot and Mazur, 1962). Here, we show the results neglecting the velocity gradients:

$$\sigma = \sum_{i=1}^m J_i X_i \quad [4.6]$$

$$\sigma = -\frac{1}{T^2} J_q \cdot \nabla T - \frac{1}{T} \sum_{k=1}^N J_k \cdot (T \nabla \frac{\mu_k}{T} - F_k) - \frac{1}{T} \sum_{j=1}^{n_{\text{rex}}} J_j A_j \geq 0 \quad [4.7]$$

The inequality holds due to the Second Law of Thermodynamics. Also note that the mass flux is due to the potential gradient, not the concentration gradient. Finally, note that external body forces,  $F_k$ , can also affect the flow of mass. This will become important when we include the effect of the electrical field on the flow of ions. In the rest of the treatment, we will neglect temperature gradients.

TIP has afforded us a broadened view of diffusion/reaction phenomena, and for that it is most useful. However, it is not applicable to most chemical engineering problems because of the restriction of linearity. For example, the use of TIP in chemical kinetics is limited to the region near equilibrium where the reaction rate is a linear function of the affinity. For an interesting discussion along these lines, see Anderson and Boyd (1971).

Because of the general difficulty of TIP in dealing with chemical reactions, violations of the Principle of Microscopic Reversibility and its mathematical imprecision, TIP has come under strong criticism by several authors: Anderson and

Boyd (1971), Astarita (1975), Truesdell (1969), Wei (1966). However, as stated by Astarita (1975): "In spite of all the comments and criticisms discussed above, TIP [the Theory of Irreversible Processes] has the great merit of having reintroduced into thermodynamic thinking the consideration of irreversibility."

One of the newer schools of thought is Rational Thermodynamics (RT), which does not try to specify the constitutive equations, but merely imposes restrictions upon them, such that they satisfy the Second Law of Thermodynamics (Truesdell, 1969, Astarita, 1974). For example, RT does not state that the flux is linearly proportional to the concentration gradient; however, it would state the following:

IF        the constitutive relation between the flux and the concentration gradient is a linear relationship (Fick's law for a single species diffusion)  
 THEN the constant of proportionality (the diffusion coefficient) must be nonnegative in order to satisfy the Second Law of Thermodynamics.

RT claims as a basis a rigorous mathematical structure, borrowed from continuum mechanics.

## 4.2 Diffusion in Nonideal Electrolyte Systems

### *4.2.1 The Flux Expression for Diffusion in Electrolyte Systems*

It may seem that the discussion of the Theory of Irreversible Processes is, at best, a diversion. However, in order to treat the absorption of an acid gas into an amine system on a fundamental level, we must be able to recognize that diffusion can be affected by thermodynamic nonideality, ionic coupling, and phenomenological coupling as well. Throughout this discussion, we will concern ourselves with diffusion in one spatial dimension only. We take as our starting point, the generalized Stefan-Maxwell equation, neglecting temperature and pressure gradients (Krishna and Standart, 1979; Standart et al., 1979):

$$\sum_{\substack{j=1 \\ j \neq i}}^N \frac{x_j J_j - x_i J_i}{C_t D_{ij}} = \frac{C_i}{RT} \nabla \mu_i - \frac{1}{C_t RT} \left( C_i F_i - \omega_i \sum_{j=1}^N C_j F_j \right) \quad [4.8]$$

The quantity  $F_j$  is the external force which operates on chemical species and  $\omega_i$  is the weight fraction of species  $i$ .  $C_t$  is the total concentration. Examples of external forces include gravity and electrical potential. For the diffusion of ions, we must take into account the electrical potential gradient, which is an external force (Krishna, 1987):

$$F_i = -z_i F \nabla \Phi \quad [4.9]$$

Now we make the simplifying approximation that the only diffusion coefficient of importance is that of the binary diffusion coefficient in the solvent. Assuming this, and bulk electroneutrality:

$$\sum_{i=1}^N z_i C_i = 0 \quad [4.10]$$

Equation [4.8] simplifies greatly:

$$J_i = -\frac{D_i C_i}{RT} \nabla \mu_i - \frac{z_i C_i D_i}{RT} F \nabla \Phi \quad [4.11]$$

Here, we have made the assumption that the solution is dilute enough such that the phenomenological coupling through the cross-diffusion coefficients may be ignored, but not so dilute that the chemical potential gradient is negligible. This assumption is reasonable for dilute solutions of ions, and has been used by Smyrl and Newman (1968). We will, however, later neglect the chemical potential gradients in the boundary layer at the gas-liquid interface, in order to save computation time - assuming that the activity coefficients are constant and equal to the values in the bulk liquid phase. For the eddy diffusivity theory (the origins of which will be discussed in more detail in the next chapter), we add the empirical modification which accounts for the turbulent flux:

$$J_i = - \frac{D_i C_i}{RT} \nabla \mu_i - \epsilon x^2 \nabla C_i - \frac{z_i C_i D_i}{RT} \mathcal{F} \nabla \Phi \quad [4.12]$$

Note that the eddy diffusivity term,  $\epsilon x^2 \nabla C_i$ , is not to be considered an external force, since it does not create a potential for transport of individual chemical species relative to the bulk fluid phase. This issue will be addressed in more detail soon.

Substituting for the chemical potential gradient:

$$\mu_i = \mu_o + RT \ln(\gamma_i C_i) \quad [4.13]$$

and assuming that the activity coefficients,  $\gamma_i$ , all constant throughout the region of diffusion, we arrive at the Nernst-Planck equation (Krishna, 1987):

$$J_i = - D_i \nabla C_i - \frac{z_i C_i D_i}{RT} \mathcal{F} \nabla \Phi \quad [4.14]$$

#### 4.2.2 The Henderson Formula for the Electrical Potential Gradient

We wish to obtain a closed form equation for the electrical potential gradient as a function of the ion concentrations and concentration gradients, for numerical solution of the material balance equations. We do this by first obtaining the expression for the flux of electrical current:

$$\begin{aligned} I &= \sum_{i=1}^N z_i J_i \\ &= - \sum_{i=1}^N \left( \frac{D_i C_i z_i}{RT} \nabla \mu_i + \frac{z_i^2 C_i D_i}{RT} \mathcal{F} \nabla \Phi \right) \end{aligned} \quad [4.15]$$

Since, during the absorption of a gas into the liquid phase, there is no external electrical potential applied to the system, we assume no flux of current (Krishna, 1987):

$$\begin{aligned}
 I = 0 &= \sum_{i=1}^N z_i J_i \\
 &= - \sum_{i=1}^N \left( \frac{D_i C_i z_i}{RT} \nabla \mu_i + \frac{z_i^2 C_i D_i}{RT} \mathcal{F} \nabla \Phi \right) \quad [4.16]
 \end{aligned}$$

Solving equation [4.16] for the electrical potential gradient, we arrive at an expression for the electrical potential gradient as a function of the chemical potential gradients of the ions:

$$- \nabla \Phi = \frac{\sum_{i=1}^N \frac{z_i D_i C_i}{RT} \nabla \mu_i}{\frac{\mathcal{F}}{RT} \sum_{i=1}^N z_i^2 D_i C_i} \quad [4.17]$$

Assuming that the activity coefficients of the ions are constant, we arrive at what is called the Henderson formula by Mills et al. (1984):

$$- \nabla \Phi = \frac{\sum_{i=1}^N z_i D_i \nabla C_i}{\frac{\mathcal{F}}{RT} \sum_{i=1}^N z_i^2 D_i C_i} \quad [4.18]$$

The Henderson formula can be considered a multicomponent extension of the common formula for binary diffusion of ionic species (Vinograd and McBain, 1941).

Is the Henderson formula (and its nonideal solution counterpart) also valid for the eddy diffusivity theory? To answer this question, we rederive the expression for the electrical potential gradient with the eddy diffusivity term added into the flux expression. In doing so, we arrive at an equation of the form:

$$-\nabla\Phi = \frac{\sum_{i=1}^N \left( \frac{z_i D_i C_i}{RT} \nabla \mu_i + z_i \epsilon x^2 \nabla C_i \right)}{\frac{\mathcal{F}}{RT} \sum_{i=1}^N z_i^2 D_i C_i} \quad [4.19]$$

Separating the second term in the numerator, and removing the term  $\epsilon x^2$  from the summation:

$$-\nabla\Phi = \frac{\sum_{i=1}^N \frac{z_i D_i C_i}{RT} \nabla \mu_i}{\frac{\mathcal{F}}{RT} \sum_{i=1}^N z_i^2 D_i C_i} + \frac{\epsilon x^2 \sum_{i=1}^N z_i \nabla C_i}{\frac{\mathcal{F}}{RT} \sum_{i=1}^N z_i^2 D_i C_i} \quad [4.20]$$

Let the net electrical charge be represented as follows:

$$\mathcal{C} = \mathcal{F} \sum_{i=1}^N z_i C_i \quad [4.21]$$

The change in the net electrical charge with respect to distance:

$$\nabla \mathcal{C} = \mathcal{F} \sum_{i=1}^N z_i \nabla C_i \quad [4.22]$$

If electrical neutrality is to exist everywhere, then the derivative of the net electrical charge must be zero, and so the second term in equation [4.20] must be zero, by equation [4.22]. Therefore, the equation potential gradient (ideal or nonideal) is valid also for the eddy diffusivity theory. An intuitive explanation as to why the second term in the electrical potential gradient cancels is as follows: Consider an element of fluid that is carried by a turbulent eddy. It is electrically neutral, and, it is mixed with fluid elements that are also electrically neutral. Therefore, the transport of ionic species due

to an eddy does not have a tendency to produce any charge separation, and does not require a potential gradient to counteract any tendency to produce such a charge separation.

If the diffusion coefficients of all of the ions are assumed to be the same, then the effective diffusion coefficient may be removed from the summation sign:

$$-\nabla\Phi = \frac{D_{\text{eff}} \sum_{i=1}^N z_i \nabla C_i}{\frac{F}{RT} \sum_{i=1}^N z_i^2 D_i C_i} \quad [4.23]$$

and, by equation [4.22] for the electrical charge density, the potential gradient is zero. This assumption is used to simplify the equations and reduce the computation time for time intensive tasks, such as parameter estimation. However, note that, under the case of diffusion in thermodynamically nonideal solutions, the same simplification does not occur:

$$-\nabla\Phi = \frac{D_{\text{eff}} \sum_{i=1}^N \frac{z_i C_i}{RT} \nabla \mu_i}{\frac{F}{RT} \sum_{i=1}^N z_i^2 D_i C_i} \quad [4.24]$$

For isothermal conditions, any activity coefficient model we use must (or should!) satisfy the following Gibbs-Duhem equation:

$$\sum_{i=1}^N C_i \nabla \ln \gamma_i = 0 \quad [4.25]$$

The chemical potential gradient may be written as follows:

$$\nabla \mu_i = RT \left( \frac{1}{C_i} \nabla C_i + \nabla \ln \gamma_i \right) \quad [4.26]$$

We can now separate the electrical potential gradient into its ideal and nonideal components:

$$-\nabla \Phi = \frac{D_{\text{eff}} \sum_{i=1}^N z_i \nabla C_i}{\frac{F}{RT} \sum_{i=1}^N z_i^2 D_i C_i} + \frac{D_{\text{eff}} \sum_{i=1}^N z_i C_i \nabla \ln \gamma_i}{\frac{F}{RT} \sum_{i=1}^N z_i^2 D_i C_i} \quad [4.27]$$

As before, the first term on the right-hand side cancels. However, the second term will cancel only if the following holds true for the activity coefficient model:

$$\sum_{i=1}^N z_i C_i \nabla \ln \gamma_i = 0 \quad [4.28]$$

Therefore, if one is going to properly account for the diffusion of ions in nonideal solutions, either the activity coefficient model must satisfy equation [4.25] and [4.28] simultaneously, or equation [4.27] must be used for the potential gradient.

### 4.3 On the Consistency Between Chemical Kinetics and Reaction Equilibria

Let us first consider ideal systems. The reaction kinetics will be represented by the general mass action kinetic laws for the supposed elementary steps of the reactions. The equation for a single reaction,  $j$ , in a general reaction network is shown in equation [4.29]:

$$r_j = k_j \prod_{i=1}^{n_r} C_i^{-\nu_{ij}} - k_{-j} \prod_{i=1}^{n_p} C_i^{\nu_{ij}} \quad [4.29]$$



In this expression,  $k_j$  and  $k_{-j}$  are concentration based forward and reverse rate constants, respectively;  $v_{ij}$  are the stoichiometric coefficients of the species of the elementary reactions, assumed positive for products and negative for reactants; and  $n_r$  and  $n_p$  designate that the products in equation [4.29] are taken over the reactants and products of the chemical reaction, respectively. We make the usual assumption that the concentration based equilibrium constant,  $K_{cj}$ , for reaction  $j$  is the ratio of the forward to reverse rate constants:

$$K_{cj} = \frac{k_j}{k_{-j}} \quad [4.30]$$

Therefore, the reaction rate is zero for every reaction at equilibrium, and equation [4.29] can be expressed as shown:

$$r_j = k_j \left( \prod_{i=1}^{n_r} C_i^{-v_{ij}} - \frac{1}{K_{cj}} \prod_{i=1}^{n_p} C_i^{v_{ij}} \right) \quad [4.31]$$

Note that nothing in equilibrium theory demands that equation [4.30] hold for general reaction schemes. In fact, equation [4.30] reflects an additional assumption known as the principle of detailed balance (Denbigh, 1948) which proposes that, at thermodynamic equilibrium, the net rate of each individual reaction is zero.

We are now faced with a difficulty for the nonideal system. Since the activity coefficients differ from unity, and in fact vary over the range of conditions encountered in this work, the use of a single equilibrium constant in equation [4.31] will not work. We *must*, however, ensure that the reaction rates all go to zero at the bulk of the liquid, or else we will get discontinuities in the concentration profiles during the numerical solution of the differential equations. One approach to this problem is to adjust the equilibrium constant at each loading such that the equilibrium condition in the bulk liquid is satisfied. This is equivalent to adjusting the reverse rate constant at each condition, but keeping the forward rate constant the same. This assumption does not necessarily provide good results, consistent with the experimental data. The general form all corrections must take becomes apparent in the discussion below:

A general formulation for reaction kinetics in nonideal systems is to base the rates on activities, not concentrations:

$$r_j = k_{aj} \left( \beta \prod_{i=1}^{n_r} a_i^{-v_{ij}} - \frac{\beta}{K_{aj}} \prod_{i=1}^{n_p} a_i^{v_{ij}} \right) \quad [4.32]$$

$K_{aj}$  is now the activity-based equilibrium constant (truly constant for constant temperature). In this formulation, the activities are used in place of the concentrations, and the constant  $\beta$  is equal to the inverse of the transition state complex activity coefficient (Boudart, 1968; Hall, 1982). Also note that  $k_a$  is an activity-based rate constant, as opposed to the concentration-based rate constant used in equation [4.31]. The difficulty with this formulation is that the transition state complex activity coefficient is not readily available except for dilute, strong electrolyte systems, using the Debye-Huckel approximation (Boudart, p. 44). Furthermore, the simplifying assumption that  $\beta = 1$  has also been demonstrated to be both qualitatively and quantitatively incorrect (Froment and Bischoff, p. 60, 1979).

If we substitute  $\gamma_i C_i$  for each activity, we obtain an expression of the form:

$$r_j = k_{aj} \beta \left( \prod_{i=1}^{n_r} \gamma_i^{-v_{ij}} C_i^{-v_{ij}} - \frac{1}{K_{aj}} \prod_{i=1}^{n_p} \gamma_i^{v_{ij}} C_i^{v_{ij}} \right) \quad [4.33]$$

The activity based equilibrium constant,  $K_{aj}$ , is the product of the concentration based equilibrium constant and the ratio of the activities to the  $v_{ij}$  power:

$$K_{aj} = K_{cj} K_{\gamma j} = \prod_{i=1}^N \gamma_i^{v_{ij}} C_i^{v_{ij}} \quad [4.34]$$

Substituting equation [4.34] into equation [4.33]:

$$r_j = k_{aj} \beta \prod_{i=1}^{n_r} \gamma_i^{-v_{ij}} \left( \prod_{i=1}^{n_r} C_i^{-v_{ij}} - \frac{1}{K_{cj}} \prod_{i=1}^{n_p} C_i^{v_{ij}} \right) \quad [4.35]$$

One can assume the following functional form for  $\beta$ :

$$\beta = \prod_{i=1}^{n_r} \gamma_i^{\nu_{ij}} \quad [4.36]$$

This assumption essentially makes the forward rate constant *constant*, while adjusting the reverse rate constants in order to ensure consistency between the kinetic equations and the equilibria. Alternatively, one can assume that  $\beta$  is of a form that adjusts the forward rate constants as a function of changing nonidealities:

$$\beta = \prod_{i=1}^{n_p} \gamma_i^{\nu_{ij}} \quad [4.37]$$

It has been found that the expression corresponding to equation [4.37] provides the best consistency between the data at high and low ionic strengths.

#### 4.4 Incorporation of Flux Expressions into Material Balance Equations

We summarize the previous results by presenting the general formulation of the reaction/diffusion equations (neglecting activity coefficient gradients) within the material balance equations. It is these equations which will be supplied with boundary conditions based upon the assumptions of the mass transfer theories, as will be discussed in the next chapter. For an unsteady-state theory, we have:

$$\frac{\partial C_i}{\partial t} = -\nabla J_i + R_i \quad [4.38]$$

accumulation = change in flux + net rate of production

Whereas, for a steady-state theory,

$$-\nabla J_i + \mathcal{R}_i = 0 \quad [4.39]$$

change in flux + net rate of production = 0

For the laminar-diffusion based theories, we have,

$$\frac{\partial C_i}{\partial t} = -\nabla J_i + \mathcal{R}_i$$

$$\frac{\partial C_i}{\partial t} = D_i \nabla^2 C_i + \frac{D_i z_i}{RT} \mathcal{F} \nabla (C_i \nabla \Phi) + \mathcal{R}_i \quad [4.40]$$

where

$$-\mathcal{R}_i = \sum_{j=1}^{n_{\text{rex}}} v_{ij} r_j \quad [4.41]$$

An the expressions for  $\nabla \Phi$  and  $r_j$  are supplied in equations [4.18] and [4.35], respectively.

For the eddy diffusivity based theories, the equations are of the form:

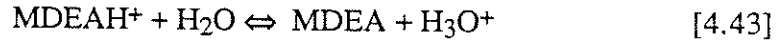
$$\frac{\partial C_i}{\partial t} = \nabla ((D_i + \epsilon x^2) \nabla C_i) + \frac{D_i z_i}{RT} \mathcal{F} \nabla (C_i \nabla \Phi) + \mathcal{R}_i \quad [4.42]$$

The steady-state theories are the same except that the derivatives with respect to time are cancelled.

#### 4.5 Two Alternative Formulations of the Material Balance Equations for Multiple Instantaneous Reactions

There are two distinct formulations of the material balance equations for mass transfer accompanied by instantaneous reaction. The first point to be stressed is that *no reaction*

is *instantaneous*. The fastest type of reactions relevant to acid gas treating processes are the proton transfer reactions, eg.:



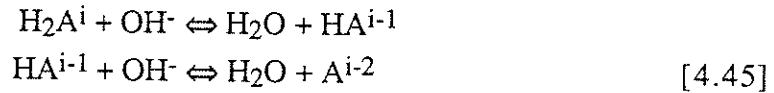
Proton transfer reactions can be considered instantaneous *with respect to the time frame for diffusion*. Therefore, for all practical purposes equilibrium equations can be used for the subset consisting of proton transfer reactions.

Two approaches were used during this work, both with success. The first approach was to write a differential equation for every species:

$$\frac{\partial C_i}{\partial t} = -\nabla J_i + \mathcal{R}_i \quad [4.44]$$

For *instantaneous* reactions, the rate constant is set to a very high value, e.g.  $1 \times 10^9$ , and equilibrium was checked calculating the equilibrium constant ratios in the boundary layer. The advantage of this approach is that it is straightforward.

An alternative approach is possible for equilibrium reactions. Consider a buffer system which is composed of the following reactions:



The original species has a charge  $i$ . Given the water and hydroxide concentrations, there are three unknowns, the concentration of  $\text{H}_2\text{A}$ ,  $\text{HA}$ , and  $\text{A}$ , and three equations may be written (assuming a steady-state theory):

$$D_{\text{H}_2\text{A}} \nabla^2 C_{\text{H}_2\text{A}} + D_{\text{HA}} \nabla^2 C_{\text{HA}} + D_{\text{A}} \nabla^2 C_{\text{A}} = -\mathcal{R}_{\text{prod,a}} \quad [4.46]$$

$$K_1 = \frac{[\text{H}_2\text{O}] [\text{HA}]}{[\text{H}_2\text{A}] [\text{OH}^-]} \quad [4.47]$$

$$K_2 = \frac{[\text{H}_2\text{O}] [\text{A}^{i-2}]}{[\text{HA}^{i-1}] [\text{OH}^-]} \quad [4.48]$$

The term  $\mathcal{R}_{\text{prod},a}$  corresponds to the net rate of production of buffer species A, which, as we shall see, may not necessarily be zero. Let us say we know the total amount of buffer species A. We have stated previously we know the amount of water and hydroxide. We may, therefore, by explicit formulation, determine each of the components of the buffer system as follows:

$$[\text{HA}^{i-1}] = K_2 \frac{[\text{H}_2\text{O}] [\text{A}^{i-2}]}{[\text{OH}^-]} \quad [4.49]$$

$$\begin{aligned} [\text{H}_2\text{A}] &= K_1 \frac{[\text{H}_2\text{O}] [\text{HA}^{i-1}]}{[\text{OH}^-]} \\ &= K_1 K_2 \frac{[\text{H}_2\text{O}] [\text{A}^{i-2}]}{[\text{OH}^-]} \end{aligned} \quad [4.50]$$

$$[\text{H}_2\text{A}] + [\text{HA}^{i-1}] + [\text{A}^{i-2}] = [\text{A}_{\text{tot}}] \quad [4.51]$$

Substituting, we find:

$$[\text{A}^{i-2}] = \frac{[\text{A}_{\text{tot}}]}{1 + K_2 \frac{[\text{H}_2\text{O}]}{[\text{OH}^-]} + K_1 K_2 \frac{[\text{H}_2\text{O}]^2}{[\text{OH}^-]^2}} \quad [4.52]$$

We can then find the concentration of the other two buffer species using equations [4.49] and [4.50]. This procedure may be extended or reduced to any arbitrary number of buffer species in an analogous manner.

## 4.6 Mass Transfer Equation Systems for Acid-Gas Absorption/Desorption with Alkanolamine-Based Systems

### *4.6.1 CO<sub>2</sub> Absorption into Mixed Amine Systems*

In the first formulation, we merely write the material balance equation for each chemical species:

$$\frac{\partial C_i}{\partial t} = -\nabla J_i + \mathcal{R}_i \quad [4.53]$$

The corresponding reaction rates at each point in the boundary layer are obtained using the reaction rate equations in Chapter 2. However, this can become unwieldy, and the second formulation offers a significant advantage - namely, the reduction in the number of differential equations. We combine the components into buffer systems - those subsets of chemical components which interchange amongst each other *instantaneously*. For the CO<sub>2</sub> - mixed alkanolamine system, the buffer systems are total DEA, total MDEA, and total carbonate. We can define a total of 6 external variables, from which all species concentrations may be determined explicitly:

$$\begin{aligned} \frac{\partial C_{\text{CO}_2}}{\partial t} &= -\nabla J_{\text{CO}_2} + \mathcal{R}_{\text{CO}_2} \\ \frac{\partial C_{\text{R}_2\text{NHT}}}{\partial t} &= -\nabla J_{\text{R}_2\text{NH}} - \nabla J_{\text{R}_2\text{NH}_2} - \mathcal{R}_{\text{R}_2\text{NCOO}} \\ \frac{\partial C_{\text{R}_2\text{NCOO}}}{\partial t} &= -\nabla J_{\text{R}_2\text{NCOO}} + \mathcal{R}_{\text{R}_2\text{NCOO}} \\ \frac{\partial C_{\text{R}_3\text{NT}}}{\partial t} &= -\nabla J_{\text{R}_3\text{N}} - \nabla J_{\text{R}_3\text{NH}} \\ \frac{\partial C_{\text{CO}_3\text{T}}}{\partial t} &= -\nabla J_{\text{HCO}_3} - \nabla J_{\text{CO}_3} + \mathcal{R}_{\text{HCO}_3} \\ \sum_{i=1}^N z_i C_i &= 0 \end{aligned} \quad [4.54]$$

where  $R_2NHT = R_2NH + R_2NH_2^+$ ,  $R_3NT = R_3N + R_3NH^+$ , and  $CO_3T = CO_3^{=} + HCO_3^-$ .  $R_2NH$  and  $R_3N$  designate secondary (or primary) and tertiary amines, respectively. Note that the carbamate species,  $R_2NCOO^-$ , is not considered part of the secondary amine buffer system since its transition to the amine  $R_2NH$ , is a finite rate reaction. For a similar reason,  $CO_2$  is not included in the total carbonate buffer system. We now have 6 equations corresponding to 6 unknowns ( $CO_2$ ,  $R_2NHT$ ,  $R_2NCOO^-$ ,  $R_3NT$ ,  $CO_3T$ , and  $OH^-$ ). The selection of hydroxide as the species corresponding to the charge balance may seem arbitrary, and to some extent this is true. However, by choosing hydroxide to be one of the external variables, we may solve for all of the internal variables, namely, the buffer species concentrations, by the explicit equations [4.49] through [4.52], shown in the previous section. This procedure then reduces the number of equations which must be solved by DASSL. Note that equations [4.54b,d,e] are obtained by linear combinations of the material balance equations for the individual species in the buffer system.

#### 4.6.2 *CO<sub>2</sub> Absorption into Mixed Amine Systems with Buffer Additives*

The addition of buffer additives may have several beneficial effects for gas absorption with chemical reaction. The model was modified to allow the addition of buffer additives, and, using the second formulation, this adds only 1 additional variable to the system. Consider a buffer additive A:

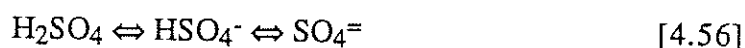
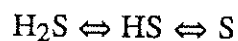
$$\frac{\partial C_{AT}}{\partial t} = -\nabla J_{H_2A} - \nabla J_{HA} - \nabla J_A \quad [4.55]$$

Once again, by defining the total amount of buffer species A as an external variable, all of the other species may be solved for explicitly using the buffer equilibrium relations. This approach has been used to simulate  $CO_2$  absorption into MDEA partially neutralized by the addition of sulfuric acid.



### 4.6.3 Simultaneous $H_2S/CO_2$ Absorption into Mixed Amine Systems

Once the methodology is developed to simulate  $CO_2$  absorption into amine systems with buffer additives, the simultaneous absorption of  $CO_2$  and  $H_2S$  is straightforward. The  $H_2S$  system is merely another buffer system, analogous to sulfuric acid:



The only difference lies in the boundary condition for the differential equation at the gas-liquid interface. For the sulfuric acid system, the boundary condition is that the net flux of the buffer species is zero, i.e. sulfuric acid is nonvolatile. For hydrogen sulfide, the boundary condition is not only tied not to the external variable,  $H_2S$ , but also to the buffer species  $H_2S$ , itself:

$$k_g (P_{H_2S} - (H_2S)_{int}) = J_{H_2S} + J_{HS} + J_S \quad [4.57]$$

## Chapter Five

### Models for Gas Absorption into a Turbulent Liquid Phase

This chapter reviews the theories for mass transfer into a turbulent liquid phase, and compares them briefly from a qualitative point of view. Each theory is then derived, showing how the assumed characteristics of the gas-liquid interface couple with the differential equations derived in Chapter 4 to provide an overall description of the gas absorption process. The effect of chemical reaction on gas absorption will be discussed from a quantitative point of view. The issue of simplifying approximations will also be discussed.

#### 5.1 Mass Transfer Models - An Overview

The oldest of the mass transfer theories studied is the film theory (Lewis and Whitman, 1924). In this theory, it is proposed that a stagnant film of liquid rests at the gas-liquid interface, and mass transfer from the gas to the liquid phase occurs by molecular diffusion only through this stagnant film. Below this film, the composition is uniform due to turbulence (see Figure 5.1). By nature, film theory is a steady-state theory and requires the solution of ordinary differential equations to determine concentration profiles in the boundary layer at a gas-liquid interface.

Penetration theory was introduced as a more realistic alternative to film theory (Higbie, 1935). Higbie proposed that elements of fluid rise from the bulk of the liquid to the interface, remain at the interface for a period of time known as the contact time, and are then swept back into solution. Danckwerts furthered this concept by assuming that the time of contact is not the same for all elements, but provided by a distribution of times (Danckwerts, 1951). His theory is known as surface renewal theory, and is characterized by the fraction of surface renewed per unit time. Under certain conditions, surface renewal theory provides a simpler analytical solution for the absorption rate; however, penetration theory is faster to solve numerically. Both penetration and surface renewal theories are unsteady-state theories, hence the

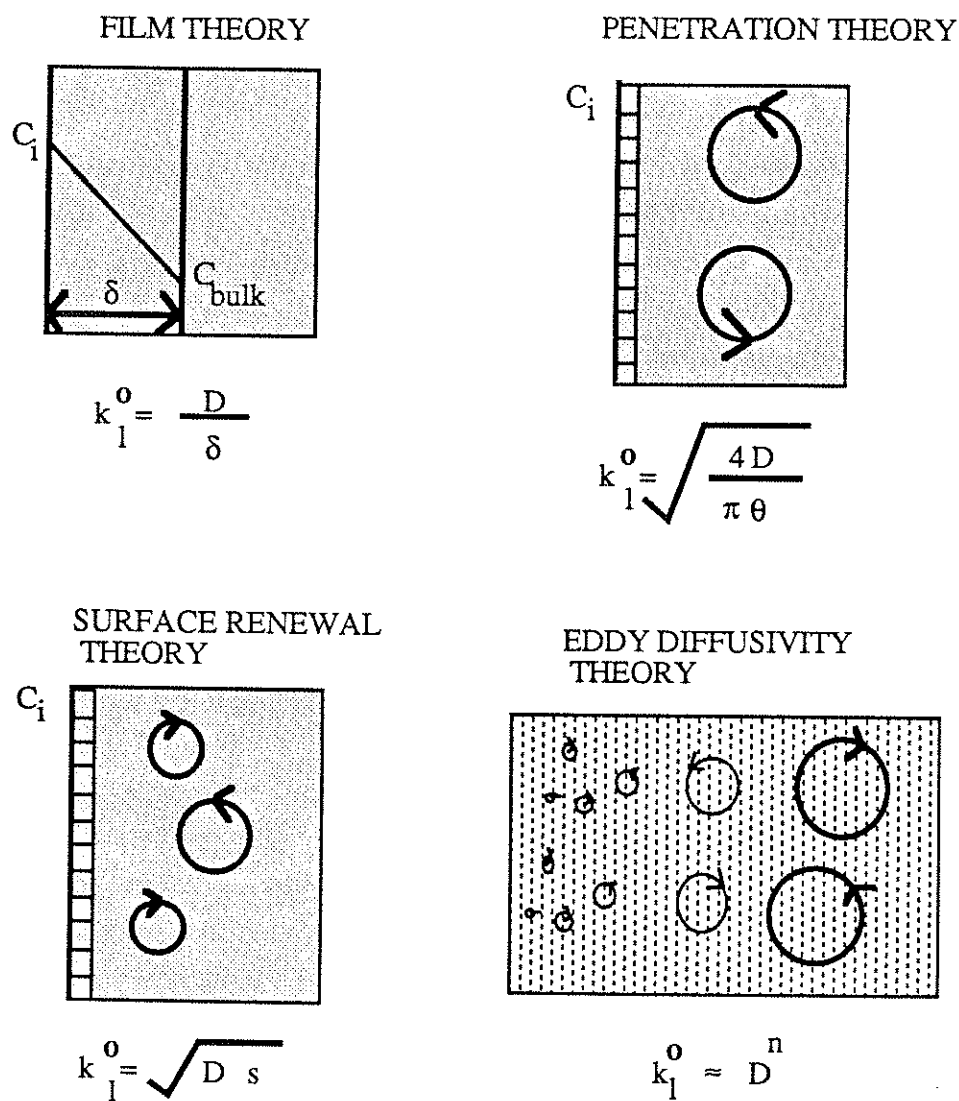


Figure 5.1 Liquid-Phase Mass Transfer Models

---

description of these theories involves the solution of partial differential equations. These theories are generally accepted as being more accurate than film theory for mass transfer at turbulent gas-liquid interfaces (Danckwerts, 1970), at the expense of additional computation time.

In all of the previously mentioned theories, the mass transfer occurs by diffusion through a laminar boundary layer, analogous to diffusion in a solid. However, in turbulent flow, a more realistic approach is the eddy diffusivity theory (King, 1966). Here, the diffusion coefficient is modified to allow for the effect of turbulent, as well as diffusive, transport in the boundary layer. We will use a simplified form of the eddy diffusivity theory (Prasher and Fricke, 1974) to reduce the number of unknown parameters. Eddy diffusivity theory can be treated as an unsteady-state theory, however, we choose to treat it as a steady-state alternative to film theory, and it will be shown that the steady-state eddy diffusivity theory, which involves the solution of ordinary, not partial, differential equations, is an excellent approximation to the unsteady-state surface renewal theory. The comparison is so good, in fact, that the use of an unsteady-state theory is not necessary for the reaction schemes considered in this work.

Approximate methods for several reaction schemes are also available. Specifically, the algebraic methods of DeCoursey (1982) and Onda et al. (1970a) are both available for second-order, reversible reactions. These methods are of limited use, however, for complex reaction schemes and will not be presented in comparison (this is not to say that the work of DeCoursey and Onda is not useful; quite to the contrary, under many circumstances, these approximations are quite valid and necessary, in light of the extensive computation time required to solve for the mass transfer theories rigorously). Another type of approximation is that due to Chang and Rochelle (1982) in which film theory is corrected to approximate surface renewal theory. This is done by adjusting the diffusion coefficients of all species (except the diffusing gas). The details and justification of this method will be discussed later.

The mass transfer models can be discriminated by observing the predicted effect of the diffusion coefficient on the mass transfer coefficient. This is difficult experimentally, however, since diffusion coefficients of gases in liquids vary over only a small range. Film theory predicts a linear dependence. Penetration and surface renewal theories predict a dependence to the one-half power, and the dependence for

the eddy diffusivity model varies, depending on parameter values. The general range for the experimentally determined diffusion coefficient dependence is 0.5 to 0.75, depending on the mass transfer equipment (Kozinski and King, 1955). However, this dependence can increase with the addition of surface active agents (Davies, 1980).

In a recent work, Seo and Lee (1988) measured the turbulence at a gas-liquid interface directly using a hot wire anemometer, and interpreted the data assuming a two-dimensional eddy model (Luk and Lee, 1986). This is significant since the interfacial behavior is measured directly, and not inferred from absorption data. An interesting analysis is provided based upon an assumed gamma distribution of contact times of elements at the gas-liquid interface (Bullin and Dukler, 1972). This model has, as limits, the surface renewal and Higbie penetration theories. It is shown that, for the stirred tank system studied, the true residence time distribution lies between the two models.

## 5.2 Unsteady-State Mass Transfer Theories

Before proceeding to discuss specific mass transfer theories in detail, let us examine the phenomenon of unsteady-state surface renewal from a general point of view. In order to determine the average absorption rate, we will need to determine the integrated absorption rate:

$$\bar{R} = \int_0^{\infty} \phi(t) R(t) dt \quad [5.1]$$

For any of the diffusion-based, unsteady-state theories, it is the fraction of surface area with the residence time  $t$ ,  $\phi(t)$ , which determines the mass transfer behavior. We show how this residence time distribution may be determined from an arbitrary surface renewal rate,  $s$ , which may or may not be a function of residence time,  $t$ .

Let us assume we know what fraction of the surface has a residence time of  $t$ , i.e., we know  $\phi(t)$ . Now, in the time interval from  $t$  to  $t + \Delta t$ , an arbitrary element will either be renewed by a turbulence mechanism, or it will remain at the interface. Therefore, we may form the following relation:

$$\phi(t) = \phi(t+\Delta t) + \int_t^{t+\Delta t} s(t') \phi(t') dt' \quad [5.2]$$

fraction of surface = fraction of surface + fraction of surface renewed  
at age  $t$  at age  $(t+\Delta t)$

We have implicitly defined the fraction of surface renewed per unit time as the product,  $s(t') \phi(t')$  (Note that  $t'$  is merely a dummy variable of integration). Now, by the mean theorem of calculus, we know

$$\exists \text{ some } \xi \in [t, t+\Delta t] : \phi(t+\Delta t) = \phi(t) + \left. \frac{d\phi}{dt} \right|_{\xi} \Delta t \quad [5.3]$$

By addition of equations [5.2] and [5.3], we arrive at the expression:

$$\left. \frac{d\phi}{dt} \right|_{\xi} = \frac{-1}{\Delta t} \int_t^{t+\Delta t} s(t') \phi(t') dt' \quad [5.4]$$

By taking the limit as  $\Delta t \Rightarrow 0$ , and  $\xi \Rightarrow t$ , we get the following:

$$\frac{d\phi}{dt} = -s(t) \phi(t) \quad [5.5]$$

Straightforward integration from 0 to  $t$  yields:

$$\phi = c \exp \left( - \int_0^t s(t') dt' \right) \quad [5.6]$$

where  $c$  is a constant of integration. We may determine this constant of integration by the necessary conditions that the the sum of surface fractions equals unity:

$$\int_0^{\infty} \phi(t) dt = 1 \quad [5.7]$$

We may now solve for the constant of integration:

$$c = \frac{1}{\int_0^{\infty} \exp\left(-\int_0^t s(t') dt'\right) dt} \quad [5.8]$$

Equations [5.6] and [5.8] are particularly useful since, given an arbitrary surface renewal function one may determine the function  $\phi$ , and the subsequent *average* mass transfer rate from equation [5.1]. The surface renewal function may be determined from the proposed physical characteristics of the system under consideration, or from the subsequent mathematical convenience it yields (we shall see this later with the Danckwert's surface renewal theory).

### 5.2.1 Penetration Theory

Given this general framework, let us assume that  $s = 0$  for  $t \in [0, \theta)$ , and  $s = \infty$  for  $t \in [\theta, \infty)$ , we have:

$$c = \frac{1}{\int_0^{\theta} \exp(-0) dt + \int_{\theta}^{\infty} \exp(-\infty) dt} = \frac{1}{\theta} \quad [5.9]$$

Using equation [5.6], we get:

$$\phi = \frac{1}{\theta} \quad \text{for } t \leq \theta$$

$$\phi = 0 \quad \text{for } t > \theta \quad [5.10]$$

This residence time distribution corresponds to the classic Higbie's penetration theory when coupled with the differential equations on an infinite domain.

We write the unsteady-state form of equation of the mass transfer equation:

$$D_i \nabla^2 C_i + z_i D_i \frac{F}{kT} \nabla(C_i \nabla \Phi) = \frac{\partial C_i}{\partial t} - R_i(C(x), t) \quad i = 1, \dots, N \quad [5.11]$$

The spatial domain,  $x$ , is on  $[0, \infty)$ . (i.e. the fluid element depth is infinite with respect to the penetration depth during the contact time). We now need the initial and boundary conditions. The initial conditions are assumed to be the same as the boundary conditions at infinity, since the fluid element is initially of uniform composition.

$$\begin{aligned} \text{at } x = 0, \text{ all } t \quad & C_1 = C_1^* \\ & J_i = 0 \quad i = 2, \dots, N \\ \text{at } x = \infty, \text{ all } t \quad & C_i = C_i^0 \quad i = 1, \dots, N \\ \text{all } x, t = 0 \quad & C_i = C_i^0 \quad i = 1, \dots, N \end{aligned} \quad [5.12]$$

Component 1 designates the absorbing gas. We assume that the interfacial concentration is known via Henry's law and the gas-phase partial pressure:

$$C_1^* = \frac{P_1}{H} \quad [5.13]$$

This assumption neglects gas-phase resistance, but is easily modified if necessary. We also assume that all other species are nonvolatile. The concentrations in the bulk are obtained from an equilibrium model, and the initial conditions assume that the infinitesimal elements are uniform in composition at the initial time.



The equations are integrated and the concentration gradient of the absorbing gas is obtained as a function of time, giving the average absorption rate:

$$\begin{aligned}\bar{R} &= \int_0^{\infty} \phi(t) R(t) dt \\ &= \frac{1}{\theta} \int_0^{\theta} R(t) dt\end{aligned}\quad [5.14]$$

The physical mass transfer coefficient for penetration theory is shown in equation [5.15] (Danckwerts, 1970). This expression is obtained by solving the material balance equation for the physical absorption of a gas, and determining the relationship between the average absorption rate, and the driving force,  $(C_1^* - C_1^0)$ :

$$k_l^0 = 2 \sqrt{\frac{D_1}{\pi \theta}} \quad [5.15]$$

The liquid-phase mass transfer coefficient is defined by the expression:

$$\bar{R}_{\text{phys}} = k_l^0 (C_1^* - C_1^0) \quad [5.16]$$

The enhancement factor is defined as the rate of absorption with chemical reaction divided by the rate of absorption without reaction:

$$E = \frac{\bar{R}}{\bar{R}_{\text{phys}}} \quad [5.17]$$

Using equations [5.14] and [5.16] we obtain the expression for the enhancement factor:

$$E = \frac{1}{\theta k_l^0 (C_1^* - C_1^0)} \int_0^{\theta} R(t) dt \quad [5.18]$$

As done by Versteeg (1986), the infinite  $x$  domain is mapped onto a finite domain using a time-dependent spatial transformation. Normally, there exists an infinite gradient in the gas concentration profile at the initial time, since the interfacial concentration is not the same as the bulk concentration. It is shown by Versteeg that this transformation compresses the spatial domain so that there is no such gradient at the initial time in  $r$  space:

$$r = \operatorname{erf} \left( \frac{x}{\sqrt{D\pi t}} \right) \quad [5.19]$$

This transformation is based upon the solution for physical absorption, and consequently the computed solution is a straight line in  $r$  space in the limit of no reaction. The derivation of the transformed equations was not presented by Versteeg; and the form of the resulting equations is not obvious, so a complete derivation is presented in Appendix A (in fact, the derivation presented in Appendix A is more general than that of Versteeg, since the possibility of electrical potential gradients is taken into account). The final equations after the error function transformation are:

$$\begin{aligned} \tau \left( \frac{\partial C_i}{\partial \tau} \right)_r = & \\ & 2\beta_i \frac{\exp(-2\xi^2)}{\pi D} \left( \frac{\partial C_i}{\partial r} \right)_\tau \left( \frac{\partial \Phi}{\partial r} \right)_\tau \\ & - \beta_i C_i \frac{2\xi \exp(-\xi^2)}{\sqrt{\pi D}} \left( \frac{\partial \Phi}{\partial r} \right)_\tau + \beta_i C_i \frac{2\exp(-2\xi^2)}{\pi D} \left( \frac{\partial^2 \Phi}{\partial r^2} \right)_\tau \\ & - D_i \frac{2\xi \exp(-\xi^2)}{\sqrt{\pi D}} \left( \frac{\partial C_i}{\partial r} \right)_\tau + D_i \frac{2\exp(-2\xi^2)}{\pi D} \left( \frac{\partial^2 C_i}{\partial r^2} \right)_\tau \end{aligned}$$

$$\begin{aligned}
& + \frac{2\xi \exp(-\xi^2)}{\sqrt{\pi}} \left( \frac{\partial C_i}{\partial r} \right)_{\tau} \\
& + 2\tau^2 \theta \mathcal{R}_i(\xi, \tau) \quad i = 1, \dots, N
\end{aligned} \tag{5.20}$$

In this equation,  $D$  is some reference variable, which should generally be set to the highest diffusion coefficient,  $\beta$  is  $\frac{z_i D_i F}{kT}$ , and  $\xi$  and  $\tau$  are dimensionless variables defined by the following equations:

$$\xi \stackrel{\text{df}}{=} \frac{x}{\sqrt{4Dt}} \tag{5.21}$$

$$\tau \stackrel{\text{df}}{=} \sqrt{\frac{t}{\theta}} \tag{5.22}$$

We may obtain the enhancement factors for penetration theory directly from the concentration profile in the transformed space as follows. By definition of the enhancement factor, we have:

$$2 \sqrt{\frac{D_1}{\pi \theta}} (C_1^* - C_1^0) E = \frac{-D_1}{\theta} \int_0^{\theta} \left( \frac{\partial C_1}{\partial x} \right)_{x=0} dt \tag{5.23}$$

From the definition of  $\tau$ , we have:

$$t = \tau^2 \theta \tag{5.24}$$

$$dt = 2\tau \theta d\tau \tag{5.25}$$

also,

$$\left(\frac{\partial C_1}{\partial x}\right)_{x=0} = \left(\frac{\partial C_1}{\partial r}\right)\left(\frac{\partial r}{\partial x}\right)_{x=0} \quad [5.26]$$

$$= \frac{e^{-\xi^2}}{\tau \sqrt{D_1 \pi \theta}} \left(\frac{\partial C_1}{\partial r}\right) \quad [5.27]$$

since  $\xi = 0$  when  $x = 0$ , we have

$$E = - \frac{\int_0^1 \left(\frac{\partial C_1}{\partial r}\right)_{\xi=0} d\tau}{(C_1^* - C_1^0)} \quad [5.28]$$

or, if  $D_1 \neq D$ , then

$$E = - \sqrt{\frac{D_1}{D}} \frac{\int_0^1 \left(\frac{\partial C_1}{\partial r}\right)_{\xi=0} d\tau}{(C_1^* - C_1^0)} \quad [5.29]$$

Using equation [5.28] or [5.29] eliminates the need to convert the concentration gradient from the transformed space into the real space in order to evaluate the enhancement factor and subsequent absorption rate.

### 5.2.2 Surface Renewal Theory

Let us assume that the function  $s(t)$  is now a constant,  $s$ . Upon solving equations [5.6] and [5.8] for our constant of proportionality and  $\phi$ , we obtain:

$$\phi = s \exp(-s t) \quad [5.30]$$

The physical mass transfer coefficient for surface renewal theory is shown in equation [5.31] (Danckwerts, 1970). As with penetration theory, this expression is obtained by solving the material balance equation for the physical absorption of a single species, and determining the relationship between the average absorption rate, and the driving force,  $(C_1^* - C_1^0)$ :

$$k_1^0 = \sqrt{D_1 s} \quad [5.31]$$

The average absorption rate with chemical reaction is:

$$\bar{R} = s \int_0^{\infty} e^{-st} R(t) dt \quad [5.32]$$

So we now obtain a different form of the enhancement factor expression:

$$E = \frac{1}{k_1^0 (C_1^* - C_1^0)} \int_0^{\infty} s e^{-st} R(t) dt \quad [5.33]$$

or, upon substitution for the mass transfer coefficient:

$$E = \frac{1}{(C_1^* - C_1^0) \sqrt{D_1 s}} s \int_0^{\infty} e^{-st} R(t) dt \quad [5.34]$$

Equation [5.34] has a desirable property. One may notice that the integral in equations [5.32] and [5.34] corresponds to the "s multiplied" Laplace transform of the absorption rate. Therefore, for a first-order reaction, one may take the Laplace transform of equation [5.11] and solve for the concentration profile and absorption rate in the Laplace transform domain. The enhancement factor and subsequent average absorption rate may then be determined without inversion of the Laplace transformed solution, leading to a simpler analytical solution than penetration theory (Danckwerts, pp. 108-109, 1970):

$$E = \sqrt{1 + M} \quad [5.35]$$

M is a measure of the importance of reaction to mass transfer rate, and the square root of M is known as the Hatta number (S. Hatta, as referenced by Sherwood and Pigford, 1952, conducted much of the original research on gas absorption with reaction):

$$M = \frac{D_1 k_1}{k_1^0{}^2} = Ha^2 \quad [5.36]$$

Equation [5.35] is much simpler than the corresponding equation for penetration theory (Danckwerts, 1970).

Numerically, we do not integrate for an infinite amount of time, of course, but up to a finite time  $\theta'$ :

$$E \equiv \frac{1}{(C_1^* - C_1^0) \sqrt{D_1 s}} \int_0^{\theta'} se^{-st} R(t) dt \quad [5.37]$$

where  $\theta' : se^{-s\theta'} R(\theta') \ll se^{-s\theta} R(\theta)$ , and  $\theta = \frac{4}{\pi s}$ , is the equivalent contact time (i.e.  $\theta$

is the contact time which gives the same physical absorption rate for penetration theory as does surface renewal theory with the distribution constant  $s$ ). Physically, we are neglecting the fraction of surface area with a contact time  $t > \theta'$ . As with penetration theory, we evaluate the enhancement factor from the concentration profile in the transformed space:

$$E \equiv \frac{-1}{(C_1^* - C_1^0) \sqrt{\pi s}} \int_0^{\theta'} \frac{1}{\sqrt{t}} se^{-st} \left( \frac{\partial C_1}{\partial r} \right)_{\xi=0} dt \quad [5.38]$$

Finally, we wish to integrate in dimensionless time  $\tau$ , where  $\tau = \sqrt{\frac{t}{\theta'}}$ . Transforming the variable of integration from  $t$  to  $\tau$ :

$$E \equiv \frac{-2 \sqrt{\theta'}}{(C_1^* - C_1^0) \sqrt{\pi s}} \int_0^1 s e^{-s\tau^2 \theta'} \left( \frac{\partial C_1}{\partial r} \right)_{\xi=0} d\tau \quad [5.39]$$

There are literally an infinite number of possible residence time distributions we can generate by this method. For example, it would be reasonable to assume that  $s$  is a constant for  $t \leq \theta$  and is infinite thereafter. However, such an endeavor would not be useful. To quote Andrew (1983): "It is the fate of theories of liquid film limited physical gas absorption to be used as a vehicle for the production of PhDs and learned papers and at the same time to be totally ignored by practicing designers...". We will stick to the classical penetration and surface renewal theory results, and indeed, show that there is only a minor difference between the two, well within the limit of experimental error.

### 5.3 Steady-State Mass Transfer Theories

#### *5.3.1 Film Theory*

Since film theory is a steady-state process, we write the steady-state form of the mass transfer equation:

$$D_i \nabla^2 C_i + z_i D_i \frac{F}{kT} \nabla(C_i \nabla \Phi) = -R_i(\underline{C}(x)) \quad i = 1, \dots, N \quad [5.40]$$

These equations are solved using the same boundary conditions as with penetration theory.

Solving equation [5.40] for the physical absorption of a nonionic species, we obtain the relationship between the physical mass transfer coefficient and the film thickness  $\delta$ . As noted earlier, the mass transfer coefficient is proportional to the diffusion coefficient to the first power:

$$k_1^0 = \frac{D_1}{\delta} \quad [5.41]$$

The enhancement factor is calculated using the results of the numerical solution, where, in this case,  $R$  is no longer a function of time.

$$E = \frac{R}{R_{\text{phys}}} = \frac{R}{k_1^0 (C_1^* - C_1^0)}$$

$$E = \frac{-\left(\frac{dC}{dx}\right)_{x=0}}{(C_1^* - C_1^0)} \quad [5.42]$$

### 5.3.2 Eddy Diffusivity Theory

For eddy diffusivity theory, we provide the following addition to the diffusion coefficient, as suggested by King (1966):

$$\nabla((D_i + \epsilon x^m)\nabla C_i) + z_i D_i \frac{F}{RT} \nabla(C_i \nabla \Phi) = \frac{\partial C_i}{\partial t} - \mathcal{R}_i(\underline{C}(x)) \quad i = 1, \dots, N \quad [5.43]$$

with  $0 \leq x < \infty$ . To solve this model, we must know at least three parameters,  $a$ ,  $m$  and at least one parameter describing a residence time distribution. We first simplify this theory to a steady-state theory, and then, following the suggestion of Prasher and Fricke (Prasher and Fricke, 1974) we assume a value of 2 for  $m$ . This provides the following relationship for the physical mass transfer coefficient:



$$k_1^0 = \frac{2}{\pi} \sqrt{\epsilon D_1} \quad [5.44]$$

In this manner, we have obtained a steady-state theory with the dependence of the mass transfer coefficient to the one-half power of the diffusion coefficient. The expression for the enhancement factor is the same as for film theory, using equation [5.44] for the mass transfer coefficient. As in the unsteady-state theories, we map the infinite domain onto a finite domain for computation:

$$r = \frac{2}{\pi} \tan^{-1} \left( x \sqrt{\frac{\epsilon}{D}} \right) \quad [5.45]$$

This transformation is based on the solution for physical absorption, and the concentration profile is a straight line in  $r$  space for physical absorption. As before, we present only the final equation, however, the complete derivation, along with the motivation for the particular transformation used in equation [5.45] is shown in Appendix A:

$$\begin{aligned} & D_i \left( \frac{2}{\pi} \cos^2 \left( \frac{\pi}{2} r \right) \sqrt{\frac{\epsilon}{D}} \right)^2 \nabla_r^2 C \\ & - D_i \frac{4}{\pi} \cos^3 \left( \frac{\pi}{2} r \right) \frac{\epsilon}{D} \sin \left( \frac{\pi}{2} r \right) \nabla_r C \\ & + 4 \tan \left( \frac{\pi}{2} r \right) \epsilon \frac{1}{\pi} \cos^2 \left( \frac{\pi}{2} r \right) \nabla_r C \\ & + \frac{D_i z_i}{RT} \mathcal{F} \left( \frac{2}{\pi} \cos^2 \left( \frac{\pi}{2} r \right) \sqrt{\frac{\epsilon}{D}} \right)^2 \nabla_r C \nabla_r \Phi \\ & + \frac{D_i z_i}{RT} \mathcal{F} C_i \left( \frac{2}{\pi} \cos^2 \left( \frac{\pi}{2} r \right) \sqrt{\frac{\epsilon}{D}} \right)^2 \nabla_r^2 \Phi \\ & - \frac{D_i z_i}{RT} \mathcal{F} C_i \left( \frac{4}{\pi} \cos^3 \left( \frac{\pi}{2} r \right) \frac{\epsilon}{D} \right) \sin \left( \frac{\pi}{2} r \right) \nabla_r \Phi = -\mathcal{R}_i(C(r)) \end{aligned} \quad [5.46]$$

One again, we arrive at an expression for the enhancement factor:

$$E = \frac{-\left(\frac{dC}{dx}\right)_{x=0}}{\frac{2}{\pi} \sqrt{\frac{\varepsilon}{D} (C_1^* - C_1^o)}} \quad [5.47]$$

We can also transform the enhancement factor expression to dimensionless space:

$$E = \frac{-\left(\frac{dC}{dr}\right)_{r=0}}{(C_1^* - C_1^o)} \sqrt{\frac{D_1}{D}} \quad [5.48]$$

### 5.3.3 Approximate Film Theory

Chang and Rochelle (1982) noted that film theory could be modified to approximate surface renewal theory if the diffusion coefficient of each species is corrected by a square root ratio of the species diffusion coefficient to the species on which the mass transfer coefficient is based, in this case, the absorbing gas:

$$D_{i,corr} = D_i \sqrt{\frac{D_1}{D_i}} \quad [5.49]$$

This approximation can be qualitatively justified by comparing the analytical solution of film and surface renewal theories for an instantaneous, irreversible, second-order reaction,  $A + B \Rightarrow C$ , in the limit of high enhancement factors (Danckwerts, 1970):

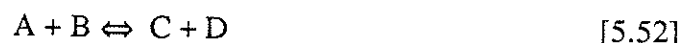
$$E_{surf} = \sqrt{\frac{D_a}{D_b}} + \frac{C_{b,bulk}}{C_{a,int}} \sqrt{\frac{D_b}{D_a}} \quad [5.50]$$

$$E_{film} = 1 + \frac{C_{b,bulk}}{C_{a,int}} \frac{D_b}{D_a} \quad [5.51]$$

Applying the correction factor will make the film theory solution quantitatively similar to surface renewal theory.

#### 5.4 Quantitative Effect of Chemical Reaction on the Gas Absorption Rate

We conclude this chapter by demonstrating quantitatively the effect chemical reaction can have on the absorption rate of a gas. We will show the results for a second-order, reversible reaction:



Upon examining Figure 5.2, we can see that, as the Hatta number (equation [5.36]) approaches 0, the enhancement factor approaches 1, as would be expected for physical absorption. At the intermediate values of the Hatta number, the enhancement factor is represented approximately by the following equation:

$$E = \sqrt{M} = Ha \quad [5.53]$$

which corresponds to equation [5.35] when  $M \gg 1$ . At this point, the enhancement factor, and subsequently the absorption rate, has a maximum sensitivity to the rate constant:

$$E \propto \sqrt{k_2} \quad [5.54]$$

It is at this condition that one should measure rate constants for a reaction using mass transfer equipment (more will be discussed on this subject in later chapters). Finally, the enhancement factor levels off, corresponding to the case when the reaction rate is *instantaneous* with respect to the mass transfer process. Under these conditions, the reaction is approaching equilibrium at all points in the boundary layer.

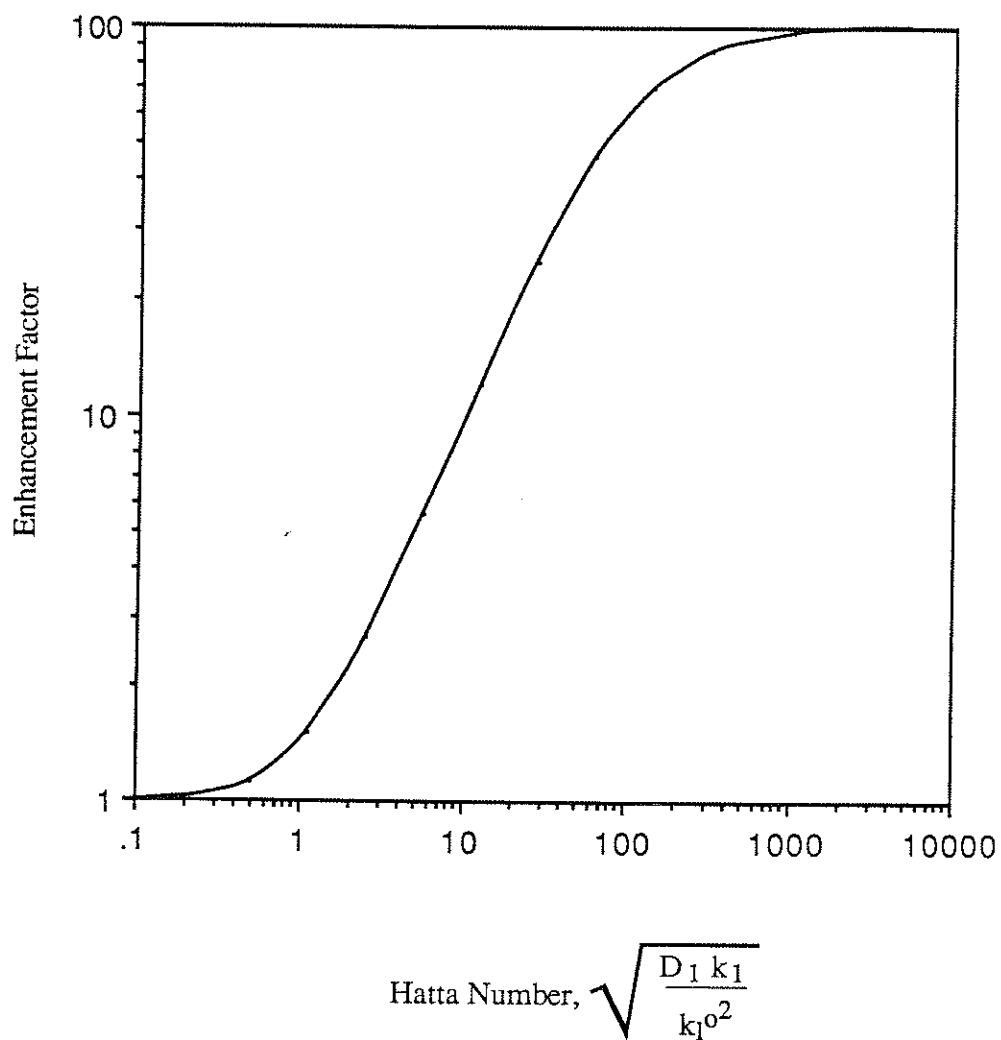


Figure 5.2 Enhancement Factor for a Second-Order, Reversible Reaction using Surface Renewal Theory,  $A + B \rightleftharpoons C + D$ .  $K_{eq} = 350$ ,  $D_B = D_C = D_D = 0.5D_A$ ,  $C_{B,bulk}/C_{A,int} = 200$ ,  $C_{A,bulk} = C_{B,bulk} = C_{C,bulk} = 0$

## Chapter Six

### Numerical Methods

#### 6.1 Review of Literature Methods for Gas Absorption with Chemical Reaction

##### *6.1.1 Unsteady-State Theories*

Analytical solutions to the penetration theory equations describing absorption with chemical reaction are available only for a few special cases (Secour and Beutler, 1967):

- (1) first-order, irreversible reaction
- (2) instantaneous, second-order, irreversible reaction
- (3) reversible reaction, first-order in both species
- (4) instantaneous, reversible reaction

When no analytical or approximate solution is available, it is necessary to rely on numerical techniques to estimate the effect of reaction rate on absorption, or to estimate a rate constant from absorption data.

The pioneering work in this field was published by Perry and Pigford (1953). They computed "point" mass transfer coefficients for the case of a second-order, reversible reaction. The average mass transfer coefficient, which is used to study the effect of reaction on absorption, must be obtained by taking the integrated average of the point mass transfer coefficient over time. The distance domain was modelled by finite differences and the explicit Euler method was used to integrate the equations in time. Due to the stiffness of the series of differential equations, the explicit technique is very inefficient for this case, and, as commented by Perry and Pigford, an "exceedingly small net size" was necessary to ensure convergence. It is interesting to note that they used an Ordvac computer, which contained 2000 vacuum tubes and 40 cathode ray tubes.

The next publication followed in 1961 by Brian et al. Results were presented for a second-order, irreversible reaction. The primary difference between this work and the previous work with respect to results is that the enhancement factors were presented for varying diffusion coefficient ratios of the reactants. Also, a wider range of the product  $k\theta$  (rate constant, contact time) was examined. The work was used to compare with an approximate solution for the enhancement factor with irreversible, second-order reaction. An implicit, finite difference technique was used for the time domain in this work; it was estimated by the authors that an explicit technique would have increased the computational time from 20 to over 1000 hours. Pearson (1963) published data very similar to that of Brian et al. (1961) at the same time. Pearson does, however, provide some interesting asymptotic expansions for limiting cases such as instantaneous reaction, and determines when such approximations are valid.

Brian (1964) studied general order, irreversible reactions ( $r=k[A]^n[B]^m$ ) for varying diffusion coefficient ratios. This work used finite differences with the Crank-Nicolson method to solve the two simultaneous differential equations. Brian noticed that when the order of reaction was less than unity, the numerical computations become unstable. This is not surprising, he notes, since this assumption (of reaction order less than unity) is not realistic at very low concentrations.

In 1965, Brian and Beaverstock studied a two step reaction:



A transformation of the distance,  $x$ , was used to generate a time dependent finite difference grid to reduce computation time:

$$\eta = \frac{x}{K'\sqrt{\theta + \epsilon'}} \quad [6.2]$$

$K'$  and  $\epsilon'$  are constants. The concentrations were predicted at half time intervals using an implicit Euler technique. These half time concentrations were then used in the

nonlinear reaction terms when predicting the concentration at the next time interval using the Crank-Nicolson method.

Secor and Beutler (1967) used an implicit Euler technique to solve the case of generalized, reversible kinetics. They transformed their infinite grid to a finite grid, independent of time:

$$x = \frac{c\eta}{1 - \eta} \quad [6.3]$$

Now,  $\eta$  is a dimensionless distance which varies from zero to one as  $x$  varies from zero to infinity.

Matheron and Sandall (1978) conducted one of the few studies on the effect of chemical reaction with Danckwert's surface renewal theory, as opposed to penetration (Higbie) theory. Their model analyzed a second-order, irreversible reaction:



To aid the computations, they divided the surface time distribution into two regions, one in which numerical computation was necessary, and the other in which an asymptotic approximation to the enhancement factor was appropriate. The enhancement factor for surface renewal theory can be calculated from an integral equation:

$$E = \frac{1}{C_{A0}\sqrt{D_{AS}}} \int_0^{\infty} se^{-st}R(t) dt \quad [6.5]$$

$R(t)$  can be obtained for many points in time from the intermediate solution of the partial differential equations. This solution is then simultaneously numerically integrated over time to obtain the enhancement factor. The asymptotic approximation used by Matheron and Sandall resulted in a two term expression for the enhancement factor:

$$E = \frac{1}{C_{Ao}\sqrt{D_{As}}} \int_0^{\tau_0} se^{-st}R(t) dt + E_{\text{asym}} \quad [6.6]$$

$\tau_0$  is the time at which the asymptotic solution,  $E_{\text{asym}}$ , is applicable. An interesting comparison between surface renewal and penetration theories was also provided. It was found that the enhancement factor was approximately the same (within 4%) for both models with the contact time defined appropriately:

$$\theta = \frac{4}{\pi s} \quad [6.7]$$

Cornelisse et al. (1980) studied the simultaneous absorption of  $\text{CO}_2$  and  $\text{H}_2\text{S}$ . The  $\text{CO}_2$  absorption rate was enhanced by reaction of amine to form carbamate, and the  $\text{H}_2\text{S}$  reaction with the amine was assumed to be instantaneous. They used a Newton-Raphson method to linearize the nonlinear reaction rate terms:

$$R_{n+1} \cong R_n + \left( \frac{\partial R}{\partial C} \right)_{C_n} (C_{n+1} - C_n) \quad [6.8]$$

This technique decoupled the simultaneous differential equations and allowed them to be solved as a set of linear equations. Cornelisse also used a three-point backward formula, instead of the standard two-point Euler or Crank-Nicolson formulas, to increase the accuracy:

$$\frac{\partial C}{\partial t} \cong \left( \frac{3C_{n+1} - 4C_n + C_{n-1}}{\Delta t^2} \right) \quad [6.9]$$

This equation is accurate to  $\Delta t^2$ , instead of  $\Delta t$ . Of course, a two-point backward formula is necessary for the first time step.



Versteeg (1986) used the same type of numerical scheme as Cornelisse et al., except he applied a time dependent transformation which significantly reduced the computational time:

$$\eta = \operatorname{erf}\left(\frac{x}{\sqrt{4Dt}}\right) \quad [6.10]$$

This transformation has a couple of interesting properties. First, it provides a time dependent spatial grid that is bounded between zero and one. Second, the grid width approaches zero as time approaches zero; therefore, concentration gradient of the absorbing gas is finite at zero time. Both of these properties aid in the numerical computation. Versteeg used this transformation to study general, reversible reactions and compared the results with approximations for second-order, reversible reactions.

Ozturk and Shah (1986) were the only authors reviewed who used orthogonal collocation on finite elements to solve the penetration theory equations. After converting the partial differential equations into a series of ordinary, coupled differential equations, they submitted them to an integrator to solve for the concentration distribution as a function of time. This technique is known as the method of lines. The interesting difference in their research, as opposed to the previous authors, is that they studied the effect of liquid-phase reactant volatility and found that increasing volatility can significantly decrease the enhancement factor. Table 6.1 presents a summary of the previous literature for the unsteady-state theories.

### 6.1.2 *Steady-State Theories*

The only steady-state theory found in the literature is the classical film theory. Generally, the solution of the film theory equations is more straightforward than the penetration theory equations. The differential equations are transformed into a set of nonlinear algebraic equations using finite differences in most cases. Some authors compared numerical solutions of film and penetration theories - comparisons will be discussed in more detail in the Chapter 8. Table 6.2 summarizes literature work on numerical solution of gas absorption with chemical reaction.

Table 6.1 Summary of Numerical Studies of Absorption with Chemical Reaction for the Unsteady-State Theories

Author	type of reaction	numerical method used	
		space	time
Perry et al. (1953)	2nd-order, reversible, irreversible	finite differences	explicit Euler
Brian et al. (1961)	2nd-order, irreversible unequal diffusion coeff.	finite differences	Crank-Nicolson
Pearson (1963)	2nd-order, irreversible unequal diffusion coeff.	finite differences	Crank-Nicolson
Brian (1964)	general, irreversible $r=k[A]^n[B]^m$ , unequal diffusion coefficients	finite differences	Crank-Nicolson
Brian et al. (1965)	2 step second-order $A+B \Rightarrow C$ , $A+C \Rightarrow D$ A is absorbing species	finite differences time dependent transformation	Crank-Nicolson
Secor et al. (1967)	general, reversible $A + B \rightleftharpoons C + D$ unequal diffusion coeff.	finite differences w/ transformation	implicit Euler

Table 6.1      Summary of Numerical Studies of Absorption with Chemical Reaction  
for the Unsteady-State Theories (Cont'd)

Author	type of reaction	numerical method used	
		space	time
Matheron et al. (1978)	2nd order, irreversible reaction, surface renewal theory	finite differences	Crank-Nicolson
Huang et al. (1980)	$A+B \Rightarrow C$ , $A+C \Rightarrow D$	collocation	method of lines
Cornelisse et al. (1980)	simultaneous absorption	finite differences	implicit, 3-point backward formula
Carta and Pigford (1983)	NO in Nitric Acid	finite-difference	implicit finite difference
Ozturk and Shah (1986)	2nd order, irreversible, volatile liquid-phase reactant	collocation on on finite elements time dep. trans.	method of lines
Versteeg (1986)	general, reversible	finite differences time dep. trans.	implicit, 3-point point backward

Table 6.2      Summary of Numerical Studies of Absorption with Chemical Reaction Using Film Theory

<u>Author</u>	<u>type of reaction</u>	<u>numerical method used</u>
Brian and Beaverstock (1965)	2 step second-order $A+B \Rightarrow C, A+C \Rightarrow D$ A is absorbing species	finite difference
Onda et al. (1970a),(1970b)	$A+B \rightleftharpoons C+D$	finite difference
Huang et al. (1980)	$A+B \Rightarrow C, A+C \Rightarrow D$	collocation
Carta and Pigford (1983)	NO in Nitric Acid	finite-difference
Ozturk and Shah (1986)	2nd order, irreversible, volatile liquid-phase reactant	collocation on on finite elements

## 6.2 Numerical Methods used in This Work

### *6.2.1 Spatial Dimension*

For each theory, a set of coupled, nonlinear differential equations must be solved. This is accomplished first by using orthogonal collocation on finite elements in the spatial dimension (Villadsen and Stewart, 1967; Villadsen and Michelson, 1978; Finlayson, 1980). The method is only briefly outlined here; the cited references contain the all the necessary background information. We first divide the domain into elements, and within each element the concentration of each species is approximated by a polynomial. The criterion for choosing the coefficients of the approximating polynomials is that the residuals of the differential equations, shown for film theory in equation [6.11] as an example, are zero at certain points, known as collocation points:

$$\text{Res} = D_i \nabla^2 C_i + z_i D_i \frac{F}{kT} \nabla(C_i \nabla \Phi) + \mathcal{R}_i(\underline{C}(x)) = 0 \quad i = 1, \dots, N \quad [6.11]$$

The residual for each component is satisfied at the collocation points, but not necessarily in between. Note that although the residual of the differential equation is satisfied at a collocation point, the solution,  $C$ , is not necessarily correct at that point. In our case, orthogonal collocation is being used, and the collocation points are the zeroes of a series of shifted Legendre polynomials on  $[0,1]$ , mapped into each element. In practice, however, we do not solve for the polynomial coefficients, but for the concentrations themselves. Consider the concentration of each species at any point in the element in terms of a Lagrange polynomial interpolated solution:

$$C_i = \sum_{k=1}^p C_{ik} l_k \quad [6.12]$$

The first and second derivatives can be expressed as a summation of derivative weights and the species concentration within each element:

$$\nabla C_{ij} = \sum_{k=1}^p C_{ik} A_{jk} \quad [6.13]$$

$$\nabla^2 C_{ij} = \sum_{k=1}^p C_{ik} B_{jk} \quad [6.14]$$

where the  $A_{jk}$  and  $B_{jk}$  are the derivatives of the Lagrange interpolation polynomial at the collocation point,  $j$ . The derivative weights are obtained from code based upon the routines in Villadsen and Michelsen (1978). Several elements are usually used, with the condition that at each element boundary, the flux is continuous:

$$J_i \Big|_{x^+} = J_i \Big|_{x^-} \quad [6.15]$$

where  $x^+$  and  $x^-$  denote the approach to the element boundary from the right and left sides, respectively.

### 6.2.2 *Unsteady-State Theories*

For the steady-state theories, the equations are subsequently transformed into a larger set of coupled, nonlinear algebraic equations. For the unsteady-state theories, applying collocation results in a set of coupled ordinary differential/algebraic equations which are integrated through time by DASSL (Petzold, 1983), a FORTRAN package which solves equations of the following form:

$$F(y, y', t) = 0 \quad [6.16]$$

This program uses backward differentiation formulas to integrate the differential equations. It can integrate using high order approximations and variable time steps. DASSL can perform numerical differencing for a Jacobian approximation, and takes advantage of banded Jacobians to reduce computation time (both of these features are utilized in this work). It is important to note that the algebraic and ordinary differential equations can be interspersed, and no extra work is required of the user than already required for packages which solve only ordinary differential equations.

This technique of transforming the partial differential equations into ordinary differential equations, and then using a general purpose program to solve the resulting set of equations, is known as the method of lines. It is a semi-discrete method, contrasted to a fully discretized method in which the time derivatives are replaced by a finite difference approximation. The method of lines is, in general, not as efficient computationally as the fully discretized methods (Kurtz et al., 1978), but it is easier to set up, and more importantly, to change problems. When used with a reliable integrating package, the method of lines can also be more robust.

For the penetration and surface renewal theories, we must integrate the concentration gradient through time. Since, in general, the solution will be available at variable time steps, we must use an integration method that does not require function evaluations at regular time intervals such as Simpson's Rule. Furthermore, we need a method that is accurate, since it would be wasteful to use smaller time steps in evaluating a set of perhaps 100 or more differential/algebraic equations in order to evaluate a single integral accurately. Therefore, we first interpolate the flux rate using Lagrange polynomials, then we integrate the interpolated solution using Gauss quadrature. This technique allows both high accuracy and does not restrict the point of function evaluation.

### 6.2.3 *Steady-State Theories*

The steady-state theories result in a set of coupled nonlinear algebraic equations. The solution to these equations is not trivial, especially when the nonlinear, complicating effect of the potential gradient coupling is included. MINPACK (Moré et al., 1980) was used with some success in solving the equations. However, this was not always successful for fast reaction rates using reasonable initial guesses. Therefore, the steady-state equations were also solved using a parametric continuation method (eg. Vickery et al., 1988). In this method, we vary a parameter continuously from a problem for which we know the solution, to a problem for which we need the solution. Let us take, for example, the film theory equations, and multiply each of the rate terms by a parameter,  $t$ :

$$D_i \nabla^2 C_i + z_i D_i \frac{F}{kT} \nabla(C_i \nabla \Phi) = -t \mathcal{R}_i(\underline{C}(x), t) \quad i = 1, \dots, N \quad [6.17]$$

When  $t$  is 0, the problem reduces to that of physical diffusion, and the solution is trivial. As  $t$  is advanced to 1, the solution changes from the trivial problem to a nontrivial problem that we wish to solve. There are many methods for tracking the solution (Watson and Scott, 1987). We choose to let DASSL integrate the equations, and have found no problems associated with this method. As discussed earlier, DASSL solves equations of the form  $F(y, y', t) = 0$ . To see how we use DASSL to solve the steady-state problem, consider the approach used by DASSL with an implicit first-order scheme for a scalar function, according to Petzold (1983):

$$F(t_n, y_n, \frac{y_n - y_{n-1}}{\Delta t_n}) = 0 \quad [6.18]$$

These equations are solved iteratively for  $y_n$  using Newton's method:

$$y_n^{m+1} = y_n^m - G^{-1} F(t_n, y_n^m, \frac{y_n^m - y_{n-1}}{\Delta t_n}) \quad [6.19]$$

where

$$G = \frac{\partial F}{\partial y'} + \frac{1}{\Delta t_n} \frac{\partial F}{\partial y} \quad [6.20]$$

and  $m$  is the iteration index. With the algebraic equation system, the first portion of the Jacobian,  $\partial F / \partial y'$  is zero, but as long as the Jacobian  $\partial F / \partial y$  is of full rank, then  $G$  may be inverted to solve the problem at each time step,  $t$ . It is interesting to note that with this method, we actually solve many real problems as we are proceeding along the path from  $t = 0$  to  $t = 1$ . If equation number [6.17] is put in dimensionless form, one sees that the effect is analogous to varying the mass transfer coefficient from infinity (no enhancement) to the finite value:

$$r = \frac{x}{\delta} \quad [6.21]$$



$$\begin{aligned}
d_i \nabla_r^2 C_i + z_i d_i \frac{F}{kT} \nabla_r (C_i \nabla_r \Phi) &= - \frac{\delta^2}{D_1} \mathcal{R}_i(x,t) \quad i = 1, \dots, N \\
&= - \frac{D_1}{k_1^{\phi 2}} \mathcal{R}_i(x,t)
\end{aligned} \tag{6.22}$$

Now  $\nabla_r$  denotes differentiation with respect to  $r$ , instead of  $x$ , and  $d_i$  are dimensionless diffusion coefficients,  $D_i/D_1$ . This method is also analogous to varying the rate constant for systems with a single reaction.

It seems unreasonable that the steady-state problem can be solved more easily as an unsteady-state problem, but this phenomenon has been noted by others (Wayburn and Seader, 1987). There is, however, one advantage that can be taken. Unlike the unsteady-state theories, the solution for  $t < 1$  does not have to be very accurate. Therefore, we use a low-order approximation in space (eg. 1 element), solve this problem until  $t = 1$ , then interpolate the solution, using Lagrange polynomials, to a new, more dense spatial grid. We solve this problem using MINPACK with the good initial guess. This general technique has been suggested before (Allgower and Georg, 1980), and it has proved to be the most reliable method we used to solve the boundary value problems. Furthermore, it has resulted in a significant reduction in computation time for the steady-state, as opposed to the unsteady-state, theories. This approach worked well for the MDEA system, however, for the faster reacting systems, we note that a number of elements must be used or else the solution itself will not converge at all. Even for these systems, the steady-state problem used much less computation time during parameter estimation as will be discussed in the section *Machine Independent Performance Enhancement*.

Since the equations for the mass transfer theories are similar, we use the same collocation code to solve all of the problems. We can neglect time derivatives for the steady-state theories, apply the appropriate transformation for each theory, and modify the diffusion coefficients for the eddy diffusivity theory. In this manner, a number of theories can be compared easily.

### 6.3 Verification of Model

The verification of the mass transfer model was carried out by comparison with the Secor and Beutler (1967) who solved for the case of a second-order, reversible reaction with penetration theory using a finite difference method in space and time. In addition, an approximate method of DeCoursey (1982) was also used to generate the enhancement factor. The results in Table 6.3 show that there is a discrepancy with the data of Secor and Beutler (1967), as indicated by Versteeg (1986), and that the approximation of Decoursey works reasonably well under the conditions shown. Decoursey's approximation, is, however, valid only for the limiting case that all species have the same diffusion coefficient.

### 6.4 Parameter Estimation

Much of the work has centered around the interpretation of experimental data using mechanistic models. It is therefore appropriate and necessary to discuss the methods used in the data regression. This section discusses two methods used: least squares and generalized least squares, and demonstrates why the method of generalized least squares is most suitable for our purposes. A most comprehensive text on the subject of nonlinear parameter estimation is the treatment of Bard (1974); however, the text by Draper and Smith (1981) and the review by Efron (1988) provide more comprehensible introductory treatments of the ideas surrounding nonlinear parameter estimation, and the underlying geometrical interpretation. The paper by Britt and Luecke (1973) provides a most comprehensible introduction to the topic of generalized least squares nonlinear parameter estimation.

Table 6.3 Comparison of Numerical Results for a Second-Order, Reversible Reaction with that of Secor and Beutler (1967) and DeCoursey (1982)

M'	K <sub>eq</sub>	q	Enhancement Factor		
			<u>This Work</u>	<u>Secor and Beutler</u>	<u>Decoursey</u>
1.0	0.20	1.0	1.20	1.20	1.19
		20.0	1.30	1.30	1.32
		100.0	1.30	1.30	1.33
	1.00	1.0	1.24	1.20	1.24
		20.0	1.30	1.30	1.30
		100.0	1.30	1.30	1.34
	5.00	1.0	1.25	1.25	1.25
		20.0	1.30	1.30	1.33
		100.0	1.30	1.30	1.34
100.0	0.20	1.0	1.35	1.35	1.34
		20.0	2.71	2.70	2.62
		100.0	4.42	-----	4.22
	1.00	1.0	1.60	1.40	1.58
		20.0	4.19	3.50	4.00
		100.0	6.51	6.05	6.24
	5.00	1.0	1.83	1.80	1.80
		20.0	5.94	5.95	5.67
		100.0	7.93	-----	7.79

$$M' = k_2 B^0 \theta$$

$$q = B^0 / A^*$$

8 elements and 2 internal collocation points were used

We assume that the errors in experimental data, denoted by the column vector  $\mathbf{e} \in \mathfrak{R}^q$ , are normally distributed about  $\mathbf{0} \in \mathfrak{R}^q$ , with a covariance matrix  $\mathbf{R} \in \mathfrak{R}^{q \times q}$ .

$$\mathbf{e} = \mathbf{z}_{\text{exp}} - \mathbf{z} \quad [6.23]$$

$$\mathbf{E}(\mathbf{e}) = \mathbf{0} \quad [6.24]$$

$$\mathbf{E}(\mathbf{e}\mathbf{e}^T) = \mathbf{R} \quad [6.25]$$

The vectors  $\mathbf{z}_{\text{exp}} \in \mathfrak{R}^q$  and  $\mathbf{z} \in \mathfrak{R}^q$  represent the experimentally observed and "true" values of the data.  $\mathbf{E}$  is the expectation functional, as indicated for an arbitrary function,  $f(\mathbf{x})$ :

$$\mathbf{E}(f(\mathbf{x})) = \int_{-\infty}^{\infty} f(\mathbf{x}) \, d\mathbf{x} \quad [6.26]$$

The diagonal elements of  $\mathbf{R}$  are the variances of the data, and the cross terms represent the covariance between the datapoints (and datasets).

It has been demonstrated by using the calculus of variations (Bard, p. 20, 1974) that the following likelihood function introduces the minimum amount of information into the parameter estimation problem:

$$L(\mathbf{z}, \theta) = (2\pi)^{-q/2} |\mathbf{R}|^{-1/2} \exp \left( -\frac{1}{2} (\mathbf{z}_{\text{exp}} - \mathbf{z})^T \mathbf{R}^{-1} (\mathbf{z}_{\text{exp}} - \mathbf{z}) \right) \quad [6.27]$$

where  $\theta \in \mathfrak{R}^P$  is a vector of parameters to be estimated\*. It is this likelihood function that must be maximized with respect to *both* the parameters  $\theta$  and the "true" data  $\mathbf{z}$  in

---

\* In order to conform to the nomenclature most often used in statistical analysis,  $\theta$  designates a vector-valued quantity of parameters estimated from the data. This is not to be confused with the quantity  $\theta$  used to designate the contact time for mass transfer used throughout the rest of the dissertation.

order to obtain a maximum likelihood estimate. If the covariance matrix is known a priori, then maximizing [6.27] is equivalent to minimizing equation [6.28].

$$\frac{1}{2} (\mathbf{z}_{\text{exp}} - \mathbf{z})^T \mathbf{R}^{-1} (\mathbf{z}_{\text{exp}} - \mathbf{z}) \quad [6.28]$$

We wish to minimize equation [6.28] subject to the condition that the model equations, say  $\mathbf{f}(\mathbf{z}, \boldsymbol{\theta}) \in \mathfrak{R}^{\text{nexp}}$   $\text{nexp} \geq q$ , are satisfied. This is a classical constrained optimization problem, which may be solved by the method of Lagrange multipliers. We form the Lagrangian  $Q$ , and find the stationary point with respect to  $\boldsymbol{\theta}$ ,  $\mathbf{z}$ , and  $\lambda$ :

$$Q = \frac{1}{2} (\mathbf{z}_{\text{exp}} - \mathbf{z})^T \mathbf{R}^{-1} (\mathbf{z}_{\text{exp}} - \mathbf{z}) + \lambda^T \mathbf{f}(\mathbf{z}, \boldsymbol{\theta}) \quad [6.29]$$

where  $\lambda \in \mathfrak{R}^{\text{nexp}}$ . The details of the derivation are provided in excellent detail by Britt and Luecke (1973), so only the results will be shown here:

$$\boldsymbol{\theta} - \boldsymbol{\theta}_i = \left[ \mathbf{F}_{\boldsymbol{\theta}}^T (\mathbf{F}_{\mathbf{z}} \mathbf{R} \mathbf{F}_{\mathbf{z}}^T)^{-1} \mathbf{F}_{\boldsymbol{\theta}} \right]^{-1} \mathbf{F}_{\boldsymbol{\theta}}^T (\mathbf{F}_{\mathbf{z}} \mathbf{R} \mathbf{F}_{\mathbf{z}}^T)^{-1} \left[ \mathbf{f}(\mathbf{z}_i, \boldsymbol{\theta}_i) + \mathbf{F}_{\mathbf{z}} (\mathbf{z} - \mathbf{z}_{\text{exp}}) \right] \quad [6.30]$$

and

$$\mathbf{z} - \mathbf{z}_i = \mathbf{z}_{\text{exp}} - \mathbf{z}_i - \mathbf{R} \mathbf{F}_{\mathbf{z}}^T (\mathbf{F}_{\mathbf{z}} \mathbf{R} \mathbf{F}_{\mathbf{z}}^T)^{-1} \left[ \mathbf{f}(\mathbf{z}_i, \boldsymbol{\theta}_i) + \mathbf{F}_{\mathbf{z}} (\mathbf{z} - \mathbf{z}_{\text{exp}}) + \mathbf{F}_{\boldsymbol{\theta}} (\boldsymbol{\theta} - \boldsymbol{\theta}_i) \right] \quad [6.31]$$

The Jacobian matrices  $\mathbf{F}_{\mathbf{z}} \in \mathfrak{R}^{n \times q}$  and  $\mathbf{F}_{\boldsymbol{\theta}} \in \mathfrak{R}^{n \times p}$  represent the partial derivatives of the function  $\mathbf{f}(\mathbf{z}, \boldsymbol{\theta})$  with respect to the data and the parameters, respectively. Equations [6.30] and [6.31] are the essence of the algorithm suggested by Deming (1943). First the Jacobian matrices are calculated, along with the values of the function  $\mathbf{f}$ . Then the parameters  $\boldsymbol{\theta}$  are updated using equation [6.30], and the data are then updated using equation [6.31]. The procedure is continued iteratively until convergence is indicated by the Euclidean norm between successive iterates of the parameters:

$$\|\theta - \theta_i\|_2 = \sqrt{\sum_{j=1}^p (\theta_j - \theta_{i_j})^2} \quad [6.32]$$

is satisfied by a given tolerance (actually Britt and Luecke also use the norm between successive iterates of the data, this was, however, disregarded in the present work).

The code that was developed and used in this work actually utilizes further assumptions about the data and error structure in order to minimize computational time. First of all, it is assumed that all of the errors between the datasets, and amongst each other within the same dataset, are uncorrelated. This has the computationally beneficial effect of rendering the matrix  $\mathbf{R}$  diagonal. It is composed of diagonal blocks  $\mathbf{R}_i \in \mathbb{R}^o$ , where  $o$  is the number of observations taken during each experiment:

$$\mathbf{R}_i = \begin{bmatrix} s_{i1}^2 & \dots & 0 \\ \vdots & \ddots & \vdots \\ 0 & \dots & s_{io}^2 \end{bmatrix} \quad [6.33]$$

therefore

$$\mathbf{R} = \begin{bmatrix} \mathbf{R}_1 & \dots & 0 \\ \vdots & \ddots & \vdots \\ 0 & \dots & \mathbf{R}_{n_{\text{exp}}} \end{bmatrix} \quad [6.34]$$

Note that, even had we not assumed the diagonal structure for  $\mathbf{R}$ , it would have had a half-bandwidth of  $o - 1$ , not  $q - 1$ , which is beneficial since, ordinarily,  $o$ , the number of observations in a single experiment, is much less than  $q$ , the number of observations per experiment times the number of experiments, i.e.  $o \ll q = o \times n_{\text{exp}}$ .

Now, the matrix product,  $\mathbf{F}_z \mathbf{R} \mathbf{F}_z^T$ , is diagonal and of the form:

$$[F_z R F_z^T]_{ii} = \begin{bmatrix} \sum_{i=1}^o f_{1i}^2 s_{1i}^2 & \dots & 0 \\ \vdots & \ddots & \vdots \\ 0 & \dots & \sum_{i=1}^o f_{1o}^2 s_{1o}^2 \end{bmatrix} \quad [6.35]$$

and

$$F_z R F_z^T = \begin{bmatrix} [F_z R F_z^T]_1 & \dots & 0 \\ \vdots & \ddots & \vdots \\ 0 & \dots & [F_z R F_z^T]_{n_{exp}} \end{bmatrix} \quad [6.36]$$

Now, the inversion that must be performed in equation [6.30] is simplified to the inverting of the diagonal elements. The elements  $f_{ji}$  correspond to the partial derivative of the constraint  $j$  with respect to the datapoint  $i$ , and is an element of the Jacobian matrix  $F_z$ . The only dense (however, symmetric) matrix which must be inverted is in equation [6.30]:

$$[F_\theta^T (F_z R F_z^T)^{-1} F_\theta]^{-1} \quad [6.37]$$

In reality, one never performs a matrix inversion unless absolutely necessary, but rather, equation [6.30] is recast in the form:

$$[F_\theta^T (F_z R F_z^T)^{-1} F_\theta] (\theta - \theta_i) = F_\theta^T (F_z R F_z^T)^{-1} [f(z_i, \theta_i) + F_z (z - z_m)] \quad [6.38]$$

Equation [6.38] is solved by standard method using LU decomposition (Noble and Daniel, 1988). The dimension of these linear equations is, however, normally quite

small compared to the total number of experiments. Most of the computation time is involved in evaluating the function  $f$  and the Jacobian matrices  $F_z$  and  $F_\theta$ . It is for this reason that much effort was put into utilizing techniques which calculate the Jacobian matrices efficiently.

For our situation, the iterative solution of the equations [6.30] and [6.31] are equivalent to minimizing the objective function:

$$S = \sum_{i=1}^{n_{\text{exp}}} \sum_{k=1}^o \left[ \frac{z_{ik,\text{pred}} - z_{ik,\text{exp}}}{s_{ik}} \right]^2 \quad [6.39]$$

Subject to the conditions:

$$f(z, \theta) = 0 \quad [6.40]$$

In order that the covariance matrix be known, we generally assume that the standard deviation is proportional to the observed error:

$$s_{ik} = s'_{ik} z_{ik,\text{exp}} \quad [6.41]$$

If we assume that only one variable is subject to error, and it can be represented in the following form:

$$y = g(z, \theta) \quad [6.42]$$

We can then reduce the problem to minimizing:

$$S = \sum_{i=1}^{n_{\text{exp}}} \left[ \frac{y_i - g_i(z_{i,\text{exp}}, \theta)}{s_i} \right]^2 \quad [6.43]$$



In this case, the Lagrangian formulation is no longer needed, since the substitution of  $g(x, \theta)$  for the predicted  $y$  has already been made. This is the standard formulation of least squares, which assumes that there is no error in the independent variables,  $z$ . The package GREG (Caracotsios, 1986) was used for the simplified least squares, and ideas from this code were used in the development of the generalized regression code developed in this work. The generalized least squares parameter estimation can, of course, default to ordinary least squares if only one variable is assumed to be subject to error. This method can, for certain situations with which we are concerned, create distressing results. It should be noted that the code GREG has a more sophisticated convergence checking procedure, and can handle the Box-Draper objective function as well. No attempt has been made to develop production quality code of this generality.

The parameter estimates are useless unless there is some idea of their certainty. For linear parameter estimation, one can calculate the covariance matrix of the estimates:

$$\mathbf{E}\{(\theta - \theta_0)(\theta - \theta_0)^T\} = [\mathbf{F}_\theta^T (\mathbf{F}_z \mathbf{R} \mathbf{F}_z^T)^{-1} \mathbf{F}_\theta]^{-1} \quad [6.44]$$

The right hand side has already been calculated (before the inversion) during the iterations. The diagonals of the inverted matrix correspond to the variances of the estimated parameters, which the off-diagonal elements correspond to the correlation between the parameters. Good parameter estimates are reflected by small values of the relative standard deviation:

$$\alpha_i = \frac{\sigma_{ii}}{\theta_i} \quad [6.45]$$

It would also be preferable to have no correlation between the parameter estimates. This correlation can be determined by evaluating the normalized covariance matrix, the elements of which are:

$$\omega_{ij} = \frac{\text{cov}(\theta_i, \theta_j)}{\sqrt{\text{Var}(\theta_i) \text{Var}(\theta_j)}} = \frac{\text{cov}(\theta_i, \theta_j)}{\sigma_i \sigma_j} \quad [6.46]$$

The off-diagonal elements are the cross-correlation coefficients between the parameters. In reality, even for a linear model, the values for the standard deviations are only an approximate view of the actual p-dimensional hypersurface. For the nonlinear problem, the situation is even worse, depending on the degree of curvature at the point of parameter estimates. The paper by Donaldson and Schnabel (1987) and the text by Bates and Watts (1988) provide much discussion on this matter. For the purposes of this work, the calculated standard deviations and the correlation matrix are taken to be valid statistical results.

## **6.5 Performance Enhancements**

Because of the relatively large amount of computation that must be performed during rate parameter estimation, much effort was made to improve the speed of the model. These techniques used fall into 2 classes:

- (1) improvements independent of the type of machine
- (2) improvements to enhance vector processor utilization

### ***6.5.1 Machine Independent Performance Enhancement***

For the parameter estimation problem, the number of calls to the actual model is:

$$\# \text{ exp } * (1 + F_{\text{jac}}(\# \text{ parms } + \# \text{ var } - 1)) * \# \text{ iterations} \quad [6.47]$$

So, the total CPU time is:

$$\# \text{ exp } * (1 + F_{\text{jac}}(\# \text{ parms } + \# \text{ var } - 1)) * \# \text{ iterations } * \text{ CPUtime/call} \quad [6.48]$$

$F_{\text{jac}}$  is, in this case, the fraction of the number of iterations during which partial derivatives with respect to the parameters and variables must be obtained.  $\# \text{ exp}$ ,  $\# \text{ parms}$ ,  $\# \text{ var}$  designate the number of experiments, number of parameters to be estimated, and the number of variables subject to error, respectively. For a typical parameter

In this case, the Lagrangian formulation is no longer needed, since the substitution of  $g(x, \theta)$  for the predicted  $y$  has already been made. This is the standard formulation of least squares, which assumes that there is no error in the independent variables,  $z$ . The package GREG (Caracotsios, 1986) was used for the simplified least squares, and ideas from this code were used in the development of the generalized regression code developed in this work. The generalized least squares parameter estimation can, of course, default to ordinary least squares if only one variable is assumed to be subject to error. This method can, for certain situations with which we are concerned, create distressing results. It should be noted that the code GREG has a more sophisticated convergence checking procedure, and can handle the Box-Draper objective function as well. No attempt has been made to develop production quality code of this generality.

The parameter estimates are useless unless there is some idea of their certainty. For linear parameter estimation, one can calculate the covariance matrix of the estimates:

$$\mathbf{E}\{(\theta - \theta_0)(\theta - \theta_0)^T\} = [\mathbf{F}_\theta^T (\mathbf{F}_z \mathbf{R} \mathbf{F}_z^T)^{-1} \mathbf{F}_\theta]^{-1} \quad [6.44]$$

The right hand side has already been calculated (before the inversion) during the iterations. The diagonals of the inverted matrix correspond to the variances of the estimated parameters, which the off-diagonal elements correspond to the correlation between the parameters. Good parameter estimates are reflected by small values of the relative standard deviation:

$$\alpha_i = \frac{\sigma_{ii}}{\theta_i} \quad [6.45]$$

It would also be preferable to have no correlation between the parameter estimates. This correlation can be determined by evaluating the normalized covariance matrix, the elements of which are:

$$\omega_{ij} = \frac{\text{cov}(\theta_i, \theta_j)}{\sqrt{\text{Var}(\theta_i) \text{Var}(\theta_j)}} = \frac{\text{cov}(\theta_i, \theta_j)}{\sigma_i \sigma_j} \quad [6.46]$$

The off-diagonal elements are the cross-correlation coefficients between the parameters. In reality, even for a linear model, the values for the standard deviations are only an approximate view of the actual p-dimensional hypersurface. For the nonlinear problem, the situation is even worse, depending on the degree of curvature at the point of parameter estimates. The paper by Donaldson and Schnabel (1987) and the text by Bates and Watts (1988) provide much discussion on this matter. For the purposes of this work, the calculated standard deviations and the correlation matrix are taken to be valid statistical results.

## **6.5 Performance Enhancements**

Because of the relatively large amount of computation that must be performed during rate parameter estimation, much effort was made to improve the speed of the model. These techniques used fall into 2 classes:

- (1) improvements independent of the type of machine
- (2) improvements to enhance vector processor utilization

### ***6.5.1 Machine Independent Performance Enhancement***

For the parameter estimation problem, the number of calls to the actual model is:

$$\# \text{ exp} * (1 + F_{\text{jac}}(\# \text{ parms} + \# \text{ var} - 1)) * \# \text{ iterations} \quad [6.47]$$

So, the total CPU time is:

$$\# \text{ exp} * (1 + F_{\text{jac}}(\# \text{ parms} + \# \text{ var} - 1)) * \# \text{ iterations} * \text{CPUtime/call} \quad [6.48]$$

$F_{\text{jac}}$  is, in this case, the fraction of the number of iterations during which partial derivatives with respect to the parameters and variables must be obtained.  $\# \text{ exp}$ ,  $\# \text{ parms}$ ,  $\# \text{ var}$  designate the number of experiments, number of parameters to be estimated, and the number of variables subject to error, respectively. For a typical parameter

estimation case, the number of experimental data points was 46, the number of parameters estimated was 2, the number of variables subject to error was 3, and the number of iterations was 8 (reasonably good initial guesses were supplied), with  $F_{jac} = 3/8$ . It was not unusual to have more experimental datapoints and more iterations until convergence. Assuming that the model takes only two CPU seconds to solve the problem, we find that the total CPU time = 1840 CPU sec.

However, the approach used in this work is slightly different. In this case, a Newton-Raphson method was used after the initial solution of the equations, in which case the typical CPU time was 0.2 seconds. A check was implemented in the program which would automatically divert the problem from the Newton-Raphson method back to the homotopy continuation method if a difficulty in convergence is detected. For the latter approach, the total CPU time is given by:

$$\begin{aligned} & \# \text{exp} * (\text{initial CPUtime/call}) + \\ & \# \text{exp} * \left( 1 + \frac{F_{jac}}{1 - \frac{1}{\# \text{iterations}}} (\# \text{parms} + \# \text{var} - 1) \right) \\ & * (\# \text{iterations} - 1) (\text{CPUtime/call}) \end{aligned} \quad [6.49]$$

This yields a total of 267 CPU sec, a factor of 7 reduction in computation time. Such a reduction in computation time makes the estimation of rate parameters using the differential equation model a much more viable option.

### 6.5.2 Machine Dependent Performance Enhancement - Vectorizability

The ability to vectorize certain types of calculations will increase the speed of a Cray X-MP/24 by approximately a factor of 10 (a higher factor, about 14, has been noted when the chaining of addition and multiplication is considered). Of course, not all of the code will vectorize efficiently, and the potential speedup of computer code on a vector processor is estimated by using Amdahl's law (Levesque and Williamson, 1988):

$$P = \frac{1}{1 - \frac{(VS-1)}{VS} * F_v} \quad [6.50]$$

where VS is the speedup factor (assume 10), and  $F_v$  is the fraction of code that is vectorized. In the case used here, analysis indicated that most of the computation time was spent in two types of routines: (1) LINPACK subroutines used by the DASSL program and the Newton-Raphson method, and (2) a subroutine which was used to calculate the first and second spatial derivatives of the concentration variables via equations [6.13] and [6.14]. The LINPACK routines already vectorize well, and, although other programs exist which perform better on the CRAY X-MP, this was not considered to be a problem. The calculation of the spatial derivatives, on the other hand, was a problem, and optimization of the code decreased computation time significantly (by about 30%). The technique used to optimize the code was to perform loop unrolling (see Levesque and Williamson).

estimation case, the number of experimental data points was 46, the number of parameters estimated was 2, the number of variables subject to error was 3, and the number of iterations was 8 (reasonably good initial guesses were supplied), with  $F_{jac} = 3/8$ . It was not unusual to have more experimental datapoints and more iterations until convergence. Assuming that the model takes only two CPU seconds to solve the problem, we find that the total CPU time = 1840 CPU sec.

However, the approach used in this work is slightly different. In this case, a Newton-Raphson method was used after the initial solution of the equations, in which case the typical CPU time was 0.2 seconds. A check was implemented in the program which would automatically divert the problem from the Newton-Raphson method back to the homotopy continuation method if a difficulty in convergence is detected. For the latter approach, the total CPU time is given by:

$$\begin{aligned} & \# \text{exp} * (\text{initial CPUtime/call}) + \\ & \# \text{exp} * \left( 1 + \frac{F_{jac}}{1 - \frac{1}{\# \text{ iterations}}} (\# \text{ parms} + \# \text{ var} - 1) \right) \\ & * (\# \text{ iterations} - 1) (\text{CPUtime/call}) \end{aligned} \quad [6.49]$$

This yields a total of 267 CPU sec, a factor of 7 reduction in computation time. Such a reduction in computation time makes the estimation of rate parameters using the differential equation model a much more viable option.

### 6.5.2 Machine Dependent Performance Enhancement - Vectorizability

The ability to vectorize certain types of calculations will increase the speed of a Cray X-MP/24 by approximately a factor of 10 (a higher factor, about 14, has been noted when the chaining of addition and multiplication is considered). Of course, not all of the code will vectorize efficiently, and the potential speedup of computer code on a vector processor is estimated by using Amdahl's law (Levesque and Williamson, 1988):

$$P = \frac{1}{1 - \frac{(VS-1)}{VS} * F_v} \quad [6.50]$$

where VS is the speedup factor (assume 10), and  $F_v$  is the fraction of code that is vectorized. In the case used here, analysis indicated that most of the computation time was spent in two types of routines: (1) LINPACK subroutines used by the DASSL program and the Newton-Raphson method, and (2) a subroutine which was used to calculate the first and second spatial derivatives of the concentration variables via equations [6.13] and [6.14]. The LINPACK routines already vectorize well, and, although other programs exist which perform better on the CRAY X-MP, this was not considered to be a problem. The calculation of the spatial derivatives, on the other hand, was a problem, and optimization of the code decreased computation time significantly (by about 30%). The technique used to optimize the code was to perform loop unrolling (see Levesque and Williamson).



## Chapter Seven

### Experimental Apparatus and Procedure

There are several methods by which to obtain rate constants for the reaction of CO<sub>2</sub> with alkanolamines. One method is the rapid mixing method (or stopped flow technique), by which the reactants are introduced in aqueous streams, and the change in a physical property is measured. Alper (1989) for example, used this method to determine the reaction rate of COS with Diglycolamine by measuring the change in conductivity once the reactants are introduced. There is inevitably, however, experimental error at the start of the experiment because of the inhomogeneous nature of the mixture at the point of introduction. This can cause problems with some of the faster reactions (the reactions of COS are analogous to those with CO<sub>2</sub> because of the similar electron structure of both molecules, however, CO<sub>2</sub> typically reacts 100 times faster with a given amine). In addition, the conductivity must be related to the ionic strength and subsequent concentration of CO<sub>2</sub>. Another method is to continuously flow the mixture through a tube and measure the reaction rate by the temperature rise (Hikita et al., 1977). This method has not been very successful, however, because the temperature effect from viscous heating is not negligible, and the heats of reaction must be known in advance.

By far, the most popular method for measuring CO<sub>2</sub> reaction rates is by chemical absorption. To be sure, this method has its own set of drawbacks. For example, mass transfer limitations can obscure the results, errors in assumed equilibrium behavior can cause error in the interpreted rates, and other transport properties, such as the diffusion coefficient of the absorbing gas, must be known in order to calculate a rate constant. The equation for absorption with first-order reaction has been used by most authors:

$$R = \frac{\sqrt{k_1 D + k_1^2}}{H} (P - P^*) \quad [7.1]$$

This equation is only valid when the diffusion of the liquid-phase reactants to the interface is negligible. Also, we see that the sensitivity of the absorption rate to the rate constant is to the  $1/2$  power. Under other conditions, when the diffusion of reactants to the interface is important, this dependence will only decrease. The compensation for this shortcoming is that the rate constants so determined will most likely be used to predict chemical absorption rates, and so the same lack of sensitivity in determining the rate constant will obscure the errors in the predicted absorption rate.

The predominance of the chemical absorption method is its ease of use, and accurate results given properly designed experiments. A fundamental model of the sort developed in this work is quite useful in checking assumptions and interpreting experimental data when equation [7.1] does not hold. Several types of equipment can be used for absorption measurements, with varying mass transfer coefficients (see Figure 7.1). The stirred tank, which was used in this work, has the lowest mass transfer coefficient, and is the easiest equipment to design and operate. Its disadvantage is that its low mass transfer coefficient makes it susceptible to the aforementioned mass transfer limitations. The wetted wall and wetted sphere are useful to obtain higher mass transfer coefficients. The laminar jet has very high mass transfer coefficients. The laminar jet can also be used to measure diffusion coefficients of slow reacting amines since the reaction rate is not fast enough to affect absorption rates. However, this piece of equipment is very difficult to operate, since the jet itself must be perfectly aligned between the exit nozzle of the jet, and the jet receptor.

## 7.1 Procedure

Because of its ease of use, and the relatively slow speed of the reaction rates to be determined in this work, the stirred tank was used for the chemical absorption measurements in this work. The same apparatus has been used previously, but modifications were made in order to improve the accuracy of the results. The procedure was carried out in a straightforward manner:

## Chapter Seven

### Experimental Apparatus and Procedure

There are several methods by which to obtain rate constants for the reaction of CO<sub>2</sub> with alkanolamines. One method is the rapid mixing method (or stopped flow technique), by which the reactants are introduced in aqueous streams, and the change in a physical property is measured. Alper (1989) for example, used this method to determine the reaction rate of COS with Diglycolamine by measuring the change in conductivity once the reactants are introduced. There is inevitably, however, experimental error at the start of the experiment because of the inhomogeneous nature of the mixture at the point of introduction. This can cause problems with some of the faster reactions (the reactions of COS are analogous to those with CO<sub>2</sub> because of the similar electron structure of both molecules, however, CO<sub>2</sub> typically reacts 100 times faster with a given amine). In addition, the conductivity must be related to the ionic strength and subsequent concentration of CO<sub>2</sub>. Another method is to continuously flow the mixture through a tube and measure the reaction rate by the temperature rise (Hikita et al., 1977). This method has not been very successful, however, because the temperature effect from viscous heating is not negligible, and the heats of reaction must be known in advance.

By far, the most popular method for measuring CO<sub>2</sub> reaction rates is by chemical absorption. To be sure, this method has its own set of drawbacks. For example, mass transfer limitations can obscure the results, errors in assumed equilibrium behavior can cause error in the interpreted rates, and other transport properties, such as the diffusion coefficient of the absorbing gas, must be known in order to calculate a rate constant. The equation for absorption with first-order reaction has been used by most authors:

$$R = \frac{\sqrt{k_1 D + k_1^{\circ 2}}}{H} (P - P^*) \quad [7.1]$$

This equation is only valid when the diffusion of the liquid-phase reactants to the interface is negligible. Also, we see that the sensitivity of the absorption rate to the rate constant is to the  $1/2$  power. Under other conditions, when the diffusion of reactants to the interface is important, this dependence will only decrease. The compensation for this shortcoming is that the rate constants so determined will most likely be used to predict chemical absorption rates, and so the same lack of sensitivity in determining the rate constant will obscure the errors in the predicted absorption rate.

The predominance of the chemical absorption method is its ease of use, and accurate results given properly designed experiments. A fundamental model of the sort developed in this work is quite useful in checking assumptions and interpreting experimental data when equation [7.1] does not hold. Several types of equipment can be used for absorption measurements, with varying mass transfer coefficients (see Figure 7.1). The stirred tank, which was used in this work, has the lowest mass transfer coefficient, and is the easiest equipment to design and operate. Its disadvantage is that its low mass transfer coefficient makes it susceptible to the aforementioned mass transfer limitations. The wetted wall and wetted sphere are useful to obtain higher mass transfer coefficients. The laminar jet has very high mass transfer coefficients. The laminar jet can also be used to measure diffusion coefficients of slow reacting amines since the reaction rate is not fast enough to affect absorption rates. However, this piece of equipment is very difficult to operate, since the jet itself must be perfectly aligned between the exit nozzle of the jet, and the jet receptor.

## 7.1 Procedure

Because of its ease of use, and the relatively slow speed of the reaction rates to be determined in this work, the stirred tank was used for the chemical absorption measurements in this work. The same apparatus has been used previously, but modifications were made in order to improve the accuracy of the results. The procedure was carried out in a straightforward manner:

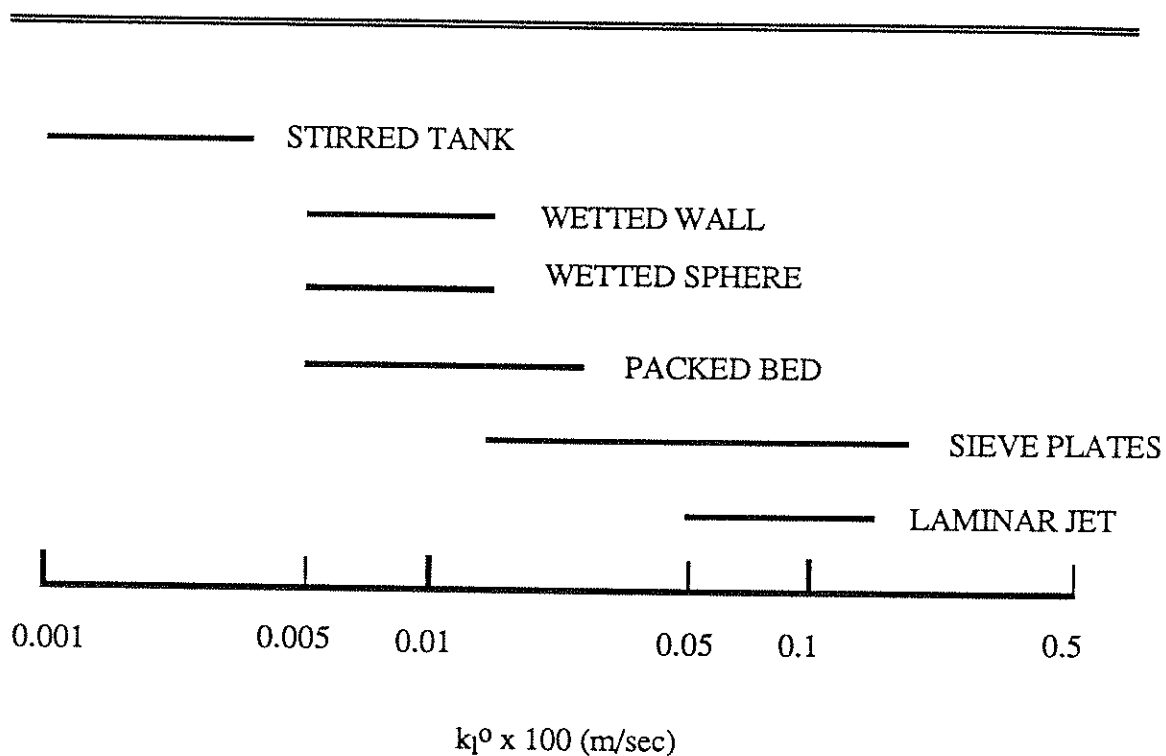


Figure 7.1 Liquid-Phase Mass Transfer Coefficients for Various Types of Equipment (Astarita et al., 1983; Fair, J., 1987)

- (1) assemble the apparatus and make improvements
- (2) calibrate supplemental equipment
- (3) calibrate the equipment with physical absorption measurements
- (4) measure the chemical absorption rates of MDEA, DEA, and mixtures of  
DEA/MDEA

Each of these tasks will be discussed in turn.

## 7.2 Apparatus Assembly and Operation

A schematic of the stirred tank apparatus used in this work is shown in Figure 7.2. The procedure was based primarily on that of Critchfield (1988). The reactor itself is made from plexiglass, with gas- and liquid-phase stirrers attached to the same shaft. The interfacial area was  $0.0146 \text{ m}^2$ . The mass transfer coefficient of the liquid phase could be adjusted by adjusting the speed of rotation of the shaft (Critchfield showed that the gas-phase mass transfer coefficient was high enough to have a negligible effect).  $\text{CO}_2$  or a mixture of  $\text{CO}_2$  and  $\text{N}_2$  were passed through a presaturator to prevent desorption of water in the reactor, causing a subsequent lowering of the interfacial temperature. The gas was passed through a condensor, which used water from an ice bath, to ensure that the water in the gas phase would not condense inside the gas-phase  $\text{CO}_2$  analyzer. The temperature was maintained at a constant level by a temperature bath which also contained the presaturator. The line from the presaturator to the reactor was heat traced to prevent condensation of water inside the line. The total pressure relative to atmospheric was determined by a pressure sensor attached to the top of the reactor. The atmospheric pressure was determined on a daily basis by the use of a mercury manometer. The  $\text{CO}_2$  partial pressure, which could be varied by varying the relative flowrates of  $\text{CO}_2$  and  $\text{N}_2$  was determined by the gas-phase outlet composition. Of course, the partial pressure of  $\text{CO}_2$  was corrected by the vapor pressure of water, a non-trivial correction for the experiments taken at  $40^\circ\text{C}$ .

The absorption rate of  $\text{CO}_2$  could be determined by two methods. First, for mixtures of  $\text{CO}_2$  and  $\text{N}_2$ , an analysis of the gas-phase composition and subsequent material balance between the inlet and outlet gas stream can provide the net rate of  $\text{CO}_2$  flux. Second, since the liquid phase is operated in a batch mode, the liquid can be analyzed for total  $\text{CO}_2$  concentration by removing small amounts of liquid samples using 10 and 100  $\mu\text{l}$  syringes, and injecting them into a total inorganic carbon analyzer. The first method is questionable for two reasons: first, the rate of absorption of  $\text{CO}_2$  is obtained by taking the difference of two relatively large numbers, in order to obtain a small number; second, the water is not totally removed by the gas-phase condenser, and can affect the material balance. The second method is considered to be more reliable because, although a single point may be in error, a number of datapoints can be taken at regular intervals, and a smooth interpolation curve may be obtained to

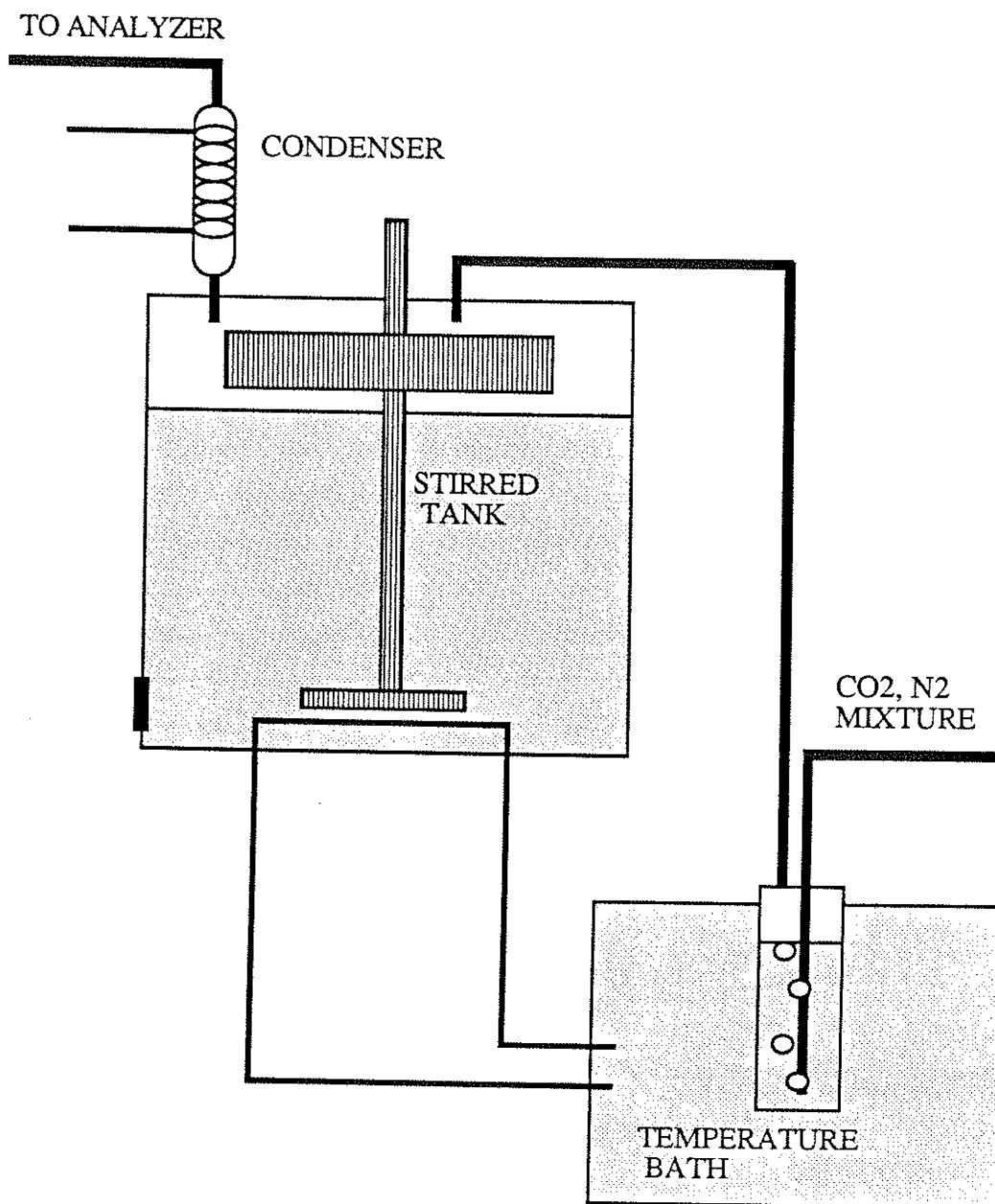


Figure 7.2 Stirred Tank System Used in CO<sub>2</sub> Absorption Experiments

reduce the effect of experimental error.

Before each experiment, the temperature bath and reactor were allowed to reach a thermal steady-state, and then the CO<sub>2</sub> was then passed over the reactive solution. Concentration measurements and gas-phase outlet compositions were measured over the course of the experiment.

### **7.3 Calibration and Use of Supplemental Equipment**

Gas flow rates were determined using Brooks model 5850E gas flow controllers. As the gas flows through the controller, it is heated. There are temperature sensors on both sides of the heater, and the flowrate may be determined by the temperature difference between the upstream and downstream temperature detectors. This temperature difference is a function of the flowrate, heat capacity, and thermal diffusivity of the gas. The accuracy is reported to be 1% of full scale; the repeatability is 0.25% of the rate.

The flowmeters were carefully calibrated before use by means of a soap film meter. An interesting problem occurs, however, if one tries to use a soap film meter to measure CO<sub>2</sub> flowrates. Most soap solutions are basic, and, at low flowrates, the reaction of the acidic CO<sub>2</sub> with the basic soap solution can provide an absorption rate comparable to the flowrate of CO<sub>2</sub>, within the soap film meter itself. This reaction can be evidenced by the solid reaction products which form in the soap solution. The result is that the interpreted absorption rate of CO<sub>2</sub> is much lower than the actual flowrate. For this reason, all of the calibrations were performed using nitrogen, and a conversion factor provided by the manufacturer was used to estimate the CO<sub>2</sub> flowrate. This conversion factor was checked using a cationic surfactant (therefore acidic in nature), Dodecyltrimethyl ammonium bromide, and was found to be valid within experimental error. Due to the widespread use of soap film meters to measure CO<sub>2</sub> absorption rates in laminar jets, the author wonders why this problem has not been mentioned in the literature before.

Gas-phase analysis was conducted using a Horiba PIR-2000 Infrared gas-phase analyzer with a 0-25 vol % range and a repeatability of 0.5% full scale. The principle of operation is the use of infrared absorption spectroscopy to determine the CO<sub>2</sub> concentration in the gas phase. This analyzer was calibrated using a premixed sample



of 10 % CO<sub>2</sub> in N<sub>2</sub>, and using mixtures of CO<sub>2</sub> and N<sub>2</sub> from the precalibrated mass flow controllers.

The liquid-phase CO<sub>2</sub> concentration was determined using an Oceanography International Model 525 Carbon Analyzer. The principle of operation is simple: Nitrogen is bubbled through a very acidic solution of 30 wt % phosphoric acid. A small amount of solution is injected into the acidic solution, which almost instantly reverses any reactions of the CO<sub>2</sub> with the basic amine. The CO<sub>2</sub> is then freed from solution and passes with the nitrogen stream to another gas-phase Horiba Analyzer (a Model PIR-2000 with a 0-0.25 vol % range). The total signal is integrated, and the integrated value is related to the total CO<sub>2</sub> concentration. This analyzer was susceptible to drift from day to day and from hour to hour. For this reason, the analyzer was *constantly* and *simultaneously* calibrated using sodium carbonate solutions, each time an experiment was run. For every experiment, a new calibration curve was developed and used to interpret the concentration of CO<sub>2</sub> in the liquid phase. Because of this procedure, more confidence was placed in the liquid-phase analysis of the CO<sub>2</sub> concentration, as opposed to the gas-phase material balance.

#### 7.4 Calibration of the Reactor

In the limit that the reaction kinetics are in the fast, pseudo first-order regime, then the mass transfer coefficient is negligible in equation [7.1], and experimental determination of the mass transfer coefficient is not necessary. It is, of course, necessary to measure the mass transfer coefficient in order to test the assumption of first-order kinetic behavior, and some data were purposefully taken under non-pseudo first-order conditions in order to provide a test of the combined mass-transfer/equilibrium model. Critchfield (1988) measured CO<sub>2</sub> absorption rates into water of varying temperatures to correlate the mass transfer coefficient. However, the viscosity of the mixed amine solutions can vary markedly from that of water, and for this reason CO<sub>2</sub> absorption rates were carried out in water (to compare with previous results) as well as solutions of ethylene glycol and water, for which diffusivity and solubility data of CO<sub>2</sub> are readily available (Hayduk and Malik, 1971). The general correlation used for the mass transfer coefficient is of the form:

$$k_{1a} = c_1 D c^2_{\text{stirrer speed}} c^3_v c^4 \quad [7.2]$$

This equation has some basis in theory (Davies, 1972a), but is considered to be an empirical correlating equation. The significance of determining the mass transfer rate of CO<sub>2</sub> into ethylene glycol solutions is to determine a statistically significant dependence of the effect of diffusivity and viscosity by means other than changing the temperature. Furthermore, the viscosity of aqueous amine solutions is much greater than that of water, and comparable to ethylene glycol solutions. The regression fit both sets of data well, certainly within the accuracy needed for the chemical absorption experiments. The dependence on the diffusivity was found to be 0.619, instead of the previously assumed 0.5 power, which demonstrates that the actual behavior of the stirred tank lies somewhere between surface renewal theory (0.5 dependence) and film theory (1.0 dependence). This result is comparable to results obtained previously in the literature (Davies, 1980; Kozinski and King, 1966). The final correlation used is shown in equation [7.3]:

$$k_{1a} \text{ (m}^3\text{/s)} = 3.626 \times 10^{-8} D \text{ (m}^2\text{/sec)}^{0.62} \text{ stirrer speed (RPM)}^{0.71} v \text{ (m}^2\text{/s)}^{-0.77} \quad [7.3]$$

The fit of the data is shown in Figure 7.3, and the data obtained in this work are documented in Appendix C.

## 7.5 Measurement of Chemical Absorption Rates

The procedure for determining chemical absorption rates is generally the same as measuring physical absorption rates. Commercial grade MDEA and DEA were obtained from DOW Chemical and Union Carbide, respectively. The major precaution taken was to vacuum distill the MDEA before use. The reason for this was to remove possible highly reactive impurities which can affect the interpreted absorption rate data at low driving forces. Solutions of various compositions of MDEA, DEA, and mixtures of the two were used. A summary of the data taken and the conditions are shown in Table 7.1. The data themselves are in Appendix C; they are distinguished from data taken previously by Critchfield (1988) and other authors for three reasons:

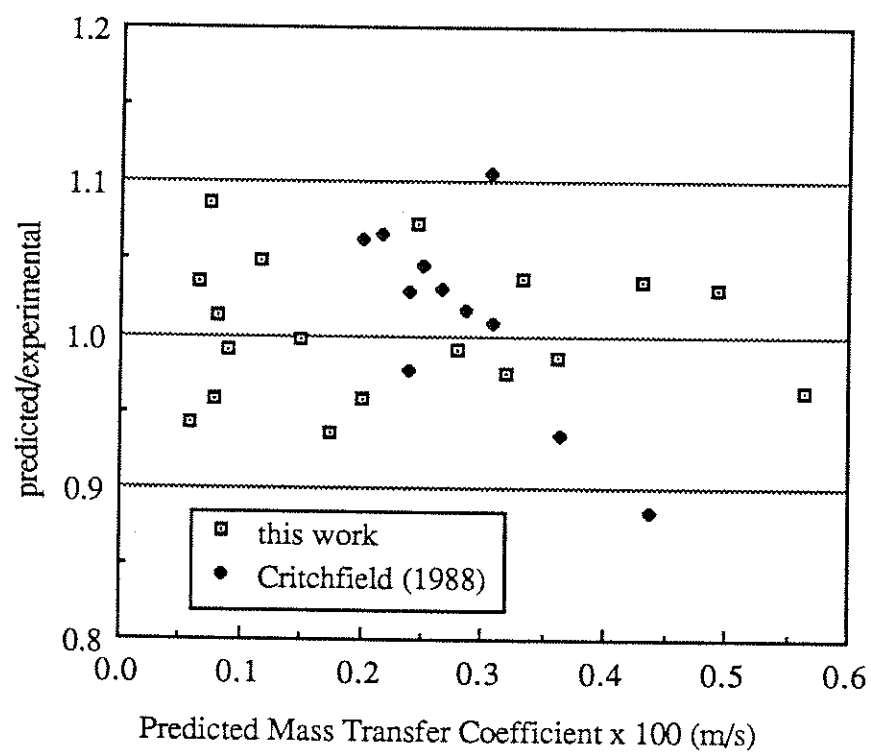


Figure 7.3 Mass Transfer Coefficients Determined by CO<sub>2</sub> Absorption into Water and Aqueous Ethylene Glycol

---

---

Table 7.1      Summary of Conditions for Chemical Absorption Data

<u>Mixture</u>	<u>Temperature</u>	<u>CO<sub>2</sub> Partial Pressure</u>
0.5,1.0 m DEA	313 K	1 - 4 kPa
1.0 m MDEA	298,313 K	5 - 100 kPa
0.1 m DEA/0.9 m MDEA	313 K	3 kPa
0.3 m DEA/0.7 m MDEA	313 K	3 kPa

first, the MDEA data were taken at low and high driving forces in order to explore the driving force effect noted with CO<sub>2</sub> absorption into MDEA; second, the mixed amine DEA/MDEA data were taken at 313 K, in order to complement the data taken previously by Critchfield at 298 K, and the DEA/MDEA data were taken for two separate amine concentration levels. The mixed amine data allow an estimation of the temperature dependence on the rate parameters, and are closer to the actual range of temperatures encountered in industrial absorption equipment. Interpretation of the data will be presented along with data of other authors in the regression analysis, the subject of Chapter 9.

## Chapter Eight

### Comparison of Mass Transfer Theories

A number of steady- and unsteady-state mass transfer theories were compared. The purpose of this comparison is to show that, for the reaction schemes under consideration, we may use a steady-state mass transfer theory in place of an unsteady-state mass transfer theory in order to predict the effect of chemical reaction on gas absorption rates. This allows for a large reduction in computation time - an important consideration for the nonlinear parameter estimation of rate constants from absorption/desorption data. Comparisons are made for a second-order, reversible reaction and for the absorption of CO<sub>2</sub> into aqueous MDEA.

Throughout the discussion, the effect of gas-phase resistance on mass transfer will be neglected. This effect can be important for absorption from mixtures of gases with accompanying high absorption rates. However, taking the gas phase resistance into account is straightforward in numerical simulation, and not pertinent to this work. Interfacial equilibrium is also assumed in the calculations. This has been demonstrated to be valid for uncontaminated surfaces during the physical absorption of slightly soluble gases into laminar jets (Scriven and Pigford, 1958). The nonionic diffusion process is assumed to obey Fick's law, except when turbulence is taken into account empirically with an eddy diffusivity model. Therefore, the only coupling of the diffusion fluxes is through electrical potential gradients and chemical reaction.

#### 8.1 Second-Order, Reversible Reaction

Before proceeding to discussion of the MDEA system, it is appropriate to compare the mass transfer theories for a simple case. We chose the bimolecular, reversible reaction:



The rate expression used for this reaction is shown in equation [8.2]:

$$r_i = \nu_i k_2 \left\{ C_A C_B - \frac{1}{K_{eq}} C_C C_D \right\} \quad [8.2]$$

The stoichiometric coefficients,  $\nu_i$ , are +1 for products and -1 for reactants. Numerical results are already available in the literature for this reaction for both penetration (Secor and Beutler, 1967; Versteeg, 1986) and film theories (Onda et al., 1970a, 1970b). We will, however, present our own results for completeness. In this simple case, we will neglect potential gradient coupling, and assume the diffusion coefficients for all species except the absorbing gas as the same. We will also consider only the case where the diffusion coefficient ratio is different from unity. In Figure 8.1 the enhancement factor is presented as a function of the dimensionless rate constant,  $M$ :

$$M = \frac{D_1 k_2 C_{Bo}}{k_l^2} \quad [8.3]$$

The primary difference between the theories occurs at the highest enhancement factors, where the gradients in the liquid phase species concentrations are largest. This region corresponds to the instantaneous upper limit.

Figure 8.2 shows the ratio of the enhancement factor of each of the four other theories to surface renewal theory. There are two regions where the theories are significantly different. The major difference is at the highest enhancement factors, where film theory deviates approximately 30%. This deviation would not be as large if the diffusion coefficients were equal, and would be larger if the diffusion coefficient ratio was greater. We note that the large difference at the instantaneous upper limit can be predicted by taking the ratio of the enhancement factors from equations [5.50] and [5.51], for irreversible reaction using surface renewal and film theories.

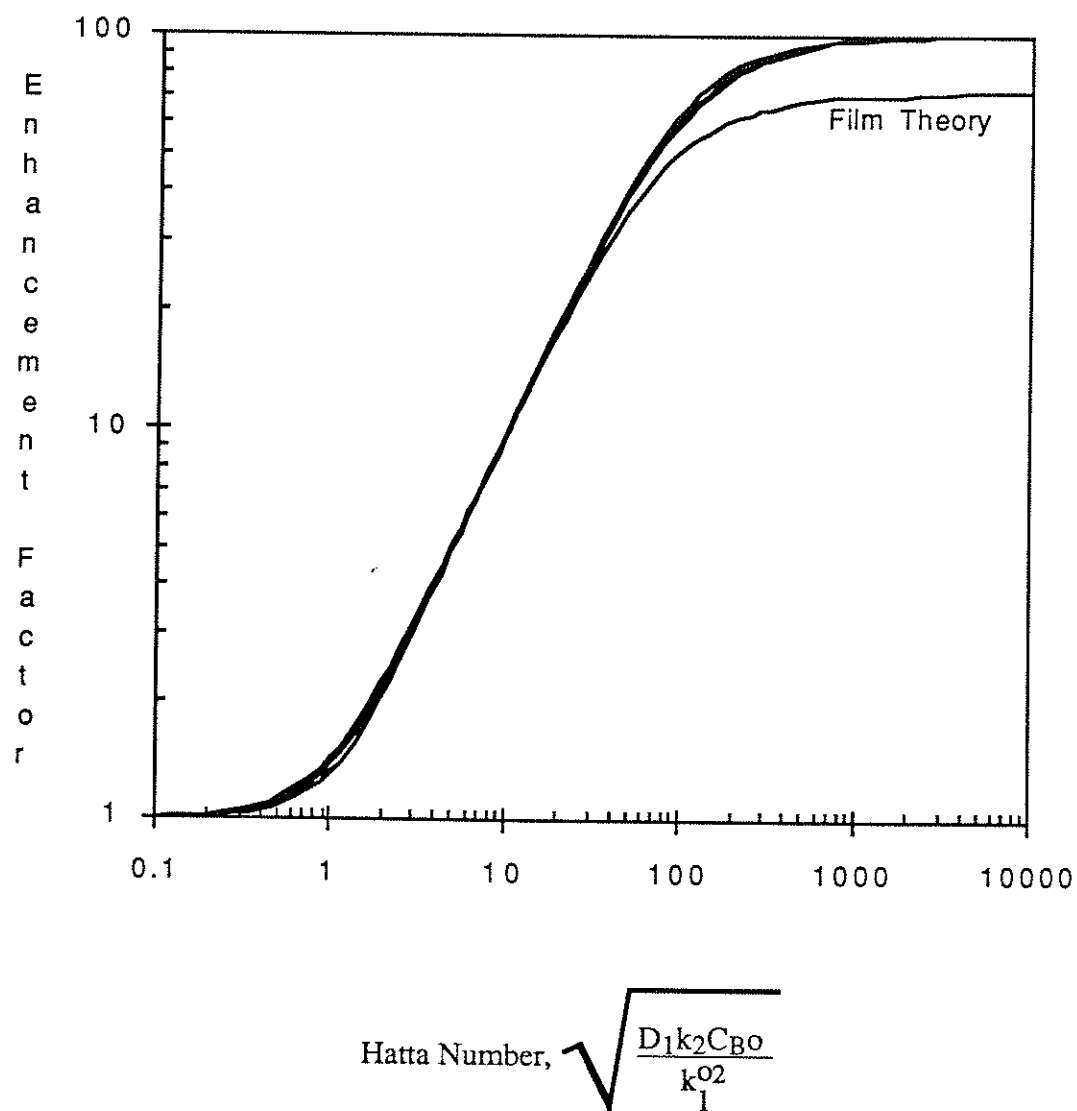


Figure 8.1 Enhancement Factor for a Second-Order, Reversible Reaction,  $A + B \rightleftharpoons C + D$ .  $K_{eq} = 350$ ,  $D_B = D_C = D_D = 0.5D_A$ ,  $C_{B,bulk}/C_{A,int} = 200$ ,  $C_{A,bulk} = C_{B,bulk} = C_{C,bulk} = 0$

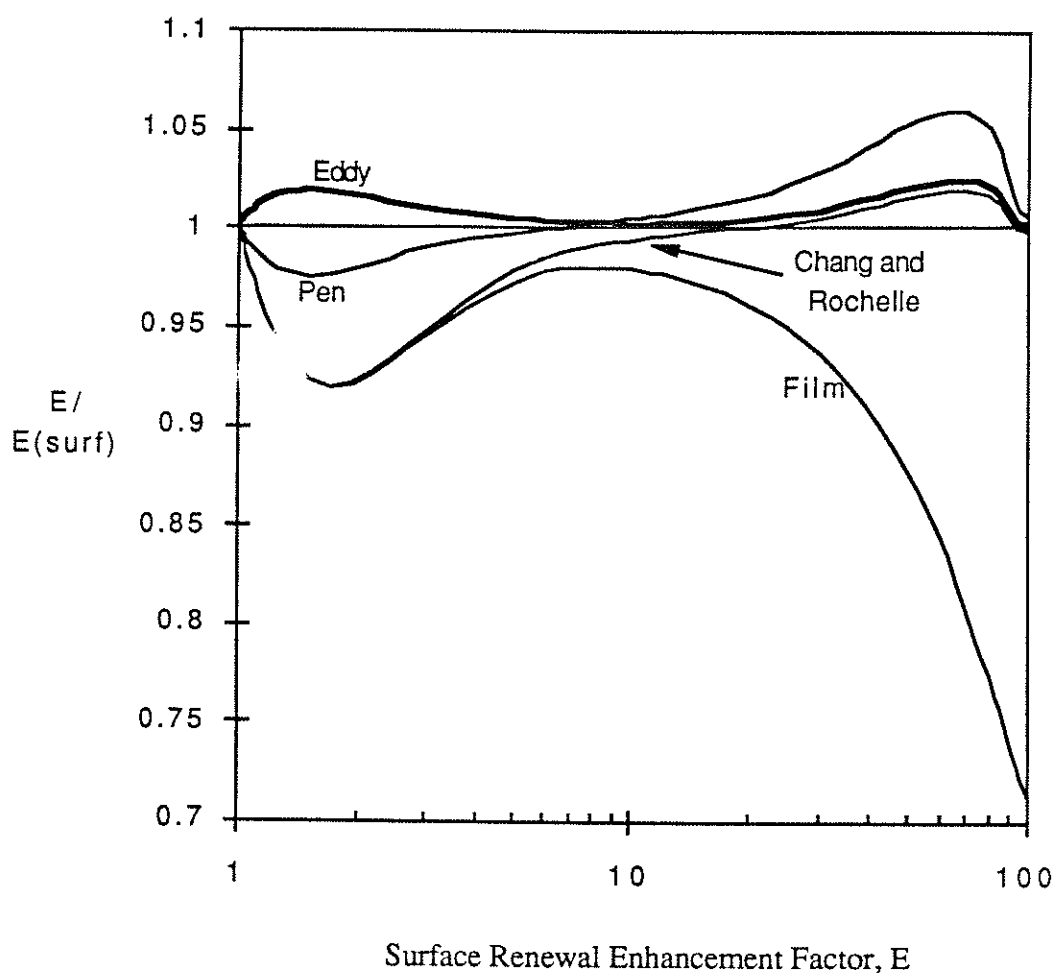


Figure 8.2 Comparison of Mass Transfer Theories to Surface Renewal Theory for a Second-Order, Reversible Reaction,  $A + B \rightleftharpoons C + D$ .  $K_{eq} = 350$ ,  $D_B = D_C = D_D = 0.5D_A$ ,  $C_{B,bulk}/C_{A,int} = 200$ ,  $C_{A,bulk} = C_{B,bulk} = C_{C,bulk} = 0$



The approximate method of Chang and Rochelle (1983) modifies only the diffusion coefficients of the nonvolatile reactants. When the approximate and film theory solutions are the same, the diffusion of liquid-phase reactants is unimportant, corresponding to a pseudo first-order reaction condition (Danckwerts, 1970). Upon examining Figure 8.2 for the low enhancement factors, one finds that there are differences in the models even when liquid-phase reactant diffusion is unimportant, reflecting the fact that the models are different even for the simple case of the first-order reaction scheme. This difference is demonstrated in Figure 8.3, where the results are shown for a simple first-order reaction scheme. At low enhancement factors, the theories have the largest deviation, but at high enhancement factors, all of the theories approach the same limit:

$$E = \sqrt{M} \quad [8.4]$$

This result has been demonstrated from the analytical solutions for penetration, film and surface renewal theories by Danckwerts (1970), and has been verified numerically for the eddy diffusivity theory.

Figures 8.4 and 8.5 show similar results for a second-order reaction at conditions studied by Chang (1979), the equilibrium constant is lower, and the interfacial concentration of the absorbing gas is higher. At both sets of conditions, high and low enhancement factors, the eddy diffusivity theory provides a good approximation to the unsteady-state theories, while the approximate method does best at higher enhancement factors. It appears, therefore, that both eddy diffusivity and the approximate model can be used to obtain the enhancement factor for the simple reaction case. The differences from the presumably more accurate unsteady-state models are, in fact, negligible compared to the uncertainty in the actual mass transfer mechanism.

## 8.2 CO<sub>2</sub> Absorption into Aqueous MDEA

Four reactions are considered for the absorption of CO<sub>2</sub> into aqueous MDEA solutions (Critchfield and Rochelle, 1987):

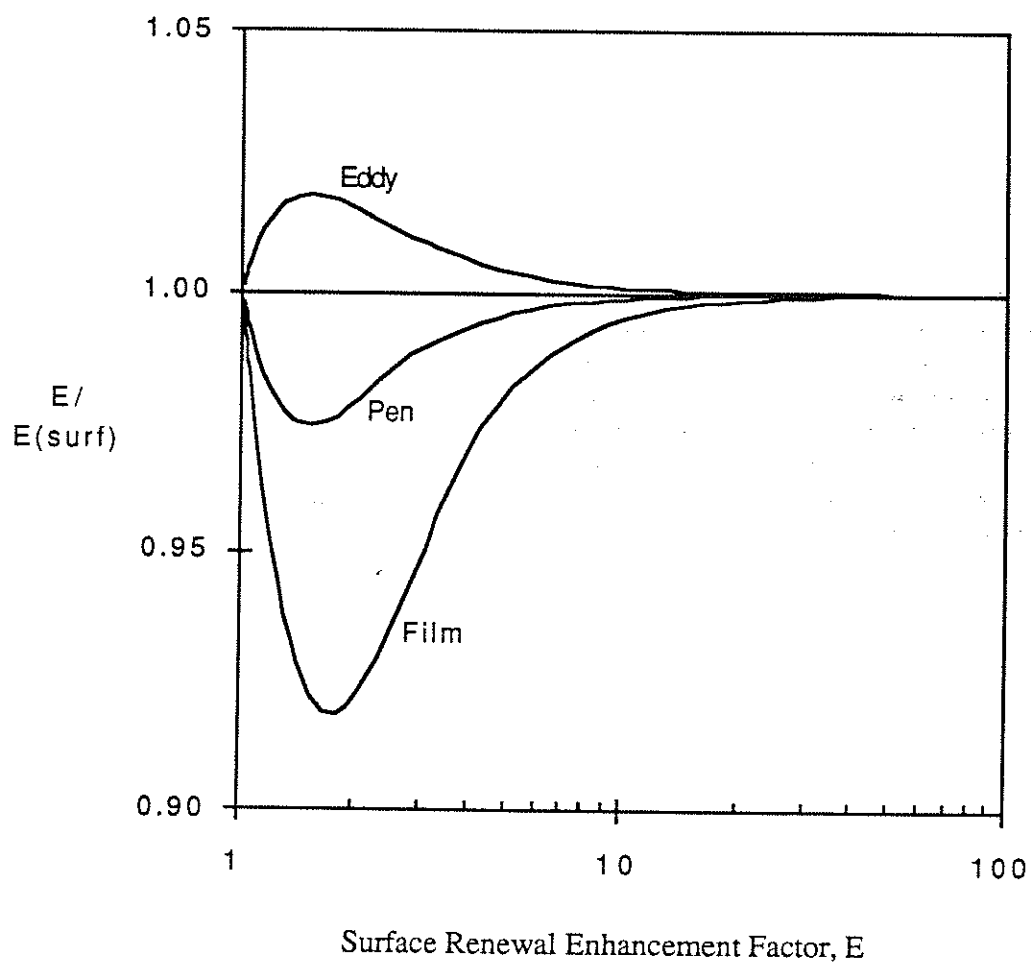


Figure 8.3 Comparison of Mass Transfer Theories to Surface Renewal Theory for a First-Order, Irreversible Reaction.

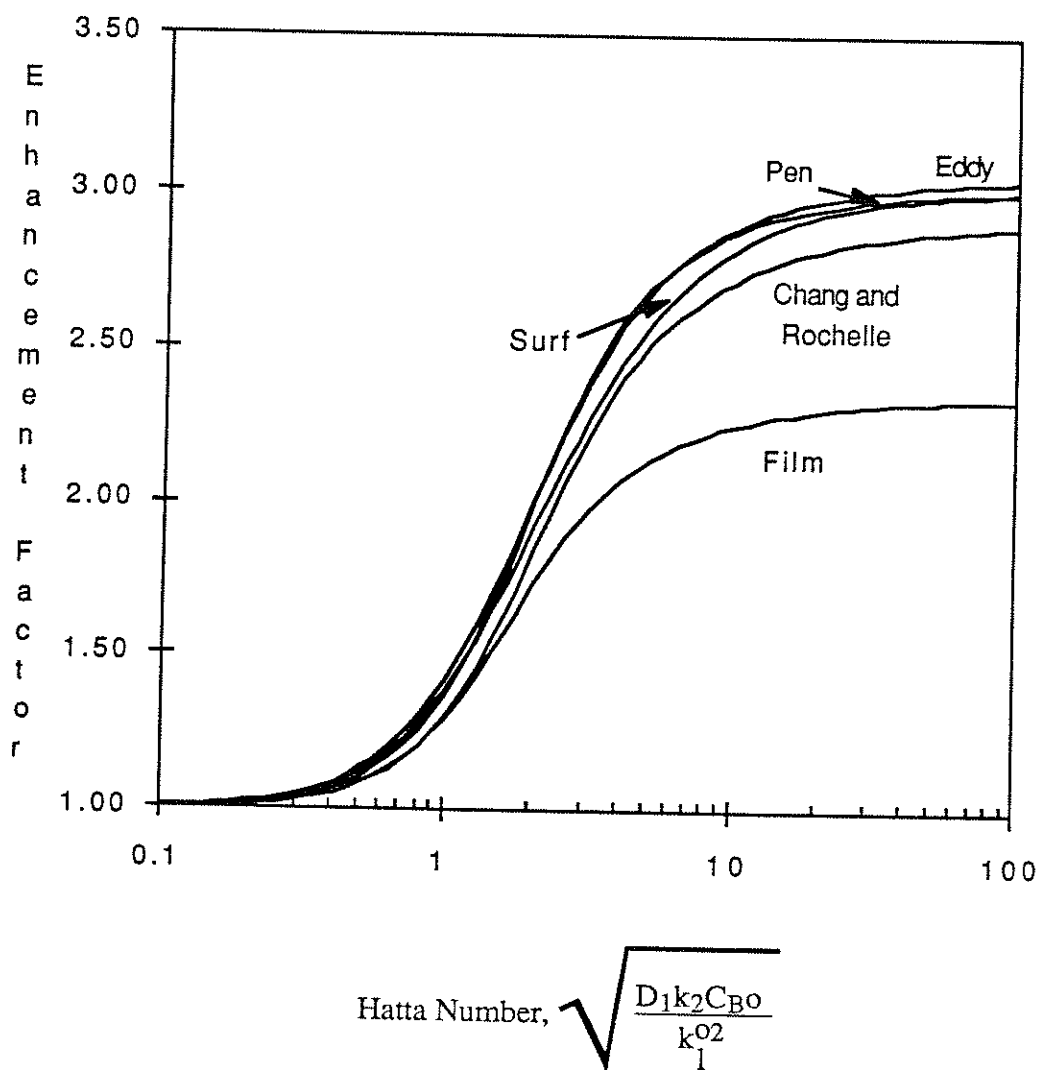


Figure 8.4 Enhancement Factor for a Second-Order, Reversible Reaction,  $A + B \rightleftharpoons C + D$ .  $K_{eq} = 1$ ,  $D_B = D_C = D_D = 0.5D_A$ ,  $C_{B,bulk}/C_{A,int} = 10$ ,  $C_{A,bulk} = C_{B,bulk} = C_{C,bulk} = 0$

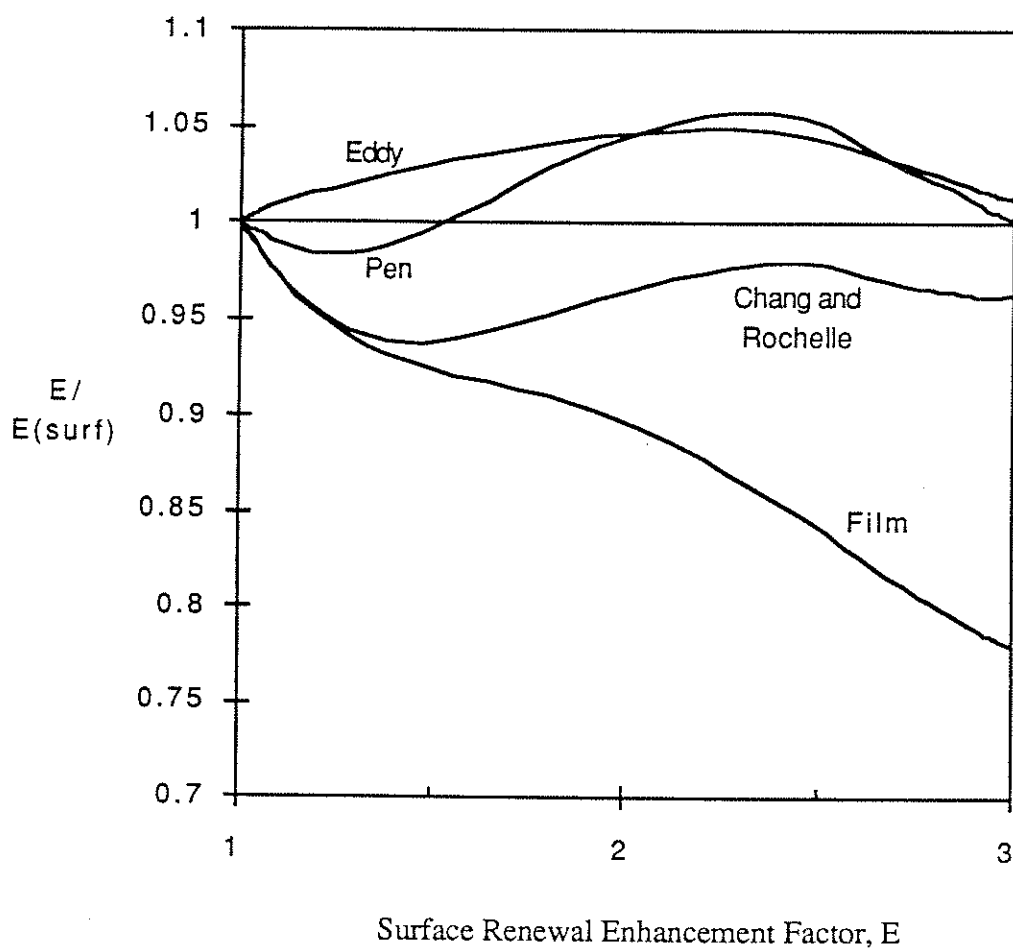
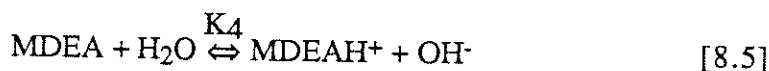
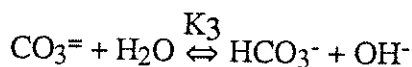
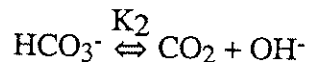
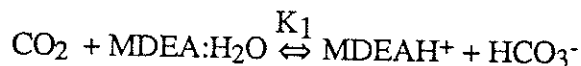


Figure 8.5 Comparison of Mass Transfer Theories to Surface Renewal Theory for a Second-Order, Reversible Reaction,  $A + B \rightleftharpoons C + D$ .  $K_{eq}=1$ ,  $D_B = D_C = D_D = 0.5D_A$ ,  $C_{B,bulk}/C_{A,int} = 10$ ,  $C_{A,bulk} = C_{B,bulk} = C_{C,bulk} = 0$



The first two reactions are finite rate reactions, the second two reactions involve only a proton transfer and will be considered instantaneous with respect to mass transfer. Neglecting water as a species, we have six simultaneous diffusion equations to solve. Since this is an ionic system, we replace the diffusion equation for bicarbonate with an algebraic charge balance equation, and use the Henderson formula to correct for the ionic effects on diffusion. The instantaneous reactions are treated by making the rate constants large enough so that the reactions are in equilibrium everywhere in the boundary layer. This assumption is easily checked using the calculated concentration profiles. The finite rate reactions are treated in the same manner as the reversible, bimolecular reaction discussed previously.

The resulting set of equations are solved with the model parameters shown in Table 8.1. The equilibrium data used are the same as in Critchfield and Rochelle (1987) for 318K. Since the equilibrium constant for the CO<sub>2</sub>-MDEA reaction is correlated as a function of ionic strength, a mean value of 0.1 is assumed in all calculations. The rate constant for hydroxide is taken from Astarita et al. (1983), evaluated at an ionic strength of 0.1. The N<sub>2</sub>O analogy is used to estimate the diffusion coefficient of CO<sub>2</sub> in 2M MDEA, using the data of Versteeg (1986) (see Appendix D). The diffusion coefficient of MDEA is assumed to be the same as DEA. All of the liquid phase reactant diffusion coefficients are adjusted using the modified Stokes-Einstein relationship and the viscosity data of Versteeg (1986). Also, the diffusion coefficient of MDEAH<sup>+</sup> is assumed to be the same as MDEA, although it is most likely smaller.

Table 8.1 Model Parameters for MDEA System at 318K

$K_1$	132	Critchfield and Rochelle, 1987
$K_2$	$4.18 \times 10^{-8} \text{ kmol/m}^3$	Critchfield and Rochelle, 1987
$K_3$	$5.96 \times 10^{-4} \text{ kmol/m}^3$	Critchfield and Rochelle, 1987
$K_4$	not independent	
$k_{\text{MDEA}}$	$10 \text{ m}^3/\text{kmol/s}$	Critchfield and Rochelle, 1987
$k_{\text{OH}^-}$	$3.47 \times 10^4 \text{ m}^3/\text{kmol/s}$	Astarita et al, 1983
$\text{HCO}_2^-$	$5 \times 10^3 \text{ kPa} \cdot \text{m}^3/\text{kmol}$	Critchfield and Rochelle, 1987
$D_{\text{N}_2\text{O}}$	$1.7 \times 10^{-9} \text{ m}^2/\text{s}$	Versteeg, 1986
$D_{\text{DEA}}$	$0.75 \times 10^{-9} \text{ m}^2/\text{s}$	Versteeg, 1986 (modified)
$D_{\text{HCO}_3^-}$	$0.94 \times 10^{-9} \text{ m}^2/\text{s}$	Kigoshi and Hashitani, 1963*
$D_{\text{CO}_3^{=}}$	$0.7 \times 10^{-9} \text{ m}^2/\text{s}$	Kigoshi and Hashitani, 1963*
$D_{\text{OH}^-}$	$4.5 \times 10^{-9} \text{ m}^2/\text{s}$	Newman, 1973*
$\text{CO}_2$ loading	0.005 kmols/kmol MDEA	
Total MDEA	$1.0 \text{ kmol/m}^3$	

\* modified according to Versteeg's Stokes-Einstein equation

In the results, we wish not only to compare the mass transfer theories, but also to establish the importance of the additional reaction of hydroxide with  $\text{CO}_2$  and the equilibrium reactions. This is readily accomplished in a numerical model by simply "turning off" the rate constants for all reactions except the primary reaction of  $\text{CO}_2$  with MDEA; the equilibrium concentrations in the bulk are still the same, however. Figure 8.6 shows the enhancement factor, now as a function of the interfacial concentration of  $\text{CO}_2$  for both the true reaction case and the "simplified" reaction scheme at an equivalent contact time of 10 seconds, which corresponds to a mass transfer coefficient of  $1.46 \times 10^{-5} \text{ m/sec}$ . At low  $\text{CO}_2$  concentrations, corresponding to low  $\text{CO}_2$  partial pressures, the enhancement factor is highest, since there is no depletion in the boundary

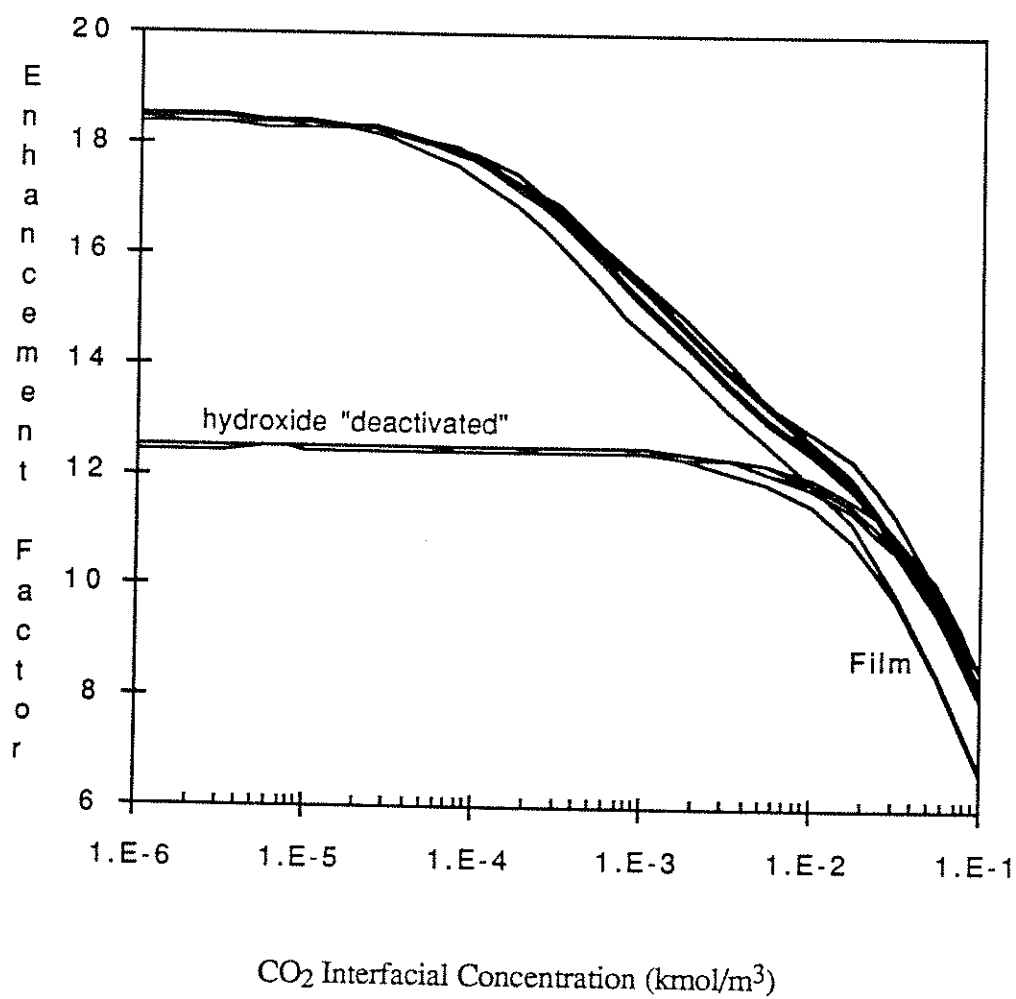


Figure 8.6 Effect of CO<sub>2</sub> Interfacial Concentration and Hydroxide Reaction for the MDEA System.  $k_1^0 = 1.46 \times 10^{-5}$  m/sec,  $T = 45^\circ\text{C}$ , CO<sub>2</sub> loading = 0.005 (d) corresponds to numerical solution with the hydroxide reaction "deactivated"

layer of the MDEA and hydroxide. This condition corresponds to the pseudo first-order reaction regime. At this point, the hydroxide reaction has its largest effect, and must be taken into account in predicting the enhancement factor. As the partial pressure is increased, the hydroxide becomes depleted in the boundary layer, the MDEA becomes the primary contributor to the absorption enhancement, and the enhancement factors become the same for both cases. This depletion effect is demonstrated explicitly in Figures 8.7 and 8.8, where boundary layer concentration profiles are shown for two selected CO<sub>2</sub> partial pressures using film theory. Figure 8.7 shows the results with a low CO<sub>2</sub> partial pressure, resulting in nearly pseudo first-order conditions (there is a small gradient in hydroxide). The contribution of each reactant, MDEA and hydroxide, can be obtained by taking the product of the concentration and the rate constant, to obtain a pseudo first-order enhancement factor:

$$k_1 = k_{\text{OH}}[\text{OH}^-] + k_{\text{MDEA}}[\text{MDEA}] \quad [8.6]$$

For these conditions, a pseudo first-order rate constant of 39 sec<sup>-1</sup> is obtained (using the interfacial concentration of hydroxide), and hydroxide contributes to about half of this value. The conditions shown in Figure 8.8, corresponding to a higher CO<sub>2</sub> concentration, show that the hydroxide is depleted at the interface, and its contribution to the enhancement factor is now less than 10%.

Figure 8.9 shows an expanded comparison of the mass transfer theories for the MDEA system (with hydroxide and the equilibrium reactions included in the simulation). Surface renewal theory is assumed to be the "correct" theory and serves as the basis for comparison. Film theory deviates the most in this case, with eddy diffusivity theory and the approximate theory both providing solutions similar to surface renewal.

The same type of data are shown in Figure 8.10 for the MDEA and the "simplified" MDEA system, except now at an equivalent contact time of 0.1 seconds ( $k_1^0 = 1.46 \times 10^{-4}$  m/s). The hydroxide reaction again contributes significantly to the absorption enhancement, until the partial pressure of CO<sub>2</sub> is large enough to cause boundary layer depletion. Now, however, the primary deviation in the models results from the differences in the theories for a pseudo first-order reaction. This region corresponds to a small value of M, shown in Figure 8.3 for a first-order reaction.



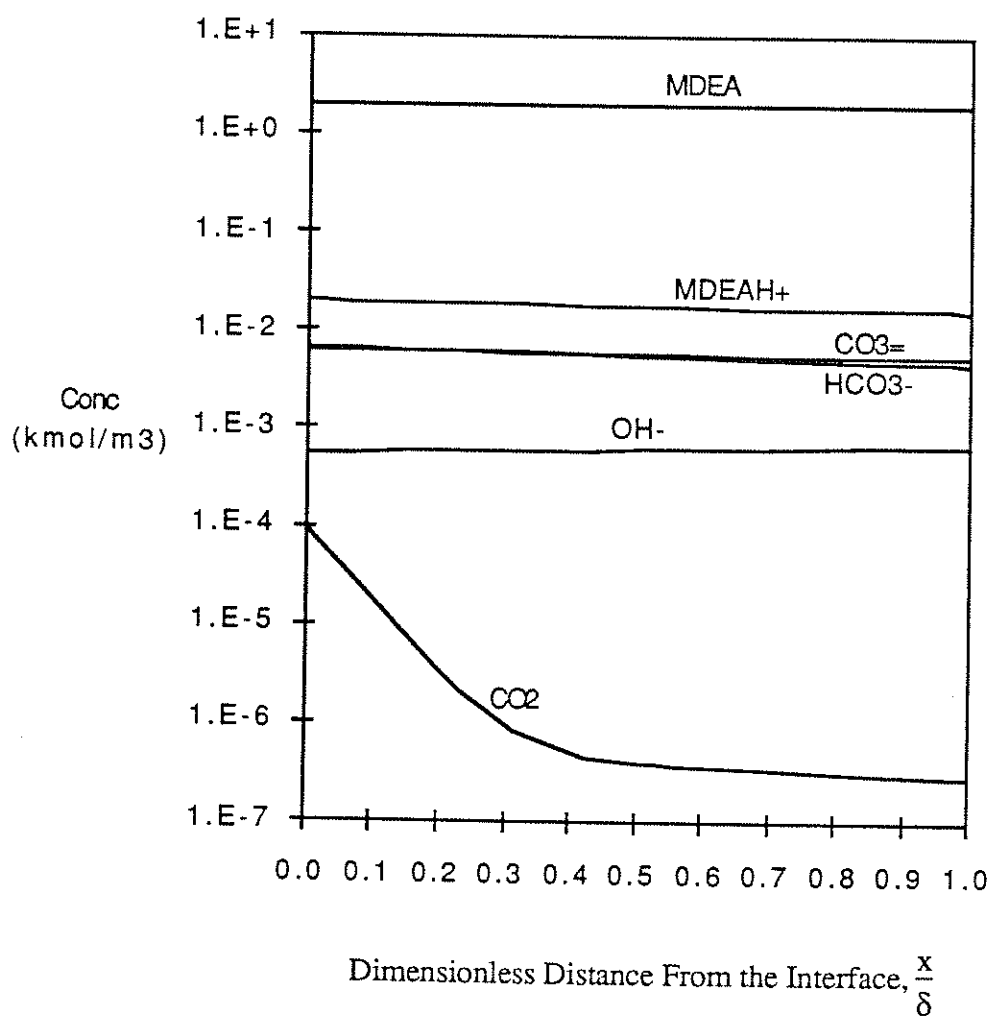


Figure 8.7 Concentration Profiles for the MDEA System with the Film Theory Solution.  $k_1^0 = 1.46 \times 10^{-5}$  m/sec,  $T = 45^\circ\text{C}$ ,  $\text{CO}_2$  loading = 0.005,  $\text{CO}_{2,\text{int}} = 1 \times 10^{-4}$  kmol/m³, Enhancement Factor = 17.5

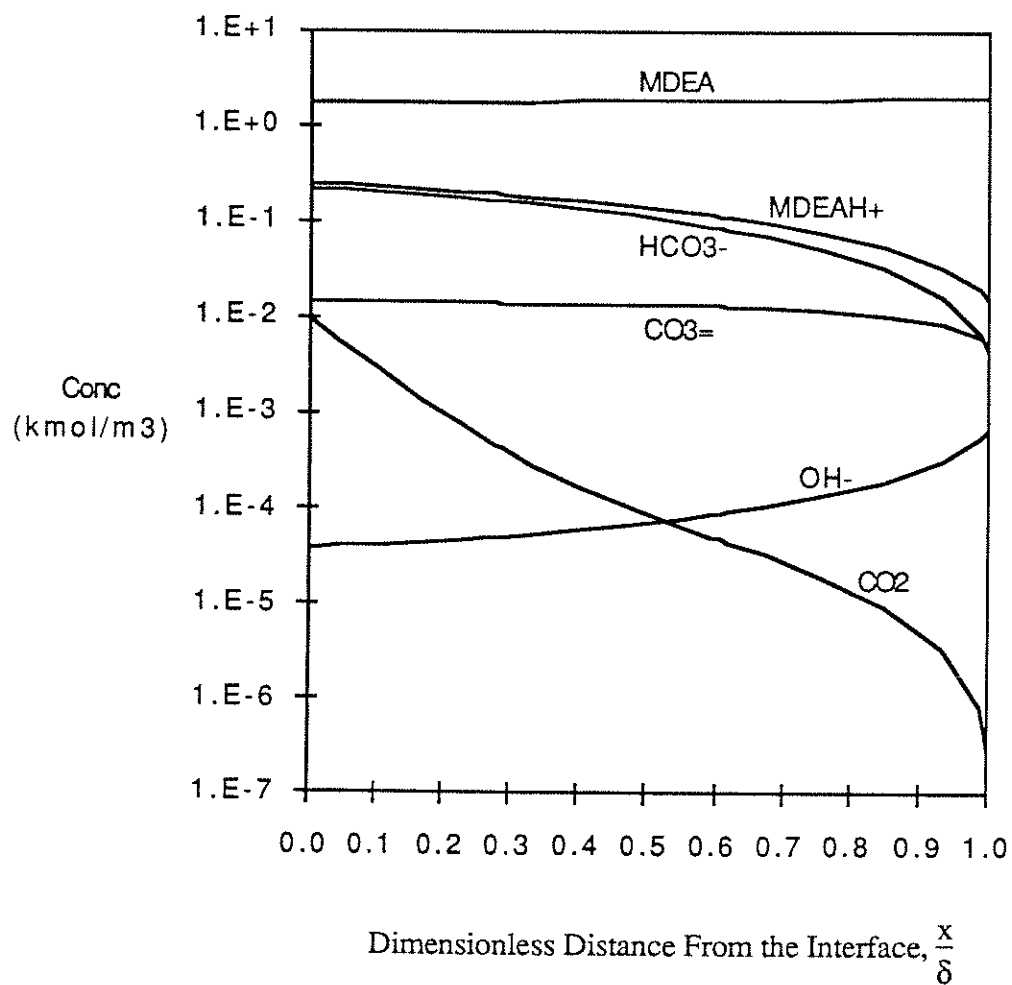


Figure 8.8 Concentration Profiles for the MDEA System with the Film Theory Solution.  $k_1^0 = 1.46 \times 10^{-5}$  m/s,  $T = 45^\circ\text{C}$ ,  $\text{CO}_2$  loading = 0.005,  $\text{CO}_{2,\text{int}} = 1 \times 10^{-2}$  kmol/m<sup>3</sup>, Enhancement Factor = 11.9

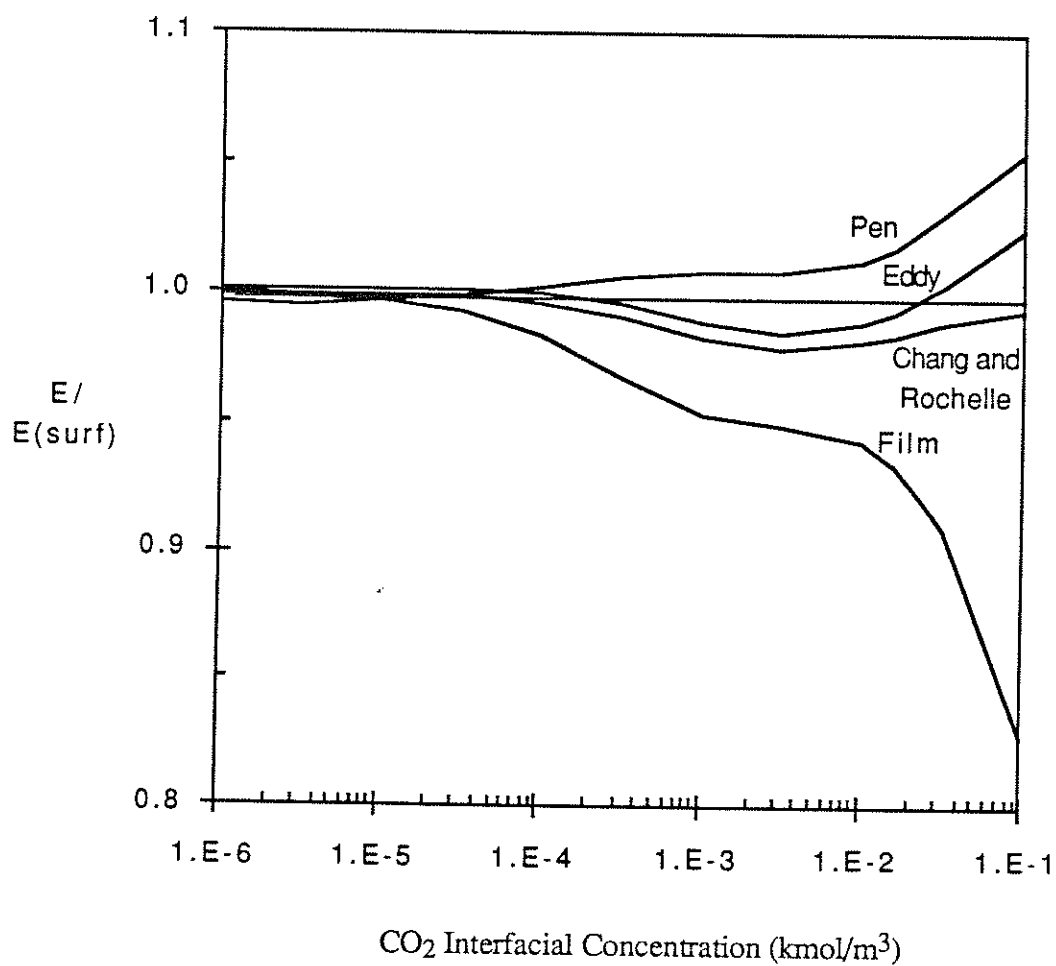


Figure 8.9 Comparison of Mass Transfer Theories to Surface Renewal Theory for the MDEA System.  $k_1^0 = 1.46 \times 10^{-5}$  m/sec,  $T = 45^\circ\text{C}$ ,  $\text{CO}_2$  loading = 0.005

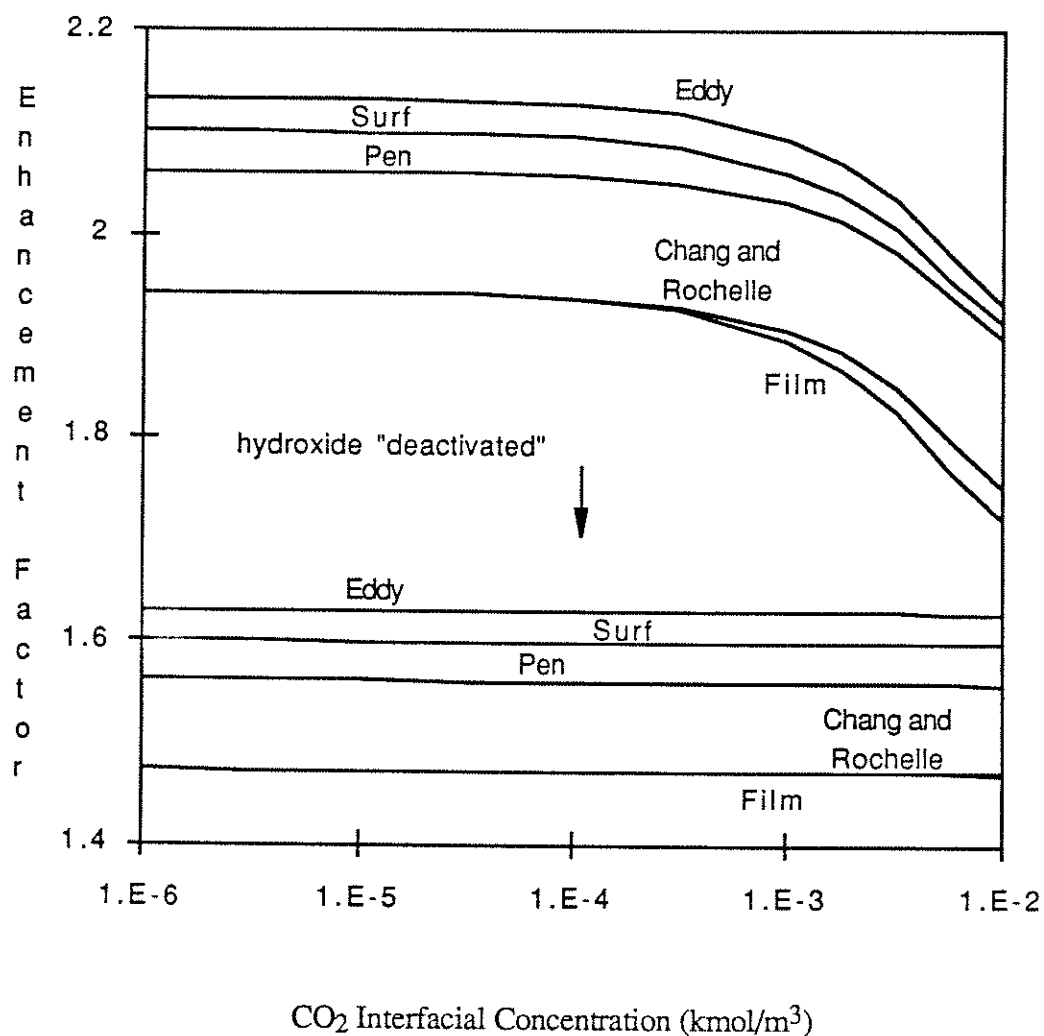


Figure 8.10 Effect of CO<sub>2</sub> Interfacial Concentration and Hydroxide Reaction for the MDEA System.  $k_1^0 = 1.46 \times 10^{-4}$  m/s,  $T = 45^\circ\text{C}$ , CO<sub>2</sub> loading = 0.005 (d) corresponds to numerical solution with the hydroxide reaction "deactivated"

It should be noted that Carta and Pigford (1983) found significant differences between penetration theory and film theory for the case of NO absorption into aqueous nitric acid solution. The distinguishing feature of this example is that the reaction is autocatalytic. Therefore, for the case of autocatalytic reactions, one must use caution in determining the appropriate mass transfer model.

## Chapter Nine

### Simulation of CO<sub>2</sub> Absorption/Desorption

In this chapter, we will concentrate on the absorption/desorption of carbon dioxide with aqueous-based alkanolamine solutions - MDEA (methyldiethanolamine), DEA (diethanolamine), MEA (monoethanolamine), and mixtures of DEA/MDEA and MEA/MDEA. Currently, DEA is the most commonly used alkanolamine while MDEA and MDEA-based solvents are increasing in popularity (Moore, 1989).

Critchfield and Rochelle (1987, 1988) studied the kinetics of these systems by means of a stirred cell absorber. Data were taken for a range of CO<sub>2</sub> partial pressures and loadings, covering both absorption and desorption conditions. It was found that the CO<sub>2</sub> desorption from DEA and MDEA solutions was greater than expected from absorption measurements. This effect was attributed to primary and secondary amine contaminants which would enhance the reaction rate. This explanation was also used by Versteeg (1986) to explain the discrepancy in the literature data.

The previous work of Critchfield and Rochelle has been extended in several ways: More data have been taken to supplement those data taken previously. We have obtained absorption data at both low and high CO<sub>2</sub> partial pressures for the MDEA-CO<sub>2</sub> system with the specific intent of observing the driving force phenomenon. In addition, we have taken data at higher temperatures for the mixed amine system DEA/MDEA to aid in prediction of amine system performance under conditions actually used in industry. Finally, we have taken a "rigorous" approach in the modelling of mass transfer rates and equilibrium phenomena. We note that for the results in this chapter, all ion diffusion coefficients have been set to that of the largest amine, allowing us to neglect the electrical potential gradient terms.

This chapter emphasizes the interpretation of experimental data and the simulation of CO<sub>2</sub> absorption into and desorption from aqueous-based alkanolamine solutions - MDEA, DEA, and MEA. These systems have been studied before, however most cases were limited to pseudo first-order conditions and/or negligible reverse reaction rates. The latter limitation was removed by Critchfield and Rochelle

(1988) who studied both absorption and desorption, but this work was still limited to pseudo first-order conditions for the data interpretation. Versteeg (1986) has developed a rigorous mass transfer model based on penetration and film theories, but the interpretation of secondary amine data is for pseudo first-order conditions only, and at low loadings, so this does not provide a check on the mass transfer model at these conditions. Bosch (1989) has extended the work of Versteeg to include both desorption and absorption data, however, he has noted difficulties in predicting the desorption rates. He indicates the importance of a good equilibrium model in simulating the desorption process. In this chapter, we analyze the experimental data using a comprehensive mass transfer model based on the simplified eddy diffusivity theory. We show that the combined mass transfer and equilibrium model can simulate the CO<sub>2</sub>-amine data under a wide range of conditions, covering both absorption and desorption. The complete scheme of reactions simulated in the model is shown in Table 9.1.

The solutions of aqueous amines loaded with CO<sub>2</sub> are characterized by high ionic strength, causing the activity coefficients to vary greatly over the range of conditions encountered. In order to provide a realistic simulation of the data, we decided it was necessary to use a "rigorous" activity coefficient model, namely the Electrolyte-NRTL model (Chen and Evans, 1986) for the activity coefficients of the liquid phase species. The parameters used in the model are based largely on the work done by Austgen et al. (1990), with some minor differences to be detailed later. This approach is in contrast with the effective equilibrium constant approach of Kent and Eisenberg (1976), and a less rigorous activity coefficient approach of Chakravarty (1985), as used by Bosch (1989) (In all fairness, the less rigorous approach of Chakravarty has advantages compared to the Electrolyte-NRTL model with respect to computation time).

Due to the type of regression method used, we take into account all variables subject to error in reporting the accuracy of fit in the data. In the tables to be referenced, the error in the model with respect to the data is defined as shown in equation [9.1]:

---

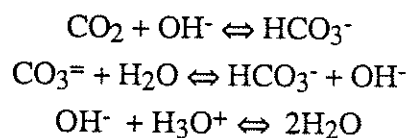


---

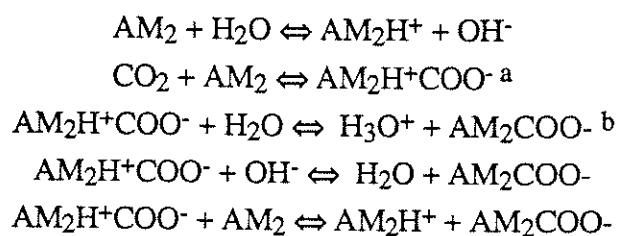
Table 9.1 Scheme of Reactions for CO<sub>2</sub>-Amine System

---

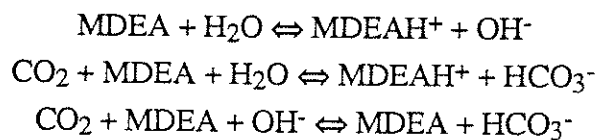
## All Systems



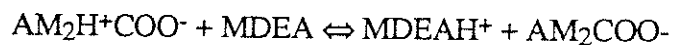
## Primary and Secondary Amines



## MDEA system



## Mixed Amine Systems

<sup>a</sup>zwitterion intermediate<sup>b</sup>amine carbamate

---



---



$$\text{error} = \frac{\sum_{i=1}^{n_{\text{exp}}} \sum_{k=1}^{n_{\text{var}}} \left( \frac{z_{ik,\text{pred}} - z_{ik,\text{exp}}}{s_{ik}} \right)^2}{n_{\text{exp}} - p} \quad [9.1]$$

We interpret this error as a measure of the ratio of actual to anticipated model error. A value much larger than 1 indicates difficulty of the model in explaining trends in the experimental data. Typically, a value of 1 to 3 would be considered an adequate fit of the data.

## 9.1 Equilibrium Data Regression

Austgen (1989) performed extensive data regression of NRTL coefficients from equilibrium data for acid-gas treating systems. However, all regression analyses were performed using the ASPEN-PLUS<sup>TM</sup> simulator and data regression system (Aspen Technology, Inc., 1985). In order to use the Electrolyte-NRTL model for rate data simulation, a stand-alone equilibrium model and regression system was developed in this work. This methodology is based primarily on the ASPEN model and Austgen's work. Using the equilibrium constants from Austgen's work, new binary interaction parameters were regressed from experimental data. The sources of data and range of conditions are summarized in Table 9.2, and the results are shown in Table 9.3. Equilibrium partial pressures less than 0.1 kPa and greater than 101 kPa were not included. Relative standard deviations of 10% of loading and 15% of pressure were assumed. The error reported reflects the relative error in the fit to the predicted error from the assumed standard deviations (see equation [9.1]). Note we have not regressed parameters over as wide of a range of temperatures due to the range of absorption data to be simulated. We have, therefore, neglected any temperature dependence of the interaction parameters. Two of the parameters for the MEA system could not be estimated with significance. In this work, they were estimated as -1/2 the value of the conjugate coefficients, whereas in Austgen's work, they were set at default values.

Table 9.2 Range of Data Used in Equilibrium and Rate Regression

Equilibrium Data

System	Temperature (K)	Acid Gas Loading	Pressure (kPa)	Wt % Amine	Refs.
MDEA	298-338	0.01-0.8	0.1-100	20-50	a - f
DEA	298-338	0.05-1.0	0.1-100	5-25	c,g-k
MEA	298-333	0.05-0.6	0.1-100	6-30	h,l-o
DEA/MDEA	298-313	0.05-0.75	0.01-100	1-20/16-23	a,c
MEA/MDEA	298-313	0.15-0.6	0.1-100	3-12/16-23	a,c

Rate Data

MDEA	298-313	$10^{-3}$ -0.7	0.1-100	10-50	c,p,q
DEA	298-313	$3 \times 10^{-3}$ -0.4	1-10	5-24	c,p,q,r
DEA/MDEA	298-313	$10^{-3}$ -0.5	0.5-8	1-6/7-22	c,p
MEA/MDEA	288-313	$3 \times 10^{-4}$ -0.25	0.02-0.05	4/16	c

<sup>a</sup>Austgen (1989)<sup>b</sup>Bhari (1984)<sup>c</sup>Critchfield (1988)<sup>d</sup>Ho and Eguren (1988)<sup>e</sup>Jou et al. (1982)<sup>f</sup>Jou et al. (1986)<sup>g</sup>Lal et al. (1985)<sup>h</sup>Lawson and Garst (1976)<sup>i</sup>Lee et al. (1972)<sup>j</sup>Mason and Dodge (1936)<sup>k</sup>Lee et al. (1974a)<sup>l</sup>Jones et al. (1959)<sup>m</sup>Lee et al. (1974b)<sup>n</sup>Lee et al. (1976)<sup>o</sup>Muhlbauer and Monaghan (1957)

Pthis work (1990)

<sup>q</sup>Toman (1990)<sup>r</sup>Blauwhoff et al. (1984)

Table 9.3 Equilibrium Regression Results

<u>interaction parameter</u>	<u>parameter estimates<sup>a</sup></u>	<u>error<sup>b</sup></u>	<u>Austgen at 25°C</u>
MDEA system			
H <sub>2</sub> O,MDEAH <sup>+</sup> ,HCO <sub>3</sub> <sup>-</sup>	8.61 ± 1.8%		9.71
MDEAH <sup>+</sup> ,HCO <sub>3</sub> <sup>-</sup> ,H <sub>2</sub> O	-3.92 ± 1.7%	1.152	-4.25
DEA system			
H <sub>2</sub> O,DEAH <sup>+</sup> ,DEACOO <sup>-</sup>	12.4 ± 6.0%		11.89
DEAH <sup>+</sup> ,DEACOO <sup>-</sup> ,H <sub>2</sub> O	-5.82 ± 7.4%		-5.58
H <sub>2</sub> O,DEAH <sup>+</sup> ,HCO <sub>3</sub> <sup>-</sup>	7.61 ± 4.0%	0.45	9.53
MEA system			
H <sub>2</sub> O,MEAH <sup>+</sup> ,MEACOO <sup>-</sup>	7.55 ± 8.7%		10.27
MEACOO <sup>-</sup> ,MEAH <sup>+</sup> ,H <sub>2</sub> O	-3.78 <sup>c</sup>		-4.0 <sup>c</sup>
H <sub>2</sub> O,MEAH <sup>+</sup> ,HCO <sub>3</sub> <sup>-</sup>	4.24 ± 29%		8.64
HCO <sub>3</sub> <sup>-</sup> ,MEAH <sup>+</sup> ,H <sub>2</sub> O	-2.12 <sup>c</sup>	0.75	-4.0 <sup>c</sup>
DEA/MDEA system			
H <sub>2</sub> O,MDEAH <sup>+</sup> ,DEACOO <sup>-</sup>	10.6 ± 10%		10.39
MDEAH <sup>+</sup> ,DEACOO <sup>-</sup> ,H <sub>2</sub> O	-4.75 ± 11%	0.57	-4.97
MEA/MDEA system			
H <sub>2</sub> O,MDEAH <sup>+</sup> ,MEACOO <sup>-</sup>	11.0 ± 23%		9.90
MDEAH <sup>+</sup> ,MEACOO <sup>-</sup> ,H <sub>2</sub> O	-5.5	0.32	-4.78

<sup>a</sup>Parameter estimates are expressed as  $\theta \pm \alpha$ , where  $\theta$  is the parameter estimate and  $\alpha$  is the relative standard deviation, i.e.  $\alpha = \sigma/\theta$ .

<sup>b</sup>See equation [9.1] for definition

<sup>c</sup>These parameters could not be estimated with significance, see text

Since the rate equations are activity-based, one must have activity coefficients to compare the results to other literature data. For this reason, activity coefficients at typical solution compositions are shown in Table 9.4.

## **9.2 Rate Data Regression**

Absorption and desorption data were used to regress the rate data after the equilibrium regression. The rate constants were regressed in the form:

$$k = k_{298} \exp \{(-E_a/R) (1/T - 1/298)\} \quad [9.2]$$

The range of data used in the regression analysis are summarized in Table 9.2. The experimental procedure used for all of the work is based primarily on that of Critchfield (1988). A stirred tank was used for the absorption apparatus. The absorption rate data could be determined from liquid-phase or gas-phase analysis. In the work of Toman (1990), both large and small stirred tanks were used with the smaller tank having a higher mass transfer coefficient than the tank used by Critchfield and the present author.

### ***9.2.1 MDEA system***

The generally accepted rate expression for the reaction of CO<sub>2</sub> with MDEA is of the form:

$$r = k[\text{CO}_2][\text{MDEA}] \quad [9.3]$$

where water concentration is neglected since it is generally quite constant. We have found some effect of driving force on the absorption rate which cannot, however, be reconciled by this rate expression. In the discussion to follow, high driving force data will refer to a CO<sub>2</sub> partial pressure of greater than 0.25 atm, and low driving force data will refer to lower CO<sub>2</sub> partial pressures. We present the regression results for MDEA using both the standard mechanism and a more complex mechanism in Table 9.5. If

Table 9.4 Typical Activity Coefficients Calculated Using the Electrolyte-NRTL Model<sup>a</sup>

DEA/MDEA system						
	Water	50% MDEA	25% DEA	25% DEA 0.5 load	10% DEA 40% MDEA	25% DEA 313K
CO <sub>2</sub>	1.0	1.3	1.2	2.0	1.35	1.04
DEA	0.11	na	0.16	0.14	0.13	0.17
H <sub>2</sub> O	1.0	1.0	0.99	1.0	1.0	0.99
HCO <sub>3</sub> <sup>-</sup>	1.0	1.5	0.59	0.62	1.2	0.64
CO <sub>3</sub> <sup>=</sup>	1.0	7.9	0.46	0.14	4.7	0.55
DEAH <sup>+</sup>	1.0	na	0.59	0.49	1.2	0.64
DEACOO <sup>-</sup>	1.0	na	1.8	0.55	2.9	1.9
H <sub>3</sub> O <sup>+</sup>	1.0	1.5	0.59	0.59	1.2	0.64
OH <sup>-</sup>	1.0	1.5	0.59	0.56	1.2	0.64
MDEA	1.0	1.0	na	na	1.0	na
MDEAH <sup>+</sup>	1.0	1.5	na	na	1.2	na
MEA/MDEA system						
	Water	25% MEA	5% MEA 45% MDEA			
CO <sub>2</sub>	1.0	1.4	1.4			
MEA	0.18	0.29	0.24			
H <sub>2</sub> O	1.0	0.98	1.0			
HCO <sub>3</sub> <sup>-</sup>	1.0	0.33	0.60			
CO <sub>3</sub> <sup>=</sup>	1.0	1.1	7.0			
MEAH <sup>+</sup>	1.0	0.95	1.5			
MEACOO <sup>-</sup>	1.0	0.82	1.6			
H <sub>3</sub> O <sup>+</sup>	1.0	0.96	1.5			
OH <sup>-</sup>	1.0	0.96	1.5			
MDEA	1.0	na	1.0			
MDEAH <sup>+</sup>	1.0	na	1.6			

<sup>a</sup>T=298K unless otherwise specified

Table 9.5 Comparison of Regression Results for MDEA System

case no.	rate expression <sup>a</sup>	parameter estimates		error
		k <sub>298</sub> (m <sup>3</sup> /kmol-s)	E <sub>a</sub> (kcal/kmol-K)	
9.5.1	MDEA, high driving force <sup>b</sup>			
	k (MDEA)(H <sub>2</sub> O)	0.0378 ± 3.6%	11070 ± 6.9%	1.9
9.5.2	MDEA, high + low driving force			
	k (MDEA)(H <sub>2</sub> O)	0.048 ± 3.0%	14000 ± 4.7%	3.5
9.5.3	MDEA, high + low driving force, H <sub>2</sub> SO <sub>4</sub>			
	k (MDEA)(H <sub>2</sub> O)	0.0727 ± 2.6%	11970 ± 5.1%	3.4
9.5.4	MDEA, high + low driving force <sup>c,d</sup>			
	k (MDEA)(H <sub>2</sub> O)	0.0212 ± 7.8%	1390 ± 120%	
	k (MDEA)(OH <sup>-</sup> )	1.46x10 <sup>5</sup> ± 7.2%	9220 ± 13.%	1.2
9.5.5	MDEA, high + low driving force, H <sub>2</sub> SO <sub>4</sub> <sup>d</sup>			
	k (MDEA)(H <sub>2</sub> O)	0.0482 ± 3.7%	5520 ± 17%	
	k (MDEA)(OH <sup>-</sup> )	1.07x10 <sup>5</sup> ± 8.9%	9420 ± 15%	2.7

---

 Table 9.5 Comparison of Regression Results for MDEA System (Cont'd)
 

---

## 9.5.6 MDEA, high + low driving force

k (MDEA)(H <sub>2</sub> O)	0.0157 ± 9.2%	3710 ± 54%	
k (MDEA)(OH <sup>-</sup> )	1.54x10 <sup>5</sup> ± 7.0%	8107 ± 4.8%	1.1

9.5.7 MDEA, high + low driving force, H<sub>2</sub>SO<sub>4</sub>

k (MDEA)(H <sub>2</sub> O)	0.0453 ± 4.2%	8170 ± 12%	
k (MDEA)(OH <sup>-</sup> )	1.11x10 <sup>5</sup> ± 8.6%	8160 ± 20%	2.4

<sup>a</sup>Rate expression corresponds to the net forward rate of reaction through the amine mechanism divided by the CO<sub>2</sub> activity (activities were used in all rate calculations).

<sup>b</sup>High and low driving force implies > 0.25 atm and ≤ 0.25 atm CO<sub>2</sub> partial pressure over solution. H<sub>2</sub>SO<sub>4</sub> indicates that 0.25 kmole H<sub>2</sub>SO<sub>4</sub>/kmole MDEA was added to solution.

<sup>c</sup>These parameters are considered to be the "correct" set and used in subsequent simulation.

<sup>d</sup>In these regressions, the hydroxide reaction, equation [2.1], was neglected.

---

we examine the high and low driving force data we find that the reaction expression incorporating hydroxide into the mechanism is substantially better than the simple mechanism. Figures 9.1, 9.2 and 9.3 show the normalized error for cases (9.5.2) and (9.5.4):

$$\text{norm. error} = ((e_{\text{pco2}}/s_{\text{pco2}})^2 + (e_{\text{load}}/s_{\text{load}})^2 + (e_{\text{flux}}/s_{\text{flux}})^2) * \text{sign}(e_{\text{flux}}) \quad [9.4]$$

where

$$e_i = \text{pred}(i) - \text{exp}(i)$$

The reason for including  $\text{sign}(e_{\text{flux}})$  in the definition is so that the data will indicate whether the flux was overpredicted or underpredicted. Relative standard deviations of 5%, 5% and 10% were assumed for the partial pressure of  $\text{CO}_2$ , the loading, and the flux, respectively. From Figures 9.1 through 9.3, we see that the flux at higher hydroxide concentrations was seriously underpredicted with the simple model, but the additional hydroxide term resolves the discrepancy in the data. In addition, by comparing Figures 9.1 and 9.2, we see that the data are more closely correlated by the product of the MDEA and hydroxide concentration as opposed to the hydroxide concentration alone. We note that, for cases (9.5.4) and (9.5.5) the hydroxide reaction itself was neglected, whereas in cases (9.5.6) and (9.5.7) the hydroxide term in the MDEA mechanism is in addition to the hydroxide reaction of  $\text{CO}_2$  alone, given by equation [2.1]. Therefore, the net rate expression is of the form:

$$r = (\text{CO}_2)(\text{MDEA})\{k_{\text{H}_2\text{O}}(\text{H}_2\text{O}) + k_{\text{OH}^-}(\text{OH}^-)\} + k'_{\text{OH}^-}(\text{CO}_2)(\text{OH}^-) \quad [9.5]$$

Both assumptions give a comparable fit to the data. In subsequent analysis, unless otherwise specified, we will use the parameters estimated in case (9.5.4).

If we correct for the water concentration in our rate constant, then compare the ratio of hydroxide to water rate constant at  $25^\circ\text{C}$ , we find the ratio is  $1.2 \times 10^5$ . This value compares favorably to the ratio of  $3.63 \times 10^5$  at  $25^\circ\text{C}$  for the uncatalyzed reactions (see equations [2.3] and [2.5]). The rate expression [9.5] corresponds to possible mechanisms proposed by Barth et al. (1981) (see section 2.3).



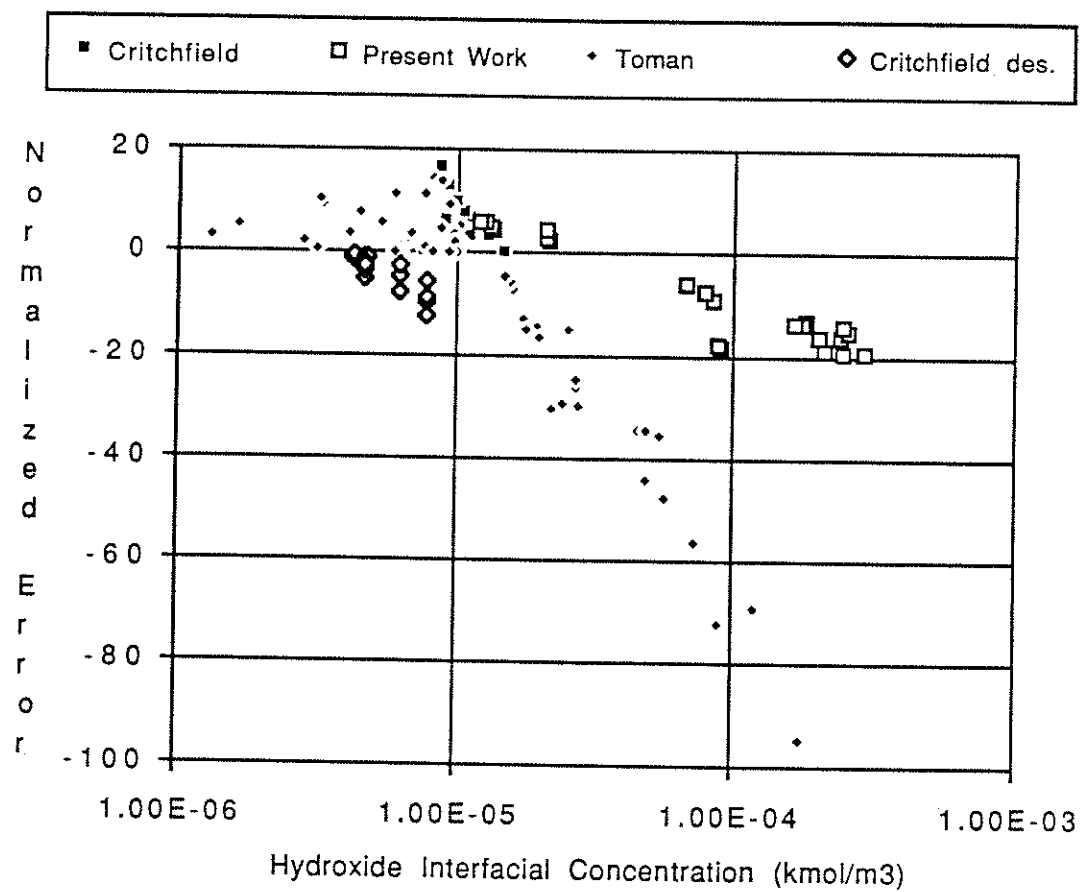


Figure 9.1 Fit of MDEA High- and Low-Driving Force Data with the Simplified Kinetic Mechanism (CO<sub>2</sub>-MDEA-H<sub>2</sub>O Term Only), Case 9.5.2. Desorption Date Designated by des.

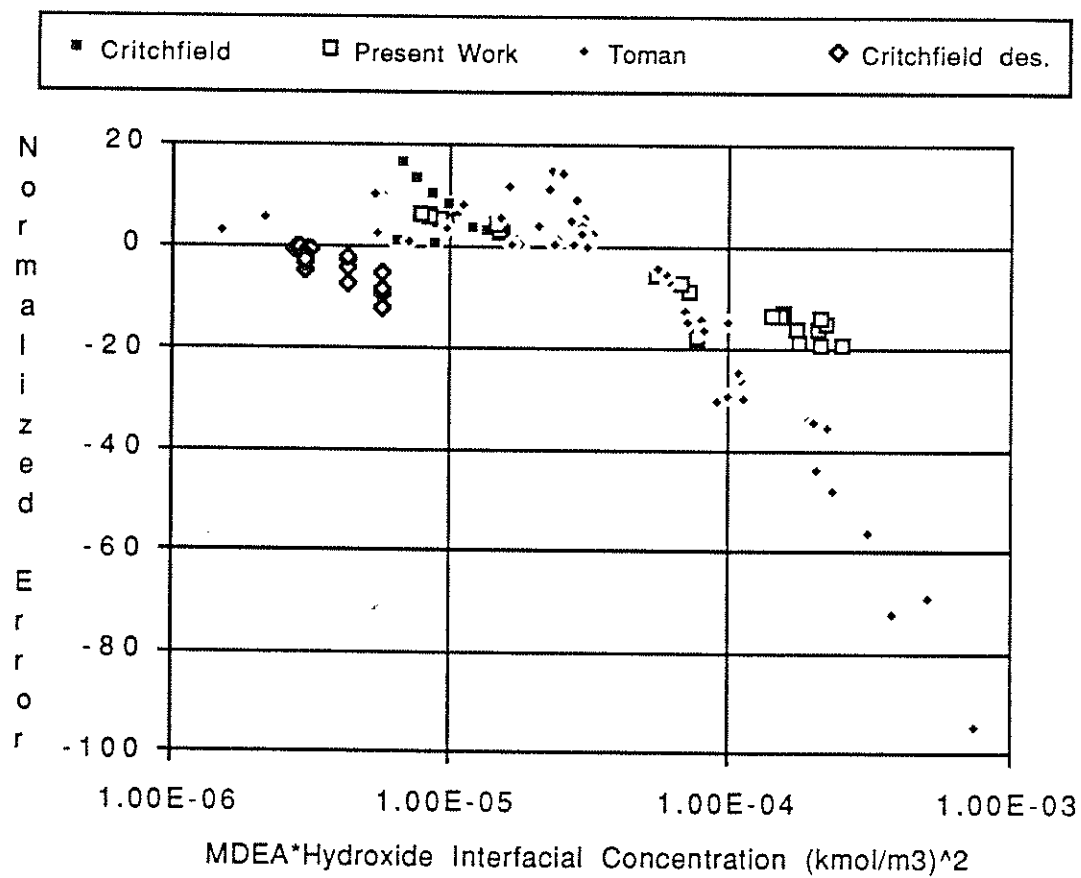
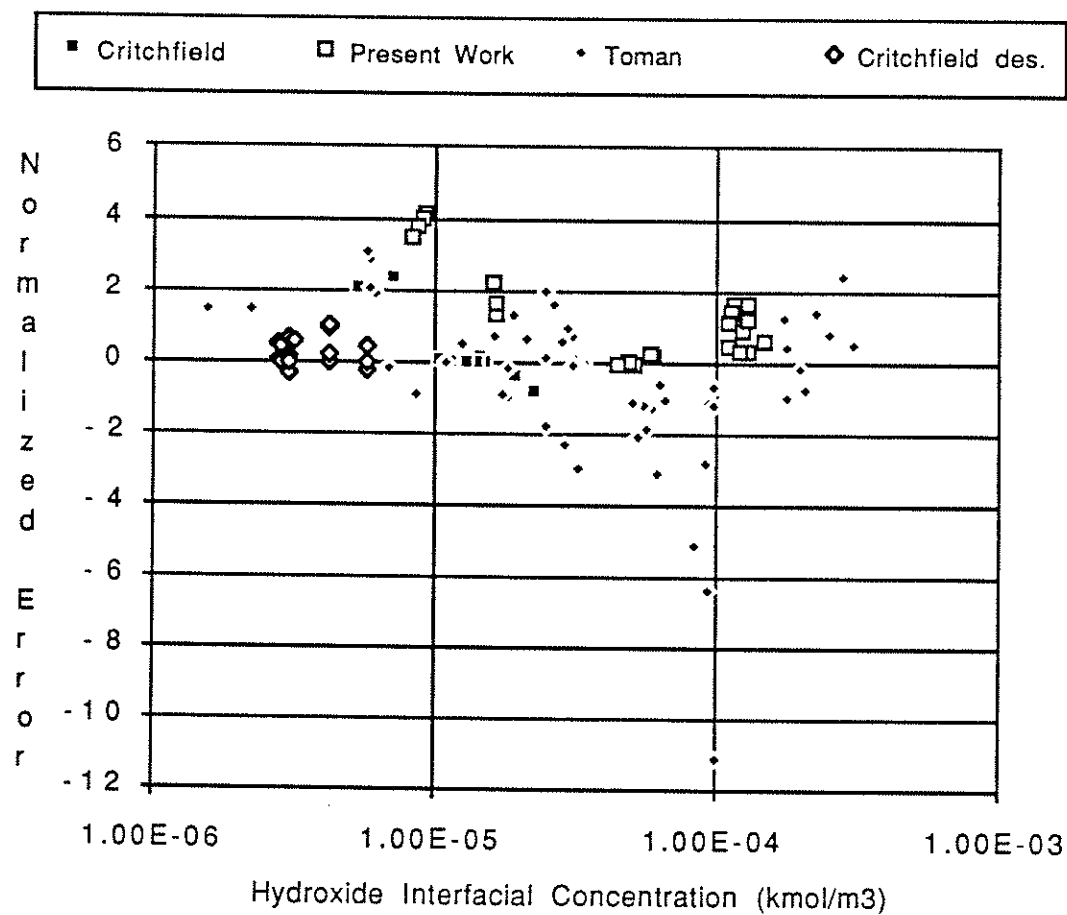


Figure 9.2 Fit of MDEA High- and Low-Driving Force Data with the Simplified Kinetic Mechanism (CO<sub>2</sub>-MDEA-H<sub>2</sub>O Term Only), Case 9.5.2.  
 • Desorption Data Designated by des.



---

Figure 9.3 Fit of MDEA High- and Low-Driving Force Data with the Hydroxide Kinetic Mechanism, Case 9.5.4. Desorption Data Designated by des.

---

---

It has been suggested (Versteeg, 1986) that primary and/or secondary amine contaminants can explain the relatively high absorption rates found at low partial pressures of CO<sub>2</sub>. In order to check this hypothesis, we had the MDEA analyzed for impurities (Benac, 1989). No primary amines were found in measurable quantities. Two secondary amines, Methyl Monoethanolamine (MMEA) and N-Methyl Diglycolamine, were found to constitute 0.037 and 0.047 wt% of the neat MDEA (the MDEA itself is 99.557% pure). Other contaminants were either tertiary amines or glycols. In order to check the impurity assumption, we lumped the impurities as 0.1 wt% MMEA and simulated CO<sub>2</sub> absorption rates at conditions shown in Table 9.6 (MMEA was assumed to have the pKa and diffusivity of MEA, both lead to a conservative estimate). It was found that the impurity effect could not account for the apparently high absorption rate at the low partial pressure. This is demonstrated in Table 9.6, where the apparent reactivity is much more sensitive to CO<sub>2</sub> partial pressure than can be demonstrated by the mass transfer model. This is because, even at the low partial pressure, the MMEA is already depleted, as will be demonstrated in section 9.4.

Also shown in Table 9.5 are results for the addition of sulfuric acid to MDEA (Toman, 1990). The results indicate that the reaction rates are "faster" than can be explained by the mass transfer model, suggesting further catalytic reaction by the ions. The details of this analysis are not in the scope of this work, but are analyzed in more detail by Toman (1990).

### 9.2.2 DEA system

Absorption and desorption data for DEA were correlated using the following rate expression (the reverse reactions are also included in the kinetic model):

$$r = k_{H_2O}(DEA)(H_2O) + k_{DEA}(DEA)(DEA) \quad [9.6]$$

This expression corresponds to the general zwitterion mechanism assuming:

$$k_2 \gg k'_{H_2O}(H_2O) + k'_{DEA}(DEA) \quad [9.7]$$

Table 9.6 Analysis of Effect of Impurities on the Absorption Rate of CO<sub>2</sub> into 10.6 wt% Aqueous MDEA at 298K

$k_l^0$ (m/s)	Loading	$P_{CO2}$ (kPa)	Flux/ $P_{CO2}$ (kmol/m <sup>2</sup> /s/kPa)	
			<u>experimental</u>	<u>predicted<sup>a</sup></u>
Low Driving Force Datapoint				
$1.31 \times 10^{-5}$	0.0182	4.38	$4.0 \times 10^{-8}$	$2.5 \times 10^{-8}$
High Driving Force Datapoint				
$1.31 \times 10^{-5}$	0.0182	97.2	$1.6 \times 10^{-8}$	$2.0 \times 10^{-8}$

<sup>a</sup>Predicted corresponds to the mass transfer model prediction using the MDEA kinetic model with parameters of case 9.5.2. All impurities are lumped and represented as 0.1 wt% MMEA.

The mass transfer model does include the full zwitterion mechanism, of which the current rate expression is a subcase; however,  $k_2$  was found to be high and could not be regressed with statistical significance. Also note that hydroxide was not included as a base - generally, it is negligible compared to DEA in effect (Blauwhoff et al., 1984).

Table 9.7 summarizes the results for DEA. Cases 9.7.1 and 9.7.2 demonstrate the effect of the rate constant formulation on consistency between absorption and desorption data. In the first case, shown in Figure 9.4, we assumed the forward rate constants were indeed "constant". In this case, the desorption data and some absorption data were seriously underpredicted. We see a much better fit and consistency between the absorption and desorption data assuming a functional form of equation [4.37], i.e. the forward rate constants increase as a function of ionic strength, as shown in Figure 9.5. We also used this same formulation for the MDEA system, and found no significant overprediction of desorption rates.

### 9.2.3 DEA/MDEA system

Thus far, we have concluded that, for MDEA data alone, the combined water and hydroxide rate expression best resolves the experimental data. Furthermore, for DEA and MDEA, we allow the rate constant to increase as a function of ionic strength. For the mixed amine system DEA/MDEA, only one additional constant need be determined - the interaction rate constant for MDEA in the DEA zwitterion mechanism. This should be interpreted as MDEA deprotonation of the zwitterion in the second step of the mechanism. In Table 9.7, we show the regression of this parameter using different expressions for the MDEA rate constants and, as expected, the MDEA rate parameters do not affect the mixed amine data significantly. The data for case 9.7.4 and 9.7.5 are shown in Figures 9.6 and 9.7, respectively. As can be seen, there are no significant trends as a function of DEA concentration. One may notice that all errors appear consistently negative. This is because a negative error in flux under desorption conditions has the opposite effect of a negative error in flux under absorption conditions. The fact that we have consistently negative errors means that the desorption data were slightly overpredicted and the absorption data were slightly underpredicted. In most cases, the agreement was within 10%, and therefore the fit was considered good.

Table 9.7 Comparison of Regression Results for the DEA and DEA/MDEA Systems<sup>a</sup>

case no.	rate expression	parameter estimates		error
		k <sub>298</sub>	E <sub>a</sub>	
9.7.1	Pure DEA data <sup>b</sup>			
	k(DEA)(H <sub>2</sub> O)	30.0 ± 19%	11000 ± 61% <sup>c</sup>	0.79
	k(DEA)(DEA)	18500 ± 10%	9314 ± 79% <sup>c</sup>	
9.7.2	Pure DEA data - forward rate concentration based			
	k(DEA)(H <sub>2</sub> O)	4.10 ± 31%	10100 ± 90%	1.3
	k(DEA)(DEA)	637 ± 8.8%	6558 ± 92%	
9.7.3	DEA/MDEA using MDEA case 9.5.1			
	k (MDEA)(DEA)	4656 ± 7.4%	6477 ± 28%	1.7
9.7.4	DEA/MDEA using MDEA case 9.5.2			
	k (MDEA)(DEA)	4570 ± 7.5%	5550 ± 34%	1.7
9.7.5	DEA/MDEA using MDEA case 9.5.4 <sup>b,d</sup>			
	k (MDEA)(DEA)	3600 ± 8.8%	2720 ± 88%	1.2
9.7.6	DEA/MDEA using MDEA case 9.5.6			
	k(MDEA)(DEA)	3310 ± 9.3%	-105 ± 2360%	1.5

<sup>a</sup>Refer to previous tables for terminology

<sup>b</sup>These parameter sets are considered to be "correct" and used in subsequent simulation

<sup>c</sup>The reason for high standard deviations is a high correlation between the water and DEA activation energies. The correlation between these two variables is -0.92.

<sup>d</sup>In this simulation, the hydroxide reaction itself was neglected

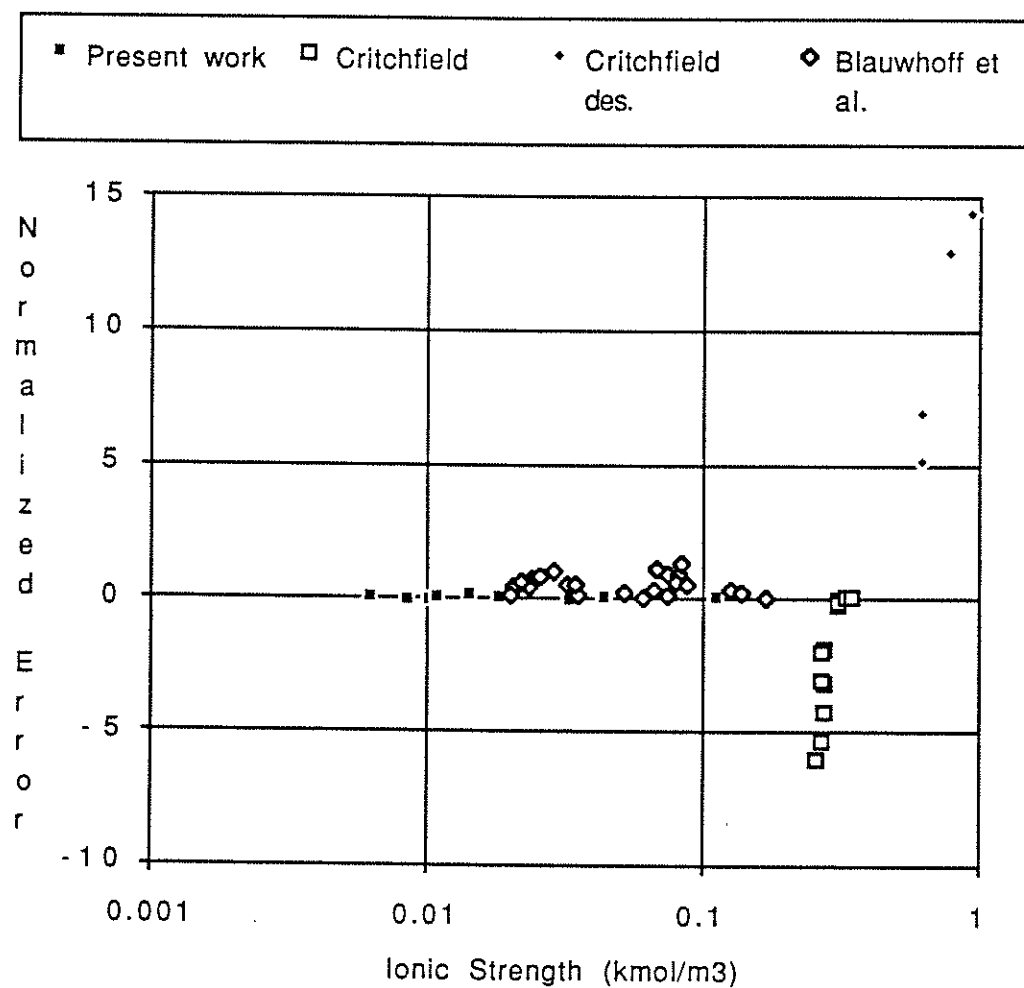


Figure 9.4 Fit of DEA Absorption/Desorption Data Using Constant Forward Rate Constants, Case 9.7.1. Desorption Data Designated by des.



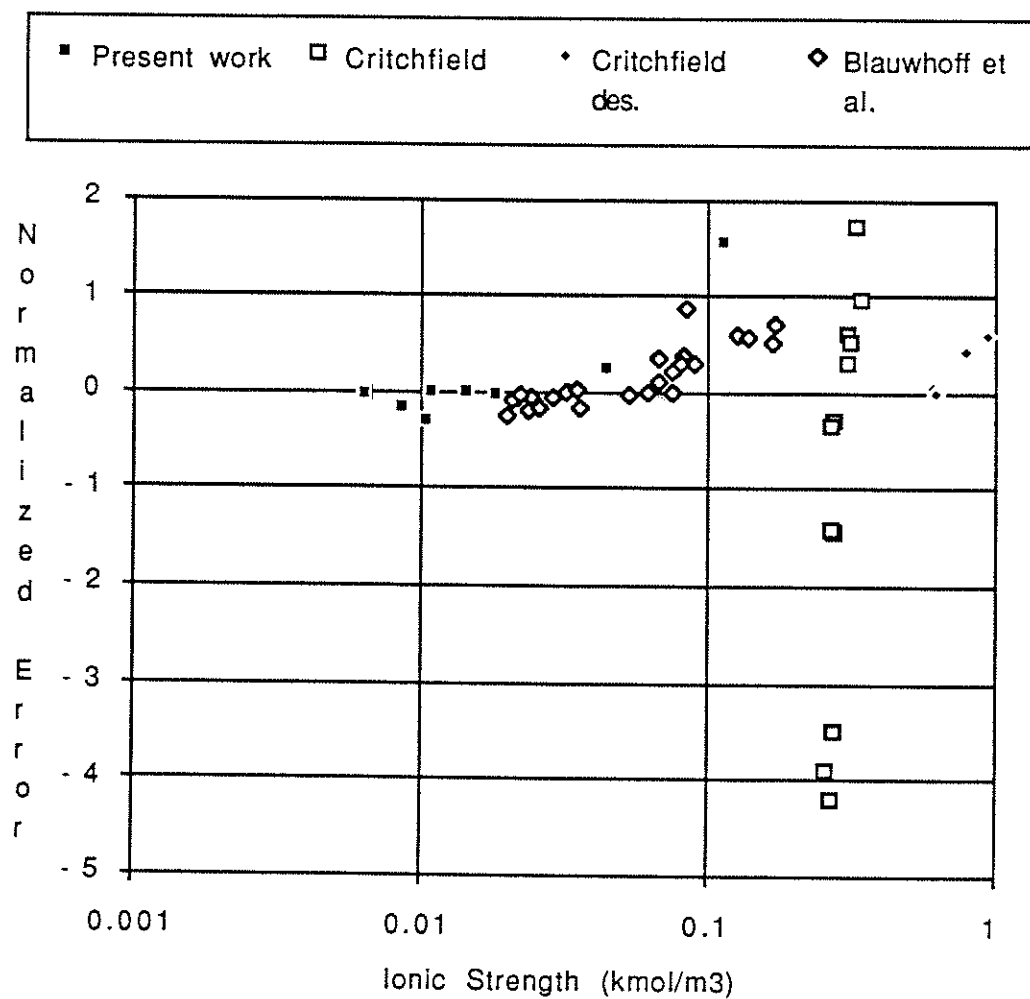


Figure 9.5 Fit of DEA Absorption/Desorption Data Assuming Forward Rate Constants Increase with Ionic Strength, Case 9.7.2. Desorption Data Designated by des.

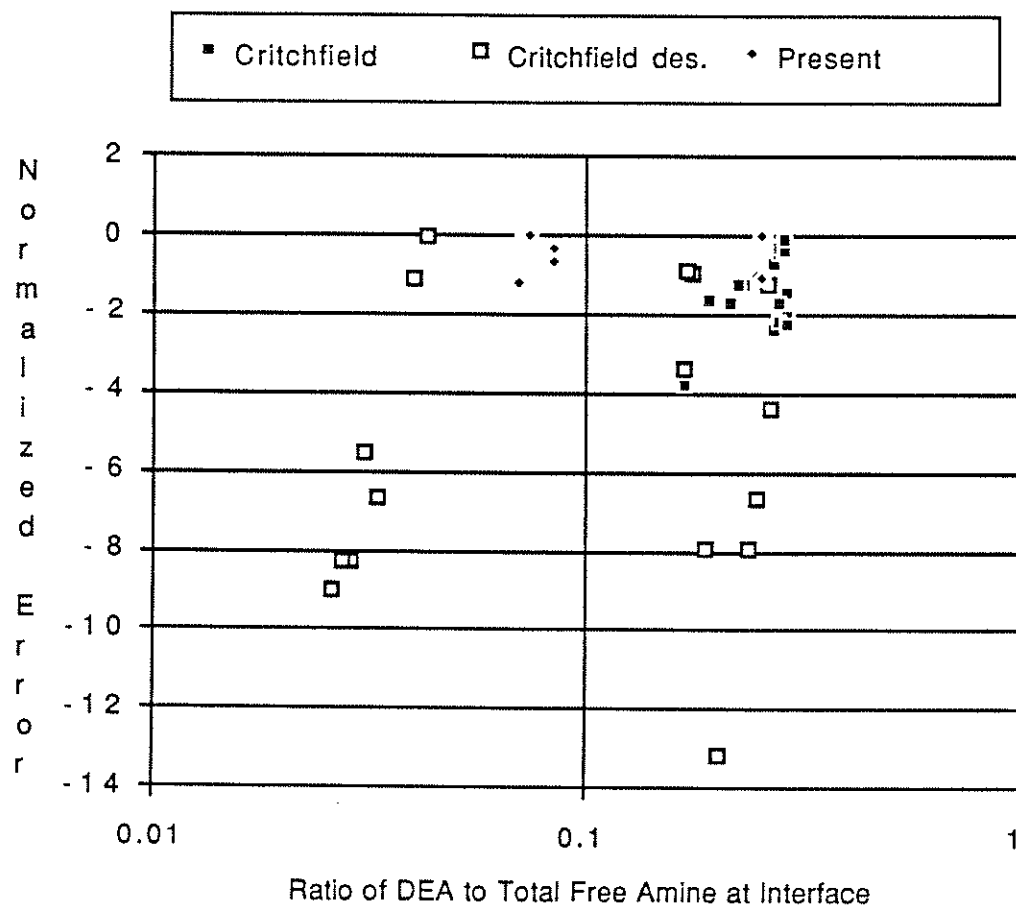


Figure 9.6 Fit of DEA/MDEA Data Using Simplified MDEA Kinetic Mechanism, Case 9.7.4. Desorption Data Designated by des.

---

---

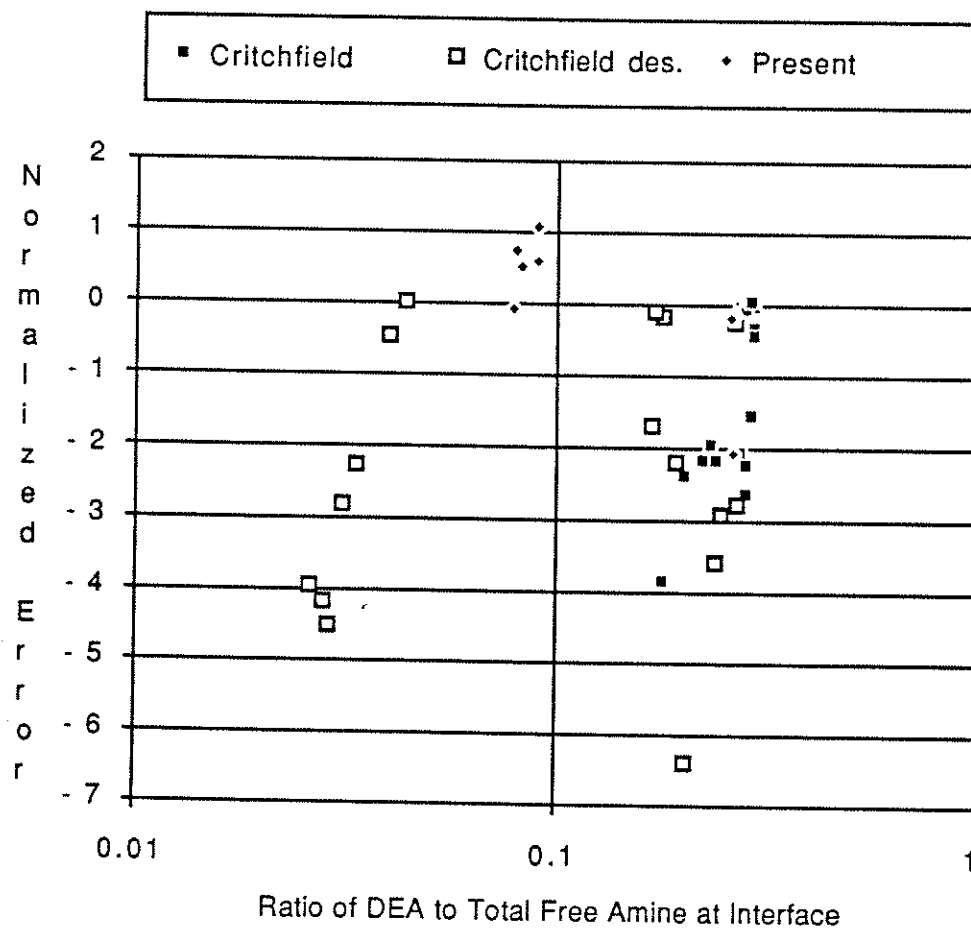


Figure 9.7 Fit of DEA/MDEA Data Using Hydroxide Kinetic Mechanism for MDEA, Case 9.7.5. Desorption Data Designated by des.

---

#### 9.2.4 MEA/MDEA system

There is apparently no significant interaction between MEA and MDEA for the mixed amine system. This conclusion was found by Critchfield (1988) and we re-ran his absorption/desorption data using the mass transfer model with the rate constant of equation [2.25] for MEA and the parameters of case 9.5.4 for MDEA. The results are shown in Figure 9.8. Note that one desorption point is significantly off. This is apparently an outlier, for a downward adjustment in loading of approximately 17% will make the model fit the data. This type of error is easily attributable to occasional experimental error. In general, the data of Critchfield and the model results are in good agreement.

### 9.3 Comparison with Previous Data

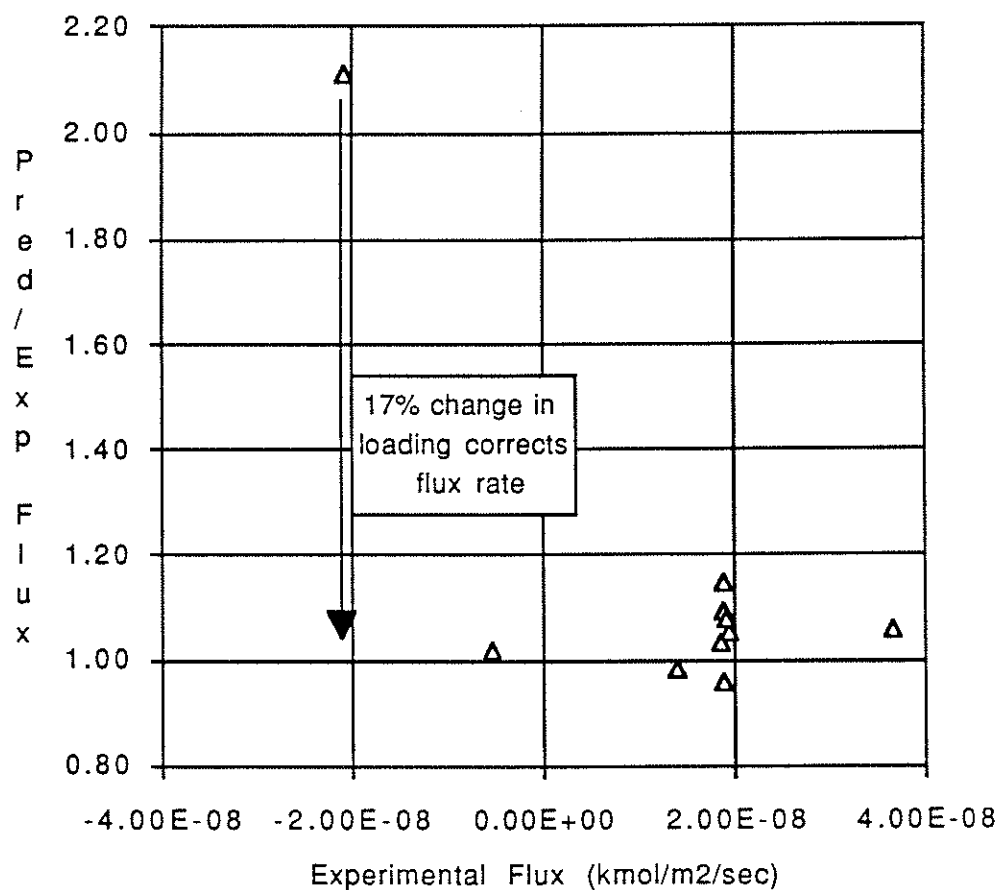
#### 9.3.1 MDEA system

Typical literature results for the second-order rate constant corresponding to the reaction of CO<sub>2</sub> with MDEA are shown in Table 9.8:



The results vary widely, ranging from 2.5 to 7.4 m<sup>3</sup>/kmol/sec at 298K. The activation energies also vary to some extent. We cannot compare our results directly to the literature data, since the kinetic expression used also includes the hydroxide ion concentration. For comparative purposes, the following approach was taken:

- (1) Calculate the concentration profiles under varying conditions for the absorption of CO<sub>2</sub> into MDEA
- (2) From the results, calculate the apparent rate constant for the reaction of CO<sub>2</sub> with MDEA:



---

Figure 9.8      Simulation of MEA/MDEA Experimental Data Using A Non-Interactive Kinetic Model, Kinetic Parameters of Case 9.5.4 for MDEA, Rate Constant of Equation [2.25] for MEA.

---

---

Table 9.8 Comparison of Results with Literature Data

MDEA system:  $r = k_2[\text{CO}_2][\text{MDEA}]$

	$k_{298}$	$E_a$
Critchfield (1988)	2.5	13700
Tomcej et al. (1986)	7.4	9400
Versteeg and Van Swaaij (1988c)	4.3	10100
Littel et al. (1990)	5.1	10700
Haimour et al. (1987)	2.5	17100
Current	1.5 - 30	6590-13600
	(see Fig. 9.9)	(see Table 9.9)

DEA system:

$$r = [\text{CO}_2] [\text{DEA}] \{k'_{\text{H}_2\text{O}} [\text{H}_2\text{O}] + k'_{\text{DEA}} [\text{DEA}] + k'_{\text{MDEA}} [\text{MDEA}]\}$$

Versteeg and van Swaaij (1988b)

$$k'_{\text{H}_2\text{O}} = 5.3$$

$$k'_{\text{DEA}} = 228.$$

Critchfield (1988)<sup>a</sup>

$$100 < k'_{\text{MDEA}} < 400$$

Current work

$$k'_{\text{H}_2\text{O}} = 4.75$$

$$k'_{\text{DEA}} = 464.$$

$$k'_{\text{MDEA}} = 468.$$

<sup>a</sup>Critchfield used a different expression for DEA. Shown is an approximate range of this interaction constant based upon conditions investigated in this work from a linearized form of Critchfield's rate expression. See text.

$$k_2 = \frac{\gamma_{\text{MDEA}} \gamma_{\text{CO}_2}}{\gamma_{\text{HCO}_3}} \left\{ k_{\text{H}_2\text{O}} \frac{\gamma_{\text{H}_2\text{O}}}{\gamma_{\text{MDEAH}^+}} [\text{H}_2\text{O}]_i + k_{\text{OH}^-} \frac{\gamma_{\text{OH}^-}}{\gamma_{\text{MDEA}}} [\text{OH}^-]_i \right\} \quad [9.8]$$

The activity coefficients in the numerators account for the fact that activities, instead of concentrations, are actually used in the rate expression. The activity coefficients in the denominators are the corrections obtained based on the products of the reaction using equation [4.37]. In this manner, we have calculated the apparent rate constant as if we had neglected the hydroxide contribution in the MDEA mechanism. Figure 9.9 shows this apparent rate constant as a function of CO<sub>2</sub> loading. The first case,  $P \rightarrow P^*$ , is the apparent rate constant in the limit that the partial pressure of CO<sub>2</sub> approaches its equilibrium partial pressure, in which case all gradients and fluxes approach zero and we are in pseudo first-order conditions. At a pressure of 10 kPa, the MDEA concentration profile is still constant, however, the hydroxide is depleted at the interface. Note that the differences between these two cases become more substantial at low loadings, where there is enough hydroxide ion in the bulk liquid phase to make a substantial contribution to the absorption rate under pseudo first-order conditions. Finally, at a pressure of 101 kPa, we have an even greater depletion of hydroxide at the interface, along with some depletion of the MDEA. Note that the apparent rate constant obtained can easily span the range of data found in the literature. We also note that a trend exists in the literature data in which equipment with higher mass transfer coefficient (a wetted sphere in the work of Tomcej et al. (1986)), and lower partial pressure of CO<sub>2</sub> (Versteeg and van Swaaij (1988c)) tend to give higher rate constants. This is the trend predicted by our mass transfer model. We cannot compare the data directly since the CO<sub>2</sub> loadings are never reported except in the work of Critchfield (1988), and have a large effect on the hydroxide concentration.

Figure 9.9 demonstrates some interesting behavior and is useful for purposes other than comparison. For example, notice that the second-order rate constant at 101 kPa increases with loading. This is due to the change in ionic strength as a function of loading, hence affecting the activity coefficients, as shown in Table 9.4, which then affect the apparent reaction rate in a manner described by equation [9.8]. The reason for the decrease and subsequent increase of the rate constant for the first two cases is a competing effect between the hydroxide depletion and the ionic strength effect. Finally, we note that no experimental data were taken at very low driving forces and low ionic

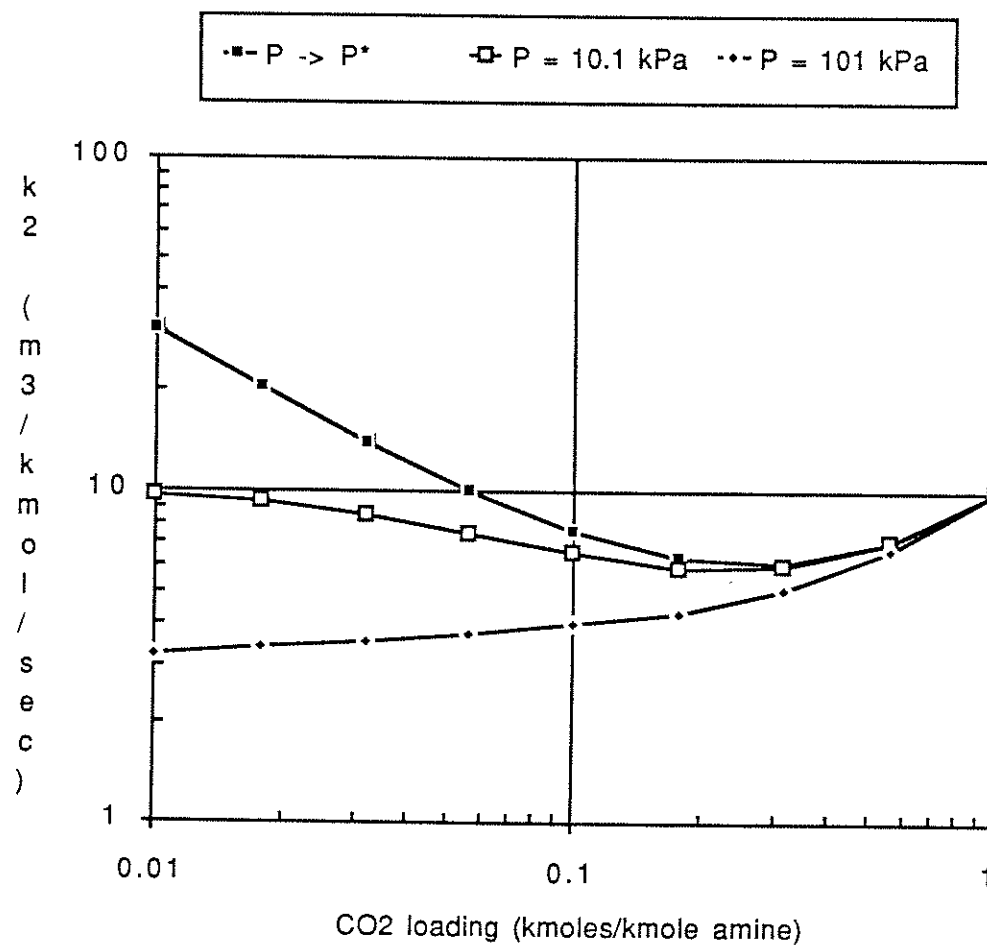


Figure 9.9 Apparent Rate Constant for the CO<sub>2</sub>-MDEA Reaction as a Function of CO<sub>2</sub> Partial Pressure and Loading. Specific Conditions: 20wt% MDEA at 298K,  $k_1^0 = 10^{-5} \text{ m/sec}$ , Derived from Case 9.5.4 for MDEA.



strengths, so the apparently very high rate constants obtained at the extreme conditions represent an extrapolation of the data, and is certainly subject to verification in future work.

Table 9.9 shows tabulated effective rate constants as a function of loading, CO<sub>2</sub> partial pressure, and temperature. The effective rate constant,  $k_2$ , is the same rate constant which is plotted in Figure 9.9. In addition, however, Table 9.9 shows the relative contribution of hydroxide to water in the hydroxide mechanism, as well as the activation energy. As can be seen, the hydroxide term dominates the kinetic expression [9.8] at most all conditions, especially at low loadings and low CO<sub>2</sub> partial pressures. The activation energy varies greatly, depending on (1) whether or not the hydroxide dominates in the kinetic expression and (2) the CO<sub>2</sub> partial pressure.

### 9.3.2 DEA and DEA/MDEA systems

The comparison of rate constants for DEA and DEA/MDEA systems is much more straightforward. The results shown in Table 9.8 indicate that the water and DEA apparent rate constants calculated in this work are comparable to the work of Versteeg and van Swaaij (1988b). For the MDEA-DEA interaction, the current work indicates that the MDEA rate constant is close to DEA. Versteeg and van Swaaij (1988a) report results for a DIPA/MDEA mixed amine system which indicate that the DIPA and MDEA rate constants are quite similar (198 and 131 m<sup>6</sup>/kmol<sup>2</sup>-sec, respectively). Both this work and the work of Versteeg and van Swaaij indicate that the partial rate constants for the secondary and tertiary amine are similar.

We cannot compare the DEA-MDEA interaction parameter directly to the work of Critchfield since he uses the rate expression of the form of Laddha and Danckwerts (1981) for DEA. His expression is of the form:

$$r = \frac{[\text{CO}_2][\text{DEA}]}{\frac{1}{1410} + \frac{1}{1200[\text{DEA}] + 2326[\text{MDEA}]}} \quad [9.9]$$

If we take conditions typical of a low CO<sub>2</sub> loading, then the rate expression in this work is approximately:

Table 9.9 Effective Rate Constants and Activation Energy for the Reaction of CO<sub>2</sub> with MDEA

loading	P (kPa)	T (K)	[OH <sup>-</sup> ] <sub>i</sub> *10 <sup>5</sup> <sup>a</sup> (kmol/m <sup>3</sup> )	f <sub>OH<sup>-</sup></sub> <sup>b</sup>	k <sub>2</sub> (m <sup>3</sup> /kmol-s)	E <sub>a</sub> (kcal/kmol-K)
0.01	P* <sup>c</sup>	298.15	18.5	0.96	30.5	13600
		313.15	28.2	0.99	91.5	
	10.1	298.15	5.37	0.89	9.62	9180
		313.15	5.96	0.94	20.2	
	101.	298.15	1.34	0.66	3.24	6950
		313.15	1.41	0.79	5.68	
0.1	P* <sup>c</sup>	298.15	3.25	0.75	7.41	11400
		313.15	4.98	0.90	18.7	
	10.1	298.15	2.67	0.71	6.42	9960
		313.15	3.69	0.87	14.4	
	101.	298.15	1.19	0.52	3.89	6590
		313.15	1.39	0.71	6.63	

<sup>a</sup> The water concentration was essentially 45 kmol/m<sup>3</sup> under all conditions.

<sup>b</sup> This is the fraction of the hydroxide contribution to the total effective rate constant.

<sup>c</sup> P\* corresponds to the equilibrium partial pressure at a given loading and temperature. In this case, there is no net flux of CO<sub>2</sub> or gradients of species in the interface, giving rise to pseudo first-order conditions.

$$r = [\text{CO}_2][\text{DEA}] \{ 4.75[\text{H}_2\text{O}] + 464[\text{DEA}] + 468[\text{MDEA}] \} \quad [9.10]$$

Both expressions give similar results under the conditions investigated in this work (see Table 9.8) however, depending on the concentration of DEA and MDEA, the rate expression of Critchfield can predict higher or lower effect of MDEA on the promotion of DEA rates. Notice that as the concentration of the amines gets large, the predictions of the two expressions will diverge. Both of these rate expressions are limiting forms of the zwitterion mechanism (see Chapter 2) and equation [9.10] was used in this work because of the suggestion by Blauwhoff et al. (1984) that it fit a wide range of data for DEA better than the expression used by Laddha and Danckwerts.

#### 9.4 Concentration Profiles Obtained using the Rate Model

Typical profiles are shown for the DEA/MDEA system in Figures 9.10 through 9.12. In Figure 9.10, we see concentration profiles for pseudo first-order conditions, in which case the algebraic approximation, [8.4] is valid. At higher partial pressures, there are significant concentration gradients of the reactants and products at the interface in Figure 9.11. At the condition shown in Figure 9.11, the enhancement factor is 7.2, compared to 9.2 which would have been predicted by equation [8.4]. Finally, we see desorption concentration profiles in Figure 9.12. In desorption, we can again use equation [8.4] since all of the species concentrations (except  $\text{CO}_2$ ) are constant under the low driving forces generally encountered in desorption.

In Figure 9.13, we see the concentration profile for a case of MMEA impurity in MDEA. As was mentioned earlier, the MMEA becomes depleted at the gas-liquid interface, hence its contribution to the overall absorption rate is small, and cannot account for the driving force effects seen with the MDEA- $\text{CO}_2$  system.

#### 9.5 Useful Results Using the Combined Equilibrium/Rate Model

The combined equilibrium/mass transfer model has now been used to predict the performance of amine systems at mass transfer coefficients and temperatures at conditions of industrial interest. In Figure 9.14, we see the effect of 30wt% DEA and 50wt% MDEA on the  $\text{CO}_2$  absorption rate at  $40^\circ\text{C}$  and a mass transfer coefficient of  $10^{-4}$  m/sec (a liquid-phase mass transfer coefficient typical of packed columns and on

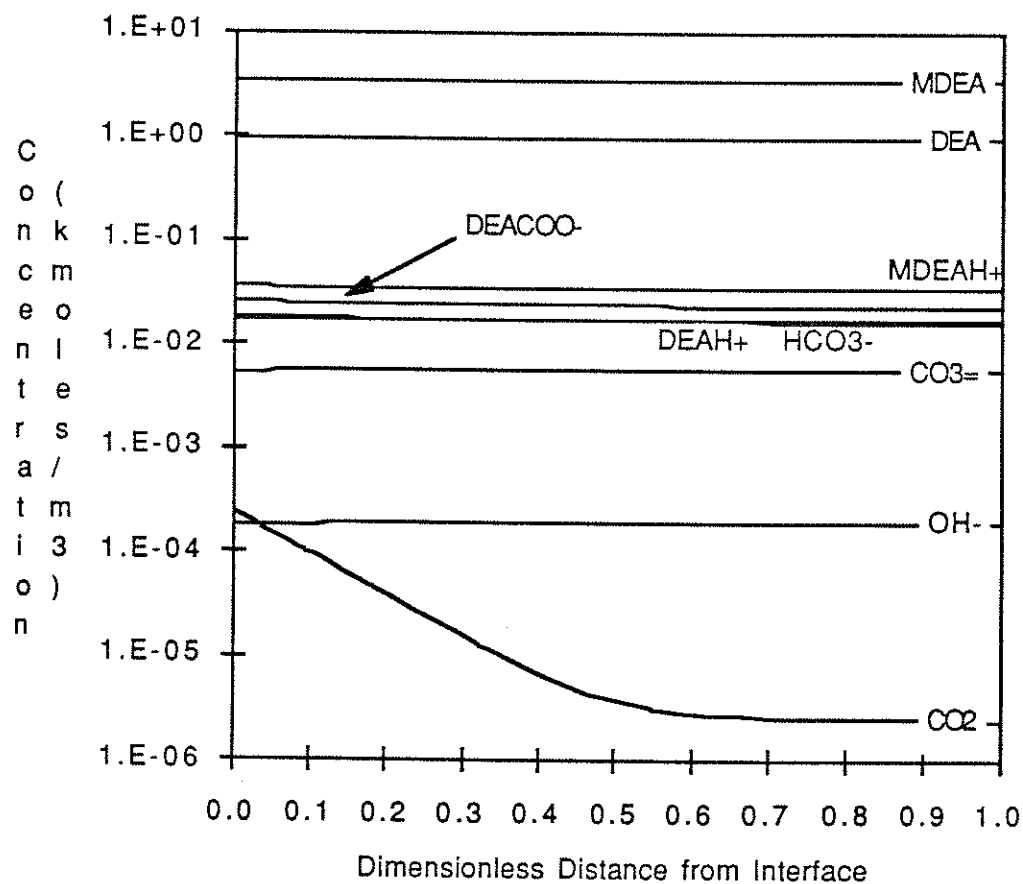


Figure 9.10 Concentration Profiles Under Low-Driving Force Absorption Conditions. 10wt% DEA, 40wt% MDEA, loading = 0.01, 313K,  $k_l^0 = 10^{-4}$  m/sec,  $P_{CO_2} = 1$  kPa, Dimensionless Distance Defined by Equation [5.45].

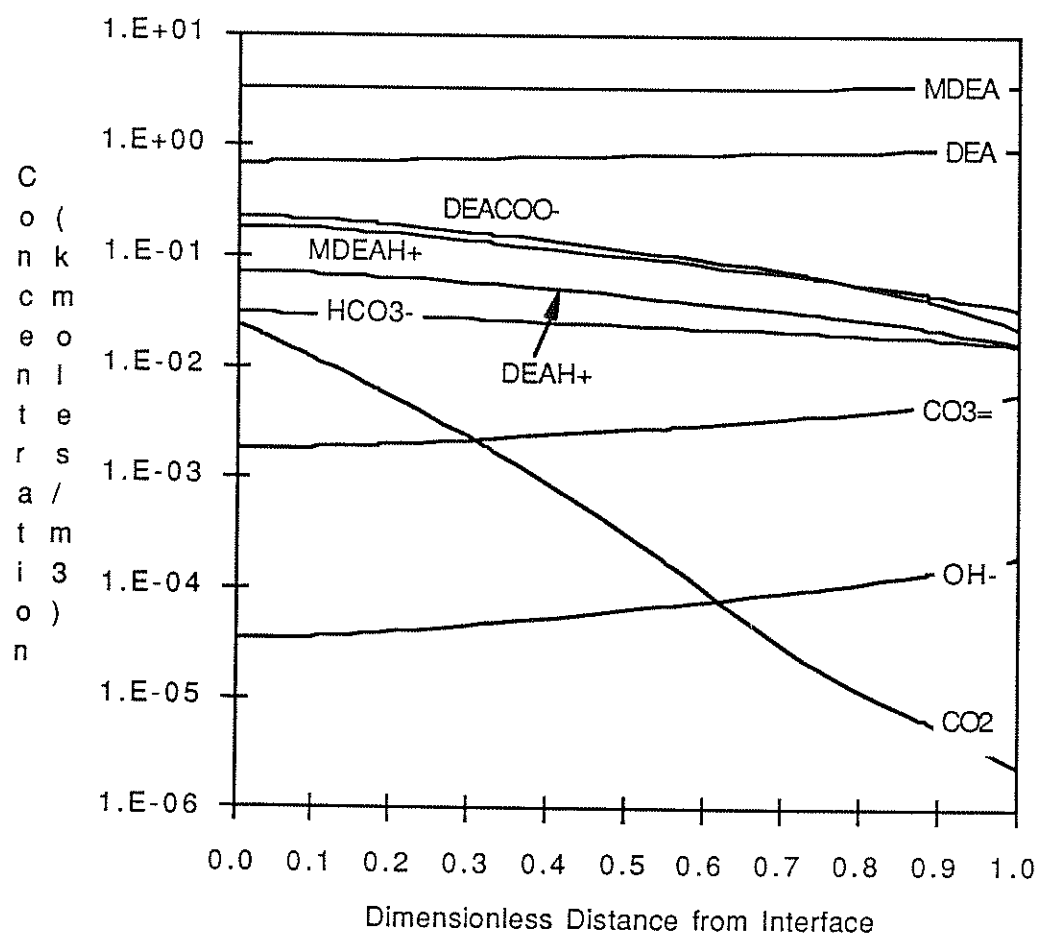


Figure 9.11 Concentration Profiles Under High-Driving Force Absorption Conditions. 10wt% DEA, 40wt% MDEA, loading = 0.01, 313K,  $k_1^0 = 10^{-4}$  m/sec,  $P_{CO_2} = 101$  kPa, Dimensionless Distance Defined by Equation [5.45].

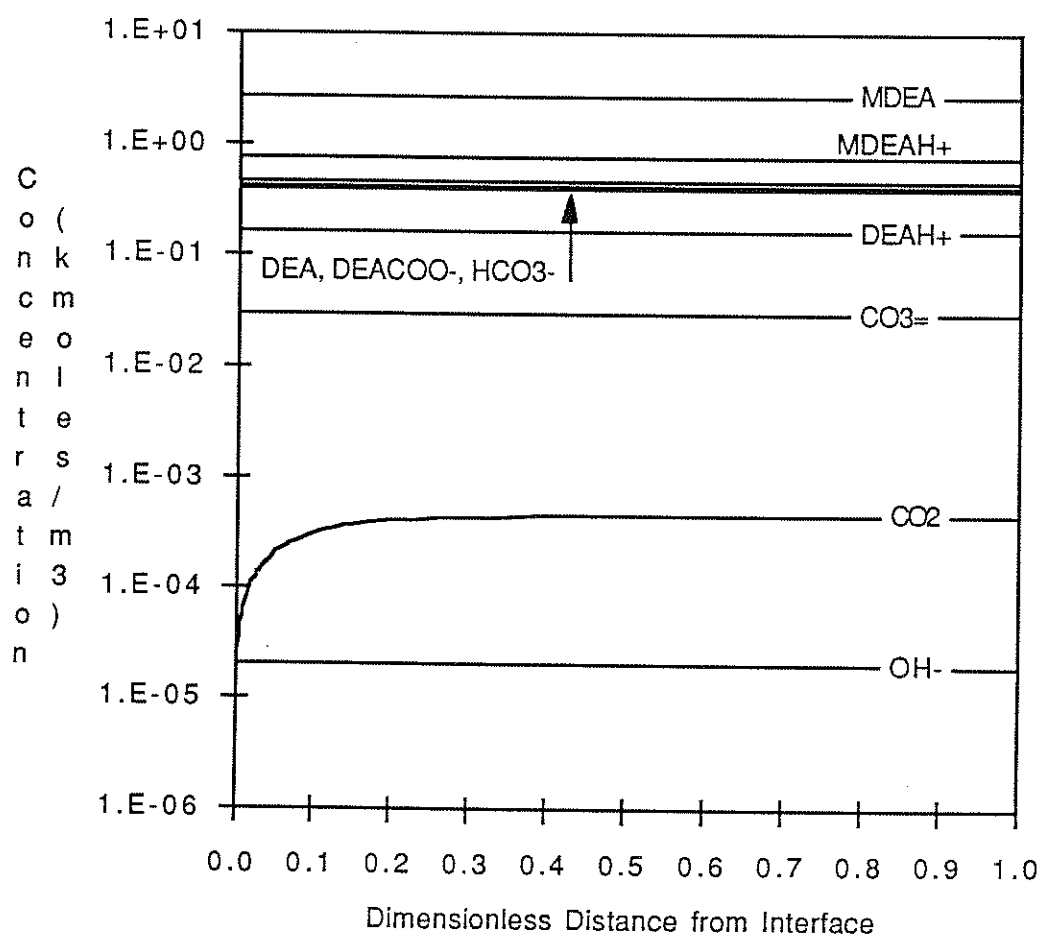


Figure 9.12 Concentration Profiles Under Desorption Conditions. 10wt% DEA, 40wt% MDEA, loading = 0.1, 313K,  $k_1^0 = 10^{-4}$  m/sec,  $P_{CO_2} = 0.1$  kPa, Dimensionless Distance Defined by Equation [5.45].

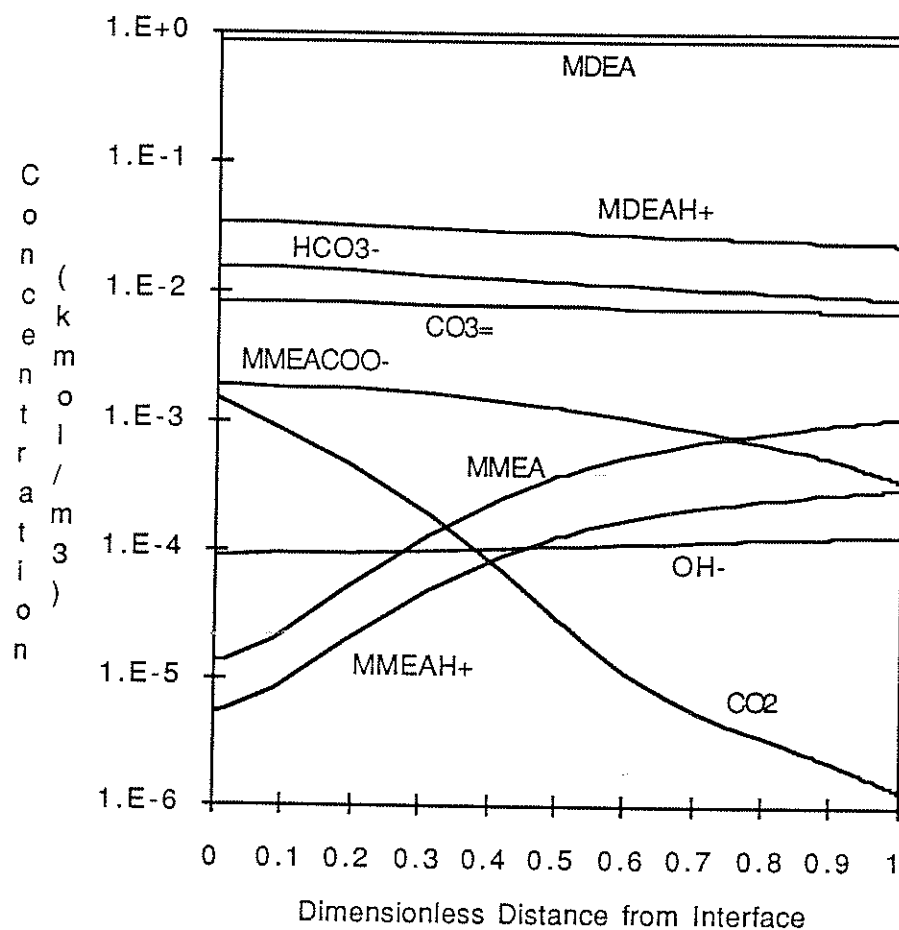


Figure 9.13 Concentration Profiles for Low-Driving Force CO<sub>2</sub> Absorption into 10.6 wt% MDEA, 0.0106 wt% MMEA, 298K, CO<sub>2</sub> loading = 0.018, P<sub>CO2</sub> = 4.4 kPa, Dimensionless Distance Defined by Equation [5.45].

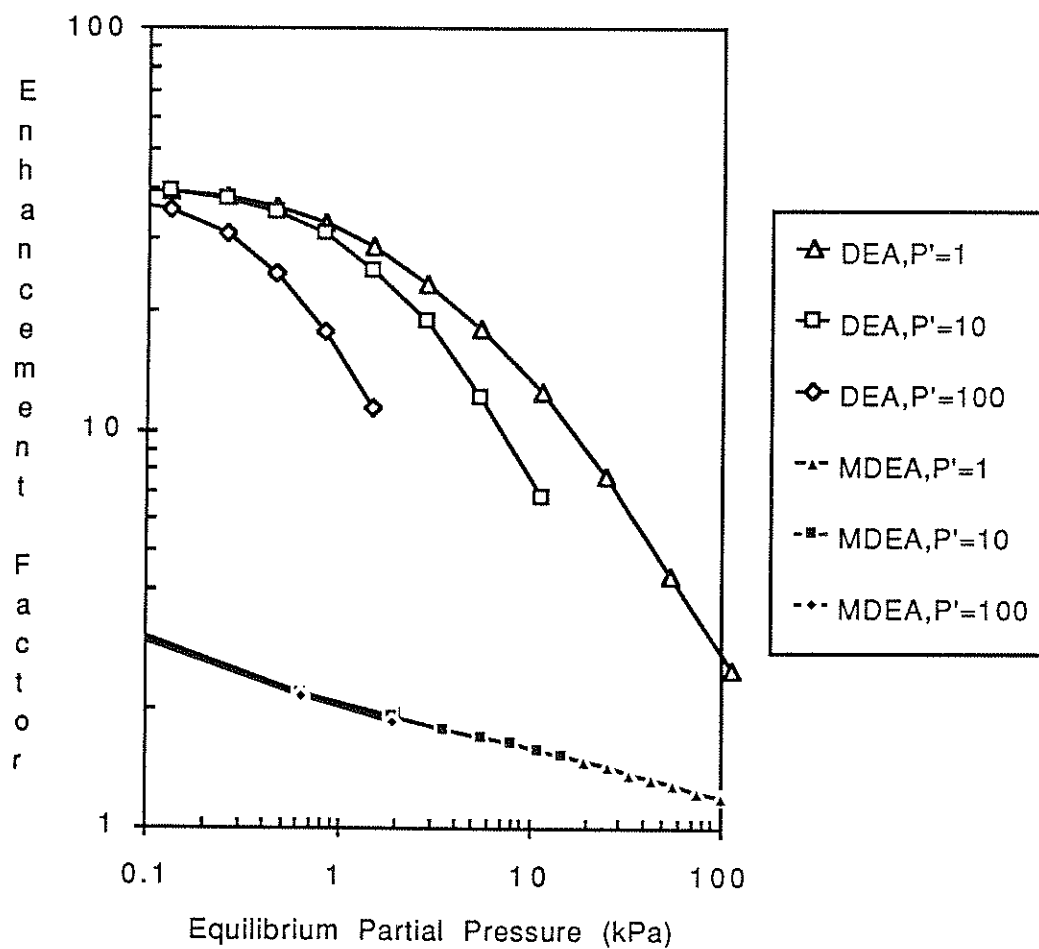


Figure 9.14 Absorption Enhancement Factor for 30wt% DEA and 50wt% MDEA for Varying Ratios of Actual to Equilibrium Partial Pressure ( $P' = P/P^*$ ). Specific Conditions: 313K,  $k_l^0 = 10^{-4}$  m/sec.



the low side for sieve trays). Here we see the enhancement factor as a function of the equilibrium partial pressure for various ratios of actual to equilibrium partial pressure:

$$P' = \frac{P_{\text{CO}_2}}{P^*_{\text{CO}_2}} \quad [9.11]$$

When the ratio,  $P'$ , is equal to 1, the conditions are pseudo first-order, and no gradients of liquid-phase reactants exist. The increasing ratios take into account successively increasing driving forces, in which depletion of the reactants can be significant. As is expected, the enhancement factor for DEA is much larger than MDEA.

Figure 9.15 shows the same information for typical mixed amine systems, 10wt% DEA/40wt% MDEA and 5wt% MEA/45wt% MDEA. The MEA/MDEA system is more effective at low loadings (corresponding to low  $\text{CO}_2$  partial pressures), however, it is also much more sensitive to loading, owing to the higher  $\text{pK}_a$  of MEA and greater carbamate stability. All of the profiles in Figures 9.14 and 9.15 exhibit the expected behavior of decreasing enhancement factor with increased loading except that of DEA/MDEA at low loadings. The reason for the increasing enhancement factor is the activity coefficient effect, whereby the reaction rates are accelerated because of decreasing ionic activity coefficients. At even higher loadings, however, the depletion of the DEA becomes the dominant effect and the enhancement factor decreases with loading as expected.

We made many runs in which we compared the predicted enhancement factor to a pseudo first-order prediction. The results are shown in Figure 9.16, where the ratio of actual to pseudo first-order enhancement factors is shown as a function of the driving force for the absorption. As can be seen, under many conditions where the driving force is less than 10 kPa, the first order approximation is accurate. The base case was taken to be a mass transfer coefficient of  $10^{-4}$  m/sec. With a larger mass transfer coefficient,  $5 \times 10^{-4}$  m/sec, the pseudo first-order approximation is valid to within 10% under the range of driving forces up to 101 kPa. We note that the AMSIM

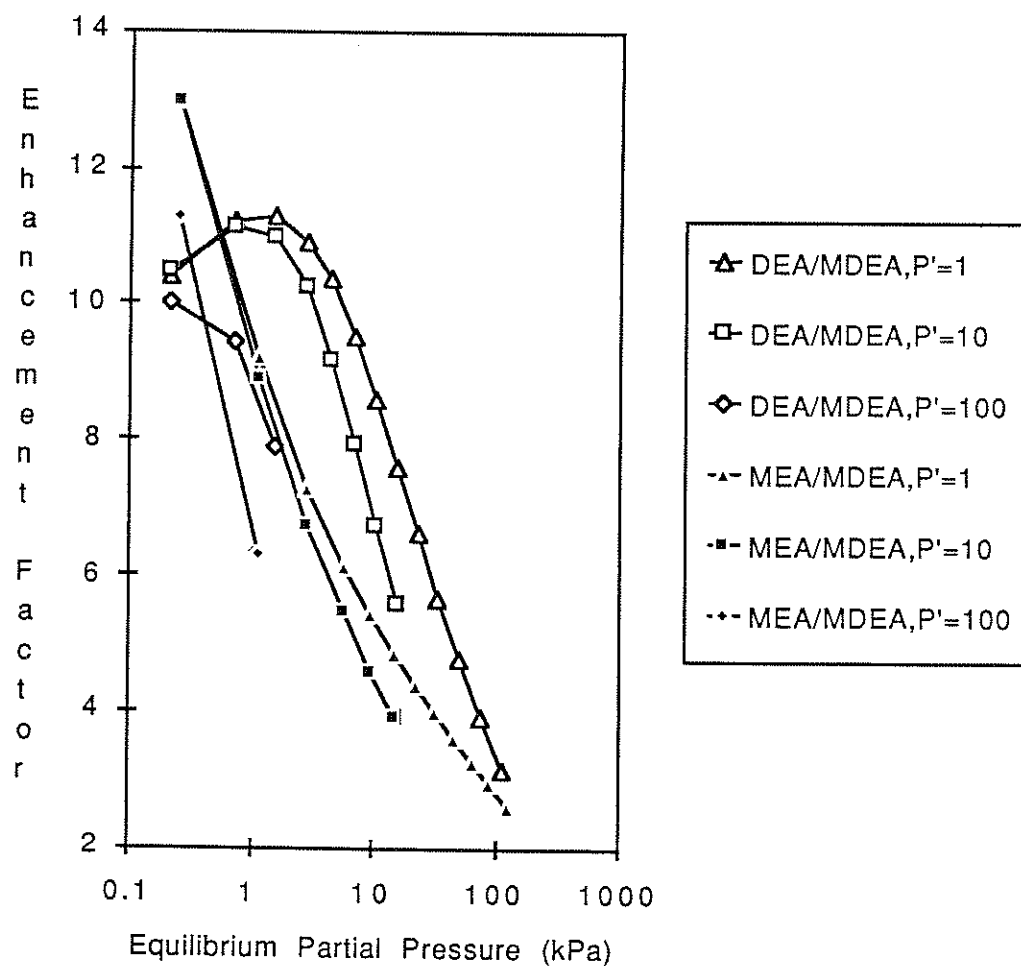


Figure 9.15 Absorption Enhancement Factor for 10wt% DEA/40wt% MDEA (mole ratio = 0.28) and 5wt% MEA/45wt%MDEA (mole ratio = 0.22) for Varying Ratios of Actual to Equilibrium Partial Pressure ( $P' = P/P^*$ ). Specific Conditions: 313K,  $k_l^0 = 10^{-4}$  m/sec.

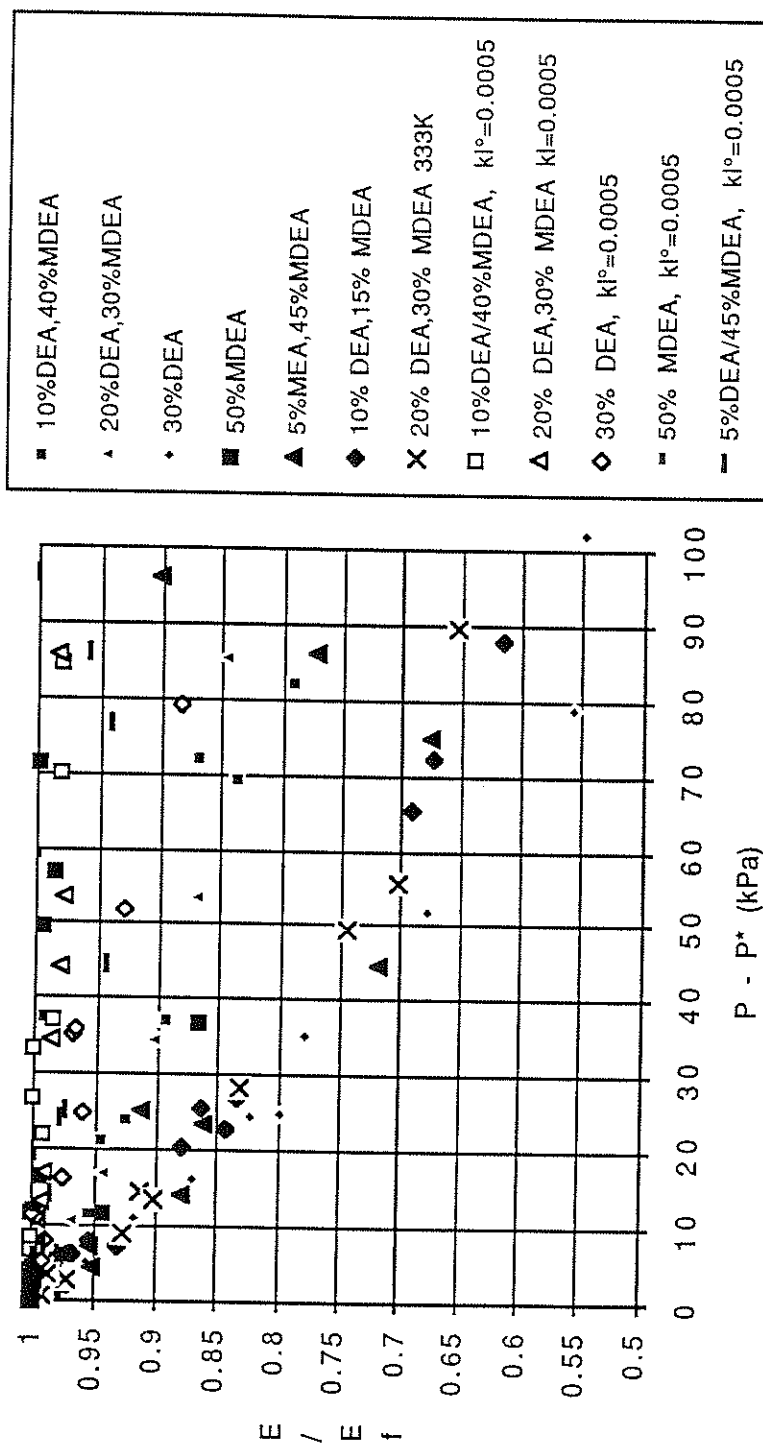


Figure 9.16 Comparison of Actual to First-Order Enhancement Factors for Various Amine Solutions.  
Base Conditions: 313K,  $k_l^0 = 10^{-4}$  m/sec, Loading Varies from 0.01 to 0.5.

simulator (Tomcej et al., 1987) uses a pseudo first-order approximation for the CO<sub>2</sub> enhancement factor. In some cases of industrial interest, we see this approximation is quite invalid and can overestimate stage efficiencies (this has been noted by Rangwala et al. (1989)).

A number of approximations have been proposed for prediction of the enhancement factor. DeCoursey (1982) and Onda et al. (1970a,b) are just a couple of the many papers presented on this subject. The difficulty with algebraic approximations is that their validity is not known under a wide range of conditions, and the approximations are valid only for a specific reaction scheme. It was for this reason that a rigorous mass transfer model was developed in this work. However, it is useful to have simplifying correlations for use in industrial column simulation due to the computation time involved in literally solving a differential equation model for the mass transfer rate within a differential equation model. Algebraic correlations can be used with some success. We review one approximation used by Sivasubramanian (1985) in which the enhancement factor is estimated from the correlation of Welleck et al. (1978):

$$\frac{1}{(E - 1)^{1.35}} = \frac{1}{(E_{\text{inst}} - 1)^{1.35}} + \frac{1}{(E_{\text{first}} - 1)^{1.35}} \quad [9.12]$$

The first-order enhancement factor,  $E_{\text{first}}$ , comes from equation [8.4], and the instantaneous enhancement factor,  $E_{\text{inst}}$ , is evaluated as follows:

$$E_{\text{inst}} = 1 + \frac{C_{\text{DEA bulk}}}{v C_{\text{CO}_2 \text{ interface}}} \sqrt{\frac{D_{\text{DEA}}}{D_{\text{CO}_2}}} \quad [9.13]$$

Equation [9.13] is for a reaction of the following form shown in equation [9.14] and is corrected for unequal diffusion coefficients by the approximation of Chang and Rochelle (1983):



In this case, the stoichiometric coefficient is assumed to be of the following form:

$$v = 1 + \frac{C_{\text{DEA}}}{C_{\text{DEA}} + C_{\text{MDEA}}} \quad [9.15]$$

This correction (not used by Sivasubramanian who assumed  $v = 2$ ) accounts for the fact that at low DEA concentrations, MDEA will be the primary deprotonator of the zwitterion (see equation [2.6]) and so only one mole of DEA will be consumed for every mole of  $\text{CO}_2$  reacting. The same type of scheme was also used for MEA/MDEA mixtures.

The results are shown for extreme cases in Table 9.10 where we see that this approximation is reasonable except for the case of MEA at high loadings. This is because the approximation does not properly account for the interaction of the MDEA in the mixed amine system. We can only suggest that the user of simplified correlations be very careful in the application of these to mixed amine systems, and preferably check such correlations with a rigorous mass transfer model. Both Versteeg (1986) and Bosch (1989) have noted the inapplicability of simplified correlations in mixed amine systems and the need for a rigorous mass transfer model.

Table 9.10 Effectiveness of Welleck Correlation for CO<sub>2</sub> Enhancement Factors at 313K,  $k_l^0 = 10^{-4}$  m/sec.

CO <sub>2</sub> loading	P <sub>eq,CO2</sub> (kPa)	P <sub>co2</sub> (kPa)	E <sub>first</sub> <sup>a</sup>	E <sub>inst</sub>	E <sub>pred</sub>	E <sub>exact</sub>	E <sub>pred</sub> /E <sub>exact</sub>
30% DEA							
0.01	3.52x10 <sup>-4</sup>	101.	37.1	40.5	23.5	20.6	1.14
0.5	1.13x10 <sup>1</sup>	112.	16.8	10.7	8.08	6.91	1.17
5% MEA, 45% MDEA							
0.01	4.45x10 <sup>-4</sup>	101.	26.4	30.9	17.4	14.1	1.23
0.01	4.45x10 <sup>-4</sup>	50.7	26.4	52.3	20.9	18.2	1.14
0.5	4.44x10 <sup>1</sup>	146.	4.37	1.57	1.54	3.26	0.47
0.5	4.44x10 <sup>1</sup>	95.0	4.37	1.88	1.78	3.43	0.52
20% DEA, 30% MDEA							
0.01	5.35x10 <sup>-3</sup>	101.	14.0	45.4	12.4	11.2	1.11
0.5	3.96x10 <sup>1</sup>	141.	9.09	9.36	5.91	5.81	1.02
10% DEA, 15% MDEA							
0.01	2.28x10 <sup>-3</sup>	101.	16.1	18.5	10.7	9.74	1.10
0.5	1.19x10 <sup>1</sup>	113.	11.1	5.75	4.78	5.45	0.88
10% DEA, 40% MDEA							
0.01	1.19x10 <sup>-2</sup>	101.	9.33	26.3	8.16	7.42	1.10
0.5	3.34x10 <sup>1</sup>	135.	7.09	5.75	4.18	4.73	0.88

<sup>a</sup>E<sub>first</sub> corresponds to pseudo first-order approximation

E<sub>inst</sub> corresponds to instantaneous for the primary or secondary amine

E<sub>pred</sub> is the prediction using the correlation of Welleck et al. (1978)

E<sub>exact</sub> is based on differential equation model prediction

## Chapter Ten

### Conclusions and Recommendations

#### 10.1 Summary

This dissertation has presented a rigorous model for the simulation of CO<sub>2</sub> absorption and desorption with chemical reaction. The activity coefficients for the alkanolamine systems studied were calculated using the Electrolyte-NRTL equation which takes into account both long range and short range interactions between the ionic species in solution. A generalized framework was constructed for the diffusion and reaction of species in ionic solutions from which the current model was derived. The differential equation material balance equations were then solved numerically to obtain liquid-phase concentration profiles and subsequent flux rates for CO<sub>2</sub> at the gas-liquid interface. This general model has been used to extract kinetic information from mass transfer experiments and predict system behavior under industrially relevant conditions.

#### 10.2 Conclusions

Four "rigorous" mass transfer theories were compared. It has been demonstrated that the simplified eddy diffusivity theory and the approximate method of Chang and Rochelle provide excellent approximations to the surface renewal theory, generally considered to be more accurate than film theory. These results have been demonstrated for a second-order, reversible reaction, and for a more complicated system of industrial interest. In light of the shorter computation time involved for the steady-state theories and the inherent uncertainty in the actual mass transfer mechanism at a gas-liquid interface, a steady-state model is most useful for experimental data interpretation and acid gas treating process design. Furthermore, since numerical implementation of the eddy diffusivity theory differs little from film theory, we prefer

the eddy diffusivity theory. It has been found through the course of this work that the ion diffusion coefficients have little effect on the  $\text{CO}_2$  absorption rate either due to insignificance of reaction products under high driving force absorption conditions or near pseudo-first order conditions occurring under low driving force absorption conditions or desorption conditions. For this reason, the potential gradient terms may be dropped by setting all ion diffusion coefficients equal to some base value (the amine is reasonable) in order to save computation time.

A differential equation-based model has been developed and used to study the reaction kinetics for  $\text{CO}_2$  with MEA (monoethanolamine), DEA (diethanolamine), MDEA (methyldiethanolamine), and the mixtures MEA/MDEA, and DEA/MDEA. The MDEA data indicate that the apparent reactivity of MDEA is a function of the  $\text{CO}_2$  partial pressure and loading. MDEA data were reconciled using a kinetic mechanism including the hydroxide ion, contrary to the rate expression commonly found in the literature. There is a theoretical basis for this mechanism, however, the justification is based upon experimental data. By detailed treatment of the reaction kinetics in nonideal solutions, absorption and desorption data for DEA have been successfully reconciled by assuming the reaction rate constants "increase" with ionic strength. It has been shown that MDEA interacts in the DEA kinetic expression, but the model can simulate MEA/MDEA mixed amine data without kinetic interaction.

The model has been used to predict the performance of amine systems and approximate correlations with mass transfer coefficients and temperatures likely to be encountered industrially. Under many conditions, a simple pseudo-first order approximation will be accurate to within 10%. This is certainly true for the MDEA system, which provides little if any enhancement of the  $\text{CO}_2$  absorption rate under the typically high mass transfer coefficients found in packed and plate columns. For faster reacting amines, the use of a more rigorous approximation would be suggested. Approximate methods have been shown to be of questionable use for MEA/MDEA under high driving force conditions, due to interaction between the MDEA and MEA in the boundary layer at the gas-liquid interface. In any case, it is recommended that a rigorous mass transfer model be used either to interpret the data or check the use of an empirical correlation for a given amine system under conditions likely to be encountered.



### 10.3 Recommendations for Future Work

It is recommended that the current model be used to predict simultaneous absorption of  $\text{H}_2\text{S}$  and  $\text{CO}_2$  in single amines and amine mixtures. The model is presently capable of simulating this system, however, more work must be done to estimate equilibrium parameters in order to produce accurate results. The simultaneous absorption of two acid gases is a complex problem which requires rigorous modelling in order to produce reliable estimates. Such an analysis can be used to develop and test semi-empirical approximations which could be of use in industrial column simulation. In addition, it is important to determine when there exists a strong interaction between the  $\text{H}_2\text{S}$  and  $\text{CO}_2$  during simultaneous absorption, since any known correlations calculate enhancement factors separately for each species. In addition, more amines should be studied and added to the existing database. Hindered amines, which are becoming very important industrially, can be simulated within the existing framework as the physical property data are determined. The current mechanism for MDEA and  $\text{CO}_2$  should also be subject to further testing by experimental absorption of  $\text{CO}_2$  into MDEA solutions with hydroxide concentration increased by addition of a base such as NaOH or KOH.

On the fundamental side, there exists much potential for research applying to areas beyond acid gas treating. Most of the equilibrium data in the literature show only the total  $\text{CO}_2$  concentration as a function of equilibrium partial pressure. These data are in reality not sufficient to give the individual ion activity coefficients obtained from the Electrolyte-NRTL model true meaning. It would be of great interest to determine concentrations of some of the individual species in solution as a function of  $\text{CO}_2$  loading and use this information along with the usual data available to estimate parameters in the Electrolyte-NRTL model. Having done this, it would be possible to perform a more detailed analysis of the interaction between the kinetic and equilibrium conditions in nonideal systems in order to test the assumption made in this work. The use of homogeneous kinetic experiments, such as the stopped flow technique, would be recommended as these experiments can be interpreted without the need for diffusion coefficient and solubility data. It would be fruitful to then reconcile the homogeneous experiments with data taken in absorption apparatus using the mass transfer model.

## Appendix A

### Derivations of the Equations of Continuity in Transformed Coordinates

#### A.1 Penetration and Surface Renewal Theories

The flux for a species relative to bulk flow and neglecting phenomenological coupling effects, is given by equation [A.1]:

$$J_i = -\beta_i C_i \frac{d\Phi}{dx} - D_i \frac{dC_i}{dx} \quad [A.1]$$

where  $\beta$  is a combination of constants,  $\frac{z_i D_i F}{kT}$ ,  $\Phi$  is the electrical potential, the gradient of which arises through the diffusion of ionic species. For the unsteady-state penetration and surface renewal theories, the equation of continuity is formed by considering the change in species concentration due to accumulation, flux, and chemical reaction:

$$\frac{\partial C_i}{\partial t} = -\frac{\partial J_i}{\partial x} + \mathcal{R}_i(\underline{C}(x,t)) \quad [A.2]$$

Substituting equation [A.1] for the flux into equation [A.2]:

$$\frac{\partial C_i}{\partial t} = \beta_i \frac{\partial C_i}{\partial x} \frac{\partial \Phi}{\partial x} + \beta_i C_i \frac{\partial^2 \Phi}{\partial x^2} + D_i \frac{\partial^2 C_i}{\partial x^2} + \mathcal{R}_i(\underline{C}(x,t)) \quad [A.3]$$

This section concentrates on the derivation of the equation of continuity when the real space  $(x,t)$  is mapped into the transformed space  $(r,\tau)$ , which, as explained in the text, is favored for numerical computation. The variable  $r$  is related to  $x$  through a time-dependent spatial transformation, the error function:

$$r \stackrel{\text{df}}{=} \frac{2}{\sqrt{\pi}} \int_0^{\xi} e^{-\zeta^2} d\zeta = \text{erf}(\xi) \quad [\text{A.4}]$$

where

$$\xi = \frac{x}{\sqrt{4Dt}} \quad [\text{A.5}]$$

Keep in mind that  $\zeta$  is merely a dummy variable of integration, with no physical significance (this will be important later). The dimensionless time is defined as follows:

$$\tau \stackrel{\text{df}}{=} \sqrt{\frac{t}{\theta}} \quad [\text{A.6}]$$

In Versteeg's (1986) definition,  $D$  is the diffusion coefficient of the absorbing gas, and  $\theta$  is the contact time for penetration theory. However, we will find it more convenient to think of these two parameters as merely constants defining the transformation, and will be given physically significant values later as needed.

Given the expressions for  $r$  and  $\tau$ , we can obtain expressions for the derivatives in the continuity equation in terms of these transformed variables. First, we express the total differential of an arbitrary variable,  $A$ , in terms of  $r$  and  $\tau$ . Then we find the derivatives of  $A$  with respect to  $x$  and  $t$  using the chain rule:

$$dA = \left( \frac{\partial A}{\partial r} \right)_{\tau} dr + \left( \frac{\partial A}{\partial \tau} \right)_{r} d\tau \quad [\text{A.7}]$$

$$\left( \frac{\partial A}{\partial t} \right)_x = \left( \frac{\partial A}{\partial r} \right)_{\tau} \left( \frac{\partial r}{\partial t} \right)_x + \left( \frac{\partial A}{\partial \tau} \right)_{r} \left( \frac{\partial \tau}{\partial t} \right)_x \quad [\text{A.8}]$$

$$\left(\frac{\partial A}{\partial x}\right)_t = \left(\frac{\partial A}{\partial r}\right)_\tau \left(\frac{\partial r}{\partial x}\right)_t + \left(\frac{\partial A}{\partial \tau}\right)_r \left(\frac{\partial \tau}{\partial x}\right)_t \quad [\text{A.9}]$$

The next step is to evaluate the derivatives to perform the transformation. First, recall Liebnitz's formula for differentiating a definite integral:

$$I = \int_a^b F(z) dz \quad [\text{A.10}]$$

$$\frac{dI}{dx} = F(b)\frac{db}{dx} - F(a)\frac{da}{dx} + \int_a^b \frac{dF(z)}{dx} dz \quad [\text{A.11}]$$

In our case, the lower limit of equation [A4] is a constant, and the integrand is a function of the dummy variable of integration only, so only one term remains to be evaluated:

$$\begin{aligned} \left(\frac{\partial r}{\partial x}\right)_t &= \frac{2}{\sqrt{\pi}} \exp\left(\frac{-x^2}{4Dt}\right) \left(\frac{\partial\left(\frac{x}{\sqrt{4Dt}}\right)}{\partial x}\right)_t \\ &= \frac{\exp\left(\frac{-x^2}{4Dt}\right)}{\sqrt{\pi Dt}} \end{aligned} \quad [\text{A.12}]$$

By the same method:

$$\left(\frac{\partial r}{\partial t}\right)_x = \frac{\exp\left(\frac{-x^2}{4Dt}\right)}{\sqrt{\pi Dt}} \frac{-x}{2t} \quad [\text{A.13}]$$

We can easily obtain the derivatives of  $\tau$  with respect to  $t$  and  $x$ :

$$\left(\frac{\partial \tau}{\partial t}\right)_x = \frac{1}{2\sqrt{t\theta}} \quad [\text{A.14}]$$

$$\left(\frac{\partial \tau}{\partial x}\right)_t = 0 \quad [\text{A.15}]$$

We can now obtain the derivatives by substitution into equations [A.8] and [A.9]:

$$\begin{aligned} \left(\frac{\partial A}{\partial t}\right)_x &= \frac{\exp\left(\frac{-x^2}{4Dt}\right)}{\sqrt{\pi Dt}} \frac{-x}{2t} \left(\frac{\partial A}{\partial r}\right)_\tau + \frac{1}{2\sqrt{t\theta}} \left(\frac{\partial A}{\partial \tau}\right)_r \\ &= \frac{-\xi \exp(-\xi^2)}{\sqrt{\pi \tau^2 \theta}} \left(\frac{\partial A}{\partial r}\right)_\tau + \frac{1}{2\tau \theta} \left(\frac{\partial A}{\partial \tau}\right)_r \end{aligned} \quad [\text{A.16}]$$

The derivative with respect to x:

$$\begin{aligned} \left(\frac{\partial A}{\partial x}\right)_t &= \frac{\exp\left(\frac{-x^2}{4Dt}\right)}{\sqrt{\pi Dt}} \left(\frac{\partial A}{\partial r}\right)_\tau \\ &= \frac{\exp(-\xi^2)}{\sqrt{\pi D \tau^2 \theta}} \left(\frac{\partial A}{\partial r}\right)_\tau \end{aligned} \quad [\text{A.17}]$$

We will also need the second derivative of A with respect to x:

$$\begin{aligned}
& \left( \frac{\partial^2 A}{\partial x^2} \right)_t \\
&= \frac{\exp\left(\frac{-x^2}{4Dt}\right)}{\sqrt{\pi Dt}} \left( \frac{-2x}{4Dt} \left( \frac{\partial A}{\partial r} \right)_\tau + \frac{\partial}{\partial x} \left( \frac{\partial A}{\partial r} \right)_\tau \right) \\
&= \frac{\exp\left(\frac{-x^2}{4Dt}\right)}{\sqrt{\pi Dt}} \left( \frac{-2x}{4Dt} \left( \frac{\partial A}{\partial r} \right)_\tau + \frac{\partial}{\partial r} \left( \frac{\partial A}{\partial r} \right)_\tau \left( \frac{\partial r}{\partial x} \right)_t \right) \\
&= \frac{\exp\left(\frac{-x^2}{4Dt}\right)}{\sqrt{\pi Dt}} \frac{-x}{2Dt} \left( \frac{\partial A}{\partial r} \right)_\tau + \frac{\exp\left(\frac{-2x^2}{4Dt}\right)}{\pi Dt} \left( \frac{\partial^2 A}{\partial r^2} \right)_\tau \\
&= \frac{-\xi \exp(-\xi^2)}{\sqrt{\pi D \tau^2 \theta}} \left( \frac{\partial A}{\partial r} \right)_\tau + \frac{\exp(-2\xi^2)}{\pi D \tau^2 \theta} \left( \frac{\partial^2 A}{\partial r^2} \right)_\tau \quad [A.18]
\end{aligned}$$

Using these results, the equation of continuity can now be expressed in the transformed coordinates:

$$\frac{-\xi \exp(-\xi^2)}{\sqrt{\pi \tau^2 \theta}} \left( \frac{\partial C_i}{\partial r} \right)_\tau + \frac{1}{2\tau\theta} \left( \frac{\partial C_i}{\partial \tau} \right)_\tau =$$

$$\beta_i \frac{\exp(-2\xi^2)}{\pi D \tau^2 \theta} \left( \frac{\partial C_i}{\partial r} \right)_\tau \left( \frac{\partial \Phi}{\partial r} \right)_\tau$$

$$\begin{aligned}
& - \beta_i C_i \frac{\xi \exp(-\xi^2)}{\sqrt{\pi D \tau^2 \theta}} \left( \frac{\partial \Phi}{\partial r} \right)_\tau + \beta_i C_i \frac{\exp(-2\xi^2)}{\pi D \tau^2 \theta} \left( \frac{\partial^2 \Phi}{\partial r^2} \right)_\tau \\
& - D_i \frac{\xi \exp(-\xi^2)}{\sqrt{\pi D \tau^2 \theta}} \left( \frac{\partial C_i}{\partial r} \right)_\tau + D_i \frac{\exp(-2\xi^2)}{\pi D \tau^2 \theta} \left( \frac{\partial^2 C_i}{\partial r^2} \right)_\tau \\
& + \mathcal{R}_i(\mathcal{C}(\xi, \tau))
\end{aligned} \tag{A.19}$$

Rearranging slightly, and multiplying every term by  $2\tau^2\theta$ :

$$\begin{aligned}
& \tau \left( \frac{\partial C_i}{\partial \tau} \right)_r = \\
& 2\beta_i \frac{\exp(-2\xi^2)}{\pi D} \left( \frac{\partial C_i}{\partial r} \right)_\tau \left( \frac{\partial \Phi}{\partial r} \right)_\tau \\
& - \beta_i C_i \frac{2\xi \exp(-\xi^2)}{\sqrt{\pi D}} \left( \frac{\partial \Phi}{\partial r} \right)_\tau + \beta_i C_i \frac{2\exp(-2\xi^2)}{\pi D} \left( \frac{\partial^2 \Phi}{\partial r^2} \right)_\tau \\
& - D_i \frac{2\xi \exp(-\xi^2)}{\sqrt{\pi D}} \left( \frac{\partial C_i}{\partial r} \right)_\tau + D_i \frac{2\exp(-2\xi^2)}{\pi D} \left( \frac{\partial^2 C_i}{\partial r^2} \right)_\tau \\
& + \frac{2\xi \exp(-\xi^2)}{\sqrt{\pi}} \left( \frac{\partial C_i}{\partial r} \right)_\tau
\end{aligned}$$

$$+ 2\tau^2\theta \mathcal{R}_i(\underline{C}(\xi, \tau)) \quad [\text{A.20}]$$

Equation [A.20] must be solved for every component. Three of the terms will drop out if there is no potential gradient:

$$\begin{aligned} \tau \left( \frac{\partial C_i}{\partial \tau} \right)_T = & \\ - D_i \frac{2\xi \exp(-\xi^2)}{\sqrt{\pi D}} \left( \frac{\partial C_i}{\partial r} \right)_\tau + D_i \frac{2\exp(-2\xi^2)}{\pi D} \left( \frac{\partial^2 C_i}{\partial r^2} \right)_\tau & \\ + \frac{2\xi \exp(-\xi^2)}{\sqrt{\pi}} \left( \frac{\partial C_i}{\partial r} \right)_\tau & \\ + 2\tau^2\theta \mathcal{R}_i(\underline{C}(\xi, \tau)) & \end{aligned} \quad [\text{A.21}]$$

Equation [A.21] is of the form presented by Versteeg (1986). Also, if the diffusion coefficient is equal to the transformation parameter  $D$ , then some cancellation occurs:

$$\begin{aligned} \tau \left( \frac{\partial C_i}{\partial \tau} \right)_T = & \\ D_i \frac{2\exp(-2\xi^2)}{\pi D} \left( \frac{\partial^2 C_i}{\partial r^2} \right)_\tau + 2\tau^2\theta \mathcal{R}_i(\underline{C}(\xi, \tau)) & \end{aligned} \quad [\text{A.22}]$$

## A.2 Eddy Diffusivity Theory

For eddy diffusivity theory, we begin with the following result:



$$\frac{\partial C_i}{\partial t} = \nabla((D_i + \epsilon x^2)\nabla C_i) + \frac{D_i z_i}{RT} \mathcal{F} \nabla(C_i \nabla \Phi) + \mathcal{R}_i \quad [\text{A.23}]$$

Although in principle an unsteady-state theory is possible, we will concern ourselves only with the steady-state formulation:

$$\nabla((D_i + \epsilon x^2)\nabla C_i) + \frac{D_i z_i}{RT} \mathcal{F} \nabla(C_i \nabla \Phi) + \mathcal{R}_i = 0 \quad [\text{A.24}]$$

Now,  $x$  may vary from 0 (the interface), to infinity (the bulk). An infinite domain is inconvenient to work with numerically, however. Following in the spirit of Versteeg (1986), we wish to define a mapping function such that the concentration profile for an absorbing gas is a straight line in the transformed domain - i.e.:

Find  $T: x \in [0, \infty) \rightarrow \zeta \in [0, 1]$  such that  $\nabla_{\zeta}^2 C_A = 0$  when  $C_A$  is described by the following equation:

$$\nabla((D_A + \epsilon x^2)\nabla C_A) = 0 \quad [\text{A.25}]$$

Integrating once, we obtain:

$$(D_A + \epsilon x^2) \nabla C_A = B_1$$

or

$$dC_A = B_1 \frac{dx}{D_A + \epsilon x^2} \quad [\text{A.26}]$$

This equation may be integrated analytically:

$$C_A = \frac{B_1}{\sqrt{D_A \epsilon}} \tan^{-1} \left( \frac{x \sqrt{D_A \epsilon}}{D_A} \right) + B_2 \quad [\text{A.27}]$$

Solving for the constants through use of the boundary conditions:

@  $x \Rightarrow \infty$ ,  $C_A = C_\infty$ , @  $x = 0$ ,  $C_A = C_0$ , we obtain:

$$C_A = \frac{2}{\pi} (C_\infty - C_0) \tan^{-1} \left( x \sqrt{\frac{\varepsilon}{D_A}} \right) + C_0 \quad [\text{A.28}]$$

(note that  $\tan^{-1}(0) = 0$ , and  $\tan^{-1}(\infty) = \frac{\pi}{2}$ ). Now, if we define the transformed space as:

$$r = \frac{2}{\pi} \tan^{-1} \left( x \sqrt{\frac{\varepsilon}{D}} \right) \quad [\text{A.29}]$$

we also have:

$$x = \sqrt{\frac{D}{\varepsilon}} \tan \left( \frac{\pi}{2} r \right) \quad [\text{A.30}]$$

We note that at  $x=0$ ,  $r = 0$ , and as  $x \Rightarrow \infty$ ,  $r \Rightarrow 1$ . Furthermore, from the equation:

$$\nabla_x C = \frac{dr}{dx} \nabla_r C \quad [\text{A.31}]$$

Taking appropriate derivatives,

$$\nabla_x C = \frac{2}{\pi} \frac{\sqrt{\frac{\varepsilon}{D}}}{1+x^2 \frac{\varepsilon}{D}} \nabla_r C \quad [\text{A.32}]$$

Substituting for  $x$ , we find:

$$\nabla_x C = \frac{2}{\pi} \cos^2 \left( \frac{\pi}{2} r \right) \sqrt{\frac{\varepsilon}{D}} \nabla_r C \quad [\text{A.33}]$$

We find the second derivative:

$$\begin{aligned}
 \nabla_x^2 C &= \frac{d}{dx} \frac{dC}{dx} = \frac{d}{dr} \left( \frac{dC}{dr} \frac{dr}{dx} \right) \frac{dr}{dx} \\
 &= \frac{d}{dr} \left( \nabla_r C \frac{2}{\pi} \cos^2 \left( \frac{\pi}{2} r \right) \sqrt{\frac{\varepsilon}{D}} \right) \frac{dr}{dx} \\
 &= \left( \frac{2}{\pi} \cos^2 \left( \frac{\pi}{2} r \right) \sqrt{\frac{\varepsilon}{D}} \right)^2 \nabla_r^2 C \\
 &\quad - \left( \frac{2}{\pi} \cos^2 \left( \frac{\pi}{2} r \right) \sqrt{\frac{\varepsilon}{D}} \right) 2 \sqrt{\frac{\varepsilon}{D}} \cos \left( \frac{\pi}{2} r \right) \sin \left( \frac{\pi}{2} r \right) \nabla_r C \quad [A.34]
 \end{aligned}$$

Now, taking our original equation,

$$\nabla((D_i + \varepsilon x^2) \nabla C_i) + \frac{D_i z_i}{RT} \mathcal{F} \nabla(C_i \nabla \Phi) + \mathcal{R}_i = 0 \quad [A.35]$$

or

$$D_i \nabla^2 C_i + 2 \times \varepsilon \nabla C_i + \frac{D_i z_i}{RT} \mathcal{F} \nabla C_i \nabla \Phi + \frac{D_i z_i}{RT} \mathcal{F} C_i \nabla^2 \Phi + \mathcal{R}_i = 0 \quad [A.36]$$

Now using the transformations, we obtain:

$$\begin{aligned}
 &D_i \left( \frac{2}{\pi} \cos^2 \left( \frac{\pi}{2} r \right) \sqrt{\frac{\varepsilon}{D}} \right)^2 \nabla_r^2 C \\
 &- D_i \frac{4}{\pi} \cos^3 \left( \frac{\pi}{2} r \right) \frac{\varepsilon}{D} \sin \left( \frac{\pi}{2} r \right) \nabla_r C \\
 &+ 4 \tan \left( \frac{\pi}{2} r \right) \varepsilon \frac{1}{\pi} \cos^2 \left( \frac{\pi}{2} r \right) \nabla_r C
 \end{aligned}$$

$$\begin{aligned}
& + \frac{D_i z_i}{RT} \mathcal{F} \left( \frac{2}{\pi} \cos^2 \left( \frac{\pi}{2} r \right) \sqrt{\frac{\varepsilon}{D}} \right)^2 \nabla_r C \nabla_r \Phi \\
& + \frac{D_i z_i}{RT} \mathcal{F} C_i \left( \frac{2}{\pi} \cos^2 \left( \frac{\pi}{2} r \right) \sqrt{\frac{\varepsilon}{D}} \right)^2 \nabla_r^2 \Phi \\
& - \frac{D_i z_i}{RT} \mathcal{F} C_i \left( \frac{4}{\pi} \cos^3 \left( \frac{\pi}{2} r \right) \frac{\varepsilon}{D} \right) \sin \left( \frac{\pi}{2} r \right) \nabla_r \Phi = -\mathcal{R}_i \quad [\text{A.37}]
\end{aligned}$$

## Appendix B

### Error Analysis

#### B.1 Introduction

Suppose we have a model of the form:

$$y = f(x_1, x_2, \dots, x_n) \quad [B.1]$$

If we wish to estimate the error in  $y$  due to the errors in  $x$ , we first assume that the model can be linearized about a point  $\mathbf{x}$ :

$$y = f(x_1, x_2, \dots, x_n)_0 + \sum_{i=1}^n (\partial y, \partial x_i) (x_i - x_{i,0}) + (\text{Higher Order Terms}) \quad [B.2]$$

Once linearized, we can obtain the variance of  $y$  as a function of the independent variables (Draper and Smith, 1981):

$$\text{Var}(y) = \sum_{i=1}^n ((\partial y, \partial x_i))^2 \text{Var}(x_i) \quad [B.3]$$

We have neglected covariance between the independent variables in this formulation. Not only can we estimate the error in  $y$  from the error in the independent variables, we can also examine the relative contributions of the error, to see which variables contribute the most to uncertainty in experimental measurement.

## B.2 Gas Phase Error Analysis

The absorption rate of CO<sub>2</sub> can be determined by taking the difference between the inlet and outlet flowrates of CO<sub>2</sub> through the stirred tank reactor:

$$\frac{A}{\rho} R_{\text{abs}} = V_{\text{CO}_2, \text{in}} - V_{\text{CO}_2, \text{out}} \quad [\text{B.4}]$$

The variable A is the interfacial area in cm<sup>2</sup>, and  $\rho$  is the density of the gas in moles/cc.  $V_i$  designates the volumetric flowrate of the gas in standard cubic centimeters per minute. The Horiba Analyzers will measure the volumetric fraction of CO<sub>2</sub> in the gas phase, defined as r:

$$V_{\text{CO}_2, \text{out}} = r (V_{\text{H}_2\text{O}, \text{out}} + V_{\text{CO}_2, \text{out}} + V_{\text{N}_2}) \quad [\text{B.5}]$$

Solving for the CO<sub>2</sub> flowrate:

$$V_{\text{CO}_2, \text{out}} = (V_{\text{H}_2\text{O}, \text{out}} + V_{\text{N}_2, \text{out}}) \frac{r}{1-r} \quad [\text{B.6}]$$

Now, if the outlet gas is fully saturated with water, we can use the water vapor pressure to determine the partial water flowrate:

$$\begin{aligned} V_{\text{H}_2\text{O}, \text{out}} &= (V_{\text{H}_2\text{O}, \text{out}} + V_{\text{CO}_2, \text{out}} + V_{\text{N}_2, \text{out}}) P_{\text{H}_2\text{O}}^* \\ &= (V_{\text{CO}_2, \text{out}} + V_{\text{N}_2, \text{out}}) \frac{P_{\text{H}_2\text{O}}^*}{1 - P_{\text{H}_2\text{O}}^*} \end{aligned} \quad [\text{B.7}]$$

Since we have provided a condenser out the outlet of the gas, we assume that the gas is no longer saturated with water, but is not completely dry either. The deviation from a perfectly dry gas is determined by a parameter  $\epsilon$ , and we can determine the volumetric flowrate of the CO<sub>2</sub>:

$$\begin{aligned}
 V_{\text{CO}_2, \text{out}} &= r \left( V_{\text{N}_2, \text{out}} \left( 1 + \varepsilon \frac{P_{\text{H}_2\text{O}}^*}{1 - P_{\text{H}_2\text{O}}^*} \right) + V_{\text{CO}_2, \text{out}} \left( 1 + \varepsilon \frac{P_{\text{H}_2\text{O}}^*}{1 - P_{\text{H}_2\text{O}}^*} \right) \right) \\
 &= \frac{(V_{\text{N}_2, \text{out}} (r + \varepsilon r \frac{P_{\text{H}_2\text{O}}^*}{1 - P_{\text{H}_2\text{O}}^*}))}{1 - r - \varepsilon r \frac{P_{\text{H}_2\text{O}}^*}{1 - P_{\text{H}_2\text{O}}^*}} \quad [\text{B.8}]
 \end{aligned}$$

The nitrogen absorption rate is negligible, so:

$$V_{\text{N}_2, \text{out}} = V_{\text{N}_2, \text{in}} \quad [\text{B.9}]$$

Therefore, the net absorption rate of  $\text{CO}_2$  can be calculated as a function of the measured nitrogen and  $\text{CO}_2$  flowrates, the vapor pressure of  $\text{CO}_2$  at the reactor temperature, and the unknown but estimated value of  $\varepsilon$ , the deviation from perfect condensation:

$$R_v = \frac{A}{\rho} R_{\text{abs}} = V_{\text{CO}_2, \text{in}} \frac{(V_{\text{N}_2, \text{in}} (r + \varepsilon r \frac{P_{\text{H}_2\text{O}}^*}{1 - P_{\text{H}_2\text{O}}^*}))}{1 - r - \varepsilon r \frac{P_{\text{H}_2\text{O}}^*}{1 - P_{\text{H}_2\text{O}}^*}} \quad [\text{B.10}]$$

Taking the appropriate partial derivatives:

$$\frac{\partial R_v}{\partial V_{\text{CO}_2}} = 1 \quad [\text{B.11}]$$

$$\frac{\partial R_v}{\partial V_{N2}} = - \frac{(r + \epsilon r \frac{P_{H2O}^*}{1 - P_{H2O}^*})}{1 - r - \epsilon r \frac{P_{H2O}^*}{1 - P_{H2O}^*}} \quad [B.12]$$

$$\frac{\partial R_v}{\partial r} = - \frac{V_{N2}}{1 - r - \epsilon r \frac{P_{H2O}^*}{1 - P_{H2O}^*}} - \frac{(V_{N2,in} (r + \epsilon r \frac{P_{H2O}^*}{1 - P_{H2O}^*}))}{(1 - r - \epsilon r \frac{P_{H2O}^*}{1 - P_{H2O}^*})^2} \quad [B.13]$$

$$\frac{\partial R_v}{\partial \epsilon} = - \frac{V_{N2} r \frac{P_{H2O}^*}{1 - P_{H2O}^*}}{1 - r - \epsilon r \frac{P_{H2O}^*}{1 - P_{H2O}^*}} - \frac{(V_{N2,in} (r + \epsilon r \frac{P_{H2O}^*}{1 - P_{H2O}^*}))}{(1 - r - \epsilon r \frac{P_{H2O}^*}{1 - P_{H2O}^*})^2} \frac{P_{H2O}^*}{1 - P_{H2O}^*} \quad [B.14]$$

$$\text{Var}(R_v) = \text{Var}(V_{CO2}) + (\frac{\partial R_v}{\partial V_{N2}})^2 \text{Var}(V_{N2}) + (\frac{\partial R_v}{\partial r})^2 \text{Var}(r) + (\frac{\partial R_v}{\partial \epsilon})^2 \text{Var}(\epsilon) \quad [B.15]$$

The following standard deviations are assumed based upon experience and manufacturers' literature:

$$\sigma_{V_{N2}} = 0.005 * V_{N2}$$

$$\sigma_{V_{CO2}} = 0.025 * V_{CO2}$$

$$\sigma_r = 0.00025$$



$$\varepsilon = 0.02, \sigma_{\varepsilon} = 0.01$$

We now take a typical case to determine the error:

$$\begin{aligned} V_{N2} &= 500 \text{ sccm} \\ V_{CO2} &= 30 \text{ sccm} \\ r &= 0.04 \\ @40^{\circ}\text{C}, P^* &= 0.072 \text{ atm} \end{aligned}$$

Taking the partial derivatives:

$$\begin{aligned} \frac{\partial R_v}{\partial V_{N2}} &= 0.0417 \\ \frac{\partial R_v}{\partial r} &= -542 \\ \frac{\partial R_v}{\partial \varepsilon} &= -1.68 \end{aligned}$$

We now calculate the variance, as well as the actual molar absorption rate:

$$\begin{aligned} \text{Var}(R_v) &= 0.59 + 0.0109 + 0.0184 + 2.82\text{e-}4 \\ \sigma_{R_v} &= 0.79 \\ R_v &= 9.13 \end{aligned}$$

We expect, therefore, about 10% error in the experimentally determined flux rates.

### B.3 CO<sub>2</sub> Partial Pressure Error Analysis

The equation for the partial pressure of CO<sub>2</sub> determined from the analyzer is shown in equation [B.16] (assuming complete water condensation):

$$r = y_{CO2,out} = \frac{P_{CO2}}{P_{CO2} + P_{N2}} \quad [B.16]$$

Inside the reactor, the partial pressure of CO<sub>2</sub> is given by the following equation:

$$P_{CO_2} = P_{TOT} - P_{N_2} - P_{H_2O} \quad [B.17]$$

We can use equation [B.16] to find the CO<sub>2</sub> partial pressure within the reactor as a function of the total pressure and the water vapor pressure:

$$\begin{aligned} (y_{N_2} + y_{CO_2}) &= 1 - y_{H_2O} \\ y_{CO_2} \left( \frac{1-r}{r} + 1 \right) &= 1 - y_{H_2O} \\ P_{CO_2} &= r (P_{TOT} - P_{H_2O}) \end{aligned} \quad [B.18]$$

Once again, take the appropriate partial derivatives to find the variance:

$$\begin{aligned} \frac{\partial P_{CO_2}}{\partial r} &= P_{TOT} - P_{H_2O} \\ \frac{\partial P_{CO_2}}{\partial P_{TOT}} &= r \\ \frac{\partial P_{CO_2}}{\partial P_{H_2O}} &= -r \end{aligned}$$

Typical conditions and standard deviations are shown below:

$$\begin{aligned} P_{TOT} &= 1, \sigma_{P_{TOT}} = 0.01 \\ P_{H_2O}^* &= 0.07, \sigma_{P^*} = 0.0007 \\ r &= 0.04, \sigma_r = 0.00025 \end{aligned}$$

We now estimate the standard deviation in the partial pressure of CO<sub>2</sub>:

$$\begin{aligned} \text{Var}(P_{CO_2}) &= 5.4e-8 + 1.6e-7 + 7.84e-10 \\ \sigma_{P_{CO_2}} &= 0.00046, \text{ or } 1.5\% \end{aligned}$$

This value seems quite small, and in the calculations a standard deviation of 5% will be assumed.

#### **B.4 Error in Concentration Measurements**

The concentration of CO<sub>2</sub> in a sample taken from the reactor by a syringe is given by equation [B.19]:

$$c = \frac{n}{V} \quad [\text{B.19}]$$

V is the volume of the syringe sample, and n is the total number of moles read by the analyzer. In order to estimate the error in V, we note that for a calibration, the concentration is constant, and we obtain a linear relationship between n and V. By regression analysis on a typical set of calibration data, we find that the standard deviation of the volume is 0.086  $\mu\text{L}$ . We can now estimate the error in concentration by equations [B.19] and [B.3]:

$$\sigma_c^2 = c^2 \frac{\sigma_v^2}{V^2} \quad [\text{B.20}]$$

Note that no error in n, the number of moles, is assumed, since this is a direct function of a digital reading on the Oceanography analyzer. Taking a typical case of  $V = 5 \mu\text{L}$ , we find the relative standard deviation of the concentration measurement:

$$\frac{\sigma_c}{c} = 1.7\% \quad [\text{B.21}]$$

Once again, this value is quite small, and we will assume an actual relative standard deviation of 5% in the parameter estimation calculations.

## Appendix C

### Experimental Data

#### MASS TRANSFER COEFFICIENT DATA

weight fraction ethylene glycol	Temp (K)	RPM	measured $k_f^{0*}a$ (cm <sup>3</sup> /sec)
0.00	298.1	150	0.229
0.00	298.1	209	0.326
0.00	298.1	180	0.282
0.00	298.1	257	0.367
0.00	298.1	113	0.211
0.00	313.1	175	0.415
0.00	313.1	119	0.321
0.00	313.1	211	0.479
0.00	313.1	255	0.586
0.25	298.1	169	0.151
0.25	298.1	209	0.186
0.25	298.1	118	0.111
0.25	298.1	66	0.0804
0.50	298.1	118	0.0616
0.50	298.1	216	0.0901
0.50	298.1	168	0.0686
0.50	298.1	138	0.0627
0.50	289.1	189	0.0801

## MDEA SYSTEM

Present work

Large Reactor, Turbine Impeller

weight fraction mdea	T (K)	$k_l^a$ (cm/sec)	CO <sub>2</sub> loading	P <sub>CO2</sub> (atm)	CO <sub>2</sub> flux (moles/cm <sup>2</sup> *sec)
0.1060	313.2	2.33e-03	2.27e-03	3.86e-02	2.62e-08
0.1060	313.2	1.93e-03	4.00e-03	3.95e-02	2.44e-08
0.1060	313.2	2.33e-03	6.15e-03	3.86e-02	2.54e-08
0.1060	313.2	2.32e-03	1.95e-02	9.15e-01	2.31e-07
0.1060	313.2	2.32e-03	2.31e-02	9.15e-01	2.32e-07
0.1060	313.2	2.32e-03	2.53e-02	9.15e-01	2.28e-07
0.1060	313.2	2.32e-03	2.77e-02	9.15e-01	2.22e-07
0.1060	313.2	2.28e-03	1.20e-03	3.10e-02	2.18e-08
0.1060	313.2	1.84e-03	1.73e-03	3.20e-02	2.03e-08
0.1060	313.2	2.31e-03	1.14e-02	3.27e-02	1.93e-08
0.1060	313.2	2.31e-03	1.23e-02	3.27e-02	1.94e-08
0.1060	313.2	2.31e-03	1.40e-02	3.27e-02	1.93e-08
0.1060	298.2	1.31e-03	1.79e-02	4.35e-02	1.78e-08
0.1060	298.2	1.31e-03	1.82e-02	4.35e-02	1.77e-08
0.1060	298.2	1.31e-03	1.83e-02	4.36e-02	1.75e-08
0.1060	298.2	1.31e-03	2.13e-02	9.59e-01	1.55e-07
0.1060	298.2	1.31e-03	3.02e-02	9.59e-01	1.55e-07
0.1060	298.2	1.31e-03	4.49e-02	9.59e-01	1.55e-07
0.1060	298.2	1.31e-03	5.87e-02	9.59e-01	1.55e-07
0.1060	313.2	2.38e-03	1.48e-03	3.93e-02	2.53e-08
0.1060	313.2	2.38e-03	2.37e-03	3.95e-02	2.47e-08
0.1060	313.2	2.35e-03	7.30e-03	1.80e-01	8.63e-08
0.1060	313.2	2.35e-03	1.16e-02	1.81e-01	8.42e-08
0.1060	313.2	2.35e-03	2.56e-02	1.82e-01	8.22e-08

<sup>a</sup> from correlation developed in this work

Critchfield (Table B.10, 1988)

Large Stirred Tank, Magnetic Stirrer

weight fraction mdea	T (K)	$k_l^0$ <sup>a</sup> (cm/sec)	CO <sub>2</sub> loading	P <sub>co2</sub> (atm)	CO <sub>2</sub> flux (moles/cm <sup>2</sup> *sec)
0.1920	282.7	8.30e-04	1.50e-01	9.90e-01	1.47e-07
0.1920	282.7	8.30e-04	2.20e-01	9.90e-01	1.40e-07
0.1920	303.7	1.05e-03	1.20e-01	9.60e-01	2.09e-07
0.1920	303.7	1.05e-03	2.06e-01	9.60e-01	1.95e-07
0.1920	313.7	1.16e-03	1.64e-01	9.20e-01	2.28e-07
0.1920	313.7	1.16e-03	1.84e-01	9.20e-01	2.22e-07
0.1920	313.7	1.16e-03	2.17e-01	9.20e-01	2.13e-07
0.1920	313.7	1.16e-03	2.56e-01	9.20e-01	2.00e-07
0.1920	313.7	1.16e-03	2.88e-01	9.20e-01	1.89e-07
0.1920	319.7	1.24e-03	1.55e-02	9.00e-01	2.86e-07
0.1920	319.7	1.24e-03	1.06e-01	9.00e-01	2.65e-07

<sup>a</sup>from Critchfield (1988) Table 5.3

Critchfield (1988)<sup>a</sup>

## Large Stirred Tank, Turbine Impeller

weight fraction mdea	T (K)	k <sub>l</sub> <sup>b</sup> (cm/sec)	CO <sub>2</sub> loading	P <sub>CO2</sub> (atm)	CO <sub>2</sub> flux (moles/cm <sup>2</sup> *sec)
0.1920	288.2	4.09e-04	5.60e-01	8.96e-04	-5.47e-09
0.1920	288.2	3.36e-04	5.61e-01	8.42e-04	-5.14e-09
0.1920	288.2	2.80e-04	5.56e-01	7.85e-04	-4.80e-09
0.1920	288.2	4.19e-04	5.55e-01	8.74e-04	-5.34e-09
0.1920	292.0	4.92e-04	5.70e-01	1.23e-03	-7.53e-09
0.1920	292.0	4.93e-04	5.64e-01	1.20e-03	-7.35e-09
0.1920	292.0	5.05e-04	5.71e-01	1.17e-03	-7.17e-09
0.1920	292.0	3.35e-04	5.71e-01	1.02e-03	-6.27e-09
0.1920	292.0	4.11e-04	5.71e-01	1.09e-03	-6.68e-09
0.1920	292.0	4.51e-04	5.71e-01	1.12e-03	-6.86e-09
0.1920	298.1	6.11e-04	5.47e-01	1.79e-03	-1.11e-08
0.1920	298.1	4.10e-04	5.47e-01	1.54e-03	-9.54e-09
0.1920	298.1	5.21e-04	5.47e-01	1.66e-03	-1.03e-08
0.1920	298.1	6.66e-04	5.47e-01	1.80e-03	-1.12e-08
0.1920	302.0	6.09e-04	5.16e-01	1.83e-03	-1.15e-08
0.1920	302.0	8.30e-04	5.16e-01	2.03e-03	-1.27e-08
0.1920	302.0	5.22e-04	5.16e-01	1.74e-03	-1.09e-08
0.1920	302.0	7.13e-04	5.16e-01	1.89e-03	-1.18e-08

<sup>a</sup>these data do not appear in tabular format in the dissertation referenced, they were taken from the original logbook

<sup>b</sup>from correlation developed in this work

## Toman (1990)

## Large Reactor, Turbine Impeller

weight fraction mdea	T (K)	$k_l^a$ (cm/sec)	CO <sub>2</sub> loading	P <sub>CO2</sub> (atm)	CO <sub>2</sub> flux (moles/cm <sup>2</sup> *sec)
0.5000	297.9	9.75e-05	2.10e-01	9.60e-01	8.80e-08
0.5000	297.9	2.40e-04	2.10e-01	9.60e-01	9.60e-08
0.5000	297.9	4.10e-04	2.10e-01	9.60e-01	1.07e-07
0.5000	297.9	5.90e-04	2.10e-01	9.60e-01	1.20e-07
0.5000	303.2	2.77e-04	2.10e-01	9.50e-01	1.04e-07
0.5000	303.2	4.75e-04	2.10e-01	9.50e-01	1.14e-07
0.5000	303.2	6.93e-04	2.10e-01	9.50e-01	1.32e-07
0.5000	308.2	5.30e-04	2.20e-01	9.40e-01	1.28e-07
0.5000	308.7	7.80e-04	2.20e-01	9.40e-01	1.47e-07
0.5000	313.2	5.91e-04	2.20e-01	9.30e-01	1.47e-07
0.5000	313.2	8.61e-04	2.20e-01	9.30e-01	1.79e-07
0.5000	298.0	9.50e-05	2.80e-01	9.60e-01	7.60e-08
0.5000	298.0	2.30e-04	2.80e-01	9.60e-01	8.80e-08
0.5000	298.0	5.70e-04	2.80e-01	9.60e-01	1.17e-07
0.5000	298.2	8.00e-04	1.17e-03	6.80e-02	2.43e-08
0.5000	297.7	8.00e-04	3.88e-03	6.90e-02	2.10e-08
0.5000	298.2	8.00e-04	6.90e-03	6.90e-02	2.18e-08
0.5000	298.2	7.50e-04	9.82e-03	6.95e-02	2.00e-08
0.5000	298.2	8.00e-04	1.98e-02	6.70e-02	1.82e-08
0.5000	298.2	1.10e-03	2.31e-02	6.70e-02	1.71e-08
0.5000	298.2	7.80e-04	3.84e-02	2.50e-01	6.24e-08
0.5000	298.2	1.00e-03	4.37e-02	2.50e-01	6.13e-08
0.5000	298.2	1.00e-03	5.16e-02	2.49e-01	6.43e-08
0.5000	298.2	1.00e-03	5.97e-02	2.48e-01	6.55e-08
0.5000	312.2	1.00e-03	6.86e-02	2.45e-01	9.98e-08
0.5000	313.2	1.00e-03	7.94e-02	2.48e-01	9.26e-08
0.5000	311.2	1.10e-03	2.59e-02	6.50e-02	2.91e-08
0.5000	313.2	1.00e-03	2.89e-02	6.50e-02	2.80e-08
0.5000	313.2	7.80e-04	3.30e-02	6.50e-02	2.76e-08

<sup>a</sup> see Toman (1990)



## Toman (1990) (Cont'd)

## Small Reactor

weight fraction mdea	T (K)	$k_l^a$ (cm/sec)	CO <sub>2</sub> loading	P <sub>CO2</sub> (atm)	CO <sub>2</sub> flux (moles/cm <sup>2</sup> *sec)
0.5000	297.6	9.67e-04	4.03e-02	9.63e-01	1.93e-07
0.5000	297.6	1.04e-03	4.12e-02	9.63e-01	2.01e-07
0.5000	297.6	1.03e-03	5.74e-02	9.63e-01	1.96e-07
0.5000	300.0	1.08e-03	5.93e-02	9.59e-01	2.21e-07
0.5000	302.4	1.12e-03	8.41e-02	9.55e-01	2.16e-07
0.5000	302.4	1.05e-03	8.50e-02	9.55e-01	2.06e-07
0.5000	302.4	1.04e-03	9.98e-02	9.55e-01	2.00e-07
0.5000	304.8	1.09e-03	1.02e-01	9.50e-01	2.21e-07
0.5000	307.2	1.10e-03	2.17e-01	9.45e-01	1.69e-07
0.5000	307.2	1.09e-03	2.33e-01	9.45e-01	1.60e-07
0.5000	307.2	1.17e-03	2.34e-01	9.45e-01	1.70e-07
0.5000	307.2	1.17e-03	2.41e-01	9.45e-01	1.67e-07
0.5000	307.2	1.36e-03	2.42e-01	9.45e-01	1.98e-07
0.5000	307.2	1.35e-03	2.64e-01	9.45e-01	1.86e-07
0.5000	302.4	1.23e-03	2.74e-01	9.55e-01	1.58e-07
0.5000	297.6	7.58e-04	2.96e-01	9.63e-01	1.24e-07
0.5000	297.6	6.79e-04	3.01e-01	9.63e-01	1.21e-07
0.5000	297.6	2.13e-04	3.01e-01	9.63e-01	9.22e-08
0.5000	297.6	2.12e-04	3.04e-01	9.63e-01	9.19e-08
0.5000	308.2	1.06e-03	5.70e-01	9.45e-01	4.76e-08
0.5000	308.2	1.06e-03	5.78e-01	9.45e-01	4.44e-08
0.5000	308.2	9.88e-04	5.78e-01	9.45e-01	4.09e-08
0.5000	308.2	9.88e-04	5.81e-01	9.45e-01	3.92e-08
0.5000	298.2	7.97e-04	6.72e-01	9.63e-01	2.77e-08
0.5000	298.2	7.86e-04	7.17e-01	9.63e-01	1.62e-08

<sup>a</sup> see Toman (1990)

MDEA/H<sub>2</sub>SO<sub>4</sub> SYSTEM

Toman (1990)

Large Reactor, Turbine Impeller

weight fraction mdea	H <sub>2</sub> SO <sub>4</sub> <sup>a</sup> loading	T (K)	kl <sup>o</sup> <sup>b</sup> (cm/sec)	CO <sub>2</sub> loading	P <sub>CO2</sub> (atm)	CO <sub>2</sub> flux (moles/cm <sup>2</sup> *sec)
0.5	0.25	298.0	1.95e-04	1.00e-05	6.37e-03	9.81e-10
0.5	0.25	298.0	1.05e-04	1.00e-05	6.66e-03	8.89e-10
0.5	0.25	298.0	2.81e-04	1.00e-05	7.09e-03	1.15e-09
0.5	0.25	298.0	1.95e-04	1.00e-05	7.29e-03	1.06e-09
0.5	0.25	298.0	1.05e-04	1.00e-05	7.52e-03	9.47e-10
0.5	0.25	313.0	5.41e-04	1.00e-05	6.92e-03	1.12e-09
0.5	0.25	313.0	3.76e-04	1.00e-05	7.07e-03	1.04e-09
0.5	0.25	313.0	2.01e-04	1.00e-05	7.35e-03	9.03e-10
0.5	0.25	297.5	2.74e-04	1.00e-05	4.53e-02	6.87e-09
0.5	0.25	298.0	1.95e-04	1.00e-05	4.97e-02	6.26e-09
0.5	0.25	298.0	1.05e-04	1.00e-05	5.33e-02	5.75e-09
0.5	0.25	312.0	5.19e-04	1.00e-05	4.46e-02	6.97e-09
0.5	0.25	308.5	3.11e-04	1.00e-05	4.67e-02	6.67e-09
0.5	0.25	313.5	2.06e-04	1.00e-05	5.10e-02	6.08e-09
0.5	0.25	298.0	1.51e-04	1.00e-05	1.87e-01	2.00e-08
0.5	0.25	298.0	2.38e-04	1.00e-05	1.77e-01	2.31e-08
0.5	0.25	298.0	3.23e-04	1.00e-05	1.67e-01	2.64e-08
0.5	0.25	297.9	1.04e-04	1.00e-05	2.74e-01	2.89e-08
0.5	0.25	298.0	6.60e-05	1.00e-05	2.76e-01	2.77e-08
0.5	0.25	298.2	3.57e-05	1.00e-05	2.75e-01	2.83e-08
0.5	0.25	298.2	3.71e-05	1.00e-05	9.60e-01	7.50e-08
0.5	0.25	298.2	5.33e-05	1.00e-05	9.60e-01	7.30e-08
0.5	0.25	298.2	8.71e-05	1.00e-05	9.60e-01	8.20e-08

<sup>a</sup> 0.25 moles of H<sub>2</sub>SO<sub>4</sub> were added for every mole of MDEA<sup>b</sup> from Toman (1990)

Toman (1990)

Small Reactor

weight fraction mdea	H <sub>2</sub> SO <sub>4</sub> <sup>a</sup> loading	T (K)	k <sub>l</sub> <sup>o b</sup> (cm/sec)	CO <sub>2</sub> loading	P <sub>CO2</sub> (atm)	CO <sub>2</sub> flux (moles/cm <sup>2</sup> *sec)
0.5	0.25	298.2	6.45e-04	3.94e-02	9.66e-01	8.88e-08
0.5	0.25	298.2	6.43e-04	4.52e-02	9.66e-01	8.78e-08
0.5	0.25	298.2	8.06e-04	6.18e-02	9.66e-01	8.88e-08
0.5	0.25	298.2	8.03e-04	6.99e-02	9.66e-01	8.78e-08
0.5	0.25	303.2	8.78e-04	7.10e-02	9.59e-01	9.32e-08
0.5	0.25	303.2	8.75e-04	8.01e-02	9.59e-01	9.12e-08
0.5	0.25	303.2	8.67e-04	1.07e-01	9.48e-01	8.45e-08
0.5	0.25	308.2	9.45e-04	1.10e-01	9.41e-01	8.85e-08
0.5	0.25	308.2	9.40e-04	1.22e-01	9.41e-01	8.52e-08
0.5	0.25	308.2	9.30e-04	1.52e-01	9.41e-01	7.90e-08
0.5	0.25	303.2	8.52e-04	1.54e-01	9.48e-01	7.67e-08
0.5	0.25	303.2	8.47e-04	1.70e-01	9.48e-01	7.17e-08

<sup>a</sup> 0.25 moles of H<sub>2</sub>SO<sub>4</sub> were added for every mole of MDEA<sup>b</sup> from Toman (1990)

## DEA SYSTEM

Present work

Large Reactor, Turbine Impeller

weight fraction dea	T (K)	$kl^0$ <sup>a</sup> (cm/sec)	CO <sub>2</sub> loading	P <sub>CO2</sub> (atm)	CO <sub>2</sub> flux (moles/cm <sup>2</sup> *sec)
0.0951	313.1	2.89e-03	1.92e-02	3.68e-02	1.22e-07
0.0951	313.1	2.36e-03	2.78e-02	3.83e-02	1.16e-07
0.0951	313.1	2.02e-03	8.48e-02	4.09e-02	1.03e-07
0.0951	313.1	2.88e-03	4.03e-03	1.10e-02	4.21e-08
0.0951	313.1	2.36e-03	6.40e-03	1.13e-02	3.98e-08
0.0951	313.1	2.02e-03	8.87e-03	1.16e-02	4.16e-08
0.0499	313.1	3.06e-03	4.58e-03	1.28e-02	3.01e-08
0.0499	313.1	2.74e-03	7.39e-03	1.29e-02	3.10e-08
0.0499	313.1	2.33e-03	1.03e-02	1.31e-02	2.94e-08

<sup>a</sup> from correlation developed in this work

## Critchfield (1988)

## Large Reactor, Turbine Impeller

weight fraction dea	T (K)	$k_l^0$ <sup>a</sup> (cm/sec)	CO <sub>2</sub> loading	P <sub>CO2</sub> (atm)	CO <sub>2</sub> flux (moles/cm <sup>2</sup> *sec)
0.2060	298.1	1.09e-03	8.53e-02	9.70e-03	4.23e-08
0.2060	298.1	1.34e-03	8.53e-02	9.60e-03	4.23e-08
0.2060	298.1	7.54e-04	8.53e-02	1.03e-02	3.93e-08
0.2060	298.1	9.73e-04	8.00e-02	2.92e-02	1.26e-07
0.2060	298.1	1.04e-03	8.35e-02	1.84e-02	7.67e-08
0.2060	298.1	1.30e-03	8.35e-02	1.82e-02	7.81e-08
0.2060	298.1	7.70e-04	8.35e-02	1.90e-02	7.40e-08
0.2060	298.1	7.97e-04	9.83e-02	6.99e-02	1.74e-07
0.2060	298.1	1.36e-03	9.83e-02	6.41e-02	2.06e-07
0.2060	298.1	1.22e-03	1.00e-01	1.33e-01	3.31e-07
0.2060	298.1	8.61e-04	1.07e-01	1.57e-01	2.76e-07
0.2060	298.1	7.43e-04	1.14e-01	1.64e-01	2.60e-07
0.2060	298.1	9.83e-04	2.27e-01	3.34e-04	-2.01e-09
0.2060	298.1	1.24e-03	2.32e-01	3.33e-04	-2.00e-09
0.2060	298.1	1.24e-03	3.10e-01	8.09e-04	-4.86e-09
0.2060	298.1	1.06e-03	3.90e-01	1.62e-03	-1.09e-08

<sup>a</sup> from correlation used by Critchfield

## Blauwhoff et al. (1984)

weight fraction dea	T (K)	$k_l^a$ (cm/sec)	CO <sub>2</sub> loading	P <sub>CO<sub>2</sub></sub> <sup>a</sup> (atm)	CO <sub>2</sub> flux (moles/cm <sup>2</sup> *sec)
0.0533	298.1	2.30e-03	2.34e-02	4.00e-02	8.03e-08
0.0541	298.1	2.30e-03	2.23e-02	4.00e-02	8.29e-08
0.0939	298.1	2.30e-03	1.28e-02	4.00e-02	1.18e-07
0.1021	298.1	2.30e-03	1.32e-02	4.00e-02	1.23e-07
0.2036	298.1	2.30e-03	3.74e-03	4.00e-02	1.85e-07
0.2090	298.1	2.30e-03	3.40e-03	4.00e-02	1.89e-07
0.2104	298.1	2.30e-03	3.23e-03	4.00e-02	1.94e-07
0.0870	298.1	2.30e-03	5.14e-02	4.00e-02	1.10e-07
0.1425	298.1	2.30e-03	2.75e-02	4.00e-02	1.44e-07
0.1787	298.1	2.30e-03	2.31e-02	4.00e-02	1.62e-07
0.1932	298.1	2.30e-03	2.03e-02	4.00e-02	1.70e-07
0.2011	298.1	2.30e-03	2.18e-02	4.00e-02	1.74e-07
0.0412	298.1	2.30e-03	1.02e-01	4.00e-02	6.59e-08
0.0614	298.1	2.30e-03	6.88e-02	4.00e-02	8.34e-08
0.0800	298.1	2.30e-03	5.05e-02	4.00e-02	9.71e-08
0.1721	298.1	2.30e-03	1.42e-02	4.00e-02	1.72e-07
0.1891	298.1	2.30e-03	5.28e-02	4.00e-02	1.62e-07
0.1891	298.1	2.30e-03	5.19e-02	4.00e-02	1.64e-07
0.1939	298.1	2.30e-03	3.53e-02	4.00e-02	1.67e-07
0.1941	298.1	2.30e-03	3.96e-02	4.00e-02	1.67e-07
0.1947	298.1	2.30e-03	7.52e-03	4.00e-02	1.87e-07
0.2014	298.1	2.30e-03	2.03e-02	4.00e-02	1.67e-07
0.2092	298.1	2.30e-03	3.74e-03	4.00e-02	1.86e-07
0.2223	298.1	2.30e-03	5.59e-03	4.00e-02	1.90e-07
0.2228	298.1	2.30e-03	6.13e-03	4.00e-02	1.90e-07
0.2367	298.1	2.30e-03	1.12e-02	4.00e-02	1.99e-07

<sup>a</sup>These data were estimated based upon the data available in the paper. During the regression procedure, these data are all treated as pseudo-first order, hence the values of the mass transfer coefficient and the partial pressure do not affect the data interpretation.

## DEA/MDEA SYSTEM

Present work

Large Reactor, Turbine Impeller

weight fraction mdea	weight fraction dea	T (K)	$k_1^0$ <sup>a</sup> (cm/sec)	CO <sub>2</sub> loading	P <sub>CO2</sub> (atm)	CO <sub>2</sub> flux (moles/cm <sup>2</sup> *sec)
0.096	0.0094	313.1	1.85E-03	1.70E-03	3.66E-02	3.24E-08
0.096	0.0094	313.1	2.19E-03	3.19E-03	3.64E-02	3.44E-08
0.096	0.0094	313.1	1.71E-03	4.16E-03	3.71E-02	3.60E-08
0.096	0.0094	333.1	3.73E-03	6.87E-03	2.96E-02	3.82E-08
0.096	0.0094	333.1	3.67E-03	1.01E-02	2.97E-02	3.84E-08
0.0748	0.0283	313.1	2.19E-03	5.26E-03	2.99E-02	5.03E-08
0.0748	0.0283	313.1	1.97E-03	9.07E-03	3.04E-02	5.04E-08
0.0748	0.0283	313.1	2.21E-03	1.45E-02	3.01E-02	5.77E-08

<sup>a</sup> from correlation developed in this work

## Critchfield (1988)

## Large Reactor, Turbine Impeller

weight fraction mdea	weight fraction dea	T (K)	$kl^0$ <sup>a</sup> (cm/sec)	CO <sub>2</sub> loading	P <sub>CO2</sub> (atm)	CO <sub>2</sub> flux (moles/cm <sup>2</sup> *sec)
0.1637	0.0619	298.1	4.64E-04	2.28E-03	8.04E-02	1.13E-07
0.1637	0.0619	298.1	7.21E-04	3.00E-03	7.77E-02	1.29E-07
0.1637	0.0619	298.1	7.23E-04	4.42E-03	3.75E-02	7.67E-08
0.1637	0.0619	298.1	5.14E-04	4.92E-03	3.87E-02	7.12E-08
0.1637	0.0619	298.1	6.19E-04	5.34E-03	3.81E-02	7.40E-08
0.1637	0.0619	298.1	6.88E-04	4.10E-04	5.62E-04	1.48E-09
0.1637	0.0619	298.1	6.88E-04	2.62E-03	5.66E-04	1.47E-09
0.1637	0.0619	298.1	4.60E-04	2.62E-03	5.82E-04	1.45E-09
0.1637	0.0619	298.1	7.28E-04	2.62E-03	5.64E-04	1.48E-09
0.1637	0.0619	298.1	4.58E-04	2.54E-03	8.08E-03	1.88E-08
0.1637	0.0619	298.1	7.28E-04	2.54E-03	7.73E-03	1.95E-08
0.1637	0.0619	298.1	6.88E-04	1.54E-03	7.74E-03	1.95E-08
0.1637	0.0619	298.1	6.88E-04	9.00E-04	2.72E-03	7.06E-09
0.1637	0.0619	288.1	2.94E-04	2.68E-03	6.54E-03	1.21E-08
0.1637	0.0619	288.1	4.40E-04	2.68E-03	6.31E-03	1.26E-08
0.1637	0.0619	288.1	4.58E-04	2.68E-03	6.30E-03	1.25E-08
0.1637	0.0619	288.1	2.96E-04	3.51E-03	2.08E-03	3.95E-09
0.1637	0.0619	288.1	4.42E-04	3.51E-03	2.05E-03	4.09E-09
0.1637	0.0619	288.1	4.60E-04	3.51E-03	2.05E-03	4.14E-09
0.1637	0.0619	298.1	6.74E-04	6.35E-02	1.61E-04	-3.81E-10
0.1637	0.0619	298.1	6.63E-04	9.80E-02	2.15E-04	-1.03E-09
0.1637	0.0619	298.1	6.64E-04	1.17E-01	3.00E-04	-1.44E-09
0.1637	0.0619	298.1	6.42E-04	2.17E-01	9.56E-04	-4.59E-09
0.1637	0.0619	298.1	6.31E-04	2.70E-01	1.42E-03	-8.56E-09
0.1637	0.0619	298.1	6.15E-04	3.50E-01	1.00E-02	-7.03E-09
0.1637	0.0619	298.1	6.02E-04	4.12E-01	1.52E-02	-1.07E-08
0.1637	0.0619	298.1	5.86E-04	4.93E-01	2.24E-02	-1.41E-08
0.1637	0.0619	298.1	6.78E-04	5.44E-02	1.22E-04	-2.10E-10
0.2223	0.0103	298.1	6.43E-04	3.78E-02	1.98E-04	-1.39E-10
0.2223	0.0103	298.1	6.35E-04	6.27E-02	4.70E-04	-3.30E-10
0.2223	0.0103	298.1	6.16E-04	1.35E-01	5.85E-04	-2.07E-09
0.2223	0.0103	298.1	6.09E-04	1.78E-01	2.80E-03	-1.96E-09
0.2223	0.0103	298.1	5.93E-04	2.30E-01	4.21E-03	-2.95E-09
0.2223	0.0103	298.1	5.88E-04	2.59E-01	5.18E-03	-3.64E-09
0.2223	0.0103	298.1	5.63E-04	3.50E-01	8.87E-03	-6.22E-09

<sup>a</sup> from correlation developed in this work



# VISCOSITY DATA USED IN CORRELATION

Al-Ghawas et al. (1988)

weight fraction mdea	weight fraction dea	weight fraction mea	T (K)	viscosity (cP)
0.000	0.000	0.000	288.2	1.14
0.000	0.000	0.000	293.2	1.01
0.000	0.000	0.000	298.2	0.90
0.000	0.000	0.000	303.2	0.80
0.000	0.000	0.000	308.2	0.72
0.000	0.000	0.000	313.2	0.66
0.000	0.000	0.000	318.2	0.60
0.000	0.000	0.000	323.2	0.56
0.000	0.000	0.000	328.2	0.50
0.000	0.000	0.000	333.2	0.48
0.100	0.000	0.000	288.2	1.71
0.100	0.000	0.000	293.2	1.48
0.100	0.000	0.000	298.2	1.29
0.100	0.000	0.000	303.2	1.14
0.100	0.000	0.000	308.2	1.01
0.100	0.000	0.000	313.2	0.91
0.100	0.000	0.000	323.2	0.75
0.100	0.000	0.000	333.2	0.63
0.200	0.000	0.000	288.2	2.65
0.200	0.000	0.000	293.2	2.26
0.200	0.000	0.000	298.2	1.94
0.200	0.000	0.000	303.2	1.69
0.200	0.000	0.000	308.2	1.47
0.200	0.000	0.000	313.2	1.30
0.200	0.000	0.000	323.2	1.05
0.200	0.000	0.000	333.2	0.86
0.300	0.000	0.000	288.2	4.40
0.300	0.000	0.000	293.2	3.69
0.300	0.000	0.000	298.2	3.09
0.300	0.000	0.000	303.2	2.61
0.300	0.000	0.000	308.2	2.25
0.300	0.000	0.000	313.2	1.94
0.300	0.000	0.000	323.2	1.51
0.300	0.000	0.000	333.2	1.21

## Al-Ghawas et al. (1988), (Cont'd)

weight fraction mdea	weight fraction dea	weight fraction mea	T (K)	viscosity (cP)
0.400	0.000	0.000	288.2	7.97
0.400	0.000	0.000	293.2	6.45
0.400	0.000	0.000	298.2	5.25
0.400	0.000	0.000	303.2	4.36
0.400	0.000	0.000	308.2	3.67
0.400	0.000	0.000	313.2	3.11
0.400	0.000	0.000	323.2	2.31
0.500	0.000	0.000	288.2	14.69
0.500	0.000	0.000	293.2	11.70
0.500	0.000	0.000	298.2	9.21
0.500	0.000	0.000	303.2	7.44
0.500	0.000	0.000	308.2	6.10
0.500	0.000	0.000	313.2	5.11
0.500	0.000	0.000	323.2	3.64
0.500	0.000	0.000	333.2	2.70

## Critchfield (1988)

weight fraction mdea	weight fraction dea	weight fraction mea	T (K)	viscosity (cP)
0.296	0.000	0.000	294.4	3.57
0.296	0.000	0.000	294.5	3.56
0.296	0.000	0.000	323.2	1.52
0.296	0.000	0.000	314.7	1.91
0.217	0.000	0.048	295.2	2.94
0.217	0.000	0.048	306.7	2.02
0.217	0.000	0.048	317.7	1.51
0.217	0.000	0.048	325.0	1.28
0.166	0.000	0.015	293.2	2.16
0.166	0.000	0.015	299.0	1.83
0.166	0.000	0.015	309.7	1.38
0.000	0.000	0.111	293.4	1.48
0.000	0.000	0.111	289.7	1.65
0.000	0.000	0.111	304.2	1.14
0.042	0.000	0.086	300.7	1.36
0.042	0.000	0.086	293.7	1.63
0.042	0.000	0.086	305.2	1.22
0.104	0.000	0.053	299.2	1.53
0.104	0.000	0.053	293.4	1.79
0.104	0.000	0.053	293.4	1.81
0.104	0.000	0.053	289.7	2.01
0.104	0.000	0.053	305.2	1.31
0.139	0.000	0.031	300.1	1.69
0.139	0.000	0.031	293.4	2.03
0.139	0.000	0.031	293.4	2.01
0.139	0.000	0.031	289.2	2.34
0.139	0.000	0.031	305.2	1.46
0.139	0.000	0.031	305.7	1.47
0.184	0.000	0.005	289.2	1.99
0.184	0.000	0.005	293.2	2.20
0.184	0.000	0.005	293.5	2.18
0.184	0.000	0.005	300.7	1.78
0.192	0.000	0.000	300.7	1.83
0.192	0.000	0.000	293.2	2.29
0.192	0.000	0.000	289.2	2.64
0.192	0.000	0.000	305.7	1.60
0.192	0.000	0.000	311.7	1.38

Sada et al. (1978)

weight fraction mdea	weight fraction dea	weight fraction mea	T (K)	viscosity (cP)
0.192	0.000	0.000	317.2	1.21
0.000	0.206	0.000	298.2	2.06
0.000	0.206	0.000	308.2	1.59
0.000	0.206	0.000	318.2	1.25
0.164	0.062	0.000	298.2	2.30
0.164	0.062	0.000	308.2	1.71
0.164	0.062	0.000	318.2	1.34
0.165	0.000	0.036	298.2	2.03
0.165	0.000	0.036	308.2	1.56
0.165	0.000	0.036	318.2	1.23
0.000	0.000	0.000	298.2	0.90
0.000	0.000	0.047	298.2	1.00
0.000	0.000	0.087	298.2	1.14
0.000	0.000	0.129	298.2	1.31
0.000	0.000	0.176	298.2	1.52
0.000	0.000	0.214	298.2	1.72
0.000	0.052	0.000	298.2	1.10
0.000	0.102	0.000	298.2	1.27
0.000	0.198	0.000	298.2	1.88
0.000	0.287	0.000	298.2	2.82
0.000	0.350	0.000	298.2	3.86

**RELATIVE VISCOSITY FOR 50 WT% MDEA AT 298K (Toman, 1990)**

loading	relative viscosity (viscosity of loaded soln./unloaded soln.)
0.001	1.001
0.050	1.046
0.111	1.101
0.162	1.139
0.321	1.283
0.353	1.315
0.408	1.388
0.440	1.430
0.500	1.440
0.510	1.527
0.547	1.528
0.569	1.616
0.673	1.776
0.710	1.724
0.760	1.784

## Appendix D

### Physical Property Correlations

#### D.1 Viscosity of the Unloaded Solution

Based upon the data of Al-Ghawas et al. (1988), Critchfield (1988) and Sada et al. (1978) the following correlation was developed:

$$w_{am} = w_{mdea} + \mathbf{0.980}w_{dea} + \mathbf{0.876}w_{mea}$$

$$\begin{aligned} B_1 &= -19.52 & - 23.40*w_{am} & - 31.24*w_{am}^2 & + 36.17*w_{am}^3 \\ B_2 &= 3912 & + \mathbf{4894}*w_{am} & + 8477*w_{am}^2 & - 8358*w_{am}^3 \\ B_3 &= 0.02112 & + 0.03339*w_{am} & + 0.02780*w_{am}^2 & - \mathbf{0.04202}*w_{am}^3 \end{aligned}$$

$$\log_e \mu = B_1 + \frac{B_2}{T} + B_3T \quad [D.1]$$

$\mu$  is in cP and  $T$  is the temperature in degrees Kelvin.  $w_{mdea}$ ,  $w_{dea}$  and  $w_{mea}$  denote the weight fractions of MDEA, DEA, and MEA, respectively. The correlation is based upon the viscosity correlation for MDEA only by Al-Ghawas et al., with the parameters in bold adjusted to fit the experimental data for all of the amines. The standard deviations for the 4 parameters are 0.980 +/- 0.0274, 0.876 +/- 0.0449, 4894 +/- 199.5, -0.04202 +/- 0.00124. The other parameters could not be adjusted with significance. All of the data (in Appendix C) fit the correlation within 10% except for one datapoint, presumed to be an outlier. This correlation is considered to be reasonable for 0 to 50 wt% total amine, and a temperature range of 290 to 320 K.

## D.2 Viscosity of the Loaded Solution

Toman (1989) determined the effect of CO<sub>2</sub> loading on the viscosity of 50 wt% MDEA at 298K. These data, shown in Appendix C, span the range of 0. to 0.76 moles of CO<sub>2</sub> per mole of amine, and are fit most adequately by a second order equation:

$$r = 1.000 + 0.8031 \cdot \text{loading} + 0.35786 \cdot (\text{loading}^2) \quad [\text{D.2}]$$

In order to estimate the viscosity of solutions other than 50 wt% MDEA, the corrected relative viscosity was estimated as follows:

$$\text{relative viscosity} = 1. + 2. \cdot (r-1) \cdot (\text{wt fraction amine}) \quad [\text{D.3}]$$

For 50 wt% amine, this equation defaults to relative viscosity = r, whereas, for pure water (wt fraction amine = 0) this equation defaults yields 1 for the relative viscosity, despite the loading. This correlation makes obvious physical sense and is used for all amine solutions.

## D.3 Density of the Solution

The density correlation of Licht and Weiland (1989) was used for all amines. The correlation is of the following form:

$$\frac{1}{\rho} = u_w V_w^0 e^{\{\beta_w (T - T_0)\}} + u_{A1} V_{A1}^0 e^{\{\beta_{A1} (T - T_0)\}} + u_{A2} V_{A2}^0 e^{\{\beta_{A2} (T - T_0)\}} + w_{CO_2} V_{CO_2}^0 e^{\{\beta_{CO_2} (T - T_0)\}} \quad [\text{D.4}]$$

where	$T_0$	=	308K
	$T$	=	temperature in degrees K
	$u_w$	=	weight fraction water
	$u_{A1}$	=	weight fraction amine 1
	$u_{A2}$	=	weight fraction amine 2 (if needed)
	$w_{CO_2}$	=	loaded basis weight fraction CO <sub>2</sub>

$V^o$	=	specific volume, shown below
$\beta$	=	bulk thermal expansivity

The density is in units of g/cm<sup>3</sup>.

	<u>Water</u>	<u>MDEA</u>	<u>DEA</u>	<u>MEA</u>	<u>CO<sub>2</sub></u>
specific volume (cm <sup>3</sup> /g)	1.01	0.918	0.894	0.964	0.0636
bulk expansivity (K <sup>-1</sup> )	0.000344	0.000528	0.000487	0.000568	0.0036

#### **D.4 Diffusion Coefficients**

##### ***D.4.1 Diffusion Coefficient of CO<sub>2</sub>***

The diffusion coefficient of CO<sub>2</sub> was estimated using the data and N<sub>2</sub>O analogy of Versteeg and van Swaaij (1988). First, the diffusion coefficients of CO<sub>2</sub> and N<sub>2</sub>O in water are calculated:

$$D_{CO_2} = 2.35 \times 10^{-6} e^{\{-2119/T\}} \quad [D.5]$$

$$D_{N_2O} = 5.07 \times 10^{-6} e^{\{-2371/T\}} \quad [D.6]$$

T is in Kelvin, and D is in m<sup>2</sup>/s. The diffusion coefficient for N<sub>2</sub>O is then calculated according to the modified Stokes-Einstein relation:

$$(D_{N_2O} \mu^{0.80})_{\text{am soln}} = (D_{N_2O} \mu^{0.80})_{\text{water}} \quad [D.7]$$

The diffusion coefficient of CO<sub>2</sub> in the amine solution is then calculated using the N<sub>2</sub>O analogy:



$$\left(\frac{D_{N_2O}}{D_{CO_2}}\right)_{\text{am soln}} = \left(\frac{D_{N_2O}}{D_{CO_2}}\right)_{\text{water}} \quad [\text{D.8}]$$

#### *D.4.2 Diffusion Coefficient of the Amines*

The amine diffusion coefficients were calculated from the data of Versteeg and van Swaaij (1988) at 298K in water for DEA and MEA. In order to estimate the diffusion coefficient of MDEA, a correlation was developed based upon the data of Versteeg and van Swaaij for a number of amines. It was found that, to a good approximation the diffusion coefficient of the amine in water could be correlated by the following equation:

$$D_{\text{am}} = 2.5 \times 10^{-10} \left(\frac{M}{\rho}\right)^{-0.54} \quad [\text{D.9}]$$

M is the molecular weight, and  $\rho$  is the mass density, obtained from Kohl and Reisenfeld (1985). The correlation coefficient of the regression,  $R^2$ , is 0.93. This correlation is based upon a general equation of the form  $D = c_1 V c^2$ , where V is the molar volume, as presented by Reid et al. (1977). The resulting diffusion coefficients in water at 298K are shown below:

$$D_{\text{MDEA}} = 8.02 \times 10^{-10} \text{ m}^2/\text{s}$$

$$D_{\text{DEA}} = 8.08 \times 10^{-10} \text{ m}^2/\text{s}$$

$$D_{\text{MEA}} = 11.72 \times 10^{-10} \text{ m}^2/\text{s}$$

The diffusion coefficients were corrected for viscosity and temperature using the modified Stokes-Einstein relationship:

$$D_{\text{am, soln}} = D_{\text{am, water}} \frac{T}{298} \left(\frac{\mu_{\text{H}_2\text{O}}}{\mu_{\text{soln}}}\right)^{0.6} \quad [\text{D.10}]$$

## Appendix E

### Program Documentation

This appendix briefly outlines the computer code used in this work, and the associated input and output files. It is not intended to provide a complete flow diagram of the program, however, the use of this Appendix, along with the internally documented computer code will guide the user through the execution of the combined equilibrium/mass transfer program.

#### E.1 Program Execution Overview

The main program is called MAXDRV in Figure E.1. This program directs the execution of the program, determining whether or not the run will be a simulation or a data regression, based upon input file data. If a data regression is to be run, then the program MAXLIK will be called. In either case, the simulation subroutine will be called to execute the model.

The main program RXN70 will call the subroutine INPUT to read the input file. A global vector VECINFO is used to store information from the input files, however, the subroutine PARM converts some of this information, such as temperature, into more meaningful variable names. Subroutine COLLOC is used to calculate the matrices of first- and second-order derivative collocation weights. Subroutine PTS is used to calculate the grid, and uses information based upon the number of collocation points and elements. Both COLLOC and PTS are called only if the differential equation-based mass transfer model is to be used. Subroutine PROP70 is then called to determine the equilibrium composition as well as the diffusion coefficients and rate constants for the chemical reactions, and will be discussed in more detail in reference to Figure E.2. If the differential equation-based mass transfer model is to be solved, then the subroutines ETRANS, PREP and CONT are solved. The subroutine ETRANS is

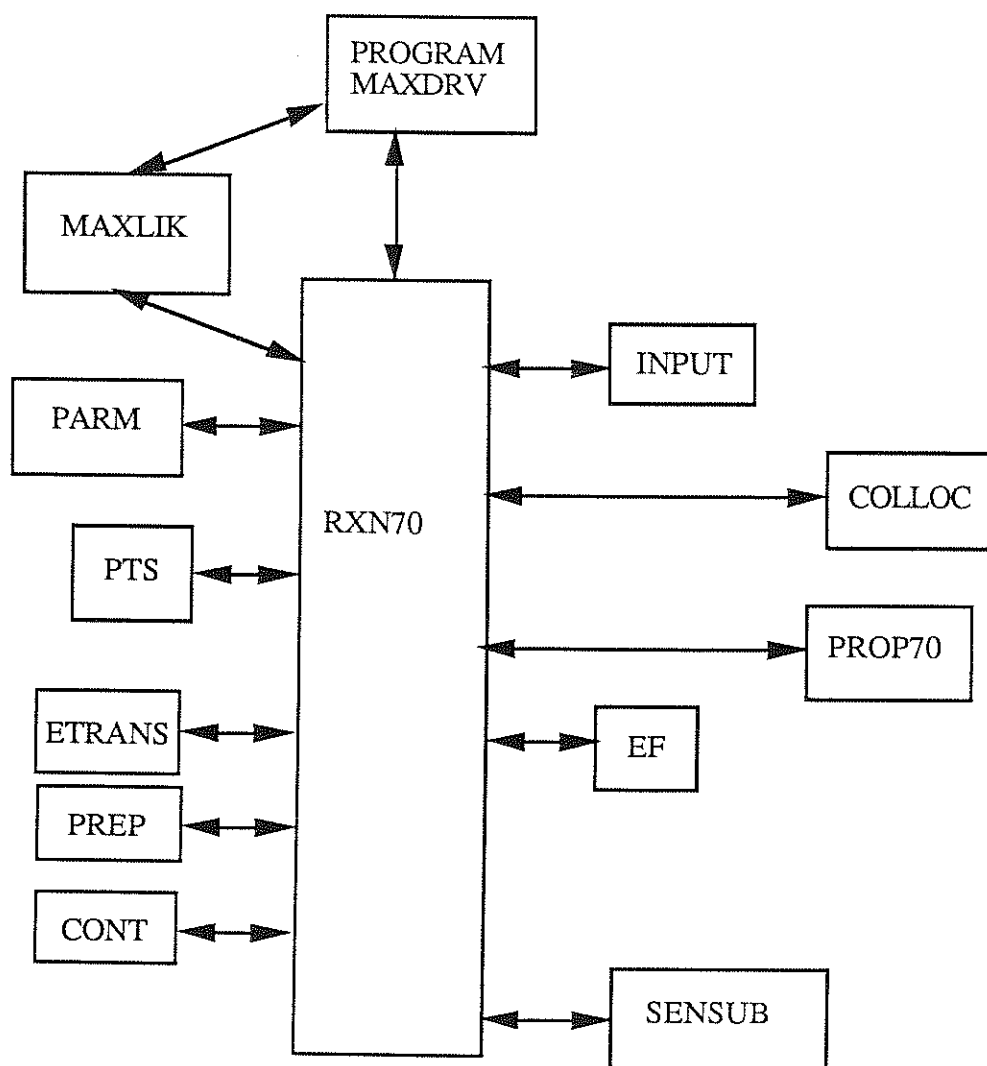


Figure E.1 Subroutine Call Chain from the Main Program

---

then called to determine the dimensionless transformation of the real distance,  $x$ , since all calculations are performed in dimensionless space. Subroutine PREP determines the initial concentration profiles for the homotopy continuation method. Subroutine CONT executes the mass transfer model and is described in Figure E.3. If pseudo-first order conditions are assumed, subroutine EF is used. Finally, subroutine SENSUB calculates the derivatives with respect to parameters for the model if needed.

Referring to Figure E.2, we see that PROP70 first determines the density of the amine system. This information is used to calculate the concentrations from weight fractions, if needed. Subroutine DATACT calculates the binary interaction parameters for the Electrolyte-NRTL model. Subroutine EQUIL, part of the EQUIL70 package, calculates the equilibrium composition by Smith and Missen's Gibbs free energy minimization algorithm. Subroutine GAMDRV is used to calculate the activity coefficients for all species in solution from the short- and long-range contributions calculated individually by the subroutines called by ACT.

After the preliminary calculations have been done for a chemical system, the subroutine CONT is called to begin execution of the mass transfer model (see Figure E.3). Subroutine DASSL is used to integrate the equations in time, and DASSL uses the subroutine RES to calculate the differential equations. Subroutine RES uses ZGRADLAPV and ZDIFTRAN to calculate the derivatives in the differential equations. Finally, subroutines BC and ELEMBV are used to calculate the equations between the elements and at the boundaries. It should be noted that if 4 internal collocation points are used, special forms for the subroutines ZGRADLAP and ELEMB used unrolled loops to calculate the equations in order to take advantage of vector processors.

Upon completion of the model, subroutine OUT prints the output file showing concentration profiles, if the run is not in the context of parameter estimation. For the case of parameter estimation, subroutine SOLVE, which used a Newton-Raphson - based method, is used after the initial solution of the model for a given problem. If the method does not converge, then the program will automatically convert to DASSL to resolve the problem using the homotopy continuation method.

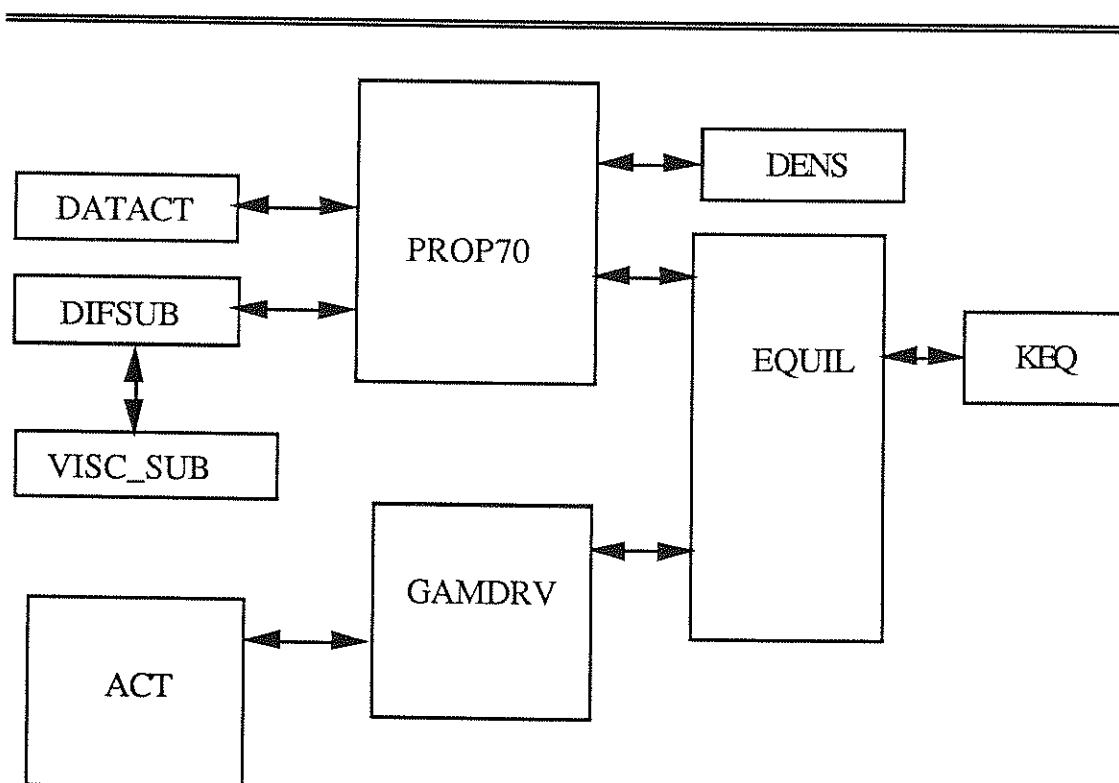


Figure E.2 Subroutine Call Chain from PROP70

---

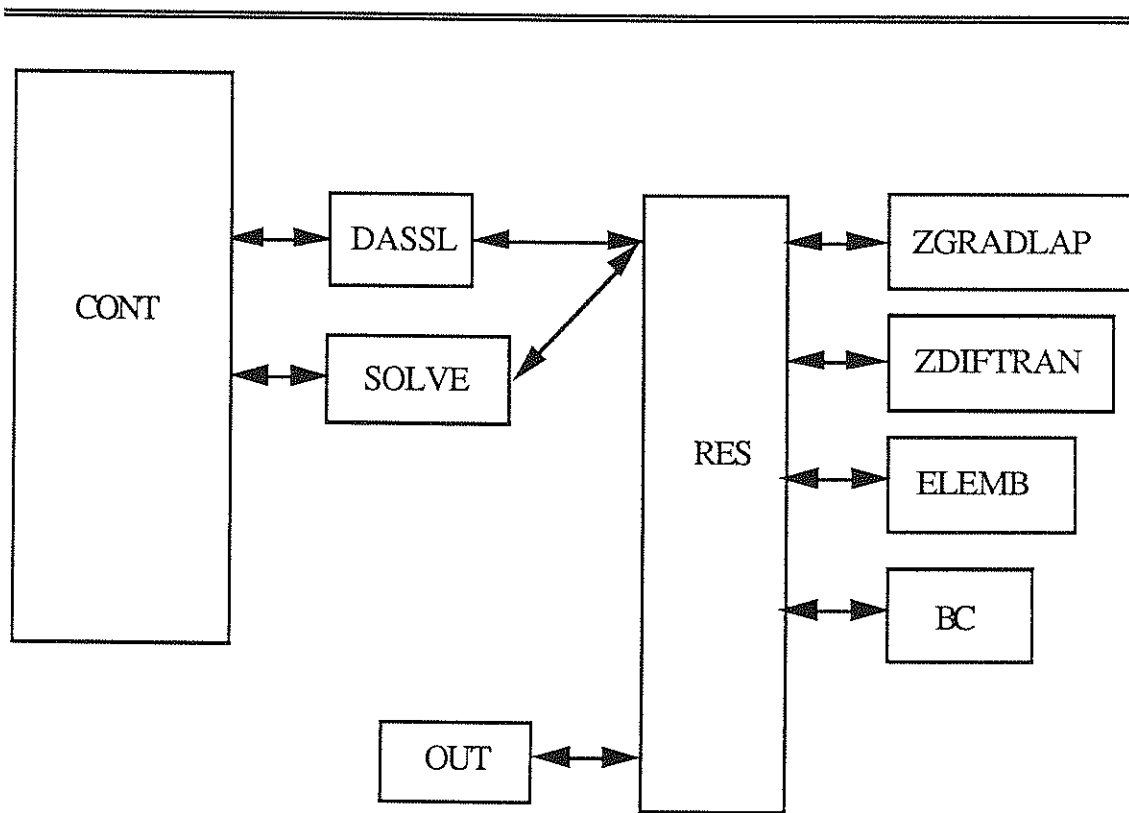


Figure E.3 Subroutine Call Chain from CONT

---

## E.2 Location of Subroutines

The subroutines written by this author are located in four files, RXN70, PROP70, UTIL70, EQUIL70, and MAXLIK and are shown in Table E.1. Program COLLOC was written by John Prindle (1986) and DASSL was developed by Linda Petzold (1983). In addition, a number of subroutines from LINPACK and BLAS levels 1 and 2 are used in the programs. The necessary LINPACK routines are included in DASSL, and the BLAS routines can be accessed automatically on the CRAY X-MP system or else are publicly available.

## E.3 Input Files

Several input files must be made available. The primary input file is designated 'RXN70.IN' and is shown in Figure E.4. Documentation is provided with the file and shown in Figure E.4. 'EQUIL.IN' is used to provide information for the equilibrium model, described in Chapter 3, and is shown in Figure E.5.

'PARM.IN', an example of which is shown in Figure E.6, lists the data used in during kinetic or thermodynamic parameter estimation. The first line shows a row of zeros, which designates that this file is to be ignored in the current simulation (no parameter estimation being performed). If parameter estimation is to be performed, then the first row should tell how many experiments will be analyzed, how much data must be read into the vector, and how many experimental datapoints are subject to error. The location of the variables subject to error is also shown. The data are read into a matrix. The first variable on each line designates the chemical system and the type of regression. The types of systems are shown in Table E.2. The data are converted into input parameters for the simulation in subroutine PROP70, so it is suggested that the reader refer to this subroutine for the definitions. Finally, the number of parameters to be regressed is input, as well as the lower bound, initial guess, upper bound, and maximum increment per iteration (MI) for each parameter. If  $MI < 0$ , then a relative increment is used.

#### E.4 Output Files

Only two of the output files will be shown here. In Figure E.7 we see the primary output file, 'RXN70.DAT' which shows the concentration profiles and run information. In Figure E.8, we shown 'RXN70.OUT', which documents the input information shown in 'RXN70.IN', the diffusion coefficients, and rate constants. This smaller output file is useful when making repeated runs, in which the cumulative file of 'RXN70.DAT' can become prohibitive. If parameter 5 is set to 1 or above in the input file 'RXN70.IN', then several plotting files are formed, 'RXN70X.PLT', 'RXN70Y1.PLT', and 'RXN70Y2.PLT' which contain the concentration profiles in a form easily downloaded into a spreadsheet for plotting. In addition, 'STEP.OUT' summarizes the equilibrium results. Finally, 'EGAMSUM.OUT', 'ECONSUM.OUT' and 'ECONINT.OUT' summarize the activity coefficients, bulk and interface compositions, respectively in a manner easily downloaded in to a spreadsheet for analysis.

#### E.5 Include Files

There are several include files which contain common blocks to allow the various subroutines to share data. RXN.INC is required by the subroutines in RXN70, PROP70, and UTIL70. NRTL.INC is required by GAMMA70. PARM.INC is used by RXN70 and PROP70. EQUIL70.INC is used by the routines in EQUIL70. Finally, SOLVE.INC is used in RXN70.



---

Table E.1      Summary of Subroutines Written by the Author

---



---

FILE LOCATION

<u>RXN70</u>	<u>PROP70</u>	<u>UTIL70</u>	<u>EQUIL70</u>	<u>GAMMA70</u>	<u>MAXLIK</u>
MAXDRV	PROP70	INPUT	EQUIL	ACT	MAXLIK
RXN70	DIFSUB	PARM	IN2	GAMM	MAXBUILD
CONT	VISC_SUB	PTS	KEND	GAMC	MAXDIR
EF	GAMDRV	ETRANS	NTOMU	GAMA	MAXOUT
SENSUB	KEQ	OUT	MATRIX	PARMDBL	MAXNEW
SENSOLV	RKEQ		UPDATE2	PARMTPL	DATSTEP
WEIGHT	DATACT		CHECK	GAMMINF	MAXCOV
STEP	RES		OUT2	GAMCINF	
NEWY	PREP		KTOMU	GAMAINF	
DAJAC2 <sup>1</sup>	BC		VTOA	GAMDEBYE	
SOLVE				CLRSUM	
GRADLAP					
DIFTRAN					
ELEMB					
GRADLAPV					
ELEMBV					
ZGRADLAP					
ZDIFTRAN					
ZGRADLAPV					
JAC <sup>2</sup>					

<sup>1</sup>Adapted from a subroutine in DASSL written by Linda Petzold

<sup>2</sup>Currently deactivated, but can be used if needed

---

---

```

80, # ELEMENTS OF INFORMATION
7,14,8,6,0., # REAL EQUATIONS, # COMP, # ELEMENTS, # COLLOCATION
POINTS,PLT
0.,1.E-5,0.001e0,.5E0,1., ;06 FIRST ORDER, (1,0,-1)
1.e-3,1.e-6,313.15, 0.0,1. ;11
0.30,0.001,0.2,1.0,1., ;16 DEA,MDEA,loading, pco2
59.,1.77828,1.,0.,0., ;21 VECINFO#, MULTIPLY VALUE, # TIMES
1.,1.,1.,1.,1., ;26 RATE CONSTANT LOCATIONS
1.,1.,1.,1.,1., ;31 RATE CONSTANT LOCATIONS
1.,1.,1.,1.,1., ;36 RATE CONSTANT LOCATIONS
0.,3.,31.,32.,33., ;41 SET 41 TO ZERO IF NO SENSITIVITY
31.,32.,33.,34.,35., ;46 SENSITIVITY VALUES
1.,1.,1.,1.,1., ;51 RATE CONSTANT LOCATIONS
1.,1.,1.,3.16228,1., ;56 56=1 WT FRACTION, 57=1 DEA, ELSE MEA
1.,1.,1.,1.,1., ;61 RATE CONSTANT LOCATIONS
0.00000001,1.,1.,1.,1., ;66 LOADING OF BUFFER SPECIES
0.,0.001,0.0001,1.,1., ;71 .EQ.1 IF H2S,PH2S, KGA
8.,1.4,0.5,1.,1., ;76 # EL EXP, EXP AND COMPRESSION FACTORS
'CO2','DEA','H2O','HCO3-','CO3=', ; COMPONENT NAMES
'DEAH+','DEACOO-','H3O+','OH-','MDEA', ; COMPONENT NAMES
'MDEAH+','H2SO4','HSO4-','SO4=',' NU ', ; COMPONENT NAMES
' DEA/MDEA ',031090000, ;TITLE OF RUN, RUN NUMBER
C
C DOCUMENTATION
C
1 THRU 5:
    1: NUMBER OF DIFFERENTIAL EQUATIONS
    2: NUMBER OF CHEMICAL COMPONENTS
    3: NUMBER OF ELEMENTS
    4: NUMBER OF INTERNAL COLLOCATION POINTS PER ELEMENT
    5: PRINT CONTROL, IF >0, THEN MORE DETAILED PRINTOUT
6 THRU 10:
    6: = 1 FOR FIRST ORDER, -1 FOR DIFFERENTIAL-EQUATIONS, AND
        0 FOR FIRST ORDER ON DESORPTION ONLY
    7: REFERENCE DIFFUSION COEFFICIENT
    8: MASS TRANSFER COEFFICIENT (CM/SEC)
    9: MAXIMUM TIME STEP (ZERO FOR AUTO)
    10: DUMMY

```

---

Figure E.4 Input File RXN70.IN

---

```

11 THRU 15:
    11: RELATIVE TOLERANCE FOR DASSL
    12: ABSOLUTE TOLERANCE FOR DASSL
    13: TEMPERATURE (K)
16 THRU 20:
    16: PRIMARY/SECONDARY AMINE CONCENTRATION OR WEIGHT FRACTION
    17: TERTIARY AMINE CONCENTRATION OR WEIGHT FRACTION
    18: CO2 LOADING
    19: CO2 PARTIAL PRESSURE (ATM)
    20: TSTOP FOR INTEGRATION
21 THRU 25:  - MULTIPLE RUN MANAGEMENT -
    21: VECINFO VALUE TO MULTIPLY, ZERO IF NO MULTIPLE RUN
    22: MULTIPLY VALUE
    23: # TIMES FOR INCREMENT
26 THRU 30: DUMMY VARIABLES
31 THRU 35: DUMMY VARIABLES
36 THRU 40: DUMMY VARIABLES
41 THRU 50: SENSIVITY INFORMATION
    41: 1 IF SENSIVITY ANALYSIS, 0 IF NOT
    42: # OF VECINFO PARAMETERS TO VARY
43 THRU 50: VECINFO REFERENCE NUMBERS
51 THRU 55: DUMMY VARIABLES
56 THRU 60:
    56: SET TO 1 IF CONCENTRATION EXPRESSED IN WEIGHT FRACTION,
        ELSE 0
    57: SET TO 1 FOR DEA, ELSE MEA IS ASSUMED
    58: IF < 0, THEN PARTIAL PRESSURE IS MADE A MULTIPLE
        OF EQUILIBRIUM PARTIAL PRESSURE
    59: MULTIPLE OF EQUILIBRIUM PRESSURE IF VEC(58) < 0
61 THRU 65: DUMMY VARIABLES
66 THRU 70:
    66: LOADING OF BUFFER SPECIES
71 THRU 75:
    71: SET TO 1 TO ACTIVATE H2S BOUNDARY CONDITION
    72: PARTIAL PRESSURE OF H2S (ATM)
    73: KGA FOR H2S ABSORPTION
76 THRU 79:
    76: # ELEMENTS FOR EXPANSION PHASE OF MESH
    77: EXPANSION RATIO
    78: COMPRESSION RATIO
COMPONENT NAMES
TITLE, RUN #

```

---

Figure E.4 (Cont'd) Input File RXN70.IN

---

---

```

8,6,      NUMBER OF REACTIONS, NUMBER OF ELEMENTS
'co2','dea','h2o','hco3','co3',      ; SPECIES IDENTIFICATION
'deah','deacoo','h3o','oh','mdea',    ; SPECIES IDENTIFICATION
'mdeah','h2so4','hso4','so4','N',    ; SPECIES IDENTIFICATION
1,      ; NUMBER OF PHASES (NOT USED)
1,1,1,1,1,      ; PHASE DESIGNATION FOR EACH SPECIES (NOT USED)
1,1,1,1,1,      ; PHASE DESIGNATION FOR EACH SPECIES (NOT USED)
1,1,1,1,1,      ; PHASE DESIGNATION FOR EACH SPECIES (NOT USED)
0.,0.,      ; INERTS IN PHASE 1, PHASE 2
0,0,-2, 0,0, 0, 0,1,1,0, 0,0, 0, 0, STOICHIOMETRIC COEFF. FOR RXN 1
-1,0,-2, 1,0, 0, 0,1,0,0, 0,0, 0, 0, '' '' RXN 2
0,0,-1,-1,1, 0, 0,1,0,0, 0,0, 0, 0, '' '' RXN 3
0,1,-1, 0,0,-1, 0,1,0,0, 0,0, 0, 0, '' '' RXN 4
0,1,-1, 1,0, 0,-1,0,0,0, 0,0, 0, 0, '' '' RXN 5
0,0,-1, 0,0, 0, 0,1,0,1,-1,0, 0, 0, '' '' RXN 6
0,0,-1, 0,0, 0, 0,0,1,0, 0,1,-1, 0, '' '' RXN 7
0,0,-1, 0,0, 0, 0,0,1,0, 0,0, 1,-1, '' '' RXN 8
0,1,0,0,0,1, 1,0,0,0,0,0,0,0,0, ELEMENT MATRIX, DEA,C,O,H,MDEA,S
1,0,0,1,1,0, 1,0,0,0,0,0,0,0,0,
2,0,1,3,3,0, 2,1,1,0,0,4,4,4,
0,0,2,1,0,1,-1,3,1,0,1,2,1,0,
0,0,0,0,0,0, 0,0,0,1,1,0,0,0,
0,0,0,0,0,0, 0,0,0,0,0,1,1,1,
4,5,7,9,11,12, ; SPECIES FOR WHICH CHEMICAL POTENTIAL IS SET TO ZERO
1.,1., ; DUMMY, DUMMY
1.E-5,0.5, ; TOLERANCE, CONVERGENCE DAMPENING FACTOR

```

---

Figure E.5 Input File EQUIL.IN

---

```

0,0,0,
8,10,0,! number of experiments,data,and variable data
' dea rate data ', ! title
5,6,10,      ! reference for variable data
locations,loading,pco2,r abs
7,8,9, ! reference for standard deviations of said variables
2.,9.5e-02,313.15,2.9e-03,1.92e-02,3.7e-02,-0.05,-0.05,-0.1,1.2e-07,
2.,9.5e-02,313.15,2.4e-03,2.78e-02,3.8e-02,-0.05,-0.05,-0.1,1.2e-07,
2.,9.5e-02,313.15,2.1e-03,8.47e-02,4.0e-02,-0.05,-0.05,-0.1,1.0e-07,
2.,2.0e-01,298.15,1.0e-03,8.35e-02,1.8e-02,-0.05,-0.05,-0.1,7.6e-08,
2.,2.0e-01,298.15,1.3e-03,8.34e-02,1.8e-02,-0.05,-0.05,-0.1,7.8e-08,
2.,2.0e-01,298.15,7.7e-04,8.35e-02,1.9e-02,-0.05,-0.05,-0.1,7.3e-08,
2.,2.0e-01,298.2,2.3e-03,3.73e-03,4.0e-02,-0.05,-0.05,-0.1,1.8e-07,
2.,2.0e-01,298.2,2.3e-03,3.39e-03,4.0e-02,-0.05,-0.05,-0.1,1.8e-07,
2,
1.,1.e6,1.e10,-1.,
1.,30.,1.e3,1.,

```

---

Figure E.6 Input File PARM.IN

Table E.2 Definition of Chemical Systems

---

<u>number</u>	<u>system</u>
1	MDEA
2	DEA
3	MEA
12	DEA/MDEA
13	MEA/MDEA

---

For equilibrium simulation only, add 100 to the numerical designation.

---

---

\*\*\*\*\*

DEA/MDEA

31090000

EDDY DIFFUSIVITY THEORY W/ CONTINUATION

ENHANCEMENT FACTOR = 0.2843E+02

EXECUTION TIME = 0.5889E+01

RESPONSE PARAMETER IDID = 2

DIMENSIONLESS TIME = 0.1000E+01

MASS TRANSFER COEFFICIENT = 0.1000E-02 CM/SEC

ABSORPTION RATE = 0.5516E-06 MOLES/CM2\*SEC

BUFFER SPECIES FLUX RATE = -.5741E-21 MOLES/CM2\*SEC

CO2 PARTIAL PRESSURE = 0.1000E+01 ATM

CO2 EQUILIBRIUM PRESSURE = 0.2486E-02 ATM

DISTANCE

CONCENTRATION

	CO2	DEA	H2O	HCO3-	CO3=
1	0.0000E+00	0.1945E-01	0.2881E+00	0.3954E+02	0.2015E+00
3	0.4925E-02	0.1714E-01	0.2902E+00	0.3954E+02	0.2015E+00
5	0.1801E-01	0.1332E-01	0.3069E+00	0.3954E+02	0.2010E+00
7	0.2809E-01	0.1138E-01	0.3248E+00	0.3954E+02	0.2005E+00
9	0.3045E-01	0.1100E-01	0.3293E+00	0.3954E+02	0.2003E+00
11	0.4457E-01	0.9007E-02	0.3579E+00	0.3954E+02	0.1995E+00
13	0.6288E-01	0.7034E-02	0.3976E+00	0.3954E+02	0.1983E+00
15	0.6978E-01	0.6425E-02	0.4132E+00	0.3954E+02	0.1978E+00
17	0.7943E-01	0.5676E-02	0.4353E+00	0.3954E+02	0.1971E+00
19	0.1051E+00	0.4149E-02	0.4957E+00	0.3954E+02	0.1952E+00
21	0.1248E+00	0.3313E-02	0.5431E+00	0.3954E+02	0.1937E+00
23	0.1295E+00	0.3151E-02	0.5542E+00	0.3954E+02	0.1933E+00
25	0.1571E+00	0.2366E-02	0.6205E+00	0.3954E+02	0.1911E+00
27	0.1930E+00	0.1695E-02	0.7051E+00	0.3954E+02	0.1882E+00
29	0.2065E+00	0.1509E-02	0.7363E+00	0.3954E+02	0.1871E+00
31	0.2255E+00	0.1293E-02	0.7793E+00	0.3954E+02	0.1855E+00
33	0.2757E+00	0.8928E-03	0.8887E+00	0.3954E+02	0.1815E+00
35	0.3145E+00	0.6933E-03	0.9681E+00	0.3954E+02	0.1784E+00
37	0.3235E+00	0.6559E-03	0.9860E+00	0.3954E+02	0.1777E+00
39	0.3778E+00	0.4815E-03	0.1088E+01	0.3954E+02	0.1735E+00
41	0.4481E+00	0.3390E-03	0.1209E+01	0.3954E+02	0.1684E+00

---

Figure E.7 Output File RXN70.DAT

---

43	0.4746E+00	0.3006E-03	0.1252E+01	0.3954E+02	0.1665E+00	0.4162E-01
45	0.5117E+00	0.2562E-03	0.1308E+01	0.3954E+02	0.1640E+00	0.4408E-01
47	0.6102E+00	0.1744E-03	0.1446E+01	0.3954E+02	0.1575E+00	0.5033E-01
49	0.6861E+00	0.1334E-03	0.1541E+01	0.3954E+02	0.1527E+00	0.5493E-01
51	0.7039E+00	0.1256E-03	0.1563E+01	0.3954E+02	0.1517E+00	0.5598E-01
53	0.8102E+00	0.8876E-04	0.1684E+01	0.3954E+02	0.1452E+00	0.6221E-01
55	0.9481E+00	0.5723E-04	0.1832E+01	0.3954E+02	0.1369E+00	0.7026E-01
57	0.1000E+01	0.4835E-04	0.1886E+01	0.3954E+02	0.1337E+00	0.7336E-01

## DISTANCE

## CONCENTRATION

	DEAH+	DEACOO-	H3O+	OH-	MDEA	
1	0.0000E+00	0.1426E+01	0.1215E+01	0.9107E-08	0.7402E-05	0.2459E-02
3	0.4925E-02	0.1425E+01	0.1214E+01	0.9037E-08	0.7460E-05	0.2473E-02
5	0.1801E-01	0.1417E+01	0.1205E+01	0.8494E-08	0.7936E-05	0.2584E-02
7	0.2809E-01	0.1408E+01	0.1196E+01	0.7977E-08	0.8451E-05	0.2699E-02
9	0.3045E-01	0.1406E+01	0.1194E+01	0.7855E-08	0.8582E-05	0.2727E-02
11	0.4457E-01	0.1392E+01	0.1179E+01	0.7158E-08	0.9418E-05	0.2903E-02
13	0.6288E-01	0.1373E+01	0.1158E+01	0.6353E-08	0.1061E-04	0.3137E-02
15	0.6978E-01	0.1365E+01	0.1150E+01	0.6080E-08	0.1109E-04	0.3225E-02
17	0.7943E-01	0.1354E+01	0.1138E+01	0.5725E-08	0.1177E-04	0.3347E-02
19	0.1051E+00	0.1325E+01	0.1107E+01	0.4919E-08	0.1370E-04	0.3662E-02
21	0.1248E+00	0.1302E+01	0.1082E+01	0.4412E-08	0.1528E-04	0.3892E-02
23	0.1295E+00	0.1297E+01	0.1076E+01	0.4306E-08	0.1566E-04	0.3944E-02
25	0.1571E+00	0.1265E+01	0.1042E+01	0.3750E-08	0.1798E-04	0.4240E-02
27	0.1930E+00	0.1223E+01	0.9977E+00	0.3193E-08	0.2111E-04	0.4586E-02
29	0.2065E+00	0.1208E+01	0.9815E+00	0.3020E-08	0.2232E-04	0.4705E-02
31	0.2255E+00	0.1188E+01	0.9591E+00	0.2804E-08	0.2404E-04	0.4862E-02
33	0.2757E+00	0.1135E+01	0.9020E+00	0.2349E-08	0.2869E-04	0.5230E-02
35	0.3145E+00	0.1096E+01	0.8606E+00	0.2084E-08	0.3235E-04	0.5473E-02
37	0.3235E+00	0.1088E+01	0.8513E+00	0.2030E-08	0.3321E-04	0.5525E-02
39	0.3778E+00	0.1038E+01	0.7978E+00	0.1756E-08	0.3840E-04	0.5805E-02
41	0.4481E+00	0.9803E+00	0.7347E+00	0.1492E-08	0.4519E-04	0.6103E-02
43	0.4746E+00	0.9600E+00	0.7126E+00	0.1411E-08	0.4776E-04	0.6200E-02
45	0.5117E+00	0.9329E+00	0.6829E+00	0.1312E-08	0.5137E-04	0.6324E-02
47	0.6102E+00	0.8672E+00	0.6109E+00	0.1104E-08	0.6108E-04	0.6601E-02

---

Figure E.7 (Cont'd) Output File RXN70.DAT

---

49	0.6861E+00	0.8215E+00	0.5607E+00	0.9807E-09	0.6874E-04	0.6777E-02
51	0.7039E+00	0.8114E+00	0.5495E+00	0.9554E-09	0.7056E-04	0.6814E-02
53	0.8102E+00	0.7537E+00	0.4855E+00	0.8233E-09	0.8188E-04	0.7015E-02
55	0.9481E+00	0.6840E+00	0.4079E+00	0.6872E-09	0.9810E-04	0.7235E-02
57	0.1000E+01	0.6586E+00	0.3794E+00	0.6426E-09	0.1049E-03	0.7310E-02

	DISTANCE	CONCENTRATION			
		MDEAH+	H2SO4	HSO4~	SO4=
1	0.0000E+00	0.6138E-02	0.1971E-23	0.2346E-14	0.4932E-07
3	0.4925E-02	0.6125E-02	0.1941E-23	0.2328E-14	0.4932E-07
5	0.1801E-01	0.6014E-02	0.1715E-23	0.2188E-14	0.4932E-07
7	0.2809E-01	0.5899E-02	0.1512E-23	0.2055E-14	0.4932E-07
9	0.3045E-01	0.5871E-02	0.1467E-23	0.2023E-14	0.4932E-07
11	0.4457E-01	0.5695E-02	0.1218E-23	0.1844E-14	0.4932E-07
13	0.6288E-01	0.5461E-02	0.9591E-24	0.1636E-14	0.4932E-07
15	0.6978E-01	0.5373E-02	0.8786E-24	0.1566E-14	0.4932E-07
17	0.7943E-01	0.5251E-02	0.7790E-24	0.1475E-14	0.4932E-07
19	0.1051E+00	0.4936E-02	0.5750E-24	0.1267E-14	0.4932E-07
21	0.1248E+00	0.4706E-02	0.4626E-24	0.1136E-14	0.4932E-07
23	0.1295E+00	0.4654E-02	0.4406E-24	0.1109E-14	0.4932E-07
25	0.1571E+00	0.4358E-02	0.3342E-24	0.9659E-15	0.4932E-07
27	0.1930E+00	0.4012E-02	0.2423E-24	0.8224E-15	0.4932E-07
29	0.2065E+00	0.3893E-02	0.2167E-24	0.7778E-15	0.4932E-07
31	0.2255E+00	0.3736E-02	0.1869E-24	0.7223E-15	0.4932E-07
33	0.2757E+00	0.3368E-02	0.1312E-24	0.6051E-15	0.4932E-07
35	0.3145E+00	0.3125E-02	0.1032E-24	0.5368E-15	0.4932E-07
37	0.3235E+00	0.3073E-02	0.9792E-25	0.5229E-15	0.4932E-07
39	0.3778E+00	0.2793E-02	0.7324E-25	0.4522E-15	0.4932E-07
41	0.4481E+00	0.2495E-02	0.5288E-25	0.3842E-15	0.4932E-07
43	0.4746E+00	0.2398E-02	0.4735E-25	0.3636E-15	0.4932E-07
45	0.5117E+00	0.2274E-02	0.4092E-25	0.3380E-15	0.4932E-07
47	0.6102E+00	0.1997E-02	0.2895E-25	0.2843E-15	0.4932E-07
49	0.6861E+00	0.1821E-02	0.2286E-25	0.2526E-15	0.4932E-07
51	0.7039E+00	0.1784E-02	0.2169E-25	0.2461E-15	0.4932E-07
53	0.8102E+00	0.1583E-02	0.1611E-25	0.2121E-15	0.4932E-07
55	0.9481E+00	0.1363E-02	0.1122E-25	0.1770E-15	0.4932E-07
57	0.1000E+01	0.1288E-02	0.9815E-26	0.1655E-15	0.4932E-07

---

Figure E.7 (Cont'd) Output File RXN70.DAT



---

	DISTANCE	ACTIVITY COEFFICIENT				
		CO2	DEA	H2O	HCO3-	CO3=
57	0.1000E+01	0.1239E+01	0.1781E+00	0.9966E+00	0.4774E+00	0.1200E+00

	DISTANCE	ACTIVITY COEFFICIENT				
		DEAH+	DEACOO-	H3O+	OH-	MDEA
57	0.1000E+01	0.5927E+00	0.8615E+00	0.4803E+00	0.4495E+00	0.1145E+01

	DISTANCE	ACTIVITY COEFFICIENT			
		MDEAH+	H2SO4	HSO4-	SO4=
57	0.1000E+01	0.4677E+00	0.1145E+01	0.4495E+00	0.1200E+00

I CHRG CHECK  
 1 0.2828E-07  
 57 -.4999E-07

#### PSEUDO-FIRST ORDER AT INTERFACE

##### % CONTRIBUTIONS OF REACTIONS

DEA	MDEA	OH
80.680	0.010	0.028

PSEUDO-FIRST ORDER RATE CONSTANT = 0.69545E+03

HATTA NUMBER = 0.88573E+02

#### FIRST ORDER BASED ON BULK

##### % CONTRIBUTIONS OF REACTIONS

DEA	MDEA	OH
80.696	0.001	0.020

PSEUDO-FIRST ORDER RATE CONSTANT = 0.13689E+05

HATTA NUMBER = 0.39296E+03

---

Figure E.7 (Cont'd) Output File RXN70.DAT

---

---

```

*****
DEA/MDEA                                     31090000

EDDY DIFFUSIVITY THEORY W/ CONTINUATION
ENHANCEMENT FACTOR      = 0.2843E+02
EXECUTION TIME          = 0.5889E+01
RESPONSE PARAMETER IDID = 2
DIMENSIONLESS TIME      = 0.1000E+01
MASS TRANSFER COEFFICIENT = 0.1000E-02 CM/SEC
ABSORPTION RATE         = 0.5516E-06 MOLES/CM2*SEC
BUFFER SPECIES FLUX RATE = -.5741E-21 MOLES/CM2*SEC
CO2 PARTIAL PRESSURE    = 0.1000E+01 ATM
CO2 EQUILIBRIUM PRESSURE = 0.2486E-02 ATM

INPUT DATA:
      NREALEQ    NEL    NCOL    NINFO
        7        8        6       80

VECTOR VECINFO
0.70000E+01  0.14000E+02  0.80000E+01  0.60000E+01  0.00000E+00
0.00000E+00  0.10000E-04  0.10000E-02  0.50000E+00  0.10000E+01
0.10000E-02  0.10000E-05  0.31315E+03  0.00000E+00  0.10000E+01
0.30000E+00  0.10000E-02  0.20000E+00  0.10000E+01  0.10000E+01
0.59000E+02  0.17783E+01  0.10000E+01  0.10000E-01  0.00000E+00
0.40200E+05  0.10000E-05  0.10000E+00  0.10000E+01  0.80000E+01
0.10000E+01  0.30000E+02  0.55360E+04  0.18500E+05  0.46870E+04
0.10000E+01  0.10000E+01  0.10000E+01  0.10000E+01  0.10000E+01
0.00000E+00  0.30000E+01  0.31000E+02  0.32000E+02  0.33000E+02
0.31000E+02  0.32000E+02  0.33000E+02  0.34000E+02  0.35000E+02

0.53400E-01  0.58880E+04  0.00000E+00  0.00000E+00  0.10000E+01
0.10000E+01  0.10000E+01  0.10000E+01  0.31623E+01  0.10000E+01
0.36000E+04  0.13700E+04  0.10000E+01  0.10000E+01  0.10000E+01
0.10000E-07  0.10000E+01  0.10000E+01  0.10000E+01  0.10000E+01
0.00000E+00  0.10000E-02  0.10000E-03  0.10000E+01  0.10000E+01
0.80000E+01  0.14000E+01  0.50000E+00  0.10000E+01  0.10000E+01

```

---

Figure E.8. Output File RXN70.OUT

---



---

VECTOR OF INTERFACE CONCENTRATIONS

0.19450E-01	0.28813E+00	0.39538E+02	0.20154E+00	0.78054E-02
0.14261E+01	0.12150E+01	0.91071E-08	0.74023E-05	0.24595E-02
0.61384E-02	0.19711E-23	0.23458E-14	0.49322E-07	

VECTOR OF BULK CONCENTRATIONS

0.48348E-04	0.18857E+01	0.39538E+02	0.13367E+00	0.73361E-01
0.65856E+00	0.37935E+00	0.64265E-09	0.10490E-03	0.73104E-02
0.12875E-02	0.98149E-26	0.16553E-15	0.49322E-07	

VECTOR OF DIFFUSION COEFFICIENTS

0.11281E-04	0.44030E-05	0.43703E-05	0.43703E-05	0.43703E-05
0.43703E-05	0.43703E-05	0.43703E-05	0.43703E-05	0.43703E-05
0.43703E-05	0.43703E-05	0.43703E-05	0.43703E-05	

VECTOR OF EQUILIBRIUM CONSTANTS

0.12726E-06	0.18876E+05	0.11683E+04	0.19446E+01	0.22595E+08
0.22595E+08	0.13906E-05	0.86065E-07	0.86721E-05	0.93751E-17
0.18082E-15	0.15040E-13	0.00000E+00	0.00000E+00	0.00000E+00

VECTOR OF RATE CONSTANTS

0.17644E+03	0.76935E+05	0.11133E+05	0.61585E+00	0.00000E+00
0.58883E+05	0.00000E+00	0.00000E+00	0.00000E+00	0.00000E+00
0.00000E+00	0.00000E+00	0.00000E+00	0.00000E+00	0.00000E+00

---

Figure E.8 (Cont'd) Output File RXN70.OUT

---



---

## **E.6 Selection of Chemical System**

If a data regression or data run is performed using the file 'PARM.IN', the first number on each line designates the chemical system (as per Table E.2) and the type of run performed. If specifying the simulation based on the input file 'RXN70.IN', MDEA is always assumed for the tertiary amine, and DEA or MEA can be chosen based upon the value of VECINFO(57) (see Figure E.4).

## **E.7 Execution of Mass-Transfer Simulation**

### ***E.7.1 One Case Only***

Set the first row of values in 'PARM.IN' equal to zero. This file will then be ignored and the file 'RXN70.IN' will be read for the parameter values.

### ***E.7.2 Multiple Cases***

#### ***- consistent parameter variation***

Same as for a single case, except now set VECINFO(23) equal to a value greater than unity. VECINFO(21) will select the input variable to be consistently multiplied by VECINFO(22).

#### ***- from datafile***

Set up the input file 'PARM.IN' as if running a parameter estimation, then set the third value on the first row (number of variables subject to error) equal to 0.

## **E.8 Execution of Equilibrium Simulation**

If running from the datafile, use system designations > 100 (see Table E.2). If running a regular simulation, then choose pseudo-first order (VECINFO(6)=1). In this case, the differential-equation based mass transfer model will not be activated.

### E.9 Nonlinear Parameter Estimation of Equilibrium and Rate Parameters

The file 'PARM.IN' should be set up as described above. The rate constants are defined in subroutine PROP70, while the equilibrium parameters are defined in subroutine DATACT (both located in the PROP70 file). The variables are defined by RPARM(1:N), where N is the number of parameters to be estimated. In the case of rate constant estimation, for example, set the appropriate rate constant, VECINFO(I), equal to RPARM(J). The vector PAR is globally defined in RXN.INC and holds the current parameter estimates.

**Appendix F**  
**SRP Annual Report**  
**Modelling and Experimental Study of CO<sub>2</sub>**  
**Absorption into Aqueous Amines**

When CO<sub>2</sub> absorbs into an aqueous solution containing an alkanolamine, both its solubility and absorption rate are increased due to its reactions with the amine and hydroxide. These properties of alkanolamine solutions allow them to remove CO<sub>2</sub> from process streams down to very low partial pressures. Therefore, alkanolamines are often used in stripper/regenerator units in hydrogen and ammonia manufacture and natural gas purification. The alcohol group on the amine is beneficial since it increases the solubility of the amine in water. The alcohol group also lowers the pK<sub>a</sub> of the amine, otherwise, the reaction would be nearly irreversible and the stripping operation would be quite difficult. In general, the reaction of CO<sub>2</sub> with primary and secondary amines is fast, with a high exothermic heat reaction; while the reaction with tertiary amines is slower, with a lower exothermic heat of reaction. Previously, amines such as the primary amine MEA (monoethanolamine) and the tertiary amine MDEA (methyldiethanolamine) have been used to remove CO<sub>2</sub>. Recently, however, mixed amine systems have been used, combining a small amount of primary or secondary amine to a tertiary amine system. The result is a promoted tertiary amine system which significantly enhances absorption, but also has a lower net heat of absorption/reaction, which must be supplied in the stripping phase of the operation (Kohl and Riesenfeld, 1985).

The absorption of CO<sub>2</sub> into an aqueous system can be described by several theories which approximate the effect of the liquid-phase fluid mechanics on mass transfer. The steady-state theories we have used are the film theory, a simplified eddy diffusivity theory, and an approximation to surface renewal theory due to Chang and Rochelle (1982). Higbie's penetration and Danckwert's surface renewal theories are

the unsteady-state theories studied. Using the differential material balance equations, one calculates the enhancement factor for  $\text{CO}_2$  (rate of absorption with chemical reaction to that without reaction) given a reaction rate of  $\text{CO}_2$  with an amine. The steady-state theories require solving ordinary differential equations describing diffusion with reaction while the unsteady-state theories require the solution of parabolic partial differential equations. However, the unsteady-state theories are considered to be more accurate than film theory for gas absorption into a turbulent liquid (Danckwerts, 1970).

Using orthogonal collocation on finite elements (Villadsen and Stewart, 1967), the equations for the steady-state theories are transformed into a larger set of nonlinear algebraic equations. For the unsteady-state theories, a system of coupled differential/algebraic equations is obtained. Initially, it may seem that the steady-state equations are easier to solve; however, if one cannot provide good initial guesses, then the solution of the nonlinear algebraic equations is quite difficult. In fact, we often solve the steady-state theories by using a continuation method, which essentially transforms the problem into an unsteady-state problem (e.g. Vickery et al., 1988). We then solve both the steady- and unsteady-state formulations using a computer program developed for differential/algebraic equations (Petzold, 1982).

It is of interest to see how well the various mass transfer theories compare in the prediction of the effect of reaction on gas absorption. If we can show that certain steady-state theories provide results comparable to surface renewal theory, then we may use the steady-state theories for experimental data interpretation and industrial equipment design, with less computation time than the unsteady-state theories. Figure F.1 shows a plot of the enhancement factor for gas absorption with a second-order, reversible reaction as a function of the Hatta number, which is essentially the ratio of chemical reaction rate to the mass transfer rate. Note that all theories, except for film theory, agree quite well over the entire range of conditions.

We have regressed the equilibrium and rate data for MDEA, DEA (diethanolamine) and mixtures of the two. We are also modelling  $\text{CO}_2$  absorption into and desorption from MEA/MDEA mixtures. We are using the Electrolyte-NRTL model (Chen and Evans, 1986) to obtain the activity coefficients for the liquid phase species, and a very efficient algorithm to obtain equilibrium compositions (Smith and Missen, 1988). Using the Electrolyte-NRTL model allows for data interpretation over a wide

range of conditions, including desorption, where activity coefficients vary so much that concentration based equilibrium constants are inadequate.

Figures F.2 and F.3 show typical results of the rate data regression analysis. In these cases, we have modelled the reaction rate of CO<sub>2</sub> with MDEA using a simplified mechanism and a more complex mechanism incorporating the hydroxide ion. These results show that the generally accepted rate expression does not account for a distinct trend in the experimental data, namely, the increase in the apparent MDEA-CO<sub>2</sub> reaction rate as a function of the increasing hydroxide concentration. Primary and secondary amine contaminants do not explain the trend, as has been suggested in the literature. Concentration profiles shown in Figure F.4 indicate the significant depletion of the fast reaction contaminant MMEA (methyl- monoethanolamine) even at the relatively low pressure of 4.4 kPa. Rate constants for DEA and the mixed amine system DEA/MDEA were also regressed from experimental data. The results indicate definite kinetic interaction between DEA and MDEA, contrary to the results for MEA/MDEA.

This work has also included the prediction of amine performance under practical conditions. Under most all conditions of industrial interest, the enhancement factor for MDEA is near one, and the pseudo-first order approximation is valid. Mixed amine systems are much more difficult, however. Typical results are shown in Figure F.5, where the model is used to calculate the enhancement factor for CO<sub>2</sub> absorption into DEA/MDEA mixtures and MEA/MDEA mixtures. These results indicate that the addition of either MEA or DEA in small amounts greatly increases the absorption rate of CO<sub>2</sub>, however, the MEA/MDEA mixture is much more sensitive to loading.



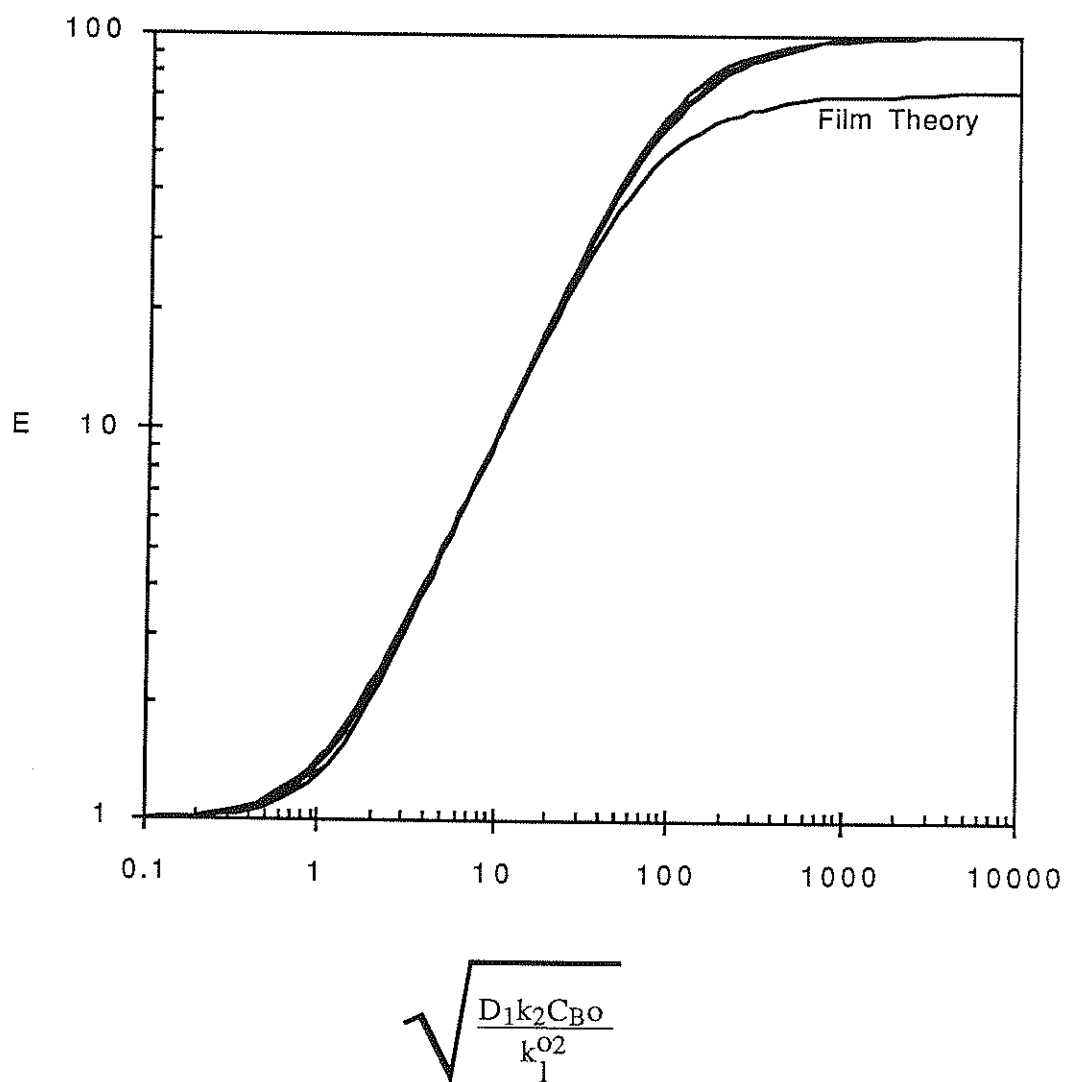
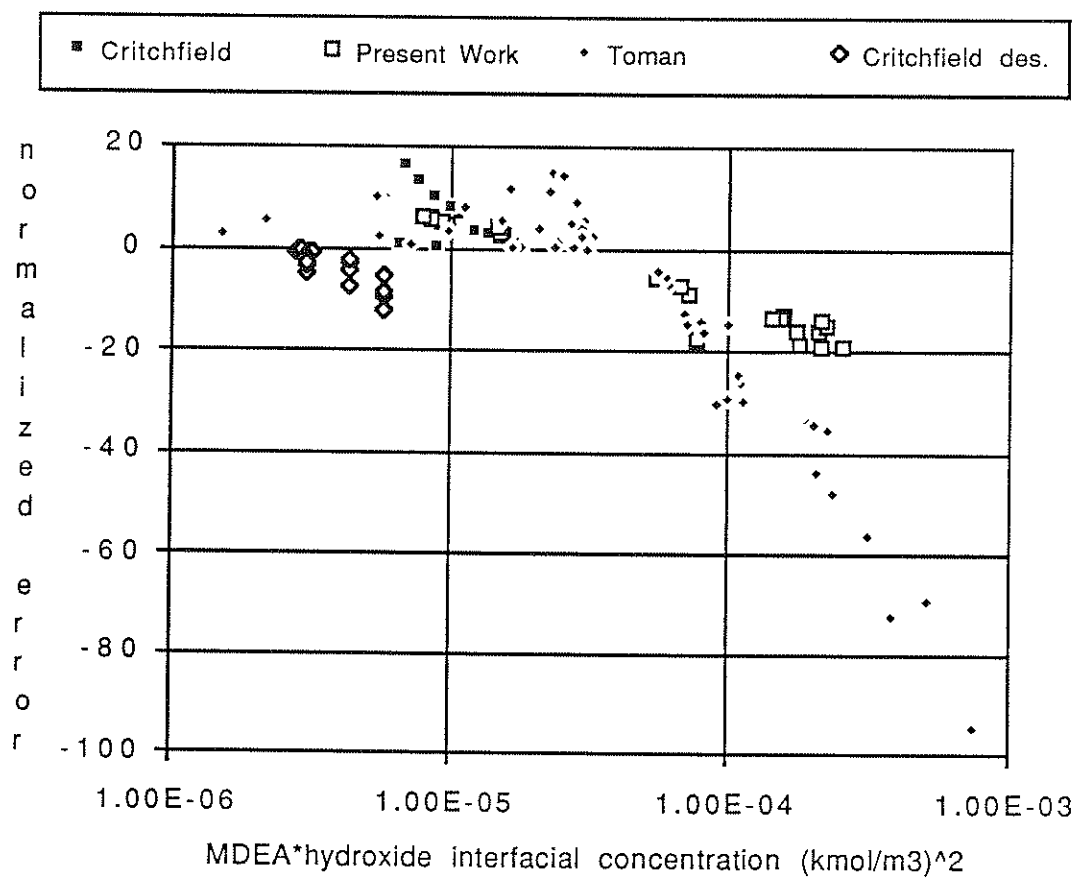


Figure F.1 Enhancement Factor for a Second-Order, Reversible Reaction,  $A + B \rightleftharpoons C + D$ .  $K_{eq} = 350$ ,  $D_B = D_C = D_D = 0.5D_A$ ,  $C_{B,bulk}/C_{A,int} = 200$ ,  $C_{A,bulk} = C_{B,bulk} = C_{C,bulk} = 0$

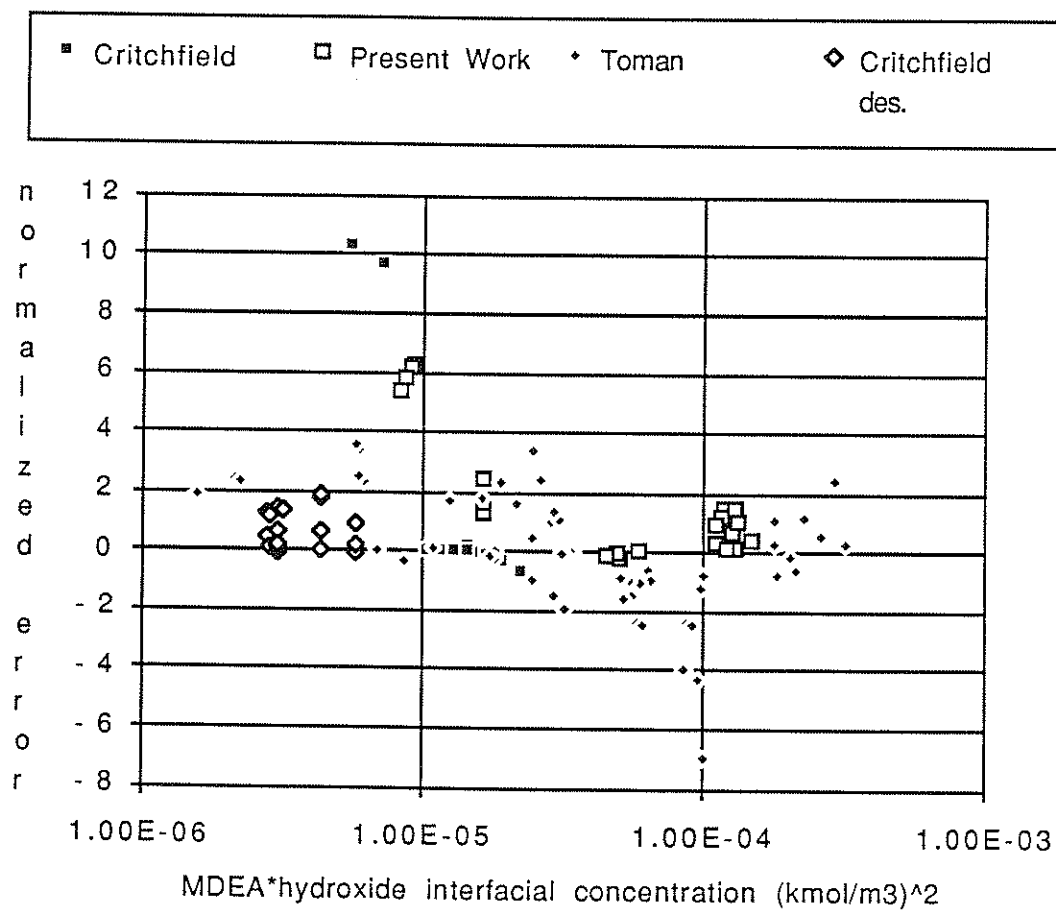


---

Figure F.2 Fit of MDEA High- and Low-Driving Force Data with the Simplified Kinetic Mechanism (CO<sub>2</sub>-MDEA-H<sub>2</sub>O Term Only)

---

---



---

Figure F.3    Fit of MDEA High- and Low-Driving Force Data with the Hydroxide Kinetic Mechanism

---

---

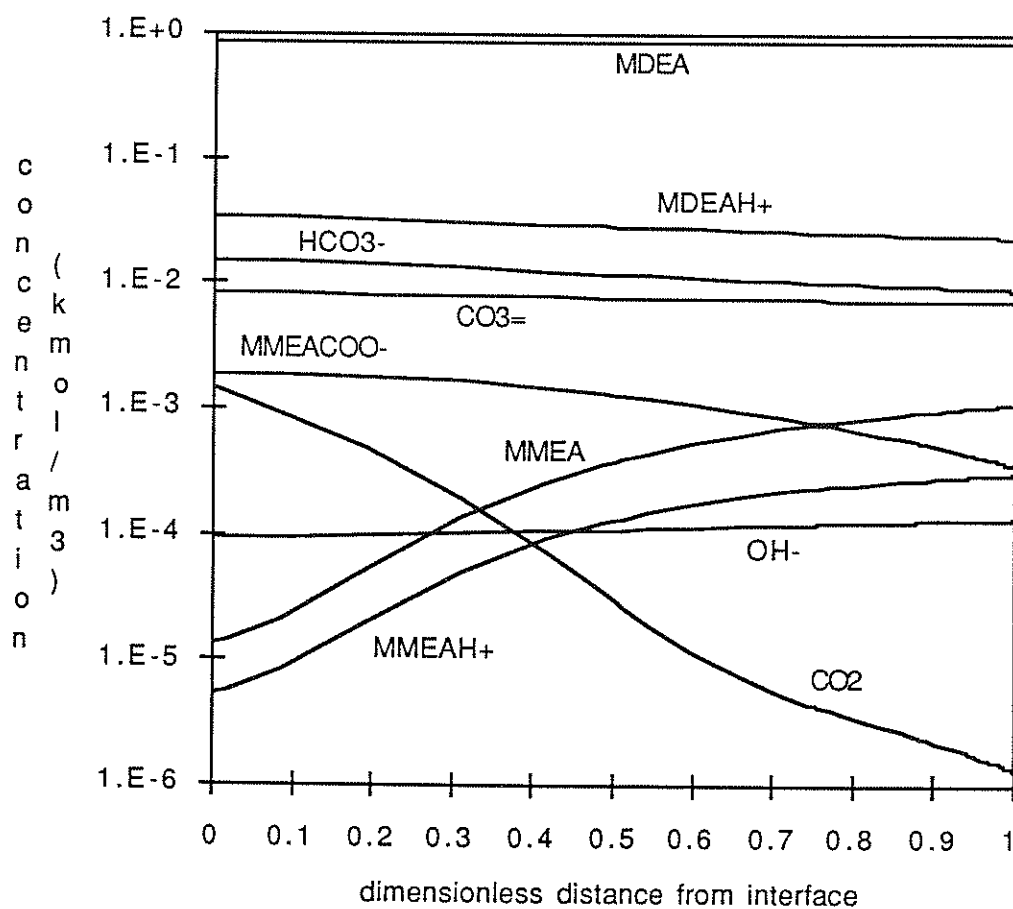


Figure F.4 Concentration Profiles for Low Driving Force  $\text{CO}_2$  Absorption into 10.6 wt% MDEA, 298K,  $\text{CO}_2$  loading = 0.018,  $P_{\text{CO}_2}$  = 4.4 kPa.

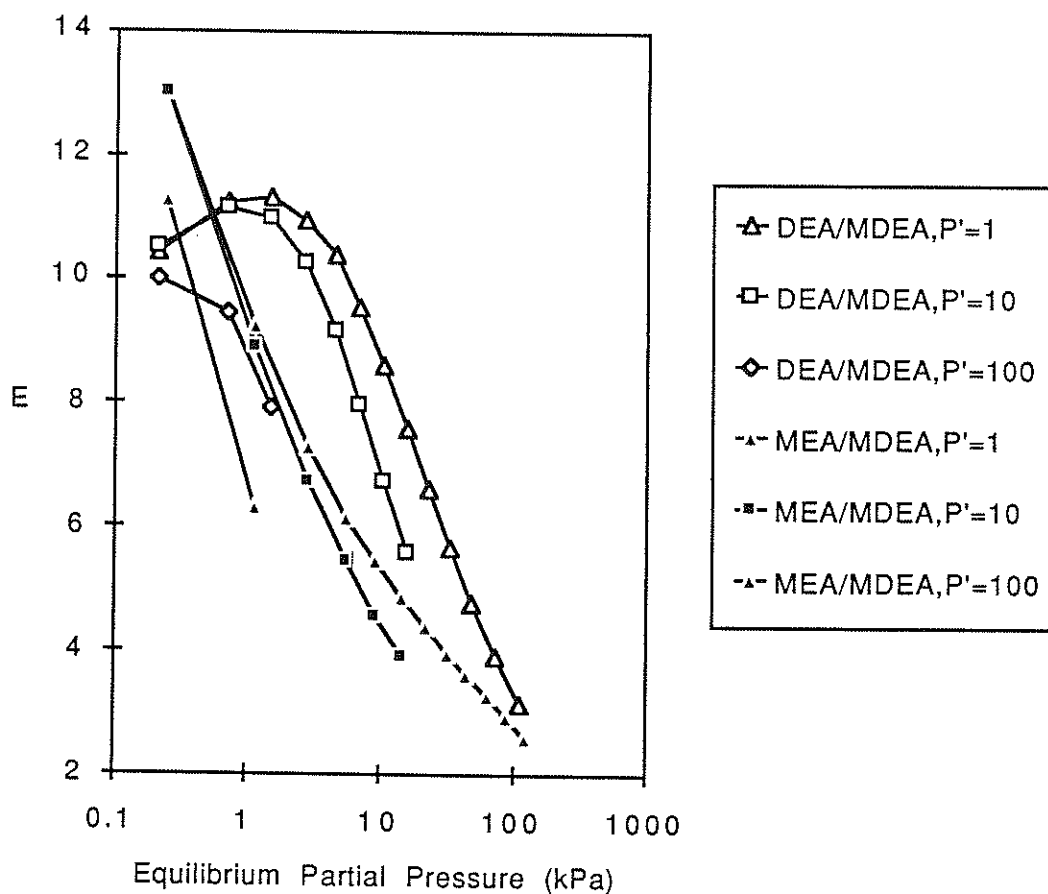


Figure F.5 Enhancement Factor for 10wt% DEA/40wt% MDEA (mole ratio = 0.28) and 5wt% MEA/45wt%MDEA (mole ratio = 0.22) for Varying Ratios of Actual to Equilibrium Partial Pressure ( $P' = P/P^*$ ). Specific Conditions: 313K,  $k_1^0 = 10^{-4}$  m/sec.

### References Cited

- Chang, C.-S., and G.T. Rochelle, "Mass Transfer Enhanced by Equilibrium Reactions," *Ind. Eng. Chem. Fundam.*, **21**, 379, 1982.
- Chen, C.-C., and L.B. Evans, "A Local Composition Model for the Excess Gibbs Energy of Aqueous Electrolyte Systems," *AIChE J.*, **32**(3), 444, 1986.
- Critchfield, J.E., *CO<sub>2</sub> Absorption/Desorption in Methyldiethanolamine Solutions Promoted with Monoethanolamine and Diethanolamine: Mass Transfer and Reaction Kinetics*, PhD. dissertation, The University of Texas at Austin, 1988.
- Danckwerts, P.V., *Gas-Liquid Reactions*, McGraw-Hill, New York, 1970.
- Kohl, A.L., and F. C. Riesenfeld, *Gas Purification*, 4th ed., Gulf Publishing Co., Houston, 1985.
- Petzold, L.R., "A Description of DASSL: A Differential/Algebraic System Solver," Sandia Report, SAND82-8637, 1982.
- Smith, W.R., and R.W. Missen, "Strategies for Solving the Chemical Equilibrium Problem and an Efficient Microcomputer-Based Algorithm," *Can. J. Chem. Eng.*, **66**, 591, 1988.
- Toman, J.J., Ph.D. dissertation, The University of Texas at Austin, Austin, TX, 1990.
- Vickery, D.J., J.J. Ferrari, and R. Taylor, "An 'Efficient' Continuation Method for the Solution of Difficult Equilibrium State Separation Process Problems," *Comput. Chem. Engng.*, **12**(1), 99, 1988.
- Villadsen, J.V., Stewart, W.E., "Solution of Boundary-Value Problems by Orthogonal Collocation," *Chem. Eng. Sci.*, **22**, 1483, 1967.

## Nomenclature

$\alpha$	thermodynamic activity
$\underline{\underline{A}}$	matrix of first derivative collocation weights
$\underline{\underline{B}}$	matrix of second derivative collocation weights
$B^0$	bulk concentration of liquid-phase reactant
$C$	concentration of an arbitrary species
$C_{ij}$	concentration of $i$ th species at point $j$
$D$	diffusion coefficient
$d$	dimensionless diffusion coefficient, $D/D_1$
$E$	enhancement factor, $R/R_{\text{phys}}$
$E_a$	activation energy
$\text{erf}$	error function
$\mathcal{F}$	Faraday's constant,
$G$	Gibb's free energy
$H$	Henry's Constant
$H_a$	Hatta number
$I$	current flux
$I_c$	concentration-based ionic strength
$I_x$	mole fraction-based ionic strength
$J$	molar flux
$K$	equilibrium constant
$k$	Boltzmann's constant, $1.381 \times 10^{-23} \text{ J K}^{-1}$ (volt-coulomb $\text{K}^{-1}$ )
$k$	rate constant
$K_a$	activity-based equilibrium constant
$k_a$	activity-based rate constant
$K_c$	concentration based equilibrium constant
$k_c$	concentration based rate constant
$k_g$	gas-phase mass transfer coefficient
$k_l^0$	liquid-phase mass transfer coefficient without reaction
$M$	dimensionless reaction rate
$N$	number of components
$n_c$	number of components
$n_{\text{exp}}$	number of experiments

$n_p$	number of products in a chemical reaction
$n_r$	number of reactants in a chemical reaction
$n_{\text{rex}}$	number of reactions
$n_{\text{var}}$	number of variables subject to error
$P$	pressure
$R$	absorption flux rate
$\mathcal{R}$	net production rate of a species
$r$	dimensionless spatial distance
$R_{\text{gas}}$	gas constant
$R_{\text{phys}}$	absorption rate with no chemical reaction
$r_i$	rate of reaction $i$
$s$	surface renewal rate, $\text{sec}^{-1}$
$s_{ik}$	standard deviation associated with $z_{ik}$
$T$	temperature
$t$	time
$x$	distance from interface
$X$	$x_i Z_i$ for ions, $x_i$ for molecules
$z$	charge number of a species
$Z$	absolute value of charge number of a species
$z_{ik}$	variable $k$ subject to error in experiment $i$
$\mathcal{R}_i$	net production rate of species $i$

### Greek Symbols

$\alpha$	relative standard deviation of parameter estimate
$\beta$	nonequilibrium rate parameter
$\delta$	film thickness
$\varepsilon$	eddy diffusivity parameter
$\phi$	fugacity coefficient, functional notation
$\Phi$	electrical potential, volt
$\gamma$	activity coefficient
$\vartheta$	stoichiometric coefficient
$\mu$	chemical potential
$\mu^0$	reference chemical potential



$v_{ij}$	stoichiometric coefficient of species $i$ in reaction $j$
$\theta$	contact time
$\sigma$	standard deviation of parameter estimate
$\tau$	Electrolyte-NRTL binary interaction parameter
$\omega$	parameter cross-correlation coefficient
$\nabla$	one dimensional differentiation operation, $\frac{\partial}{\partial x}$
$\nabla^2$	one dimensional Laplacian operator, $\frac{\partial^2}{\partial x^2}$

### Subscripts

$l$	absorbing chemical species
$=$	matrix notation
$-$	vector notation
$b$	base designation

### Superscripts

$'$	time derivative
$*$	corresponds to an interface concentration
$o$	corresponds to a bulk phase concentration
$ex$	excess property
$sr$	short-range interaction
$lr$	long-range interaction

## Bibliography

- Al-Ghawwas, H.A., G. Ruiz-Ibanez, and O.C. Sandall, "Absorption of Carbonyl Sulfide in Aqueous Methyldiethanolamine," *Chem. Eng. Sci.*, **44**(3), 631, 1989.
- Allgower, E., and K. Georg, "Simplicial and Continuation Methods for Approximating Fixed Points and Solutions to Systems of Equations," *SIAM Rev.*, **22**(1), 28, 1980.
- Alper, E., "Reaction Kinetics of Carbonyl Sulfide with Aqueous Diglycolamine by the Stopped Flow Technique," Presented at the 1989 Spring National AIChE Meeting, April 2-6, 1989, Houston, TX.
- Alper, E., and B. Abu-Sharkh, "Performance of an RTL Contactor for Gas-Liquid Systems: Effective Interfacial Area and Volumetric Mass Transfer Coefficient by Oxidation of Sodium Sulphite Solution," *Chem. Eng. Technol.*, **12**, 15, 1989.
- Alvarez-Fuster, C., N. Midoux, A. Laurent, and J.C. Charpentier, "Chemical Kinetics of the Reaction of Carbon Dioxide with Amines in Pseudo m-nth Order Conditions in Aqueous and Organic Solutions," *Chem. Eng. Sci.*, **35**, 1717, 1980.
- Alvarez-Fuster, C., N. Midoux, A. Laurent, and J.C. Charpentier, "Chemical Kinetics of the Reaction of CO<sub>2</sub> with Amines in Pseudo m-nth Order Conditions in Polar and Viscous Organic Solutions," *Chem. Eng. Sci.*, **36**(9), 1513, 1980.
- Anderson, M.L., and R.K. Boyd, "Nonequilibrium Thermodynamics in Chemical Kinetics," *Can. J. Chem.*, **49**, 1001, 1971.
- Andrew, S.P.S., "Rejuvenation and Renewal," *Chem. Eng. Sci.*, **38**(1), 9, 1983.
- Andrews, F.C., "Macroscopic Approach to Reciprocal Relations in Irreversible Thermodynamics," *Ind. Eng. Chem. Fundam.*, **6**(1), 48, 1967.
- Asher, W., and J. F. Pankow, "Direct Observation of Concentration Fluctuations Close to a Gas-Liquid Interface," *Chem. Eng. Sci.*, **44**(6), 1451, 1989.
- Asolekar, S.R., D. Desai, P.K. Deshpande, and R. Kumar, "Effect of Surface Resistance on Gas Absorption Accompanied by a Chemical Reaction in a Gas-Liquid Contactor," *Can. J. Chem. Eng.*, **63**, 336, 1985.
- Aspen Technology, Inc., *ASPEN PLUS™ Data Regression Manual*, Cambridge, MA, 1985.
- Astarita, G., "Carbon Dioxide Absorption in Aqueous Monoethanolamine Solutions," *Chem. Eng. Sci.*, **16**, 202, 1961.
- Astarita, G., "Gas Absorption with First-Order Chemical Reaction in a Spherical Liquid Film," *Chem. Eng. Sci.*, **17**, 708, 1962.

- Astarita, G., "Modern Thermodynamics in Chemical Engineering and Chemistry - I," *La Chimica E L'Industria*, **57**(10), 680, 1975.
- Astarita, G., "A Note on Homogeneous and Heterogeneous Chemical Equilibria," *Chem. Eng. Sci.*, **31**, 1225, 1976.
- Astarita, G., "On the Principle of Microscopic Reversibility," *Quad. Chim. Ital.*, **14**(1-2), 1978.
- Astarita, G., and D.W. Savage, "Gas Absorption and Desorption with Reversible Instantaneous Chemical Reaction," *Chem. Eng. Sci.*, **35**, 1755, 1980.
- Astarita, G., and D.W. Savage, "Simultaneous Absorption with Reversible Instantaneous Chemical Reaction," *Chem. Eng. Sci.*, **37**(5), 677, 1982.
- Astarita, G., D.W. Savage, and A. Bisio, *Gas Treating with Chemical Solvents*, John Wiley & Sons, New York, 1983.
- Austgen, D.M., *A Model of Vapor-Liquid Equilibria for Acid Gas-Alkanolamine-Water Systems*, Ph.D. dissertation, The University of Texas at Austin, 1989.
- Austgen, D.M., G.T. Rochelle, and C.-C. Chen, "Modeling the Solubility of  $H_2S$  and  $CO_2$  in Aqueous Solutions of MDEA and Mixtures of MDEA with MEA and DEA using the Electrolyte-NRTL Equation," accepted for publication, *Ind. Eng. Chem. Res.*, 1990.
- Austgen, D.M., G.T. Rochelle, X. Peng, and C.-C. Chen, "A Model of Vapor-Liquid Equilibria for Aqueous Acid Gas-Alkanolamine Systems using the Electrolyte-NRTL Equation," *Ind. Eng. Chem. Res.*, **28**, 1060, 1989.
- Bard, Y., *Nonlinear Parameter Estimation*, Academic Press, Inc., New York, 1974.
- Barth, D., C. Tondre, and J.-J. Delpuech, "Stopped-Flow Determination of Carbon Dioxide-Diethanolamine Reaction Mechanism: Kinetics of Carbamate Formation," *Int. J. Chem. Kinetics*, **15**, 1147, 1983.
- Barth, D., C. Tondre, and J.-J. Delpuech, "Kinetics and Mechanisms of the Reactions of Carbon Dioxide with Alkanolamines: A Discussion Concerning the Cases of MDEA and DEA," *Chem. Eng. Sci.*, **39**(12), 1753, 1984.
- Barth, D., C. Tondre, and J.-J. Delpuech, "Stopped-Flow Investigations of the Reaction Kinetics of Carbon Dioxide with Some Primary and Secondary Alkanolamines in Aqueous Solutions," *Int. J. Chem. Kinetics*, **18**, 445, 1986.
- Barth, D., C. Tondre, G. Lappai, and J.-J. Delpuech, "Kinetic Study of Carbon Dioxide Reaction with Tertiary Amines in Aqueous Solutions," *J. Phys. Chem.*, **85**, 3660, 1981.
- Bates, D.M., and D.G. Watts, *Nonlinear Regression Analysis and Its Applications*, John Wiley & Sons, Inc., New York, 1988.
- Bates, D.M., and D.G. Watts, "Relative Curvature Measures of Nonlinearity," *Journal of the Royal Statistical Society*, **B42**(1), 1, 1980.
- Bates, R.G., and G.D. Pinching, "Acidic Dissociation Constant and Related Thermodynamic Quantities of Monoethanolammonium Ion in Water from 0° to 50°C," *J. Research National Bureau of Standards*, **46**(5), 349, 1951.

- Benac, B., personal communication, Texaco Chemical Co., Austin Laboratories, Austin, TX, 1989.
- Bhairi, A. M., *Experimental Equilibrium Between Acid Gases and Ethanolamine Solutions*, Ph.D. dissertation, Oklahoma State University, Stillwater, OK, 1984.
- Bhattacharaya, A., R.V. Gholap, and R.V. Chaudhari, "Gas Absorption with Exothermic Bimolecular (1,1 Order) Reaction," *AIChE J.*, **33**(9), 1507, 1987.
- Biardi, G., and M.G. Grottoli, "Development of a New Simulation Model for Real Trays Distillation Column," *Comput. Chem. Engng.*, **13**(4/5), 441, 1989.
- Biegler, L.T., J.J. Damiano, and G.E. Blau, "Nonlinear Parameter Estimation: A Case Study Comparison," *AIChE J.*, **32**(1), 29, 1986.
- Billingley, D.S., and A. Chirachavala, "Numerical Solution of Nonequilibrium Multi-component Mass Transfer Operations," *AIChE J.*, **27**(6), 968, 1981.
- Bin, A.K., "Comments on the Effect of Diffusivity on Gas-Liquid Mass Transfer in Stirred Vessels. Experiments at Atmospheric and Elevated Pressures," *Chem. Eng. Sci.*, **43**, 3113, 1988.
- Bin, A.K., "Mass Transfer to the Free Interface in Stirred Vessels," *Chem. Eng. Commun.*, **31**, 155, 1984.
- Bird, R.B., C.F. Curtiss, and J.O. Hirschfelder, "Fluid Mechanics and the Transport Phenomena," *Chem. Eng. Symp. Ser.*, **16**(51), 69, 1955.
- Blanc, C., and G. Demarais, "The Reaction Rate of CO<sub>2</sub> with Diethanolamine," *Int. Chem. Eng.*, **24**(1), 43, 1984.
- Blauwhoff, P.M.M., and W.P.M. van Swaaij, "Simultaneous Mass Transfer of H<sub>2</sub>S and CO<sub>2</sub> with Complex Chemical Reactions in an Aqueous Diisopropanolamine Solution," *Chem. Eng. Process.*, **19**, 67, 1985.
- Blauwhoff, P.M.M., B. Kamphuis, W.P.M. van Swaaij, and K.R. Westerterp, "Absorber Design in Sour Natural Gas Treatment Plants: Impact of Process Variables on Operation and Economics," *Chem. Eng. Process.*, **19**, 1, 1985.
- Blauwhoff, P.M.M., G.F. Versteeg, and W.P.M. van Swaaij, "A Study on the Reaction Between CO<sub>2</sub> and Alkanolamines in Aqueous Solutions," *Chem. Eng. Sci.*, **39**(2), 207, 1984.
- Bosch, H., *Solvents and Reactors for Acid Gas Treating*, Ph.D. dissertation, University of Twente, The Netherlands, 1989.
- Bosch, H., G.F. Versteeg, and W.P.M. van Swaaij, "Gas-Liquid Mass Transfer with Parallel Reversible Reactions. Part I: Absorption of CO<sub>2</sub> into Solutions of Sterically Hindered Amines," *Chem. Eng. Sci.*, **44**(11), 2723, 1989a.
- Bosch, H., G.F. Versteeg, and W.P.M. van Swaaij, "Gas-Liquid Mass Transfer with Parallel Reversible Reactions. Part II: Absorption of CO<sub>2</sub> into Amine Promoted Carbonate Solutions," *Chem. Eng. Sci.*, **44**(11), 2735, 1989b.
- Bosch, H., G.F. Versteeg, and W.P.M. van Swaaij, "Gas-Liquid Mass Transfer with Parallel Reversible Reactions. Part III: Absorption of CO<sub>2</sub> into Solutions of Blends of Amines," *Chem. Eng. Sci.*, **44**(11), 2745, 1989c.

- Bottoms, R.R., U.S. Patent 1,783,901; 1930.
- Boudart, M., *Kinetics of Chemical Processes*, Prentice-Hall, Inc., New Jersey, 1968.
- Bowen, R.M., "On the Stoichiometry of Chemically Reacting Materials," *Arch. Rational Mech. Anal.*, **29**(2), 114, 1968.
- Boyd, R.K., "Macroscopic and Microscopic Restrictions on Chemical Kinetics," *Chem. Rev.*, **77**(1), 93, 1977.
- Brian, P.L.T., and M.C. Beaverstock, "Gas Absorption Accompanied by a Two-Step Chemical Reaction," *Chem. Eng. Sci.*, **20**, 47, 1965.
- Brian, P.L.T., "Gas Absorption Accompanied by an Irreversible Reaction of General Order," *AIChE J.*, **10**(1), 5, 1964.
- Brian, P.L.T., J.F. Hurley, and E.H. Hasseltine, "Penetration Theory for Gas Absorption Accompanied by a Second Order Chemical Reaction," *AIChE J.*, **7**(2), 226, 1961.
- Britt, H.I., and R.H. Luecke, "The Estimation of Parameters in Nonlinear, Implicit Models," *Technometrics*, **15**(2), 233, 1973.
- Broyden, C.G., "A Class of Methods for Solving Nonlinear Simultaneous Equations," *Math. Comp.*, **19**, 577, 1965.
- Bullin, J.A., and A.E. Dukler, "Random Eddy Models for Surface Renewal: Formulation as a Stochastic Process," *Chem. Eng. Sci.*, **27**, 439, 1972.
- Bunch, D.S., "Maximum Likelihood Estimation of Probabilistic Choice Models," *SIAM J. Sci. Stat. Comput.*, **8**(1), 56, 1987.
- Byrne, G.D., and P.R. Ponzi, "Differential-Algebraic Systems, Their Applications and Solutions," *Comput. Chem. Engng.*, **12**(5), 377, 1988.
- Campbell, S.W., and R.H. Weiland, "Modelling CO<sub>2</sub> Removal by Amine Blends," Presented at the AIChE Spring National Meeting, Houston, TX, 1989.
- Caplow, M., "Kinetics of Carbamate Formation and Breakdown," *J. Am. Chem. Soc.*, **90**, 6795, 1968.
- Caracotsios, M., *Model Parametric Sensitivity Analysis and Nonlinear Parameter Estimation. Theory and Applications*, Ph.D. Dissertation, The University of Wisconsin - Madison, 1986.
- Caracotsios, M., and W.E. Stewart, "Sensitivity Analysis of Initial Value Problems with Mixed ODEs and Algebraic Equations," *Comput. Chem. Engng.*, **9**(4), 359, 1985.
- Caram, H.S., and L.E. Scriven, "Non-Unique Reaction Equilibria in Nonideal Systems," *Chem. Eng. Sci.*, **31**, 163, 1976.
- Carnahan, B., H.A. Luther, and J.O. Wilkes, *Applied Numerical Methods*, John Wiley & Sons, New York, N.Y., 1969.
- Carta, G., and R.L. Pigford, "Absorption of Nitric Oxide in Nitric Acid and Water," *Ind. Eng. Chem. Fundam.*, **22**, 329, 1983.

- Castier, M., P. Rasmussen, and A. Fredenslund, "Calculation of Simultaneous Chemical and Phase Equilibria in Nonideal Systems," *Chem. Eng. Sci.*, **44**(2), 237, 1989.
- Chakravarty, T., *Solubility Calculations for Acid Gases in Amine Blends*, Ph.D. dissertation, Clarkson University, 1985.
- Chan, H.M., and P.V. Danckwerts, "Equilibrium of MEA and DEA with Bicarbonate and Carbamate," *Chem. Eng. Sci.*, **36**, 229, 1981.
- Chan, W.C., and L.E. Scriven, "Absorption into Irrotational Stagnation Flow: A Case Study in Convective Diffusion Theory," *Ind. Eng. Chem. Fund.*, **9**(1), 114, 1970.
- Chandrasekharan, K., Calderbank, P.H., "The Evaluation of Mass Transfer Product from Unsteady-State Gas Absorption/Desorption," *Chem. Eng. Sci.*, **35**, 1473, 1980.
- Chang, C.-S., *Mass Transfer with Equilibrium Chemical Reaction, Sulfur Dioxide Absorption in Aqueous Solutions*, Ph.D. Dissertation, The University of Texas at Austin, 1979.
- Chang, C.-S., and G.T. Rochelle, "Mass Transfer Enhanced by Equilibrium Reactions," *Ind. Eng. Chem. Fundam.*, **21**, 379, 1982.
- Chang, C.-Y., and D.-C. Hwang, "Interfacial Resistance in Exothermic Gas Absorption with Chemical Reaction," *Chem. Eng. J.*, **38**, 187, 1988.
- Chang, Y.A., and J.D. Seader, "Simulation of Continuous Reactive Distillation by a Homotopy-Continuation Method," *Comput. Chem. Engng.*, **12**(12), 1243, 1988.
- Chatterjee, S.G., and E.R. Altwick, "Film and Penetration Theories for a First-Order Reaction in Exothermic Gas Absorption," *Can. J. Chem. Eng.*, **65**, 454, 1987.
- Chen, C.-C., H.I. Britt, J.F. Boston, and L.B. Evans, "Local Composition Model for Excess Gibbs Energy of Electrolyte Systems," *AIChE J.*, **28**(4), 588, 1982.
- Chen, C.-C., and L.B. Evans, "A Local Composition Model for the Excess Gibbs Energy of Aqueous Electrolyte Systems," *AIChE J.*, **32**(3), 444, 1986.
- Connor, W. M. Curtis Jr., and J.A. Schwarz, "A Consistent Theoretical Framework for Analysis of Diverse Rate Processes," *Chem. Eng. Comm.*, **55**, 129, 1987.
- Cornelisse, R., A.A.C.M. Beenackers, F.P.H. Van Beckum, and W.P.M. Van Swaaij, "Numerical Calculation of Simultaneous Mass Transfer of Two Gases Accompanied by Complex Reversible Reactions," *Chem. Eng. Sci.*, **35**, 1245, 1980.
- Cornelissen, A.E., "Simulation of Absorption of H<sub>2</sub>S and CO<sub>2</sub> into Aqueous Alkanolamines in Tray and Packed Columns," *Trans. IChemE*, **58**, 242, 1980.
- Cowell, W.R., "Transforming Fortran DO Loops to Improve Performance on Vector Architectures," *ACM Trans. Math. Soft.*, **12**(4), 324, 1986.
- Critchfield, J. E. and G. T. Rochelle "CO<sub>2</sub> Desorption from DEA and DEA-Promoted MDEA Solutions," Presented at the AIChE National Meeting, Paper No. 68b, New Orleans, LA, March, 1988.

- Critchfield, J. E. and G. T. Rochelle, "CO<sub>2</sub> Absorption into Aqueous MDEA and MDEA/MEA Solutions," Presented at the AIChE National Meeting, Paper No. 43e, Houston, TX, March, 1987.
- Critchfield, J.E., *CO<sub>2</sub> Absorption/Desorption in Methyldiethanolamine Solutions Promoted with Monoethanolamine and Diethanolamine: Mass Transfer and Reaction Kinetics*, PhD. dissertation, The University of Texas at Austin, 1988.
- Cullin, E.J., and J.F. Davidson, "Absorption of Gases into Liquid Jets," Trans. Faraday Soc., **53**, 113, 1957.
- Danckwerts, P.V., "Absorption by Simultaneous Diffusion and Chemical Reaction into Particles of Various Shapes and into Falling Drops," Trans. Faraday Soc., **47**, 1014, 1951.
- Danckwerts, P.V., and A.M. Kennedy, "Kinetics of Liquid-Film Process in Gas Absorption. Part I: Models of the Absorption Process," Trans. Inst. Chem. Eng., **32**, S49, 1954.
- Danckwerts, P.V., "Gas-Absorption Accompanied by a First-Order Reaction: Concentration of Product, Temperature-Rise and Depletion of Reactant," Chem. Eng. Sci., **22**, 472, 1967.
- Danckwerts, P.V., *Gas-Liquid Reactions*, McGraw-Hill, New York, 1970.
- Danckwerts, P.V., "Significance of Liquid-Film Coefficients in Gas Absorption," Ind. Eng. Chem., **43**(6), 1460, 1951.
- Danckwerts, P.V., "The Reaction of CO<sub>2</sub> with Ethanolamines," Chem. Eng. Sci., **34**, 443, 1979.
- Davies, J.T., *Interfacial Mass Transfer*, Academic Press, New York, 1972a.
- Davies, J.T., "Turbulence Phenomena at Free Surfaces," AIChE J., **18**(1), 169, 1972b.
- Davies, J.T., "Diffusion and Heat Transfer at the Boundaries of Turbulent Liquids," Physicochemical Hydrodynamics, **I**, 3, 1977.
- Davies, J.T., "Interfacial Effects in Gas Transfer to Liquids," Chem. Ind. (London), **5**, 189, 1980.
- Davies, J.T., A.A. Kilner, and G.A. Ratcliff, "The Effect of Diffusivities and Surface Films on Rates of Gas Absorption," **19**, 583, 1964.
- Davies, J.T., and F.J. Lozano, "Turbulence and Surface Renewal at the Clean Surface of a Stirred Vessel," AIChE J., **30**(3), 502, 1984.
- Davies, J.T., and F.J. Lozano, "Turbulence Characteristics and Mass Transfer at Air-Water Surfaces," AIChE J., **25**(3), 405, 1979.
- Davies, J.T., and R.W. Makepeace, "Measurement of the Surface Ages of Water Jets," **24**(3), 524, 1978.
- Dawodu, O., and A. Meisen, "Degradation Products Resulting from COS-DEA Interactions," Presented at the Spring National AIChE Meeting, Houston, TX, April 1989.
- D.B. Robinson & Associates Ltd., Edmonton, Alberta, Canada.

- de Groot, S.R., and P. Mazur, *Non-Equilibrium Thermodynamics*, North-Holland Publishing Co., Amsterdam, 1962.
- de Boor, C., and B. Swartz, "Collocation at Gaussian Points," *Siam J. Numer. Anal.*, **10**(4), 582, 1973.
- DeCoursey, W.J., "Absorption with Chemical Reaction: Development of a New Relation for the Danckwerts Model," *Chem. Eng. Sci.*, **29**, 1867, 1974.
- DeCoursey, W.J., "Enhancement Factors for Gas Absorption with Reversible Reaction," *37*(10), 1483, 1982.
- Degreve, J., P. Dimitriou, J. Puszynski, and V. Hlavacek, "Modeling of Strongly Exothermic Reaction on a Supercomputer," *Chem. Eng. Comm.*, **58**, 105, 1987.
- Deming, W.E., *Statistical Adjustment of Data*, Dover Publications, New York, 1943.
- Denbigh, K.G., *The Thermodynamics of the Steady State*, John Wiley and Sons, Inc., New York, 1958.
- Deshmukh, R.D., and A.E. Mather, "A Mathematical Model for Equilibrium Solubility of Hydrogen Sulfide and Carbon Dioxide in Aqueous Alkanolamine Solutions," *Chem. Eng. Sci.*, **36**, 355, 1981.
- Dissinger, G.R., and W.E. Schiesser, "Some Methods for Minimizing Jacobian and Derivative Evaluations in Large-Scale ODE Problems," *IMACS Transactions on Scientific Computation*, **I**, 69, 1983.
- Donaldson, J.R., and R.B. Schnabel, "Computational Experience with Confidence Regions and Confidence Intervals for Nonlinear Least Squares," *Technometrics*, **29**(1), 67, 1987.
- Donaldson, T.L., and Y.N. Nguyen, "Carbon Dioxide Reaction Kinetics and Transport in Aqueous Amine Membranes," *Ind. Eng. Chem. Fundam.*, **19**, 260, 1980.
- Dow Chemical, *Gas Spec Gas Treating from Dow*, 1987.
- Draper, N.R., and H. Smith, *Applied Regression Analysis*, 2nd Ed., John Wiley & Sons, New York, 1981.
- Duda, J.L., and J.S. Vrentas, "Laminar Liquid Jet Diffusion Studies," *AIChE J.*, **14**(2), 286, 1968.
- Duprat, F., R. Gassend, and G. Gau, "Reactive Distillation Process Optimization by Empirical Formulae Construction," *Comput. Chem. Engng.*, **12**(11), 1141, 1988.
- Eckert, C.A., C.K. Hsieh, and J.R. McCabe, "Molecular Thermodynamics for Chemical Reaction Design," *AIChE J.*, **20**(1), 20, 1974.
- Edwards, T.J., J. Newman, and J.M. Prausnitz, "Thermodynamics of Aqueous Solutions Containing Volatile Weak Electrolytes," *AIChE J.*, **21**(2), 248, 1975.
- Efron, B., "Computer-Intensive Methods in Statistical Regression," *SIAM Rev.*, **30**(3), 421, 1988.



- Eriksson, G., "Thermodynamic Studies of High Temperature Equilibria III. SOLGAS, a Computer Program for Calculating the Composition and Heat Condition of an Equilibrium Mixture," *Acta Chemica Scandinavica*, **25**, 2651, 1971.
- Eriksson, G., and E. Roson, "Thermodynamic Studies of High Temperature Equilibria VIII. General Equations for the Calculation of Equilibria in Multiphase Systems," *Chemical Scripta*, **4**, 193, 1973.
- Ewing, S.P., D. Lockshon, and W.P. Jencks, "Mechanism of Cleavage of Carbamate Anions," *J. Am. Chem. Soc.*, **102**(9), 3072, 1980.
- Fair, J.R., personal communication, The University of Texas at Austin, 1987.
- Finlayson, B.A., *Nonlinear Analysis in Chemical Engineering*, McGraw-Hill, New York, 1980.
- Froment, G.F., and K.B. Bischoff, *Chemical Reactor Analysis and Design*, John Wiley and Sons, New York, 1979.
- Fortescue, G.E., and J.R.A. Pearson, "On Gas Absorption into a Turbulent Liquid," *Chem. Eng. Sci.*, **22**, 1163, 1967.
- Gaffney, P.W., "Using the Methods of Lines Technique to Solve Initial Boundary Value Partial Differential Equations," *Scientific Computing*, IMACS, North-Holland Publishing Co., 79, 1983.
- Gear, C.W., and L.R. Petzold, "ODE Methods for the Solution of Differential/Algebraic Equations," *SIAM J. Numer. Anal.*, **21**(4), 716, 1984.
- Glasscock, D.A., and G.T. Rochelle, "Comparison of Steady- and Unsteady-State Theories for Multicomponent Diffusion/Reaction in Gas Absorption Processes," *AIChE J.*, **35**(8), 1271, 1989.
- Glasscock, D.A., and G.T. Rochelle, "Modelling of CO<sub>2</sub> Absorption/Desorption in Mixtures of Methyldiethanolamine with Monoethanolamine or Diethanolamine," Presented at the AIChE National Meeting, Paper No. 15b, Orlando, FL, March, 1990.
- Goettler, L.A., and R.L. Pigford, "Computational Studies of the Simultaneous Chemical Absorption of Two Gases," *AIChE J.*, **17**(4), 793, 1971.
- Goodgame, T.H., and T.K. Sherwood, "The Additivity of Resistances in Mass Transfer Between Phases," *Chem. Eng. Sci.*, **3**(2), 37, 1954.
- Gupta, R.K., and T. Sridhar, "Effect of Interfacial Resistance on Quiescent Gas-Liquid Absorption," *Chem. Eng. Sci.*, **39**(3), 471, 1984.
- Guthrie, J.P., "Energetic Restrictions on the Allowed Range of Catalyst pK<sub>a</sub>s for General-Acid- or General-Base-Catalyzed Reactions of Carbonyl Compounds," *J. Am. Chem. Soc.*, **102**, 5286, 1980.
- Haimour, N., A. Bidarian, and O.C. Sandall, "Kinetics of the Reaction Between Carbon Dioxide and Methyldiethanolamine," *Chem. Eng. Sci.*, **42**(6), 1393, 1987.
- Haimour, N., and O.C. Sandall, "Absorption of Carbon Dioxide into Aqueous Methyldiethanolamine," *Chem. Eng. Sci.*, **39**(12), 1791, 1984.

- Hall, D.G., "The Relationship between Thermodynamics and the Kinetics of Elementary Reactions in Non-ideal System," *Zeitschr. f. physik. Chemie Neue Folge*, **129**, 109, 1982.
- Harriot, P., "A Random Eddy Modification of the Penetration Theory," *Chem. Eng. Sci.*, **17**, 149, 1962.
- Hayduk, W., and S.C. Cheng, "Review of Relation Between Diffusivity and Solvent Viscosity in Dilute Liquid Solutions," *Chem. Eng. Sci.*, **26**, 635, 1971.
- Hayduk, W., and V.K. Malik, "Density, Viscosity, and Carbon Dioxide Solubility and Diffusivity in Aqueous Ethylene Glycol Solutions," *J. Chem. Eng. Data*, **16**(2), 143, 1971.
- Hermes, J.E., and G.T. Rochelle, "A Mass Transfer-Based Process Model of Acid Gas Absorption/Stripping using Methyldiethanolamine," Presented at the ACS National Meeting, August 30-September 4, 1987.
- Hiebert, K.L., "An Evaluation of Mathematical Software that Solves Systems of Nonlinear Equations," *ACM TOMS*, **8**(1), 5, 1982.
- Higbie, R., "The Rate of Absorption of a Pure Gas into a Still Liquid During Short Periods of Exposure," *Trans. Am. Inst. Chem. Eng.*, **31**, 365, 1935.
- Hikita, H., and S. Asai, "Gas Absorption with (m,n)-th Order Irreversible Chemical Reaction," *Kagaku Kogaku (Abridged edition)*, **2**(1), 77, 1964.
- Hikita, H., S. Asai, H. Ishikawa, and M. Honda, "The Kinetics of Reactions of Carbon Dioxide with Monoethanolamine, Diethanolamine and Triethanolamine by a Rapid Mixing Method," *Chem. Eng. J.*, **13**, 7, 1977.
- Ho, B.S., and R.R. Eguren, "Solubility of Acidic Gases in Aqueous DEA and MDEA Solutions," Presented at the AIChE National Meeting, Paper No. 69a, New Orleans, LA, March, 1988.
- Huang, D.T.-J., J.J. Carberry, and A. Varma, "Gas Absorption with Consecutive Second-Order Reactions," *AIChE J.*, **26**(5), 832, 1980.
- Imaishi, N., M. Hozawa, and K. Fujinawa, "The Effect of Interfacial Turbulence on Mass Transfer - An Expression of the Enhancement Factor -," *J. Chem. Eng. Japan*, **9**(6), 499, 1976.
- Jensen, A., M.B. Jensen, and C. Faurholt, "Studies on Carbamates X. The Carbamates of Di-n-Propylamine and Di-iso-Propylamine," *Acta Chemica Scandinavica*, **8**, 1129, 1954a.
- Jensen, M.B., E. Jorgensen, and C. Faurholt, "Reactions between Carbon Dioxide and Amino Alcohols I. Monoethanolamine and Diethanolamine," *Acta Chemica Scandinavica*, **8**, 1137, 1954b.
- Joffrion, L.L., D.R. McGregor, M.G. Johnson, and A. Akgerman, "The Effect of Experimental Uncertainties on Rate Modeling and Reactor Simulation," *Chem. Eng. Comm.*, **76**, 41, 1989.
- Johnson, S.L., and D.L. Morrison, "Kinetics and Mechanism of Decarboxylation of N-Arylcarbamates. Evidence for Kinetically Important Zwitterionic Carbamic Acid Species of Short Lifetime," *J. Am. Chem. Soc.*, **94**(4), 1323, 1972.

- Jones, J. H., H. R. Froning, and E. E. Claytor, "Solubility of Acidic Gases in Aqueous Monoethanolamine," *J. Chem. Eng. Data*, **4**(1), 85, 1959.
- Jorgensen, E., and C. Faurholt, "Reactions between Carbon Dioxide and Amino Alcohols II. Triethanolamine," *Acta Chemica Scandinavica*, **8**, 1141, 1954.
- Jorgensen, E., "Reactions between Carbon Dioxide and Amino Alcohols III. Diethanolamine," *Acta Chemica Scandinavica*, **10**, 747, 1956.
- Jou, F.Y., A.E. Mather, and F.D. Otto, "Solubility of H<sub>2</sub>S and CO<sub>2</sub> in Aqueous Methyldiethanolamine Solutions," *Ind. Eng. Chem. Process Des. Dev.*, **21**, 539, 1982.
- Jou, F. Y., F. D. Otto, and A. E. Mather, "Solubility of Mixtures of H<sub>2</sub>S and CO<sub>2</sub> in a Methyldiethanolamine Solution," Presented at the AIChE National Meeting, Miami Beach, FL, Nov, 1986.
- Ju, L.-K., and C.S. Ho, "The Structure-Breaking Effect of Oxygen Diffusion Coefficients in Electrolyte and Polyelectrolyte Solutions," *Can. J. Chem. Eng.*, **67**, 471, 1989.
- Kataoka, K., Y. Okada, Y. Morikawa, and A. Iwata, "Mass Transfer Across an Interface of Stagnant Liquid Layer with Periodical Vortex Motion," *J. Chem. Eng. Japan*, **20**(4), 363, 1987.
- Katti, S.S., and R.A. Wolcott, "Fundamental Aspects of Gas Treating with Formulated Amine Mixtures," Presented at AIChE National Meeting, Minneapolis, MN, August, 1987.
- Kee, R.J., and J.A. Miller, "A Structured Approach to the Computational Modeling of Chemical Kinetics and Molecular Transport in Flowing Systems," *Complex Chemical Reaction Systems, Mathematical Modelling and Simulation*, **47**, 196, 1987.
- Kent, R.L., and B. Eisenberg, "Better Data for Amine Treating," *Hydr. Proc.*, Feb., 87, 1976.
- Kikuchi, K.-I., T. Sugawara, and H. Ohashi, "Correlation of Liquid-Side Mass Transfer Coefficient Based on the New Concept of Specific Power Group," *Chem. Eng. Sci.*, **43**(9), 2533, 1988.
- Kim, C.J., and D.W. Savage, "Kinetics of Carbon Dioxide Reaction with Diethylaminoethanol in Aqueous Solutions," *Chem. Eng. Sci.*, **42**(6), 1481, 1987.
- King, C.J., "The Additivity of Individual Phase Resistances in Mass Transfer Operations," *AIChE J.*, **10**(5), 671, 1964.
- King, C. J., "Turbulent Liquid Phase Mass Transfer at a Free Gas-Liquid Interface," *Ind. Eng. Chem. Fund.*, **5**(1), 1, 1966.
- Kirkwood, J.G., and B. Crawford, Jr., "The Macroscopic Equations of Transport," *J. Phys. Chem.* **56**, 1048, 1952.
- Kohl, A.L., and F.C. Riesenfeld, *Gas Purification*, 4th ed., Gulf Publishing Co., Houston, 1985.

- Koppel, L.B., R.D. Patel, and J.T. Holmes, "Statistical Models for Surface Renewal in Heat and Mass Transfer: Part II. Techniques for Measurement of Age Distribution at Transport Surfaces," *AIChE J.* **12**(5), 947, 1966.
- Kozinski, A.A., and C.J. King, "The Influence of Diffusivity on Liquid Phase Mass Transfer to the Free Interface in a Stirred Vessel," *AIChE J.*, **12**(1), 109, 1966.
- Krishna, R., "A Note on the Film and Penetration Models for Multicomponent Mass Transfer," *Chem. Eng. Sci.*, **33**, 765, 1978.
- Krishna, R., "A Unified Theory of Separation Processes Based on Irreversible Thermodynamics," *Chem. Eng. Comm.*, **59**, 33, 1987.
- Krishna, R., and G.L. Standart, "Mass and Energy Transfer in Multicomponent Systems," *Chem. Eng. Comm.*, **3**, 201, 1979.
- Krishna, R., "Diffusion in Multicomponent Electrolyte Systems," *Chem. Eng. J.*, **35**, 19, 1987.
- Krishna, R., "Penetration Depths in Multicomponent Mass Transfer," *Chem. Eng. Sci.*, **33**, 1495, 1978.
- Krishnamurthy, R., and R. Taylor, "A Nonequilibrium Stage Model of Multicomponent Separation Processes. Part I: Model Description and Method of Solution," *AIChE J.*, **31**(3), 449, 1985a.
- Krishnamurthy, R., and R. Taylor, "A Nonequilibrium Stage Model of Multicomponent Separation Processes. Part II: Comparison with Experiment," *AIChE J.*, **31**(3), 456, 1985b.
- Krishnamurthy, R., and R. Taylor, "A Nonequilibrium Stage Model of Multicomponent Separation Processes. Part III: The Influence of Unequal Component-Efficiencies in Process Design Problems," *AIChE J.*, **31**(12), 1973, 1985c.
- Kunerth, W., "Solubility of CO<sub>2</sub> and N<sub>2</sub>O in Certain Solvents," *Phys. Rev., Ser. 2*, **19**(5), 512, 1922.
- Kuno, M., J.D. Seader, "Computing All Real Solutions to Systems of Nonlinear Equations with a Fixed-Point Homotopy," *Ind. Eng. Chem. Res.*, **27**, 1320, 1988.
- Kurtz, L.A., R.E. Smith, C.L. Parks, and L.R. Boney, "A Comparison of the Method of Lines to Finite Difference Techniques in Solving Time-Dependent Partial Differential Equations," *Computers and Fluids*, **6**, 49, 1978.
- Laddha, S.S., and P.V. Danckerts, "The Absorption of CO<sub>2</sub> by Amine-Potash Solutions," *Chem. Eng. Sci.*, **37**(5), 665, 1982.
- Laddha, S.S., and P.V. Danckwerts, "Reaction of CO<sub>2</sub> with Ethanolamines: Kinetics from Gas Absorption," *Chem. Eng. Sci.*, **36**, 479, 1981.
- Laddha, S.S., J.M. Diav, and P.V. Danckwerts, "The N<sub>2</sub>O Analogy: the Solubilities of CO<sub>2</sub> and N<sub>2</sub>O in Aqueous Solutions of Organic Compounds," *Chem. Eng. Sci.*, **36**, 228, 1981.

- Lal, D., F.D. Otto, and A.E. Mather, "The Solubility of  $\text{H}_2\text{S}$  and  $\text{CO}_2$  in a Diethanolamine Solution at Low Partial Pressures," *Can. J. Chem. Eng.*, **63**, 681, 1985.
- Lamont, J.C., and D.S. Scott, "An Eddy Cell Model of Mass Transfer into the Surface of a Turbulent Liquid," *AIChE J.*, **16**(4), 513, 1970.
- Lawson J. D. and A. W. Garst, "Gas Sweetening Data: Equilibrium Solubility of Hydrogen Sulfide and Carbon Dioxide in Aqueous Monoethanolamine and Aqueous Diethanolamine Solutions," *J. Chem. Eng. Data*, **21**(1), 20, 1976.
- Leaist, D., "Simplified Theory of Diffusion of Mixed Electrolytes with Simultaneous Chemical Reactions," *J. Chem. Soc., Faraday Trans. 1*, **78**, 3069, 1982.
- Leder, F., "The Absorption of  $\text{CO}_2$  into Chemically Reactive Solutions at High Temperatures," *Chem. Eng. Sci.*, **26**, 1381, 1971.
- Lee, J. I., F. D. Otto, and A. E. Mather, "Solubility of Carbon Dioxide in Aqueous Diethanolamine Solutions at High Pressures," *J. Chem. Eng. Data*, **17**(4), 465, 1972.
- Lee, J. I., F. D. Otto, and A. E. Mather, "The Solubility of Mixtures of Carbon Dioxide and Hydrogen Sulfide in Aqueous Diethanolamine Solutions," *Can. J. Chem. Eng.*, **52**, 125, 1974a.
- Lee, J. I., F. D. Otto, and A. E. Mather, "The Solubility of  $\text{H}_2\text{S}$  and  $\text{CO}_2$  in Aqueous Monoethanolamine Solutions," *Can. J. Chem. Eng.*, **52**, 803, 1974b.
- Lee, J. I., F. D. Otto, and A. E. Mather, "Equilibrium Between Carbon Dioxide and Aqueous Monoethanolamine Solutions," *J. Appl. Chem. Biotechnol.*, **26**, 541, 1976.
- Levesque, J.M., and J.W. Williamson, *A Guidebook to Fortran on Supercomputers*, Academic Press, Inc., New York, 1988.
- Lewis, W.K., and W.G. Whitman, "Principles of Gas Absorption," *Ind. Eng. Chem.*, **16**(12), 1215, 1924.
- Lindner, J.R., C.N. Schubert, and R.M. Kelly, "Influence of Hydrodynamics on Physical and Chemical Gas Absorption in Packed Columns," *Ind. Eng. Chem. Res.*, **27**, 636, 1988.
- Linek, V., J. Mayrhoferová, and J. Mošnerová, "The Influence of Diffusivity on Liquid Phase Mass Transfer in Solutions of Electrolytes," *Chem. Eng. Sci.*, **25**, 1033, 1970.
- Littel, R.J., W.P.M. van Swaaij, and G.F. Versteeg, "The Kinetics of Carbon Dioxide with Tertiary Amines in Aqueous Solution," Presented at the AIChE Spring National Meeting, Orlando, FL, March, 1990.
- Liu, Y., A.H. Harvey, and J.M. Prausnitz, "Thermodynamics of Concentrated Electrolyte Solutions," *Chem. Eng. Comm.*, **77**, 43, 1989.
- Liu, Y., M. Wimby, and U. Gren, "An Activity-Coefficient Model for Electrolyte Systems," *Comp. Chem. Eng.*, **13**(4/5), 405, 1989.

- Lucia, A., and S. Macchietto, "New Approach to Approximation of Quantities Involving Physical Properties Derivatives in Equation-Oriented Process Design," *AIChE J.*, **29**(5), 705, 1983.
- Luk, S., and Y.H. Lee, "Mass Transfer in Eddies Close to Air-Water Interface," *AIChE J.*, **32**(9), 1546, 1986.
- Maddox, R.N., A.H. Bhairi, J.R. Diers, and P.A. Thomas, *Equilibrium Solubility of Carbon Dioxide or Hydrogen Sulfide in Aqueous Solutions of Monoethanolamine, Diglycolamine, Diethanolamine and Methyldiethanolamine* GPA Research Report, RR-104, 1987.
- Mahajani, V.V., and J.B. Joshi, "Kinetics of Reactions Between Carbon Dioxide and Alkanolamines," *Gas Separation & Purification*, Butterworth & Co., Ltd., **2**, 50, 1988.
- Mann, R., and H. Moyes, "Exothermic Gas Absorption with Chemical Reaction," *AIChE J.*, **23**(1), 17, 1977.
- Marcio, J.E., D. M. Cardoso, and J.P. O'Connell, "Activity Coefficients in Mixed Solvent Electrolyte Solutions," *Fluid Phase Equil.*, **33**, 315, 1987.
- Markham, A.E., and K.A. Kobe, "The Solubility of Carbon Dioxide and Nitrous Oxide in Aqueous Salt Solutions," *J. Am. Chem. Soc.*, **63**, 449, 1941.
- Martin, J.L., F.D. Otto, and A.E. Mather, "Solubility of Hydrogen Sulfide and Carbon Dioxide in a Diglycolamine Solution," *J. Chem. Eng. Data*, **23**(2), 163, 1978.
- Mason, J.W., and B.F. Dodge, "Equilibrium Absorption of Carbon Dioxide by Solutions of the Ethanolamines," *AIChE Trans.*, **32**, 27, 1936.
- Matheron, E.R., and O.C. Sandall, "Gas Absorption Accompanied by a Second-Order Chemical Reaction Modeled According to the Danckwerts Surface Renewal Theory," *AIChE J.*, **24**(3), 552, 1978.
- McCready, M.J., and T.J. Hanratty, "Concentration Fluctuations Close to a Gas-Liquid Interface," *AIChE J.*, **30**(5), 816, 1984.
- Mehra, A., and M.M. Sharma, "Simultaneous Absorption of Two Gases with Chemical Reactions: Selectivity Variation in Microheterogeneous Media," *Chem. Eng. Sci.*, **43**(9), 2541, 1988.
- Meldon, J.H., K.A. Smith, and C.K. Colton, "The Effect of Weak Acids Upon the Transport of Carbon Dioxide in Alkaline Solutions," *Chem. Eng. Sci.*, **32**, 939, 1977.
- Meldon, J.H., K.A. Smith, and C.K. Colton, "An Analysis of Electrical Effects Induced by Carbon Dioxide Transport in Alkaline Solutions," *Rec. Devel. Sep. Sci.*, **V**, 1, 1979.
- Miller, D.G., "Application of Irreversible Thermodynamics to Electrolyte Solutions. I. Determination of Ionic Transport Coefficients  $l_{ij}$  for Isothermal Vector Transport Processes in Binary Electrolyte Systems," *J. Phys. Chem.*, **70**(8), 2639, 1966.
- Miller, D.G., "Application of Irreversible Thermodynamics to Electrolyte Solutions. II. Ionic Coefficients  $l_{ij}$  for Isothermal Vector Transport Processes in Ternary Systems," *J. Phys. Chem.*, **71**(3), 616, 1967a.

- Miller, D.G., "Application of Irreversible Thermodynamics to Electrolyte Solutions. III. Equations for Isothermal Vector Transport Processes in n-Component Systems," *J. Phys. Chem.*, **71**(11), 3588, 1967b.
- Mills, R., A. Perera, J.P. Simonin, L. Orcil, and P. Turq, "Coupling of Diffusion Processes in Multicomponent Electrolyte Solutions," **89**, 2722, 1985.
- Mock, B., L. B. Evans, and C. C. Chen, "Thermodynamic Representation of Phase Equilibria of Mixed-Solvent Electrolyte Systems," *AIChE J.*, **32**(10), 1655, 1986.
- Moore, T.F., personal communication, Texaco Chemical Co., Austin Laboratories, Austin, TX, 1989.
- More, J.J., B.S. Garbow, and K.E. Hillstrom, User Guide for MINPACK-1, ANL-80-74, Applied Mathematics Division, Argonne National Laboratory, Argonne, Ill., 1980.
- Muhlbauer, H. G., and P. R. Monaghan, "Sweetening Natural Gas With Ethanolamine Solutions," *Oil Gas J.*, **55**(17), 139, 1957.
- Nagy, E., and A. Ujhidy, "Model of the Effect of Chemical Reaction on Bulk-Phase Concentrations," *AIChE J.*, **35**(9), 1564, 1989.
- Newman, J.S., *Electrochemical Systems*, Prentice-Hall, Inc, Englewood Cliffs, N.J., 1973.
- Noble, B., and J.W. Daniel, *Applied Linear Algebra*, 3rd Ed., Prentice Hall, Englewood Cliffs, NJ, 1988.
- Nunge, R.J., and W.N. Gill, "Gas-Liquid Kinetics: the Absorption of Carbon Dioxide in Diethanolamine," *AIChE J.*, **9**(4), 469, 1963.
- Onda, K., E. Sada, T. Kobayashi, and M. Fujine, "Gas Absorption Accompanied by Complex Chemical Reactions - I. Reversible Chemical Reactions," *Chem. Eng. Sci.*, **25**, 753, 1970a.
- Onda, K., E. Sada, T. Kobayashi, and M. Fujine, "Gas Absorption Accompanied by Complex Chemical Reactions - II. Consecutive Chemical Reactions," *Chem. Eng. Sci.*, **25**, 761, 1970b.
- Onsager, L., "Reciprocal Relations in Irreversible Processes. II.," *Phys. Rev.*, **38**, 2265, 1931.
- Onsager, L., "Theories of Concentrated Electrolytes," *Chem. Rev.*, **XIII**, 73, 1933.
- Otto, N.C., and J.A. Quinn, "The Facilitated Transport of Carbon Dioxide Through Bicarbonate Solutions," *Chem. Eng. Sci.*, **26**, 949, 1971.
- Ozturk, S.S., and Y.T. Shah, "Gas Absorption with Chemical Reaction Involving a Volatile Liquid Reactant: Penetration Theory Solution," *Chem. Eng. Commun.*, **46**, 65, 1986.
- Pantelides, C.C., D. Gritsis, K.R. Morison, and R.W.H. Sargent, "The Mathematical Modelling of Transient Systems Using Differential-Algebraic Equations," *Comput. Chem. Engng.*, **12**(5), 449, 1988.
- Pearson, J.R.A., "Diffusion of One Substance into a Semi-Infinite Medium Containing Another with Second-Order Reaction," *Appl. Sci. Res.*, **11**(A), 321, 1963.

- Perlmutter, D. D., "Surface-Renewal Models in Mass Transfer," *Chem. Eng. Sci.*, **16**, 287, 1961.
- Perry, R.H., and R.L. Pigford, "Kinetics of Gas-Liquid Reactions," *Ind. Eng. Chem.*, **45**(6), 1247, 1953.
- Petzold, L., "Differential/Algebraic Equations are not ODEs," *SIAM J. Sci. Stat. Comput.*, **3**(3), 367, 1982.
- Petzold, L.R. "A Description of DASSL: A Differential/Algebraic System Solver," *Scientific Computing*, IMACS/North-Holland Publishing Co., R. Stepleman et al. (eds.), 65, 1983.
- Pinsent, B.R.W., L. Pearson, and F.J.W. Roughton, "The Kinetics of Combination of Carbon Dioxide with Hydroxide Ions," *Trans. Faraday Soc.*, **52**, 1512, 1956.
- Pinto, N.G., and B. Newman, "Estimation of Diffusivities in Concentrated Electrolyte Solutions," *AIChE Annual Meeting*, New York, Nov., 1987.
- Pinto, N.G., and E.E. Graham, "Multicomponent Diffusion in Concentrated Electrolyte Solutions: Effect of Solvation," *AIChE J.*, **33**(3), 436, 1987.
- Pitzer, K.S., "Thermodynamics of Electrolytes. I. Theoretical Basis and General Equations," *J. Phys. Chem.*, **77**(2), 268, 1973.
- Pitzer, K.S., and G. Mayorga, "Thermodynamics of Electrolytes. II. Activity and Osmotic Coefficients for Strong Electrolytes with One or Both Ions Univalent," *J. Phys. Chem.*, **77**(19), 2300, 1973.
- Pitzer, K.S., and J.J. Kim, "Thermodynamics of Electrolytes. IV. Activity and Osmotic Coefficients for Mixed Electrolytes," *J. Am. Chem. Soc.*, **96**(18), 5701, 1974.
- Pitzer, K.S., "Electrolyte Theory - Improvements since Debye and Huckel," *Accounts Chem. Res.*, **10**, 371, 1977.
- Pitzer, K.S., "Electrolytes. From Dilute Solutions to Fused Salts," *J. Am. Chem. Soc.*, **102**(9), 2902, 1980.
- Pohorecki, R., and W. Moniuk, "Plate Efficiency in the Process of Absorption with Chemical Reaction - General Relations," *Chem. Eng. J.*, **39**, 27, 1988a.
- Pohorecki, R., and W. Moniuk, "Plate Efficiency in the Process of Absorption with Chemical Reaction - Experiments and Example Calculations," *Chem. Eng. J.*, **39**, 37, 1988b.
- Portalski, S., and A.J. Clegg, "Interfacial Area Increase in Rippled Film Flow on Wetted Wall Columns," *Chem. Eng. Sci.*, **26**, 773, 1971.
- Powers, M.F., D.J. Vickery, A. Arehole, and R. Taylor, "A Nonequilibrium Stage Model of Multicomponent Separation Processes- V. Computation Methods for Solving the Model Equations," *Comput. Chem. Engng.*, **12**(12), 1229, 1988.
- Prasher, B.D., and A.L. Fricke, "Mass Transfer at a Free Gas-Liquid Interface in Turbulent Thin Films," *Ind. Eng. Chem., Process Des. Develop.*, **13**(4), 336, 1974.



- Quicker, G., E. Alper, and W.-D. Deckwer, "Gas Absorption Rates in a Stirred Cell With Plane Interface in the Presence of Fine Particles," *Can. J. Chem. Eng.*, **67**, 32, 1989.
- Rahman, M.A., R.N. Maddox, and G.J. Mains, "Kinetic Aspects of the Reactions of Acid Gases with Alkanolamines," Presented at the AIChE Spring National Meeting, Houston, TX, March, 1989.
- Raimondi, P., and H.L. Toor, "Interfacial Resistance in Gas Absorption," *AIChE J.*, **5**(1), 86, 1959.
- Rangwala, H.A., R.A. Tomcej, S. Xu, A.E. Mather, and F.D. Otto, "Absorption of Carbon Dioxide in Amine Solutions," Presented at the AIChE Spring National Meeting, Houston, TX, 1989.
- Raymond, D.R., and S.A. Zieminski, "An Investigation of Oxygen Transfer Rates to Flowing Films of Various Electrolyte Solutions," *Can. J. Chem. Eng.*, **54**, 425, 1976.
- Reid, R.C., J.M. Prausnitz, and T.K. Sherwood, *The Properties of Gases and Liquids*, 3rd ed., McGraw-Hill Book Co., New York, 1977.
- Rennotte, J., and B. Kalitventzeff, "Contribution to the Thermodynamic Study of Electrolyte Solutions," *Comput. Chem. Engng.*, **12**(5), 461, 1988.
- Rennotte, J., H. Massillon, and B. Kalitventzeff, "A New Model for the Simulation of the Behaviour of Electrolytic Aqueous Solutions. Comparison with Three Well-Known Previous Models," *Comput. Chem. Engng.*, **13**(4/5), 411, 1989.
- Riazi, M., and A. Faghri, "Gas Absorption with Zero-Order Chemical Reaction," *AIChE J.*, **31**(12), 1967, 1985.
- Rice, R.G., J.A. King, and X.Y. Wang, "Absorption Kinetics and Mixing Studies in Pressure Response Cells," *Ind. Eng. Chem.*, **28**, 1431, 1989.
- Ruckenstein, E., "On Turbulent Mass Transfer Near a Liquid-Fluid Interface," *Chem. Eng. J.*, **2**, 1, 1971.
- Sada, E., H. Kumazawa, and M.A. Butt, "Gas Absorption with Consecutive Chemical Reaction: Absorption of Carbon Dioxide into Aqueous Amine Solutions," *Can. J. Chem. Eng.*, **54**, 421, 1976.
- Sada, E., H. Kumazawa, and M.A. Butt, "Solubilities of Gases in Aqueous Solutions of Amine," *J. Chem. Eng. Data*, **22**(3), 277, 1977.
- Sada, E., H. Kumazawa, and M.A. Butt, "Solubility and Diffusivity of Gases in Aqueous Solutions of Amines," *J. Chem. Eng. Data*, **23**(2), 161, 1978.
- Sada, E., H. Kumazawa, M.A. Butt, and J.E. Lozano, "Interfacial Turbulence Accompanying Chemical Absorption," *Can. J. Chem. Eng.*, **55**, 293, 1977.
- Sada, E., H. Kumazawa, M.A. Butt, and J.E. Lozano, "Interfacial Turbulence During Absorption with Reaction," *J. Chem. Eng. Japan*, **10**(6), 487, 1977.
- Sada, E., H. Kumazawa, Y. Ikehara, and Z.Q. Han, "Chemical Kinetics of the Reaction of Carbon Dioxide with Triethanolamine in Non-Aqueous Solvents," *Chem. Eng. J.*, **40**, 7, 1989.

- Sada, E., H. Kumazawa, Y. Osawa, M. Matsuura, Z.Q. Han, "Chemical Kinetics of the Reaction of Carbon Dioxide with Amines in Non-Aqueous Solvents," *Chem. Eng. J.*, **33**, 87, 1986.
- Sagara, N., and M. Fukushima, "An Efficient Predictor-Corrector Method for Solving Nonlinear Equations," *J. Comp. Appl. Math.*, **19**, 343, 1987.
- Sanyal, D., N. Vasishtha, and D.N. Saraf, "Modeling of Carbon Dioxide Absorber Using Hot Carbonate Process," *Ind. Eng. Chem. Res.*, **27**, 2149, 1988.
- Sardar, H., and R.H. Weiland, "Simulation of Commercial Amine Treating Units," 1985 Gas Conditioning Conference, 43 pp.
- Sartori, G., and D.W. Savage, "Sterically Hindered Amines for CO<sub>2</sub> Removal from Gases," *Ind. Eng. Chem. Fundam.*, **22**, 239, 1983.
- Savage, D.W., E.W. Funk, W.C. Yu, and G. Astarita, "Selective Absorption of H<sub>2</sub>S and CO<sub>2</sub> into Aqueous Solutions of Methyldiethanolamine," *Ind. Eng. Chem. Fundam.*, **25**, 326, 1986.
- Scaufaire, P., D. Richards, and C.-C. Chen, "Ionic Activity Coefficients of Mixed-Solvent Electrolyte Systems," submitted *AIChE J.*, 1989.
- Scriven, L.E., and R.L. Pigford, "Fluid Dynamics and Diffusion Calculations for Laminar Liquid Jets," *AIChE J.*, **5**(3), 397, 1959.
- Scriven, L.E., and R.L. Pigford, "Phase Equilibrium at the Gas-Liquid Interface During Absorption," *AIChE J.*, **4**(4), 439, 1958.
- Scriven, L.E., "Flow and Transfer at Fluid Interfaces. Part I - Lessons from Research," *Chem. Eng. Educ.*, Fall, 150, 1968.
- Scriven, L.E., "Flow and Transfer at Fluid Interfaces. Part II - Models," *Chem. Eng. Educ.*, Winter, 26, 1969.
- Scriven, L.E., "Flow and Transfer at Fluid Interfaces. Part III - Convective Diffusion," *Chem. Eng. Educ.*, Spring, 94, 1969.
- Seader, J.D., *Computer Modeling of Chemical Processes*, AIChE Monograph Series, **81**(15), 1985.
- Seader, J.D., "The Rate-based Approach for Modeling Staged Separations," *Chem. Eng. Prog.*, **85**(10), 41, 1989.
- Secor, R.M., and J.A. Beutler, "Penetration Theory for Diffusion Accompanied by a Reversible Chemical Reaction with Generalized Kinetics," *AIChE J.*, **13**(2), 365, 1967.
- Seo, Y.G., and W.K. Lee, "Single-Eddy Model for Random Surface Renewal," *Chem. Eng. Sci.*, **43**(6), 1395, 1988.
- Sharma, M.M., and P.V. Danckwerts, "Catalysis by Bronsted Bases of the Reaction Between CO<sub>2</sub> and Water," *Trans. Faraday Soc.*, **59**, 386, 1963.
- Sharma, M.M., and P.V. Danckwerts, "Fast Reactions of CO<sub>2</sub> in Alkaline Solutions - (a) Carbonate Buffers with Arsenite, Formaldehyde and Hypochlorite as Catalysts (b) Aqueous Monoisopropanolamine (1-Amino-2-Propanol) Solutions," *Chem. Eng. Sci.*, **18**, 729, 1963.

- Sharma, M.M., "Kinetics of Reactions of Carbonyl Sulphide and Carbon Dioxide with Amines and Catalysis by Bronsted Bases of the Hydrolysis of COS," *Trans. Faraday Soc.*, **61**, 681, 1965.
- Sherwood, T.K., and R.L. Pigford, *Absorption and Extraction*, McGraw-Hill, New York, 1952.
- Sherwood, T.K., R.L. Pigford, and C.R. Wilke, *Mass Transfer*, McGraw-Hill, New York, 1975.
- Sivasubramanian, M.S., *The Heat and Mass Transfer Rate Approach for the Simulation and Design of Acid Gas Treating Units*, Ph.D. Dissertation, Clarkson University, 1985.
- Sivasubramanian, M.S., and J.F. Boston, "Rate Based Separation Processes," Presented at the AIChE National Meeting, Washington, D.C., Nov., 1988.
- Smith, W.R., and R.W. Missen, *Chemical Reaction Equilibrium Analysis: Theory and Algorithms*, John Wiley & Sons, Inc., New York, 1982.
- Smith, W.R., and R.W. Missen, "Strategies for Solving The Chemical Equilibrium Problem and an Efficient Microcomputer-Based Algorithm," *Can. J. Chem. Eng.*, **66**, 591, 1988.
- Smyrl, W.H., and J. Newman, "Potential of Cells with Liquid Junctions," *J. Phys. Chem.*, **72**(13), 4660, 1968.
- Springer, T.G., and R.L. Pigford, "Influence of Surface Turbulence and Surfactants on Gas Transport through Liquid Interfaces," *Ind. Eng. Chem. Fundam.*, **9**(3), 458, 1970.
- Standart, G.L., R. Taylor, and R. Krishna, "The Maxwell-Stefan Formulation of Irreversible Thermodynamics for Simultaneous Heat and Mass Transfer," *Chem. Eng. Commun.*, **3**, 277, 1979.
- Sun, E.T., and M.A. Stadtherr, "Issues in Nonlinear Equation Solving in Chemical Engineering," *Comput. Chem. Engng.*, **12**(11), 1129, 1988.
- Tamir, A., and Y. Taitel, "Absorption of a Multicomponent Gaseous Mixture in the Presence of Instantaneous Surface Reaction," *Chem. Eng. Sci.*, **29**, 669, 1974.
- Teramoto, M., K. Hashimoto, and S. Nagata, "Effect of Mass Transfer on the Selectivity of (m,n)-(p,q) Order Consecutive Gas-Liquid Reactions," *J. Chem. Eng. Japan*, **6**(6), 522, 1973.
- Theofanous, T.G., R.N. Houze, and L.K. Brumfield, "Turbulent Mass Transfer at Free, Gas-Liquid Interfaces, with Applications to Open-Channel, Bubble and Jet Flows," *J. Heat Mass Transfer*, **19**, 613, 1976.
- Toman, J.J., Ph.D. dissertation, The University of Texas at Austin, Austin, TX, 1990.
- Tomcej, R.A., and F.D. Otto, "Absorption of CO<sub>2</sub> and N<sub>2</sub>O into Aqueous Solutions of Methyldiethanolamine," *AIChE J.*, **35**(5), 861, 1989.
- Tomcej, R.A., D. Lal, H.A. Rangwala, and F.D. Otto, "Absorption of Carbon Dioxide into Aqueous Solutions of Methyldiethanolamine," Presented at the AIChE Annual Meeting, Miami Beach, Florida, Nov., 1986.

- Tomcej, R.A., F.D. Otto, H.A. Rangwala, and B.R. Morrell, "Tray Design for Selective Absorption," Presented at the Gas Conditioning Conference, Norman, OK, March, 1987.
- Toor, H.L., "Solution of the Linearized Equations of Multicomponent Mass Transfer: I," *AIChE J.*, **10**(4), 448, 1964a.
- Toor, H.L., "Solution of the Linearized Equations of Multicomponent Mass Transfer: II. Matrix Methods," *AIChE J.*, **10**(4), 460, 1964b.
- Truesdell, C., *Rational Thermodynamics*, McGraw-Hill Book Co., New York, 1969.
- van Krevelen, D.W., and P.J. Hoftijzer, "Kinetics of Simultaneous Absorption and Chemical Reaction," *Chem. Eng. Prog.*, **44**(7), 529, 1948.
- Vaz, R.N., G.J. Mains, and R.N. Maddox, "Ethanolamine Process Simulated by Rigorous Calculation," *Hydro. Process.*, 139, April 1981.
- Versteeg, G.F., *Mass Transfer and Chemical Reaction Kinetics in Acid Gas Treating Processes*, dissertation, University of Twente, The Netherlands, 1986.
- Versteeg, G.F., P.M.M. Blauwhoff, and W.P.M. van Swaaij, "The Effect of Diffusivity on Gas-Liquid Mass Transfer in Stirred Vessels. Experiments at Atmospheric and Elevated Pressures," *Chem. Eng. Sci.*, **42**(5), 1103, 1987.
- Versteeg, G.F., and W.P.M. van Swaaij, "Absorption of CO<sub>2</sub> in Aqueous Solutions of Mixtures of Alkanolamines," Presented at the AIChE Spring National Meeting, New Orleans, LA, 1988a.
- Versteeg, G.F., and W.P.M. van Swaaij, "On the Kinetics Between CO<sub>2</sub> and Alkanolamines both in Aqueous and Non-aqueous Solutions. Part I: -Primary and Secondary Amines," *Chem. Eng. Sci.*, **43**(3), 573, 1988b.
- Versteeg, G.F., and W.P.M. van Swaaij, "On the Kinetics Between CO<sub>2</sub> and Alkanolamines both in Aqueous and Non-aqueous Solutions. Part II: -Tertiary Amines," *Chem. Eng. Sci.*, **43**(3), 587, 1988c.
- Versteeg, G.F., and W.P.M. van Swaaij, "Solubility and Diffusivity of Acid Gases (CO<sub>2</sub>, N<sub>2</sub>O) in Aqueous Alkanolamine Solutions," *J. Chem. Eng. Data*, **33**, 29, 1988d.
- Versteeg, G.F., and M.H. Oyeveaar, "The Reaction between CO<sub>2</sub> and Diethanolamine at 298K," *Chem. Eng. Sci.*, **44**(5), 1264, 1989.
- Versteeg, G.F., J.A.M. Kuipers, F.P.H. van Beckum, and W.P.M. van Swaaij, "Mass Transfer with Complex Reversible Chemical Reactions," accepted *Chem. Eng. Sci.*, 1989.
- Vickery, D.J., J. J. Ferrari, and R. Taylor, "An 'Efficient' Continuation Method for the Solution of Difficult Equilibrium Stage Separation Process Problems," *Comput. Chem. Engng.*, **12**(1), 99, 1988.
- Villadsen, J. V., and W.E. Stewart, "Solution of Boundary-Value Problems by Orthogonal Collocation," *Chem. Eng. Sci.*, **22**, 1483, 1967.
- Villadsen, J.V., and M.L. Michelsen, *Solution of Differential Equation Models by Polynomial Approximation*, Prentice-Hall, Englewood Cliffs, 1978.

- Vinograd, J.R., and J.W. McBain, "Diffusion of Electrolytes and of the Ions in their Mixtures," J. Amer. Chem. Soc., **63**, 2008, 1941.
- Ward, C.A., "The Rate of Gas Absorption at a Liquid Interface," J. Chem. Physics, **67**(1), 229, 1977.
- Watson, L.T., and L.R. Scott, "Solving Galerkin Approximations to Nonlinear Two-Point Boundary Value Problems by a Globally Convergent Homotopy Method," SIAM J. Sci. Stat. Comput., **8**(5), 768, 1987.
- Watson, L.T., and L.R. Scott, "Solving Spline-Collocation Approximations to Nonlinear Two-Point Boundary-Value Problems by a Homotopy Method," Appl. Math. and Comp., **24**, 333, 1987.
- Wayburn, T.L., and J.D. Seader, "Homotopy Continuation Methods for Computer-Aided Process Design," Comput. Chem. Engng., **11**(1), 7, 1987.
- Webb, T.J., "The Free Energy of Hydration of Ions and the Electrostriction of the Solvent," J. Am. Chem. Soc., **48**(10), 2589, 1926.
- Wei, J., "Axiomatic Treatment of Chemical Reaction Systems," J. Chem. Phys., **36**(6), 1578, 1962.
- Wellek, R.M., R.J. Brunson, and F.H. Law, "Enhancement Factors for Gas-Absorption with Second-Order Irreversible Chemical Reaction," Can. J. Chem. Eng., **56**(4), 181, 1978.
- Westman, K.R., A. Lucia, and D.C. Miller, "Flash and Distillation Calculations by a Newton-Like Method," Comp. Chem. Engng., **8**(3/4), 219, 1984.
- Weston, R.E. Jr., and H.A. Schwarz, *Chemical Kinetics*, Prentice-Hall, Inc., Englewood Cliffs, NJ, 1972.
- White, D. Jr., and L.E. Johns, "The Diffusional Limitation on the Temperature Rise in the Absorption of Chemically Reactive Gases," Chem. Eng. Commun., **48**, 177, 1986.
- White, W.B., S.M. Johnson, and G.B. Dantzig, "Chemical Equilibrium in Complex Mixtures," J. Chem. Phys., **28**(5), 1958.
- Wijn, G., G.F. Versteeg, and A.A.C.M. Beenackers, "Mass-Transfer Enhancement Factors for Reversible Gas-Liquid Reactions: Comparison of DeCoursey's and Onda's Methods," Chem. Eng. Sci., **41**(9), 2440, 1986.
- Yourgrau, W., A. van der Merwe, and G. Raw, *Treatise on Irreversible and Statistical Thermophysics: An Introduction to Nonclassical Thermodynamics*, Dover Publications, Inc., New York, 1982.
- Yu, W.-C., G. Astarita, and D.W. Savage, "Kinetics of Carbon Dioxide Absorption in Solutions of Methyldiethanolamine," Chem. Eng. Sci., **40**(8), 1585, 1985.
- Zwietering, Th. N., "The Degree of Mixing in Continuous Flow Systems," Chem. Eng. Sci., **11**(1), 1, 1959.

## VITA

David Arnold Glasscock was born in Oklahoma City, Oklahoma, on April 22, 1964, the son of James E. and Doris A. Glasscock. After graduation from Laverne High School in 1982, he entered Oklahoma State University. He was married in August, 1983 to Kathleen Marie Clevenger. He earned the B.S. degree in Chemical Engineering in July, 1986. During the summer of 1985, he was employed at the Amoco Production Company research center in Tulsa, Oklahoma. In August, 1986 he entered The Graduate School of The University of Texas at Austin. He received the M.S. degree in Chemical Engineering in December, 1989. Upon completion of requirements for the Ph.D. in Chemical Engineering, he will be employed in the Field Engineering Program of E.I. Du Pont de Nemours and Co. in Newark, Delaware.

Permanent address: Route 2, Box 78  
Laverne, OK  
73848

This dissertation was typed by the author.